THÈSE

Présentée à

L'UNIVERSITE DES SCIENCES ET TECHNOLOGIES DE LILLE

Pour l'obtention du titre de

DOCTEUR DE L'UNIVERSITE DE LILLE 1

École doctorale Biologie-Santé

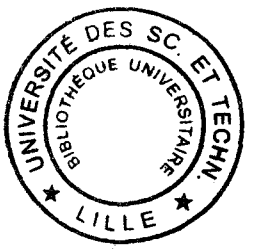

Par

Chann LAGADEC

INCIDENCE DE LA SUREXPRESSION DE TRKA SUR LA CROISSANCE DES CELLULES CANCEREUSES DE SEIN

Soutenue le 9 novembre 2007 devant la commission d'examen :

Rapporteurs :	Dr. Jean-Jacques DIAZ
	Pr. Philippe BOUGNOUX
Membres :	Pr. Philippe DELANNOY
	Dr. Victor NURCOMBE
	Pr. Hubert HONDERMARCK
Directeur de thèse :	Pr. Xuefen LE BOURHIS

A Alix,

A toute ma famille,

A mes amis.

Pour leur amour, le soutien et

leur éternel désir de découvrir

Avant propos

Mes travaux de thèse présentés dans ce mémoire ont été réalisés sous le tutorat scientifique de Madame le Professeur Xuefen LE BOURHIS au sein du laboratoire INSERM ERI-8 (JE 2488) « Signalisation des facteurs de croissance dans le cancer du sein. Protéomique fonctionnelle », IFR147 de l'Université des sciences et technologies de Lille.
Pendant les trois premières années, un soutien à ces recherches a été apporté par une allocation du ministère de la recherche, puis par une bourse de soudure d'une année financée par l'Association de Recherche contre le Cancer (ARC).

Je tiens à remercier Monsieur le Professeur Hubert HONDERMARCK, qui dirige l'équipe INSERM ERI-8, pour l'accueil au sein du laboratoire et pour ses « contrôles positifs et négatifs » de chaque expérience, « n'oubliez pas trop le club-jeune de la SFEAP ».

Je remercie de tout cœur Madame le Professeur Xuefen LE BOURHIS qui m'a dirigé et soutenu lors de mon stage de DEA puis lors de ma thèse. Ta patience, ta disponibilité légendaire et ta gentillesse (malgré tes yeux d'un noir profond !) m'ont permis de mener à bien ce travail. Merci pour nos discussions scientifiques et pour la confiance que tu m'as accordé.

Je souhaite remercier vivement les membres du jury pour l'honneur qu'ils me font :

Monsieur le Professeur Jean-Jacques DIAZ (INSERM E 0211, Tours)
Monsieur le Professeur Philippe BOUGNOUX (INSERM U369, CNRS UMR 5534, Lyon)
Qui ont accepté de juger ce travail.

Monsieur le Professeur Philippe DELANNOY (UMR 8576, Villeneuve d'Ascq)
Monsieur le Professeur Dr. Victor NURCOMBE (IMCB, VNSC Group, Singapore)
Monsieur le Professeur Pr. Hubert HONDERMARCK (INSERM ERI-8, Villeneuve d'Ascq)
Qui ont bien voulu examiner ce travail.

Alessandro merci pour ces heures de « culture » passées en salle de culture à écouter ton papa au « Sergio Show ».

Elsa fait attention à ne pas te faire agresser par les tableaux du couloir.

Samuel, merci pour ton « expert » tease… si jamais tu ne sais plus quoi faire, je serai par loin d'Hollywood !

Merci Steph pour les quelques heures en tête à tête passées le soir au fond du labo (attention je sens que çà va jaser !). Prends bien soin de nos bêtes à poils…Yohann dit Yohbacca.

Un ahUUU spécial à Rodrigue.

Virginie, vive les pissettes… ce sera mieux quand elles auront des ailes ou des air-bags.

Christophe, un immense merci pour nos échanges professionnels et personnels… tu auras été pour nous « le changement en douceur mais efficace ».

Vaïk, ne change pas de sourire, en revanche les chaussures tu peux…

Claude, merci de m'avoir ouvert sur le MONDE de la recherche.

Gabriel merci pour nos discussions politico-scientifiques.

Bob dit l'âne, Adeline, Eric l'équarisseur, Rick Hunter, Manu et Emma, Nath, Albin, Anne, Chantal, Fabien, Nathalie J., l'ensemble du CJ-SFEAP, Ikram, Frank, Fanny, Toufik, Johann, Valérie B., Véronique, Sylvain, Christian, Valérie C. …. et tous les autres (çà c'est pour dire que je n'ai oublié personne) merci de m'avoir suivi ces dernières années.

En attendant que nos routes se recroisent un jour, je n'aurai que deux mots pour tous vous remercier : « Cendrier et Hippopotame » !

SOMMAIRE

QUELQUES MOTS D'INTRODUCTION

TrkA est le récepteur tyrosine kinase du Nerve Growth Factor (NGF). Il a été découvert pour la première fois dans le cancer du colon par Matin-Zanca (Martin-Zanca et al. 1986) pour son rôle oncogénique au sein d'une protéine de fusion. Depuis, l'implication de TrkA dans de nombreux cancers (neuroblastomes, adénocarcinomes thyroïdien, pancréatique et prostatique) a été décrite. De manière, très intéressante, l'axe NGF/TrkA peut dans certains cas inhiber le développement tumoral en induisant la différenciation cellulaire (neuroblastomes) ou au contraire stimuler la croissance, la survie et l'invasion contribuant ainsi à l'augmentation de l'agressivitité tumorale (carcinomes thyroïdien et pancréatique). Notre laboratoire a été le premier à montrer l'effet mitotique et protecteur du NGF sur les cellules cancéreuses de sein (Descamps et al. 1998; Descamps et al. 2001). Dans les cellules de cancer du sein, TrkA induit une augmentation de la prolifération *via* l'activation de la voie EKR MAPK. Malgré ces études, l'effet de TrkA sur les cellules cancéreuses mammaires ainsi que les voies de signalisation restaient mal décrites.

Afin d'introduire les travaux réalisés au cours de ma thèse, je décrirai tout d'abord le développement normal et cancéreux de la glande mammaire ainsi que leurs régulations par les facteurs de croissance. Je ferai ensuite, le point sur les données concernant le NGF et sa signalisation, et en particulier TrkA. Enfin, je ferai l'état des lieux des connaissances de l'influence de l'axe NGF/TrkA dans les différents cancers.

La présentation des résultats se fait sous forme d'articles. La discussion générale qui suit reprend l'ensemble de mes travaux afin d'en tirer les principaux enseignements et d'ouvrir les perspectives.

En plus de ce travail principal, j'ai poursuivi un autre axe de recherche développé au sein du laboratoire. Il s'agissait d'étudier les effets des inhibiteurs physiologiques et pharmacologiques sur la croissance des cellules de cancer du sein. Mes travaux ont abouti à 2 publications qui sont présentées au dernier chapitre de la thèse. On pourra suivre, au travers de ces deux articles, nos interrogations et nos points de vue concernant l'importance des inhibiteurs étudiés dans le traitement du cancer du sein.

Nous avons alors entrepris d'établir des clones surexprimant stablement TrkA afin d'étudier l'effet de cette surexpression sur la croissance, la survie et la motilité cellulaire. Nous avons pu confirmer que l'activation de TrkA augmente la croissance des cellules. De plus, la surexpression de TrkA induit une large inhibition de l'apoptose et l'anoïkis ainsi qu'une augmentation la migration et l'invasion cellulaire. Les résultats obtenus montrent que les voies PI3K/Akt et ERK MAPK sont essentielles aux effets biologiques observés dans les cellules surexprimant TrkA. D'autre part, des modèles de xénogreffes chez des souris *SCID* ont montré que la surexpression de TrkA induit une augmentation importante de la croissance tumorale et du nombre de métastases pulmonaires, hépatiques et cérébrales.

Nous avons ensuite analysé les protéines impliquées dans la signalisation de TrkA ainsi que les protéines cibles de la surexpression de TrkA par des approches de protéomique fonctionnelle basées sur les compétences du laboratoire. Nous avons immunoprécipité TrkA et identifié ses partenaires à l'aide d'outils de spectrométrie de masse. Nous avons en particulier identifié la protéine Ku70 comme partenaire privilégier de TrkA et des études approfondies ont montré que Ku70 est essentielle à l'effet de survie induit par TrkA (Com et al. 2007). Enfin, une approche de protéomique globale par électrophorèse bidimensionnelle a révélé une augmentation de l'expression de la protéines Ku86 dans les cellules surexprimant TrkA. Nous avons alors montré que l'augmentation d'expression de Ku86 est retrouvée au niveau de la surface cellulaire où il participe à la migration cellulaire.

C'est dans ce contexte que j'ai initié mes travaux de thèse. L'objectif principal de mes travaux était de déterminer l'influence de l'axe NGF/TrkA sur la croissance des cellules cancéreuses de sein. Pour cela, nous avons entrepris d'établir des cellules surexprimant stablement TrkA en utilisant la lignée MDA-MB-231. Ceci nous permet d'obtenir à la fois le modèle cellulaire voulu et son contrôle déjà riche d'une expérimentation approfondie disponible dans la littérature scientifique.

INTRODUCTION

I. La glande mammaire normale et les tumeurs mammaires

I. A. La glande mammaire

I. A. 1. Anatomie et histologie

La glande mammaire est une glande cutanée au même titre que les glandes sudoripares et sébacées. Cette glande est entièrement incluse dans le tissu adipeux sous-cutané et est rattachée à la peau par ses seuls canaux excréteurs. C'est une glande tubulo-acineuse, de type composé, formée de 15 à 20 unités glandulaires indépendantes nommées lobes mammaires. La glande mammaire est une glande exocrine dont la fonction est la sécrétion lactée (Figure 1).

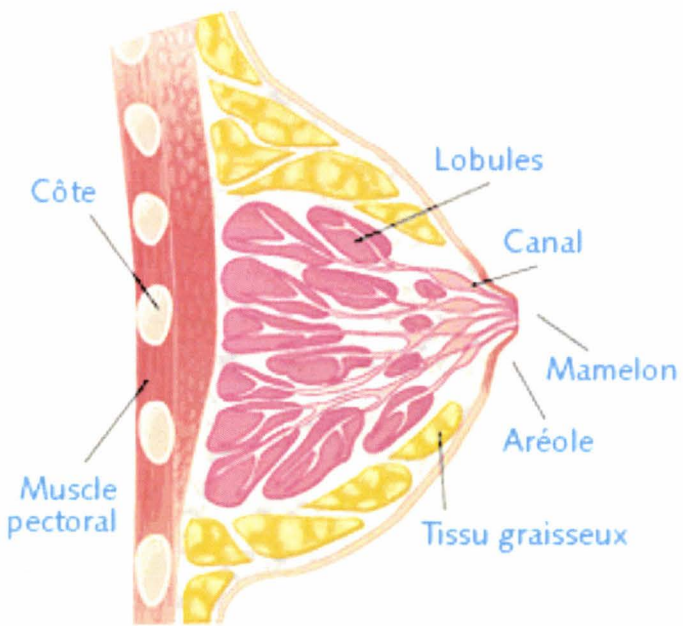

Figure 1 : *Anatomie et structure de la glande mammaire* (http://www.sanofi-aventis.com/healthcare/cancer_research/pathologic/breast/p_breast_desc.asp).

Chaque lobe s'organise autour d'un canal excréteur (canal galactophore) qui conduit le lait au niveau de l'extrémité du mamelon par un orifice qui lui est propre. Juste avant de s'ouvrir au niveau du mamelon, le canal galactophore forme une dilatation nommée

« sinus lactofère ». À l'autre extrémité, la canal galactophore se divise en plusieurs canaux dits lobulaires qui se divisent à leur tour en canaux alvéolaires autour desquels se réunissent de façon très dense les acini. Un lobule est ainsi constitué d'acini, de canaux alvéolaires et de canaux lobulaires, alors que l'on désigne lobe l'ensemble des lobules drainés par un seul et même canal galactophorique (Figure 2).

A.

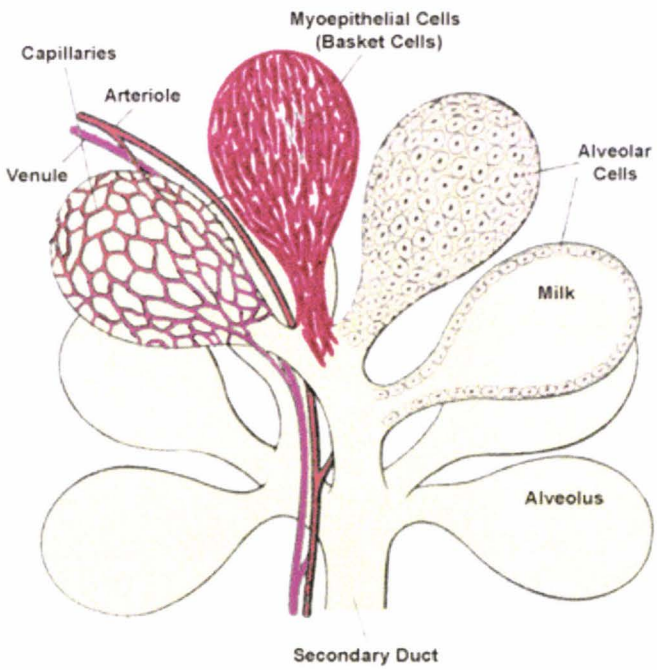

B.

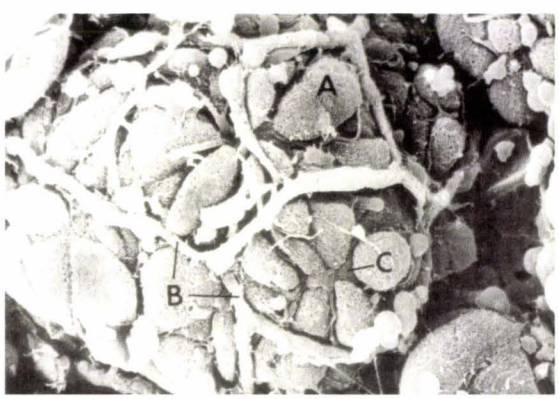

Figure 2 : *Organisation générale d'un lobule mammaire.* A. Schéma de l'organisation alvéolaire de l'extrémité d'un canal secondaire (Austin and Short 1984). B. Photo d'une alvéole durant la lactation a. cellules épithéliales, b. capillaires sanguins, c. cellules myoépithéliales (Anderson & Larson, 1995).

La glande mammaire est composée de plusieurs types cellulaires distincts. Le système lobulo-canalaire est constitué d'une assise continue de cellules épithéliales, doublée d'une couche externe discontinue de cellules myoépithéliales. Ces deux couches cellulaires reposent sur une lame basale recouverte d'un manchon fibroblastique plus ou moins développé. De la même manière, les acini ou alvéoles sont composés des cellules épithéliales et myoépithéliales qui sont entourées d'une lame basale et d'un tissu mésenchymateux (tissu palléal), composé de fibroblastes et d'adipocytes. Il est à noter que chaque acinus est fortement irrigué par les vaisseaux sanguins. Les cellules épithéliales sont d'une forme cylindrique, ce sont ces cellules qui sécrètent le lait, alors que les cellules myoépithéliales sont fusiformes et permettent l'évacuation du lait par contraction (Figure 2 et 3).

A. **B.**

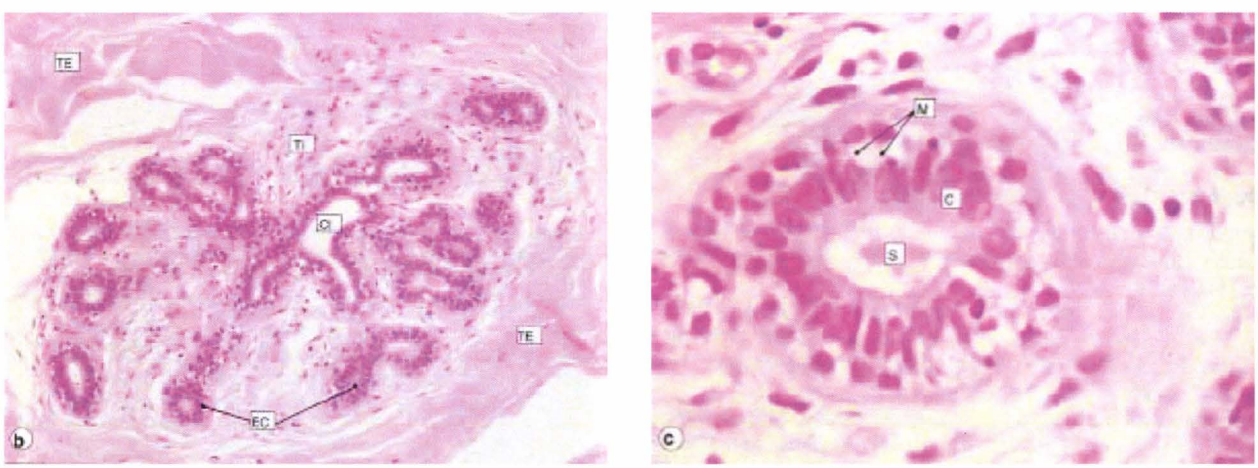

Figure 3 : *Histologie de la glande mammaire normale.* A) Lobule mammaire. CI : canal intralobulaire ; EC : extremités canalaires ; TI : tissu de soutien intralobulaire ; TE : tissu de soutien extralobulaire. B) Canal terminal intralobulaire. La couche interne de l'épithélium a un aspect cubique (C), tandis que la couche externe est constituée de cellules myoépithéliales (M) (d'après Stevens and Lowe 1992).

I. A. 2. Développement et son contrôle

La glande mammaire débute sa croissance au cours de la vie fœtale et se poursuit lentement tout au long de l'existence. Ce développement s'effectue en plusieurs étapes et ne s'achève réellement que pendant la gestation et la lactation (Figures 4).

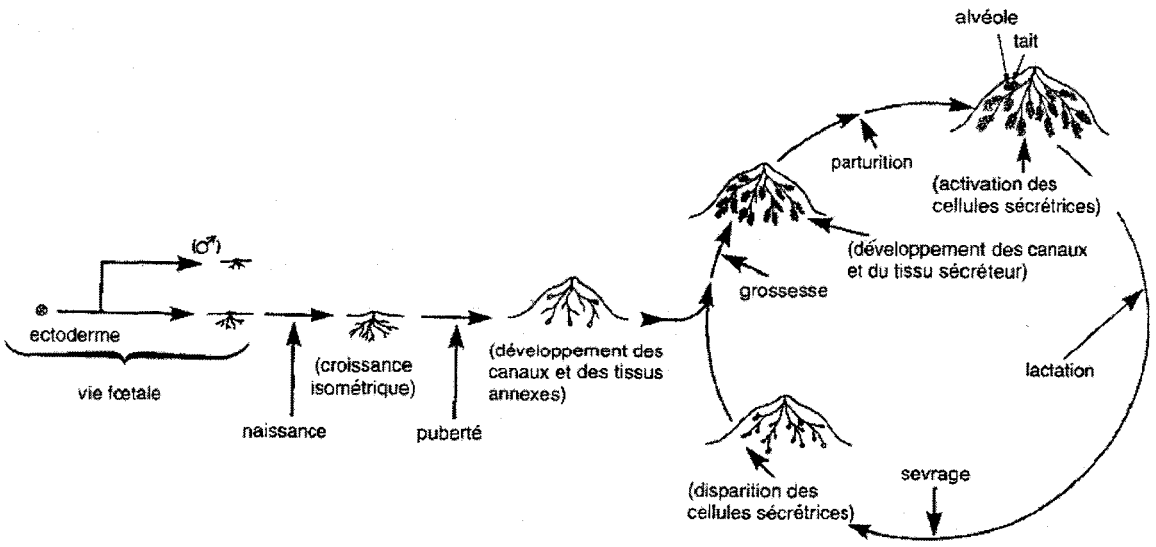

Figures 4 : *Différentes étapes de la croissance et du fonctionnement de la glande mammaire (d'après (Espie et al. 1995).*

I. A. 2. a) Étape prénatale

Les premiers signes de développement apparaissent dès la 4ème semaine de la vie embryonnaire. Une paire de bourgeons mammaires primitifs se forme le long de la crête mammaire (ligne lactéale). Ces bourgeons correspondent à un épaississement de l'ectoderme. À la 6ème semaine, la crête mammaire disparaît, seuls les bourgeons mammaires subsistent à la 7ème semaine, c'est la fin du développement embryonnaire. Ces premières étapes sont sous le contrôle de différents gènes tels que wnt et FGF-R2b. Par la suite, un dialogue entre les cellules épithéliales et les cellules mésenchymateuses se met en place faisant intervenir les facteurs de croissance comme le FGF et l'EGF qui stimulent la migration et la prolifération des cellules épithéliales. Au cours du 5ème mois de grossesse, les bourgeons mammaires émettent des prolongements cylindriques (10 à 20) dans le

mésoderme sous-jacent. Entre le 7ème et 8ème mois, ces prolongements se ramifient, se dilatent et se creusent afin de former la lumière des futurs canaux galactophoriques.

Ainsi, à la naissance, la glande se limite à un système de 15 à 20 tubules très courts s'ouvrant au sommet de l'ébauche du futur mamelon qui a fait saillie alors que l'aréole se pigmente légèrement. Les glandes mammaires des individus féminins et masculins sont, à cette étape du développement, identiques. Ce n'est que par la suite que la glande mammaire de la femme poursuivra son développement contrairement à celle de l'homme.

I. A. 2. b) Étape pubertaire

De la naissance à la puberté, la croissance de la glande mammaire est minime et isométrique. A la puberté, la maturation des follicules ovariens est accélérée sous l'influence des hormones pituitaires FSH (follicle stimulating hormone) et LH (Luteinizing hormone), on observe alors la production d'une quantité croissante d'œstrogènes, en particulier d'estradiol. La croissance de la glande s'accélère et des modifications morphologiques se produisent. Sous l'effet de ces hormones, le développement des canaux galactophoriques s'accélère, le mamelon fait également saillie et l'aréole se pigmente plus fortement.

L'hormone pituitaire GH (Growth Hormone), en association avec les œstrogènes ovariens, déclenche une série d'interaction entre les cellules épithéliales et les cellules du stroma (Figure 5). Ces interactions se font via les facteurs de croissance (IGF1, EGF, FGF, TGFβ) et les métalloprotéases (MMP2, 3, 14 et Adam17). Ces molécules ont pour effet de stimuler la prolifération, la survie et la migration des cellules épithéliales, aboutissant à la mise en place de l'arborescence de la glande.

Lors des premières ovulations, les acini lobulo-alvéolaires se forment, le sein prend alors la forme caractéristique d'une jeune femme nullipare (Figure 6). La formation de ces structures est sous le contrôle d'hormones ovariennes (progestérone et œstrogènes) et de l'hormone pituitaire GH. Ces hormones agissent en augmentant l'expression de facteurs de croissance tels que l'HGF, l'EGF et l'IGF qui, à leur tour, stimulent (de manière paracrine ou autocrine) la croissance et la différenciation des cellules mammaires.

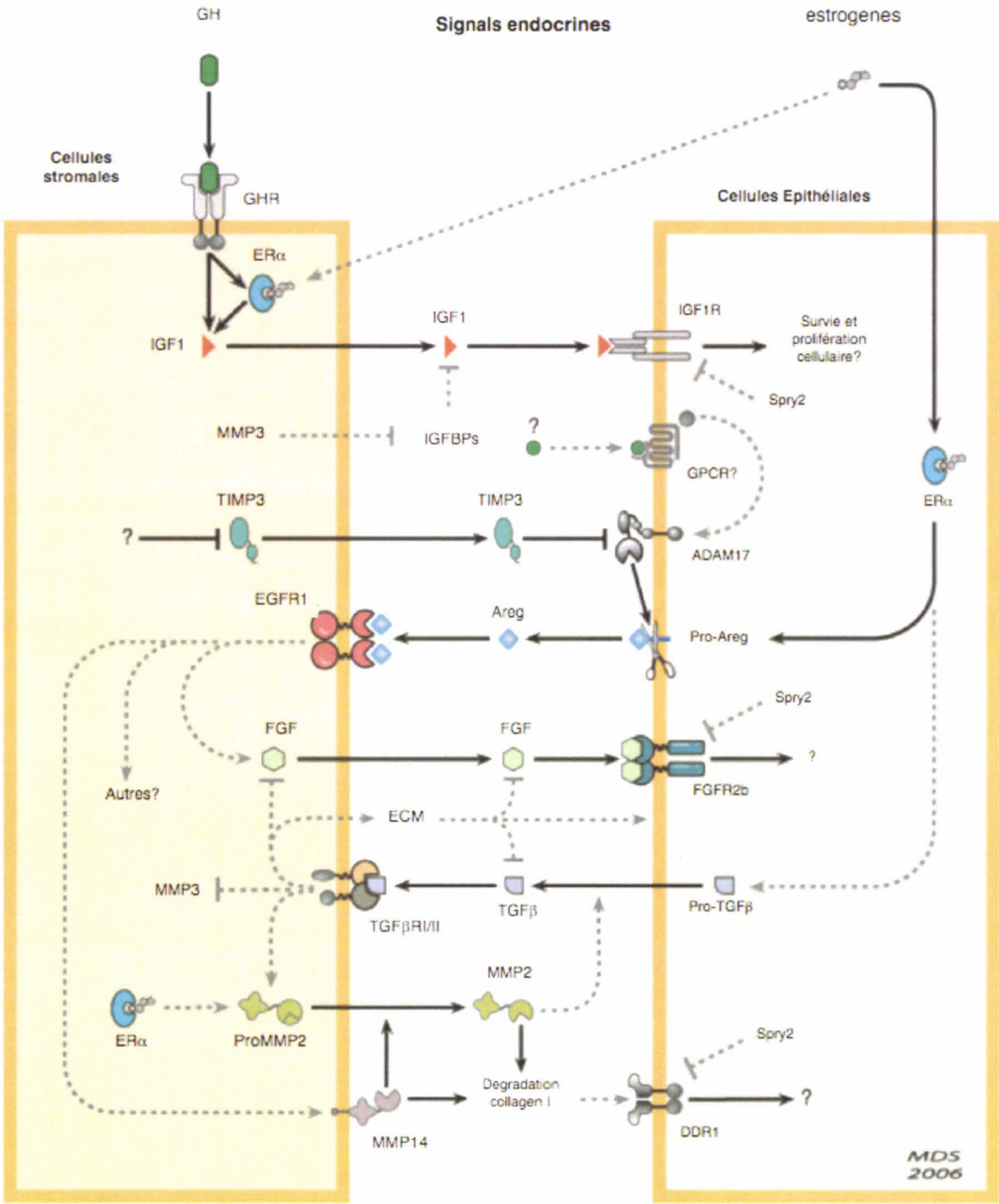

Figure 5 : *Facteurs endocrines et paracrines impliqués dans la formation de l'arborescence mammaire pendant la phase pubertaire.* GH : Growth Hormone ; GHR : Growth Hormone Receptor ; IGF1 : Insulin-like Growth Factor ; IGFBPs : IGF Binding Proteins ; (Pro-)MMP : Matrix Metalloprotease (Precursor); Spry2 : Protein Sprouty homolog 2 ; ERα : Estrogen Receptor α ; TIMP3 : Tissue inhibitor of metalloproteinases 3 ; ADAM17 : A disintegrin and metalloproteinase domain 17 ; EGFR : Epithelial Growth Factor Receptor ; (Pro-)Areg : Amphiregulin (Precursor) ; FGF : Fibroblast Growth Factor ; ECM : Extracellular Matrix ; (Pro-)TGFβ : Transforming Growth Factor β (Precursor) ; TGFβRI/II : TGFβ Receptor I and II ; DDR1 : Epithelial discoidin domain receptor 1.
⋯➤ Représentent les liens directs, alors que ⋯➤ représentent les liens indirects ou non démontrés (d'après Sternlicht et al. 2006).

I. A. 2. c) Gestation et lactation

Au cours de la gestation, l'extension des canaux galactophores et la différenciation des acini glandulaires s'effectuent sous le contrôle des œstrogènes et de la progestérone. La glande mammaire est totalement mature lors de la lactation pendant laquelle les cellules sécrétrices des acini sont parfaitement différenciées sous l'effet des hormones lactogènes (la prolactine, les glucocorticoïdes, la GH et l'hormone placentaire lactogène) dont les concentrations restent élevées durant toute la gestation et la période d'allaitement. En fin de lactation, après une période de sevrage, la glande régresse et les cellules sécrétrices de lait disparaissent (Figure 6).

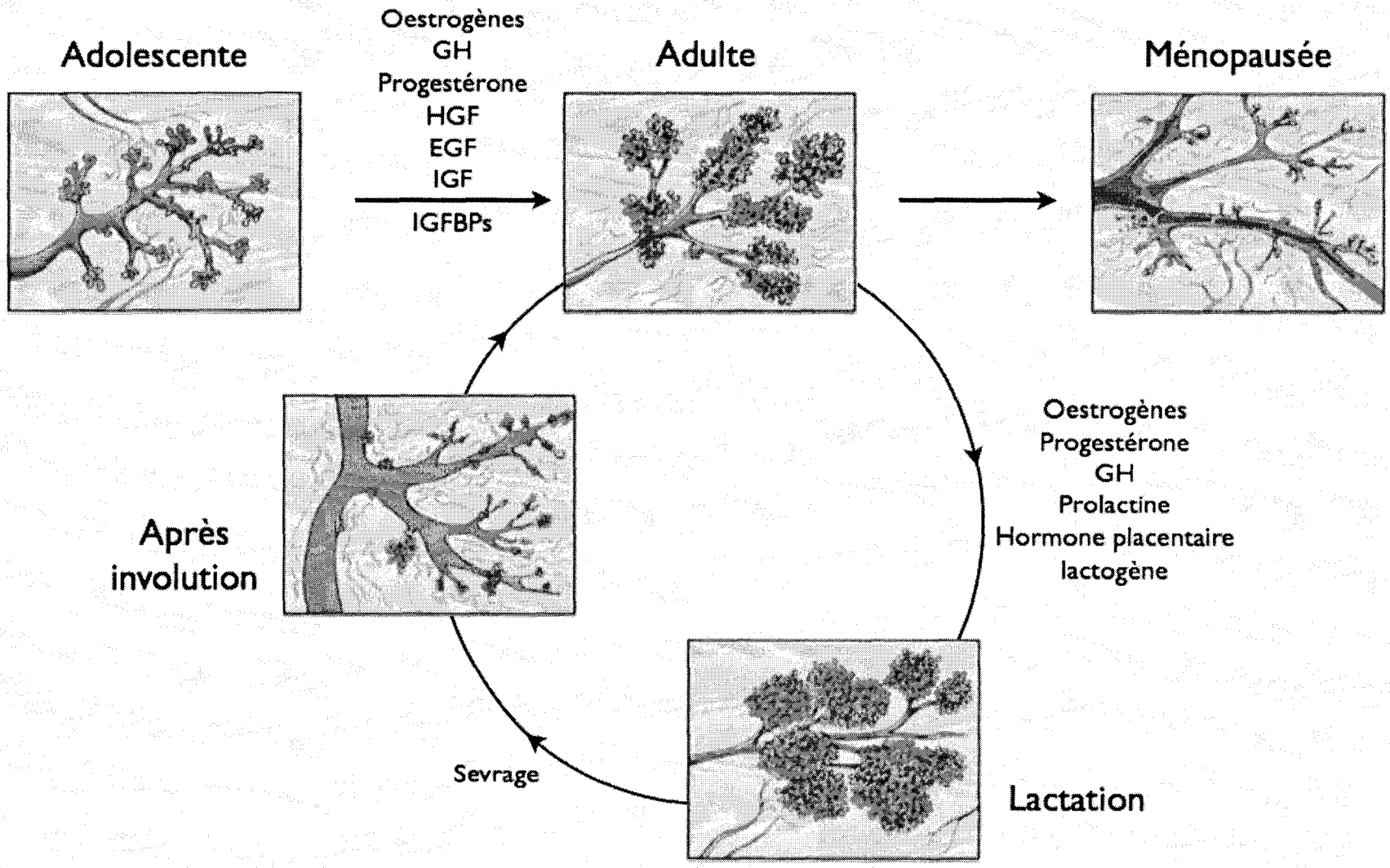

Figure 6 : *Développement de la glande mammaire à partir de l'adolescence.* À la puberté, la glande mammaire subit l'effet de nombreuses hormones et facteurs de croissance provoquant un développement de l'arborescence et des alvéoles. Lors d'une grossesse, les hormones lactogènes induisent la différenciation des cellules épithéliales des acini en cellules productrices de lait. Le sevrage entraîne la disparition de ces cellules et l'involution de la glande.

I. B. Les tumeurs mammaires

Le cancer du sein est le premier cancer féminin de l'Union Européenne avec environ 210 000 nouveaux cas par an et 73 000 décès chaque année. Les études statistiques permettent d'estimer qu'une femme sur huit développera un cancer du sein au cours de sa vie. C'est une maladie grave qui représente la première cause de morbidité chez les femmes de 35 à 55 ans issues des pays développés. En France, malgré la prévention, l'évolution du dépistage et des traitements, le taux de mortalité due aux cancers du sein a légèrement augmenté en 20 ans, passant de 18,7 en 1980 à 19,8 décès pour 100 000 habitants en 2000 (Ligue contre le cancer).

Cependant, ce cancer est une pathologie à évolution lente caractérisée par l'apparition fréquente de métastases pulmonaires, hépatiques, cérébrales et osseuses. Il faut compter 6 à 8 ans pour qu'à partir d'une seule cellule apparaisse une tumeur d'un volume de 1 cm^3 détectable par mammographie classique. Pendant cette période infra-clinique (période de non-détection de la tumeur), la tumeur évolue, pouvant ainsi passer d'un stade *in situ* (non invasif) à un stade invasif par des phénomènes d'invasion microscopique de la membrane basale. Les cellules néoplasiques peuvent alors être essaimées à partir du site de la tumeur primaire *via* les voies lymphatiques ou sanguines. C'est ainsi que les premiers relais ganglionnaires (ganglions axillaires inférieurs, moyens puis supérieurs) sont colonisés. S'en suit l'invasion des chaînes mammaires internes et enfin les ganglions sus-claviculaires en cas de tumeur externe (Figure 7). Cet envahissement des ganglions lymphatiques est le reflet du potentiel métastatique des cellules tumorales et sa présence est corrélée à la taille et au grade histologique de la tumeur. Ce n'est que plus tardivement que l'on peut retrouver des sites de métastases secondaires à distance notamment au niveau des os, du foie, des poumons, du cerveau, de la plèvre et de la peau.

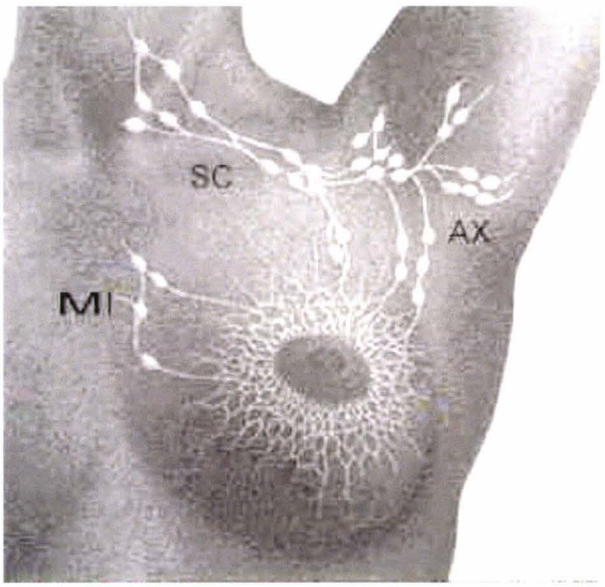

Figure 7 : *Premiers sites de métastases, les ganglions axillaires (AX), les chaînes mammaires internes (MI) et les ganglions sus-claviculaires (SC)* (http://www.arcs.asso.fr/content/seinhistnat.htm).

La carcinogenèse mammaire est le résultat d'une succession d'étapes contribuant à l'évolution d'une cellule normale en une cellule cancéreuse sous l'influence d'une multitude de facteurs tels que les agents environnementaux, les facteurs physiologiques (hormones, facteurs de croissance, cytokines…) et les altérations géniques (Figure 8).

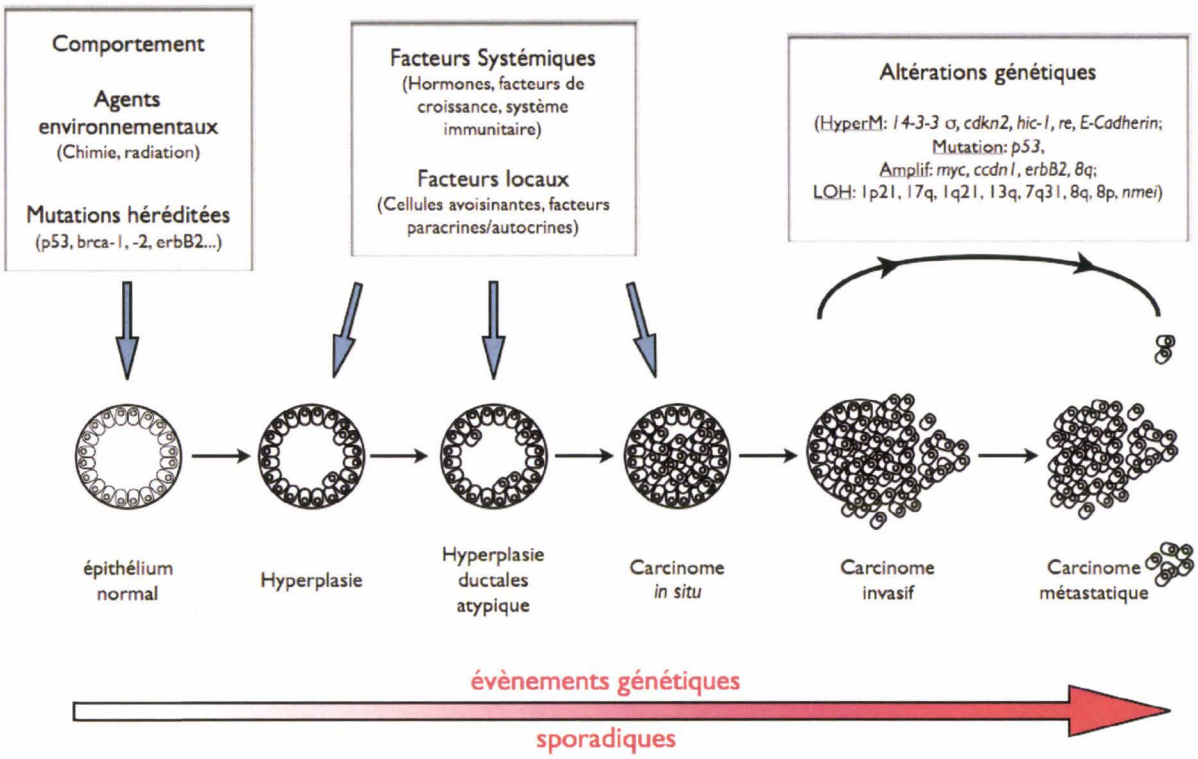

Figure 8 : *Facteurs influençant la cancérogenèse mammaire.* HyperM : Hypermethylation ; Amplif : amplification ; LOH : Lost of heterozygoty (d'après Bieche and Lidereau 1997; Lakhani et al. 1999; Polyak 2001).

Les cellules cancéreuses acquièrent les caractéristiques suivantes :

- *Immortalité* : réplication à l'infini et résistance à l'apoptose.
- *Indépendance :* échappement partiel ou total au contrôle des facteurs de croissance.
- *Métastase* : invasion des tissus conjonctifs adjacents et colonisation d'organes distants.

I. B. 1. Différents types de cancer du sein

Classiquement, les cancers du sein sont classés selon des critères histologiques en 2 catégories :

- Les carcinomes primitifs du sein (adénocarcinomes). Ils représentent 99% des cancers du sein et correspondent à des tumeurs issues des cellules épithéliales à différentiation glandulaire.

- Les autres tumeurs malignes du sein. Elles représentent un groupe de lésions disparates comportant des sarcomes, des lymphomes non hodgkiniens et des métastases mammaires témoignant d'un cancer primitif de nature variable. Etant donnée leur rareté, ces tumeurs ne seront plus évoquées ultérieurement.

Les adénocarcinomes peuvent encore être classés en 3 types en fonction de leur caractère infiltrant ou non des tissus environnants. On distingue alors les carcinomes in situ, les carcinomes invasifs (Figure 8) et la maladie de Paget:

- **Les carcinomes *in situ*** (non infiltrants). Ils sont dits soit *canalaires* (CCIS) soit *lobulaires* (CLIS) en fonction de la zone de développement. Les CCIS sont définis comme « des carcinomes du galactophore n'infiltrant pas le tissu conjonctif ». Ils ne franchissent donc pas la lame basale et sont associés à un bon pronostic de survie. D'autre part, les CLIS sont « des carcinomes associés aux canalicules intralobulaires qui sont comblés et distendus par une forte prolifération des cellules peu jointives sans envahissement du tissu conjonctif ». Ces carcinomes sont bilatéraux et évoluent dans 20 à 50% des cas vers une forme infiltrante.

- **Les carcinomes infiltrants**. Ces carcinomes sont souvent *canalaires* (75 à 80% des cas de cancers) ou *lobulaires* (4 à 11%). Il existe des formes plus rares qui sont les carcinomes *médullaires* (5%), *tubulaires* (2%), *mucineux*, *colloïdes, phyllodes, inflammatoires et bulbaires* (http://infocancer.nexenservices.com).

- **La maladie de Paget du mamelon** (2% des carcinomes). Cette lésion correspond à une extériorisation au niveau du mamelon d'un carcinome mammaire sous-jacent de nature *canalaire* et parfois infiltrant.

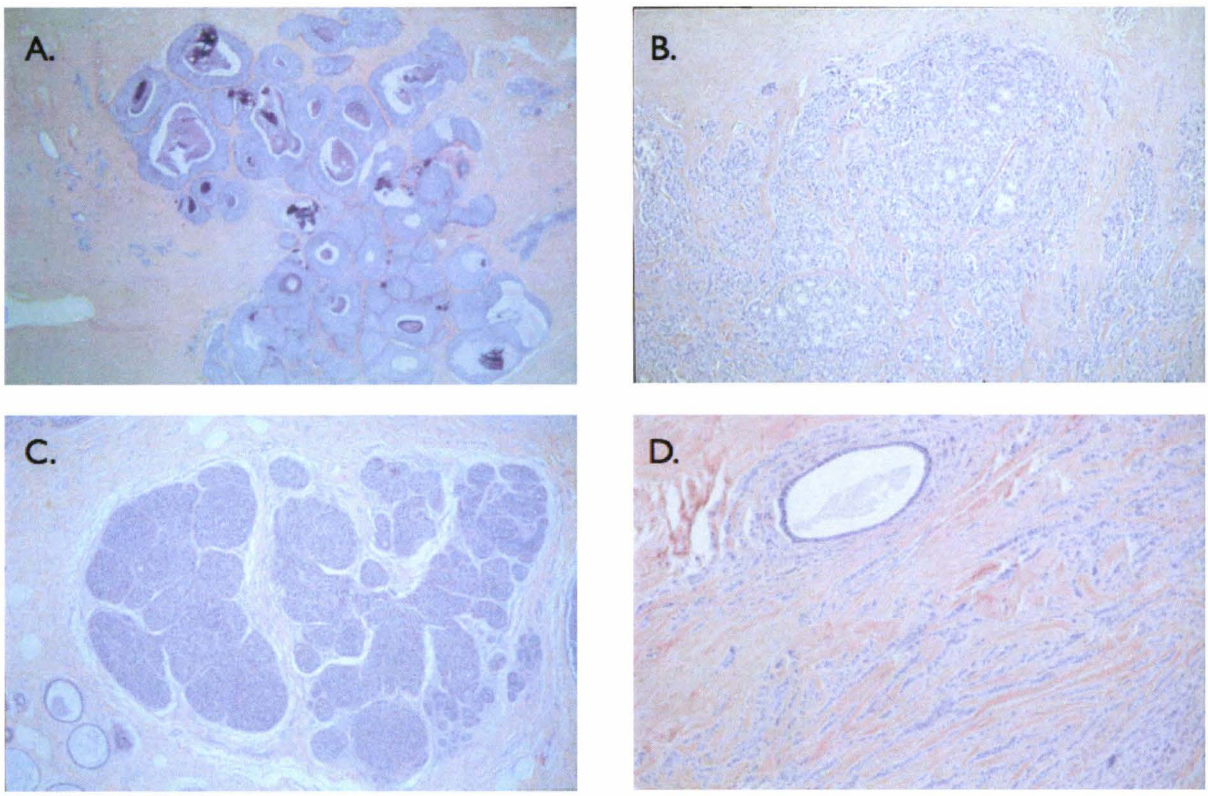

Figure 9 : *Principaux types de carcinomes de sein.* Les carcinomes canalaires in situ (A) et invasifs (B) et les carcinomes lobulaires in situ (C) et invasifs (D) (http://www.med.univ-rennes1.fr/resped/s/gyneco/kcsein/).

Plus récemment, les études transcriptionnelles ont permis d'identifier 5 sous-types majeurs de cancer du sein sur la base de l'expression d'un demi-millier de gènes (Sorlie et al. 2003; Birnbaum et al. 2004; Charafe-Jauffret et al. 2005) :

- Luminal A. Ce sous-type correspond à des cancers généralement de bas grade, exprimant des récepteurs hormonaux et d'évolution plutôt favorable. Les gènes exprimés dans ces cancers sont associés au récepteur des œstrogènes (ERα) et à la différenciation luminale (GATA3).

Ras...) et à des facteurs de transcription (c-Myc, Rel...), elles peuvent aussi être directement impliquées dans le contrôle du cycle cellulaire (cycline D1, Cdk...) ou encore dans le contrôle de la survie cellulaire (famille Bcl-2, Akt...). Dans les cancers du sein, l'activation des oncogènes par amplification génique a été fréquemment décrite. En revanche, les mutations ponctuelles, les insertions ou les réarrangements géniques ont été moins observés (Bieche and Lidereau 1997). Les amplifications les plus fréquentes concernent 3 oncogènes : *c-myc*, *ccdn1* et *c-erbB2*.

L'oncogène *c-myc* est l'un des premiers oncogènes étudiés. Il est localisé en 8q24, et code un facteur de transcription impliqué dans la prolifération, la différenciation et l'apoptose (Blancato et al. 2004). Sa fréquence d'amplification est retrouvée de manière plus importante dans les tumeurs envahissant les ganglions axillaires et les tumeurs de grade histopronostique élevé.

Le deuxième oncogène le plus souvent amplifié dans les tumeurs mammaires est *ccdn1*. Ce gène code la cycline D1 qui régule le passage G1/S et G2/M. Il est amplifié dans 13 à 20 % des carcinomes mammaires (Arnold and Papanikolaou 2005). Comme *c-myc*, la surexpression de la cycline D1 seule n'a pas un pouvoir oncogénique suffisant.

Enfin, l'oncogène *c-erbB2* (HER2) est l'homologue humain du gène *neu* isolé de cellules de neuroblastomes de rat. Il représente le 3ème gène le plus fréquemment amplifié dans les tumeurs mammaires. La protéine ErbB2 appartient à la famille des récepteurs à l'EGF (ErbB1). ErbB2 est surexprimée dans 10 à 46 % des cancers essentiellement canalaires (Jacobs et al. 2000), sa surexpression est associée à l'agressivité tumorale (grade histologique élevé et absence du récepteur aux oestrogènes).

I. B. 2. b) Inactivation de gènes suppresseurs de tumeurs

Les gènes suppresseurs de tumeurs agissent à différents niveaux de la vie cellulaire. Communément, on les subdivise en 3 groupes, les garants de la stabilité du génome (p53, BRCA...), les inhibiteurs de la croissance cellulaire au sens large (Rb, PTEN...) et les modulateurs du microenvironnement cellulaire (E-Cadhérine, CD44...).

Afin de clarifier l'exposé, nous prendrons un exemple de gènes suppresseurs de tumeurs pour chaque subdivision : *p53*, *rb* et *E-cadherine.*

Des mutations du gène *p53*, considéré comme le gardien du génome, sont retrouvées dans 15 à 60 % des cancers du sein (Gasco et al. 2002). On retrouve une perte d'hétérozygotie dans la région du gène de p53 dans près de 50 % des cancers mammaires. p53 joue un rôle majeur dans le contrôle du cycle cellulaire, la réparation et la synthèse d'ADN, dans la différenciation et l'apoptose. L'inhibition de *p53* augmente le pool de cellules en prolifération et la probabilité de leur transformation maligne par déficience de l'induction de l'apoptose.

Le gène *rb* est le premier gène suppresseur de tumeurs à avoir été étudié pour son implication dans les rétinoblastomes de l'enfant. La protéine Rb intervient dans le contrôle de la prolifération, en se liant avec d'autres protéines comme les cyclines. On observe une expression aberrante de Rb dans 20 à 30% des cancers du sein, provoquée par une perte d'hétérozygotie ou une perte totale de l'expression de *rb* (Bosco and Knudsen 2007). De plus, 20 % des tumeurs mammaires présentent une anomalie de la structure de la protéine Rb.

La E-Cadhérine est impliquée dans l'interaction cellule-cellule, elle possède également un pouvoir de signalisation cellulaire. Le niveau d'expression de l'E-Cadhérine est inversement corrélé au caractère invasif des cellules cancéreuses lobulaires (Heimann et al. 2000). La diminution d'expression est souvent due à une perte d'hétérozygotie de *l'E-cadhérine.* L'E-Cadhérine est donc considérée comme un suppresseur de tumeur et un suppresseur de métastases (Cowin et al. 2005).

I. B. 3. Rôle des facteurs de croissance

Les facteurs systémiques et locaux, notamment les facteurs de croissance, jouent un rôle important dans l'évolution de la tumeur en favorisant la croissance de la tumeur primaire et la formation des métastases. Les facteurs de croissance peuvent être sécrétés par les cellules cancéreuses elles-mêmes et des cellules du stroma (fibroblastes, cellules myoépithéliales et cellules immunitaires…) (Figure 10).

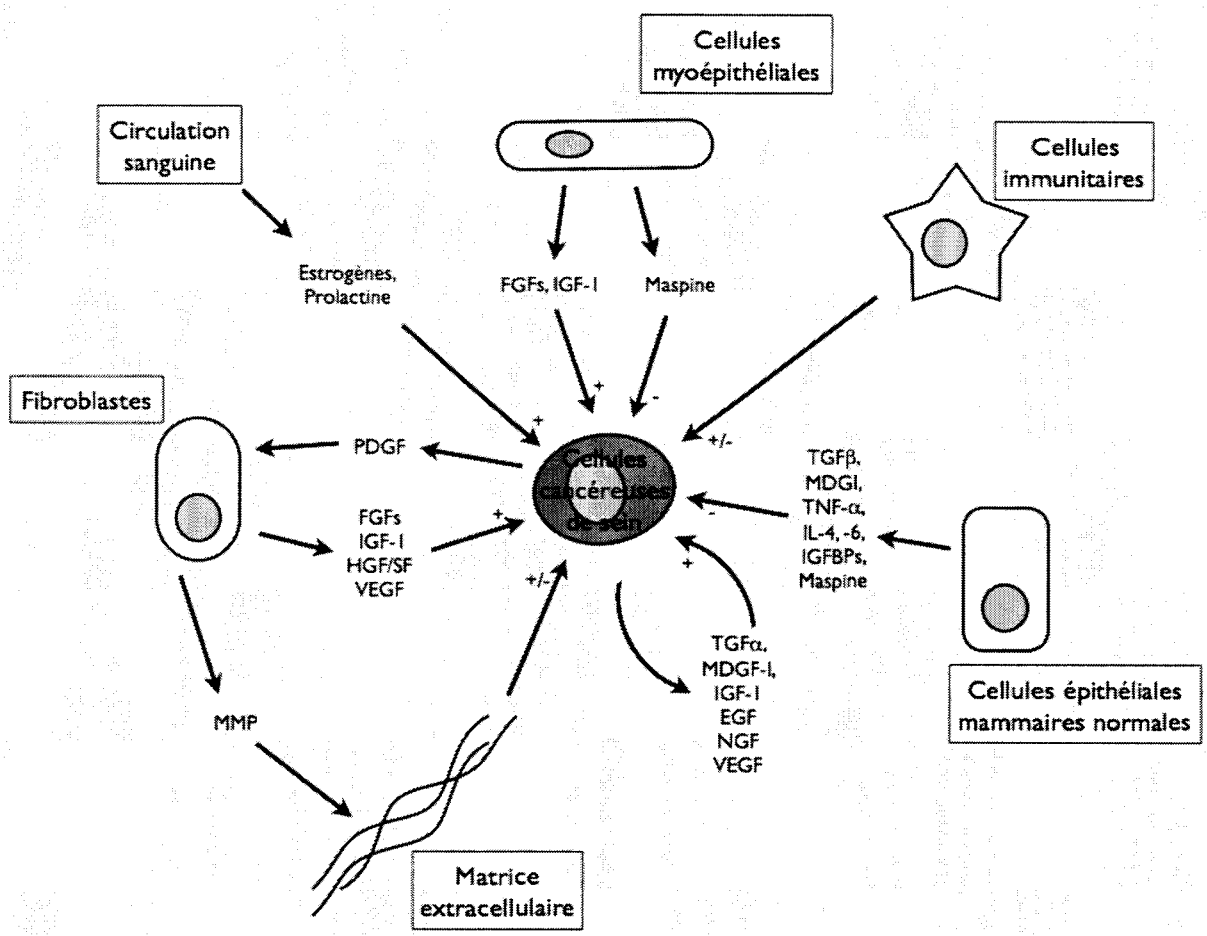

Figure 10 : *Contrôles paracrine et autocrine de la croissance des cellules cancéreuses.* Ce schéma résume les divers facteurs impliqués dans le contrôle de la croissance mammaire, ainsi que l'influence des cellules avoisinantes. Les « + » correspondent à un effet stimulateur sur le croissance des cellules cancéreuses alors que les « - » corespondent à un effet inhibiteur. IGF-1 : Insulin-like Growth Factor 1 ; IGFBPs : IGF Binding Proteins ; FGFs : Fibroblaste Growth Factor ; EGF : Epidermal Growth Factor ; NGF : Nerve Growth Factor ; PDGF : Platelet Derived Growth Factor ; HGF/SC: Hepatocyte Growth Factor / Scator Factor ; VEGF : Vascular Growth Factor ; MDGF-1 : Mammary Derived Growth Factor 1 ; MDGI : MDGF Inhibitor ; TGFβ : Transforming Growth Factor β ; TGFα : Transforming Growth Factor α ; TNF-α : Tumor Necrosis Factor α; IL-4/-6 : Interleukine-4/-6.

Les facteurs de croissance peuvent être classés en 2 catégories principales en fonction de leurs récepteurs : les récepteurs à activité tyrosine kinase et les récepteurs à activité sérine/thréonine). La première catégorie représente la majorité des facteurs de croissance connus comme l'EGF, l'HGF, l'IGF, le VEGF et le NGF. Alors que la seconde concerne essentiellement le TGFb. Les facteurs de croissance peuvent agir directement sur les cellules cancéreuses en stimulant la prolifération, la survie, la migration et l'invasion. Ils peuvent aussi agir sur les cellules du stroma induisant des modifications micro-environnementales tumorales (modifications de la matrice extracellulaire, recrutement et activation des cellules endothéliales…), ce qui favorise l'angiogenèse et la métastase (Figure 11).

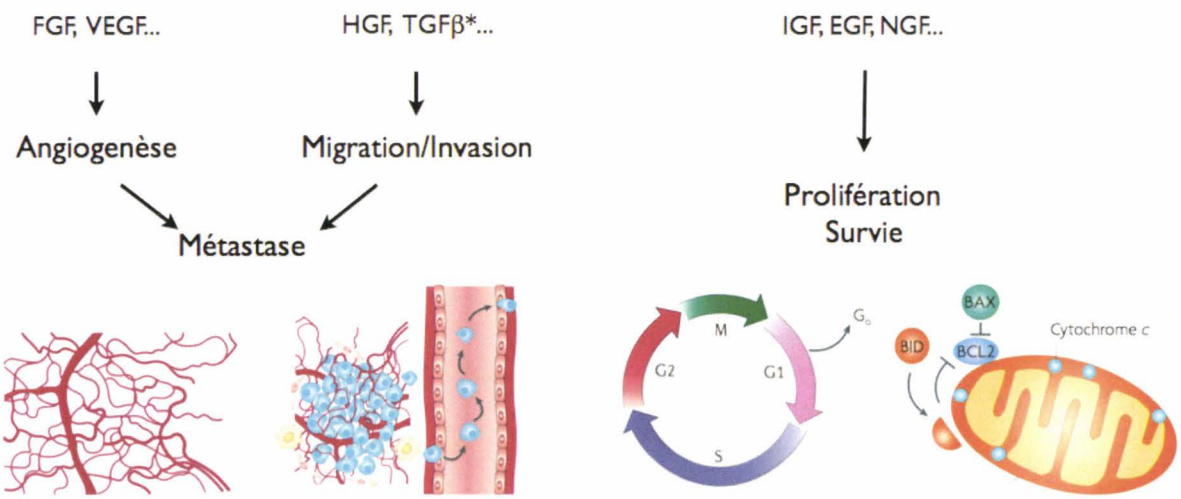

Figure 11 : *Effets pléiotropiques des facteurs de croissances sur le développement tumoral.* * fait référence à la dualité temporelle de l'effet du TGFβ sur la progression tumorale (Nass and Davidson 1999; Dickson et al. 2000; Elliott et al. 2002; Burger et al. 2005; Mercurio et al. 2005; Buck and Knabbe 2006; Chan et al. 2006; Dewan et al. 2006; Chang et al. 2007; Chong et al. 2007; Roussidis et al. 2007; Ursini-Siegel et al. 2007).

Parmi les facteurs de croissance les plus étudiés, l'EGF est bien connu pour stimuler la prolifération, la survie et la migration des cellules cancéreuses de sein *in vitro* (Chan et al. 2006). La surexpression de son récepteur (EGF-R) (20 à 40 % des tumeurs mammaires) est associée à un mauvais pronostic (Hutcheson et al. 2003). Le ciblage d'un récepteur de la famille de l'EGF-R, ErbB2, a permis la mise au point d'un traitement rationnel des cancers de sein métastatiques grâce à un anticorps monoclonal humanisé appelé

« trastuzumab » (Herceptin). Ce traitement est maintenant utilisé en clinique afin de traiter les cancers du sein surexprimant ErbB2 (Vogel and Tan-Chiu 2005).

Un second facteur de croissance connu pour son implication dans l'angiogenèse est le VEGF. Le VEGF participe à la mise en place des vaisseaux sanguins au sein de la tumeur en recrutant les précurseurs des cellules endothéliales, en stimulant la prolifération et la migration des cellules endothéliales. De plus, le VEGF augmente la perméabilité des vaisseaux sanguins, ce qui favorise la nutrition de la tumeur et l'essaimage des cellules cancéreuses. Le VEGF peut être sécrété par les cellules cancéreuses et stromales (Lee et al. 2007). Sa surexpression est associée à un mauvais pronostic (Mohammed et al. 2007). Le ciblage du VEGF et de ses récepteurs (VEGFR1, VEGFR2, neurophilin-1) est actuellement en phase d'essai clinique et constitue une approche thérapeutique angiogénique prometteuse (Hayes et al. 2007).

Enfin, le TGFβ peut inhiber la prolifération des cellules cancéreuses ; à ce titre, il est considéré comme suppresseur de tumeur. Cependant, des études récentes montrent qu'à un stade plus avancé de la progression tumorale, le TGFβ augmente l'agressivité des cellules cancéreuses en stimulant l'invasion et la métastase. L'inhibition de la signalisation du TGFβ (inhibiteurs pharmacologiques des récepteurs, anticorps neutralisants anti-TGFβ, antisens anti- TGFβ) dans des modèles animaux) induit une forte diminution de la croissance tumorale, de l'angiogenèse et des métastases. Ainsi, le TGFβ apparaît comme une cible privilégiée pour le développement de nouvelles stratégies cliniques (Chang et al. 2007).

De nombreux autres facteurs de croissance influencent également la progression tumorale. Nous avons montré au sein du laboratoire le rôle du NGF dans le cancer du sein. Ainsi, les cellules cancéreuses mammaires sécrètent du NGF qui agit de manière autocrine pour stimuler la survie et la prolifération cellulaire. L'inhibition de la signalisation du NGF (inhibiteur pharmacologique des récepteurs, anticorps neutralisants anti-NGF, antisens anti-NGF) dans des modèles animaux réduit fortement la croissance tumorale, l'angiogenèse et les métastases. L'intérêt du NGF et de ses récepteurs dans le cancer du sein sera décrit plus en détail dans le chapitre II de cette introduction (II.D.7).

II. La signalisation du NGF et son rôle dans les tumeurs

II. A. Le NGF

L'existence du Nerve Growth Factor (NGF) a été suspectée dès 1934 par Rita Levi-Montalcini mais ne sera purifié qu'en 1954 avec l'aide de Stanley Cohen (Hamburger 1993). Ce peptide appartient à la famille des neurotrophines qui compte également le Brain-Derived Neutrophic Factor (BDNF), les neurotrophines (NT)-3 et -4/5. D'abord connu pour son rôle essentiel dans la survie et le développement des neurones, on sait aujourd'hui qu'il joue un rôle important dans de nombreux types cellulaires non neuronaux.

Le NGF de haut poids moléculaire ou 7S-NGF est un complexe de 130 à 140 kDa constitué de sous-unités α_2, β, et γ_2 (Dolle et al. 2003) dont les gènes se localisent de manière rapprochée sur le chromosome 1. La sous-unité β est responsable de l'activité biologique du complexe, le γ-NGF possède une activité protéolytique fortement spécifique capable de cliver le précurseur du NGF en forme mature, et le α-NGF ne semble pas avoir d'activité propre. Le β-NGF est une glycoprotéine dimérique de 26 kDa formée de 2 sous-unités identiques de 118 acides aminés associées de manière non-covalente. Par la suite nous utiliserons le terme NGF pour désigner ce dimère actif de β-NGF.

Le gène du NGF est situé sur le bras court du chromosome 1 chez l'homme et code un précurseur de 34 kDa, le pré-pro-NGF. Ce précurseur est clivé en pro-NGF, lui même clivé après action de la furine (Serine protease plasmin) ou de convertases (MMP7) pour générer la molécule mature. La structure du NGF est relativement bien conservée entre les espèces chez les vertébrés, il existe par exemple 90 % d'homologie entre la protéine humaine et la protéine de souris.

Le NGF forme des homodimères de manière non-covalente pour activer deux types de récepteur : le récepteur $p75^{NTR}$ (récepteur commun aux neurorophines) liant l'ensemble des neurotrophines ainsi que les pro-neurotrophines (Chao 1994), et le

récepteur TrkA (Tropomyosin receptor kinase A) comportant une activité tyrosine-kinase intrinsèque (Papatsoris et al. 2007).

II. B. Le récepteur p75^{NTR} et sa signalisation

p75^{NTR} est codé par un gène localisé sur le chromosome 17 et est exprimé sous la forme d'une glycoprotéine de 75 kDa (Dolle et al. 2003). C'est une protéine transmembranaire de type I (domaine C-terminal intracellulaire) de la famille des récepteurs de mort et présente une très forte homologie avec le récepteur p75 du TNF (Rabizadeh and Bredesen 2003). p75^{NTR} est composé de 425 acides aminés dont un peptide signal de 29 acides aminés, il possède un domaine extracellulaire contenant 4 pseudo-séquences répétitives riches en cystéines (6 cystéines par répétition) et en acides aminés basiques (Arg, Lys, Asn) responsables de la liaison des différentes neurotrophines à ce récepteur. Il subit également des modifications post-traductionnelles de N- et O-glycosylation de sa partie extracellulaire alors que sa partie intracellulaire peut subir une palmitoylation sur la Cys 250. Le domaine transmembranaire du récepteur p75^{NTR} est unique et hautement conservé quelle que soit l'espèce animale considérée. Le domaine intracellulaire est constitué de 155 acides aminés. On y trouve une partie juxta-membranaire nommée domaine «*Chopper*» de 60 acides aminés structurellement très flexible suivie d'un « domaine de mort » constitué de 6 hélices a (Figure 12).

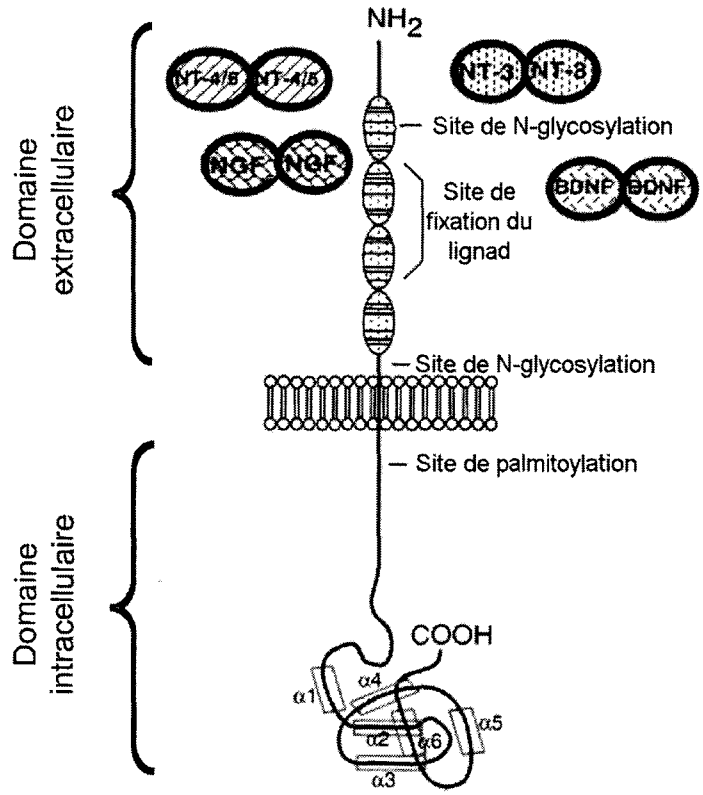

Figure 12 : *Schéma de la structure de p75^{NTR}* (Rabizadeh and Bredesen 2003).

Selon le type et le contexte cellulaires, p75^{NTR} peut recruter des adaptateurs intracellulaires différents conduisant à des effets biologiques divers tels que l'apoptose, la différenciation et la survie.

En absence du ligand, p75^{NTR} peut induire l'apoptose sous forme monomérique. Les adaptateurs comme TRAF2, NRAGE, MAGE et NRIF s'y associent conduisant à l'activation de la voie apoptotique mitochondriale. De plus, l'association de TRAF4 avec p75^{NTR} a pour effet de bloquer la dimérisation de p75^{NTR} et de maintenir la signalisation de la voie pro-apoptotique (Figure 13). Cependant, il a été décrit que le NGF est capable d'induire l'apoptose via p75^{NTR} en produisant des céramides dans certains types de cellules neuronales (Brann et al. 2002). De manière intéressante, p75^{NTR} intervient également dans l'action pro-apoptotique des pro-neurotrophines (Beattie et al. 2002; Pedraza et al. 2005).

L'effet de survie de p75^{NTR} semble impliquer la fixation du NGF et l'homodimérisation de p75^{NTR}. Le dimère p75^{NTR} recrute des protéines adaptatrices RIP2 et TRAF6 au niveau du domaine intracellulaire, entraînant l'activation d'une PKC

atypique (Mamidipudi et al. 2004) qui à son tour active le facteur de transcription NF-κB responsable de la survie des cellules. Le recrutement d'autres adaptateurs tels que p38β2 par $p75^{NTR}$ peut également activer NF-κB (Wang et al. 2000). Cependant, dans un certain contexte, $p75^{NTR}$ (en absence ou en présence de NGF) peut aussi provoquer un arrêt du cycle cellulaire et la différenciation des cellules nerveuses (Ito et al. 2002; Chittka et al. 2004).

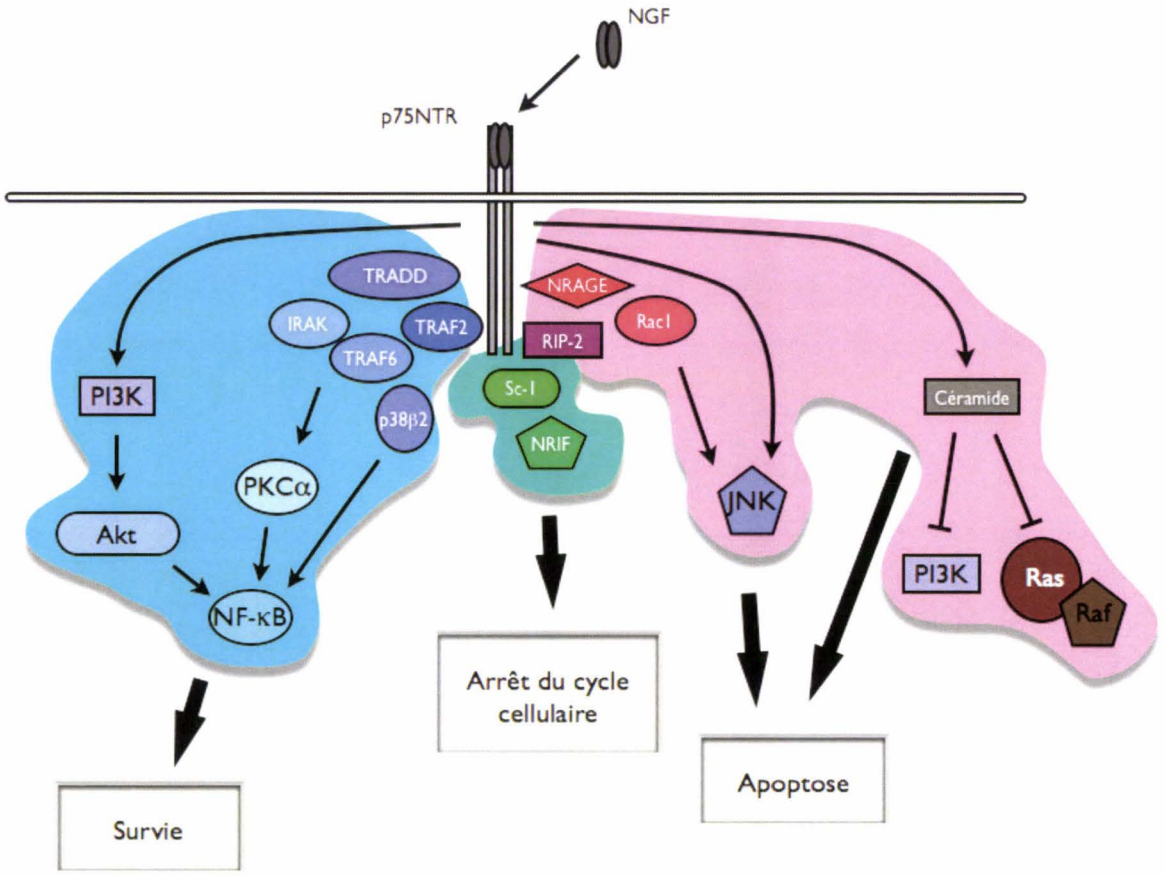

Figure 13 : *Schéma de la signalisation de $p75^{NTR}$.* Le récepteur $p75^{NTR}$ est capable d'induire l'apoptose via l'activation de la voie apoptotique mitochondriale, l'arrêt du cycle cellulaire et la survie des cellules. NRIF : neurotrophin receptor-interacting factor, NRAGE : Neurotrophin receptor-interacting MAGE homolog ; JNK : c-jun N-terminal Kinase ; TRAF2/6 : TNF receptor-associated factor 2/6; IRAK : Interleukin-1 receptor-associated kinase ; p38β2 : MAP kinase p38 β 2RIP-2 : Receptor-interacting protein 2 ; Rac-1; PKCα : Protein Kinase C α ; PI3K : Phosphatidyl Inositol Tri-Phosphate ; NF-κB : Nuclear Factor κB ; Ras : Ras GTPase activating protein ; Raf : Raf proto-oncogene serine/threonine-protein kinase ; Sc-1 : Schwann Cell Factor-1 ; TRADD : Tumor Necrose Factor Receptor Associated Death Domain).

II. C. Le récepteur TrkA et sa signalisation

TrkA est un récepteur tyrosine-kinase appartenant à la famille des Trk (TrkA, TrkB et TrkC). Ces récepteurs partagent une grande similarité dans leur domaine intracellulaire catalytique, mais sont activés par des ligands spécifiques (NGF, NT4/5 et BDNF, NT3 respectivement).

II. C. 1. TrkA : du gène à la protéine

Le gène *trkA* a été découvert quelques années après celui de $p75^{NTR}$, il se nomme également *NTRK1* (Neurotrophine receptor kinase 1). L'oncogène *trkA* se situe sur le chromosome 1, sa localisation exacte est 1q21-q22. Dans cette région du chromosome 1, on y retrouve, entre autres, l'*HDGF* (Hepatoma-Derived Growth Factor) et l'*INSRR* (Insulin Receptor-Related Receptor). Le gène *trkA* contient 17 exons répartis sur 25 kb, au niveau de son promoteur, il n'y a pas de TATA box mais de nombreux sites de fixation putatifs de facteurs de transcription comme Sp1, AP1, AP2, Ap3, ATF et GCF.

A ce jour, 3 isoformes de TrkA ont été décrites : TrkA-I, TrkA-II, TrkA-III. Les isoformes TrkA-I et -II sont issues d'un épissage alternatif de l'exon 9 (Figure 14). L'isoforme TrkA-I est préférentiellement exprimée dans les tissus non-neuronaux alors que l'isoforme TrkA-II est essentiellement exprimée dans les tissus neuronaux. L'isoforme TrkA-III est le fruit d'un épissage alternatif plus important (il lui manque les exons 6, 7 et 9) (Tacconelli et al. 2004). Elle a été découverte récemment du fait de son expression en condition d'hypoxie (Tacconelli et al. 2005).

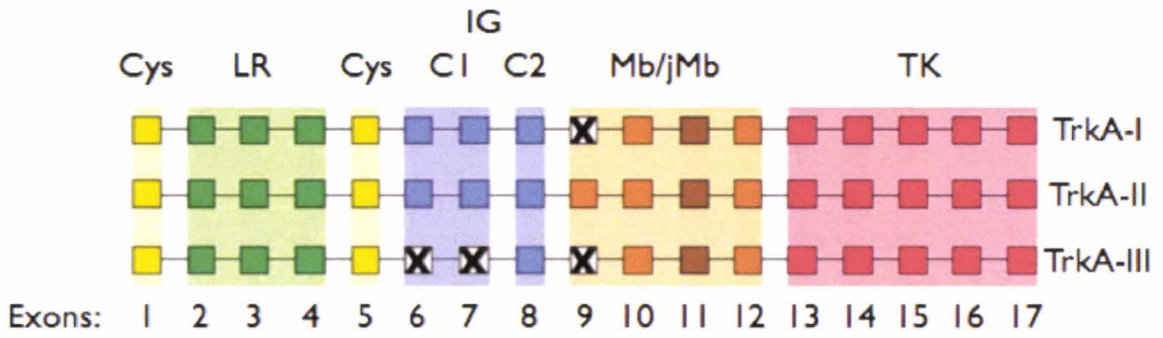

Figure 14 : *Transcrits des 3 isoformes du gène trkA.* Domaines fonctionnels de TrkA répartis le long des 17 exons (carrés), les isoformes TrkA-I et -II diffèrent par l'excision de l'exon 9, alors qu'il manque les exons 6,7 et 9 à l'isoforme TrkA-III. Cys : Cluster de Cystéines (jaune), LR : Région riche en leucines (vert), IG-C1 et –C2 : Domaine « immunoglobulin-like » 1 et 2 (bleu) , Mb/jMb : Domaine membranaire (marron) et juxta-membranaire (orange), TK : domaine tyrosine-kinase (rouge) (adapté de (Benito-Gutierrez et al. 2006).

Les isoformes TrkA-I et –II présentent peu de différences au niveau protéique et sont de ce fait appelées communément TrkA. TrkA est une glycoprotéine transmembranaire de 140 kDa de type I (avec un seul domaine transmembranaire). Au niveau du domaine extracellulaire, on trouve 2 régions riches en cystéine, 3 régions riches en leucines (LRR), 2 régions « immunoglobulin-like » (IG-C1 et IG-C2) responsables de la fixation du NGF ainsi qu'une région riche en prolines (Figure 15). Le domaine extracellulaire possède aussi 13 sites de N-glycosylation. La protéine TrkA immature de 86 kDa subit une glycosylation qui augmente très sensiblement le poids de TrkA jusqu'à 140 kDa. La glycosylation permet la localisation membranaire de TrkA et prévient son activation spontanée en absence de NGF (Watson et al. 1999). Au niveau du domaine intracellulaire juxtamembranaire, on trouve un domaine responsable de la fixation des SNT (Suc-associated Neurotrophine Target). Enfin, au niveau du domaine intracellulaire, on trouve un domaine tyrosine-kinase avec 4 sites tyrosines phosphorylables (Y490, Y674/675, Y751 et Y785).

A.

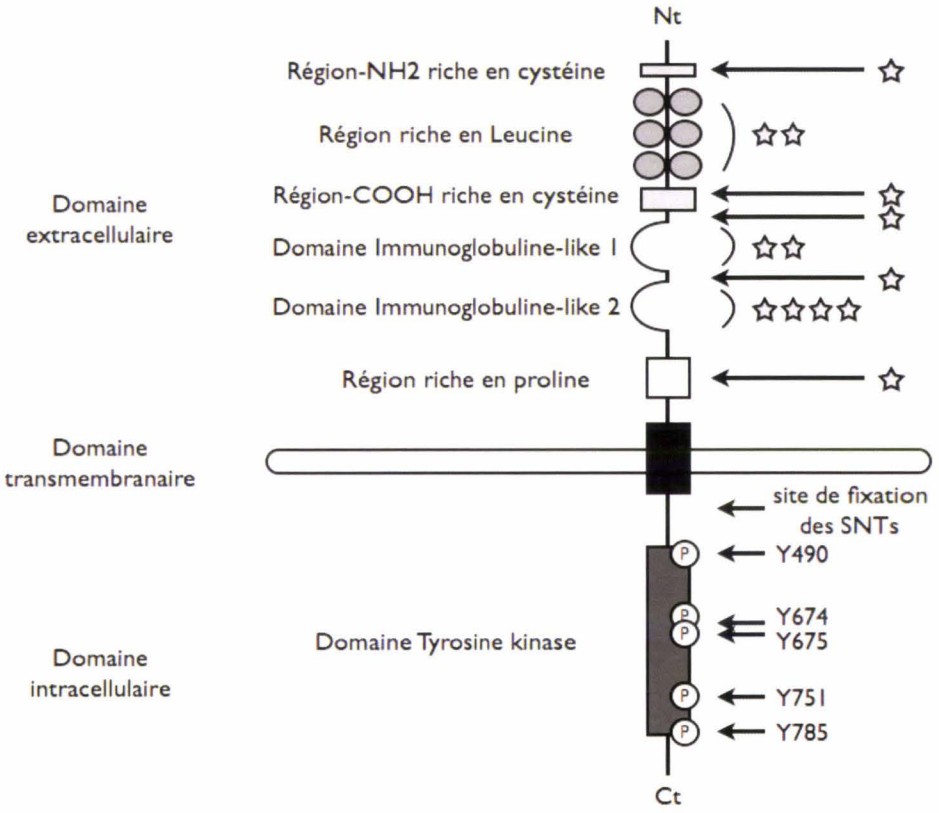

B.

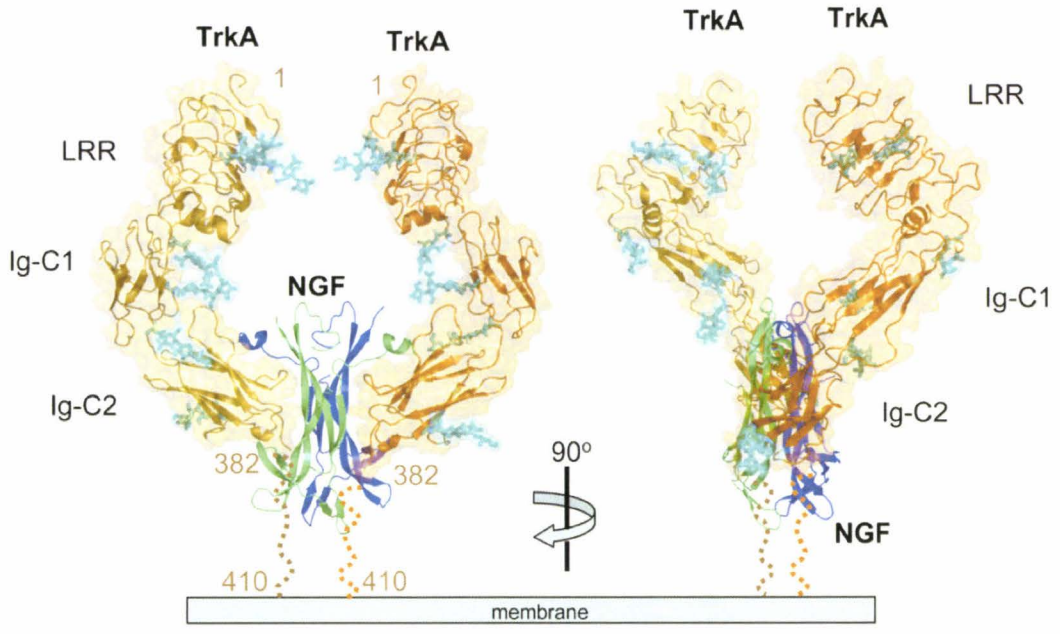

Figure 15 : *Schéma de la structure de TrkA (A) et cristallographie des domaines extracellulaires de 2 molécules TrkA liant le NGF (B).* (A) les étoiles indiquent les sites de glycosylation. (B) Structure tridimensionnelle de 2 récepteurs TrkA liant le NGF (Bleu/Vert) sous 2 angles perpendiculaires. Les glycosylations sont indiquées en cyan alors que les domaines juxta-membranaires sont en pointillés (Dolle et al. 2003; Wehrman et al. 2007).

II. C. 2. Différentes voies de signalisation activées par TrkA

Les voies de signalisation du NGF via TrkA ont été établies notamment dans les cellules neuronales. La liaison du NGF sur le récepteur TrkA induit d'abord une homodimérisation du récepteur, suivie d'une trans-phosphorylation des tyrosines et de l'activation du domaine kinasique. De nombreux adaptateurs se fixent alors à TrkA conduisant à l'activation de 3 voies de signalisation principales et à des effets biologiques divers (Figure 16) :

- *La voie des **MAP kinases*** :

Shc se fixe sur la tyrosine Y490, le recrutement de Grb2/SOS par Shc nécessite la phosphorylation des tyrosines Y674/675, il y a alors activation successive par phosphorylation de Ras/Raf, de MEK1/2 puis de p38 et de Erk1/2. De plus, d'autres adaptateurs comme les protéines SNT interviennent dans l'activation de la voie MAPK. Cette voie semble principalement impliquée dans la prolifération et la différenciation cellulaires.

- *La voie **PI3K/Akt/NF-kB*** :

La phosphorylation de la tyrosine Y751 provoque le recrutement de Src qui active la PI3K, aboutissant à l'activation d'Akt, de NF-κB et de la PKCζ. Cette voie est impliquée dans la survie, la migration et l'invasion cellulaires.

- *La voie **PLCγ/PKC*** :

La tyrosine Y785 phosphorylée permet le recrutement et l'activation de la phospholipase Cγ qui, à son tour, active les PKCα, β, δ et ε, par l'intermédiaire de la PI4,5P et la DAG. Cette activation induit à son tour une cascade de phosphorylations pouvant entraîner des modifications du flux calcique et l'activation de JNK et de p38. Cette voie peut être impliquée dans la mobilité et la survie cellulaire.

L'expression de l'isoforme TrkA-III a pour conséquence l'activation constitutive de l'activité tyrosine kinase et de la voie PI3K/Akt, mais pas de celle de Ras/MAPK. Ainsi,

l'isoforme TrkA-III antagonise l'arrêt de la croissance et la différenciation cellulaire provoqués par le couple NGF/TrkA (Tacconelli et al. 2004).

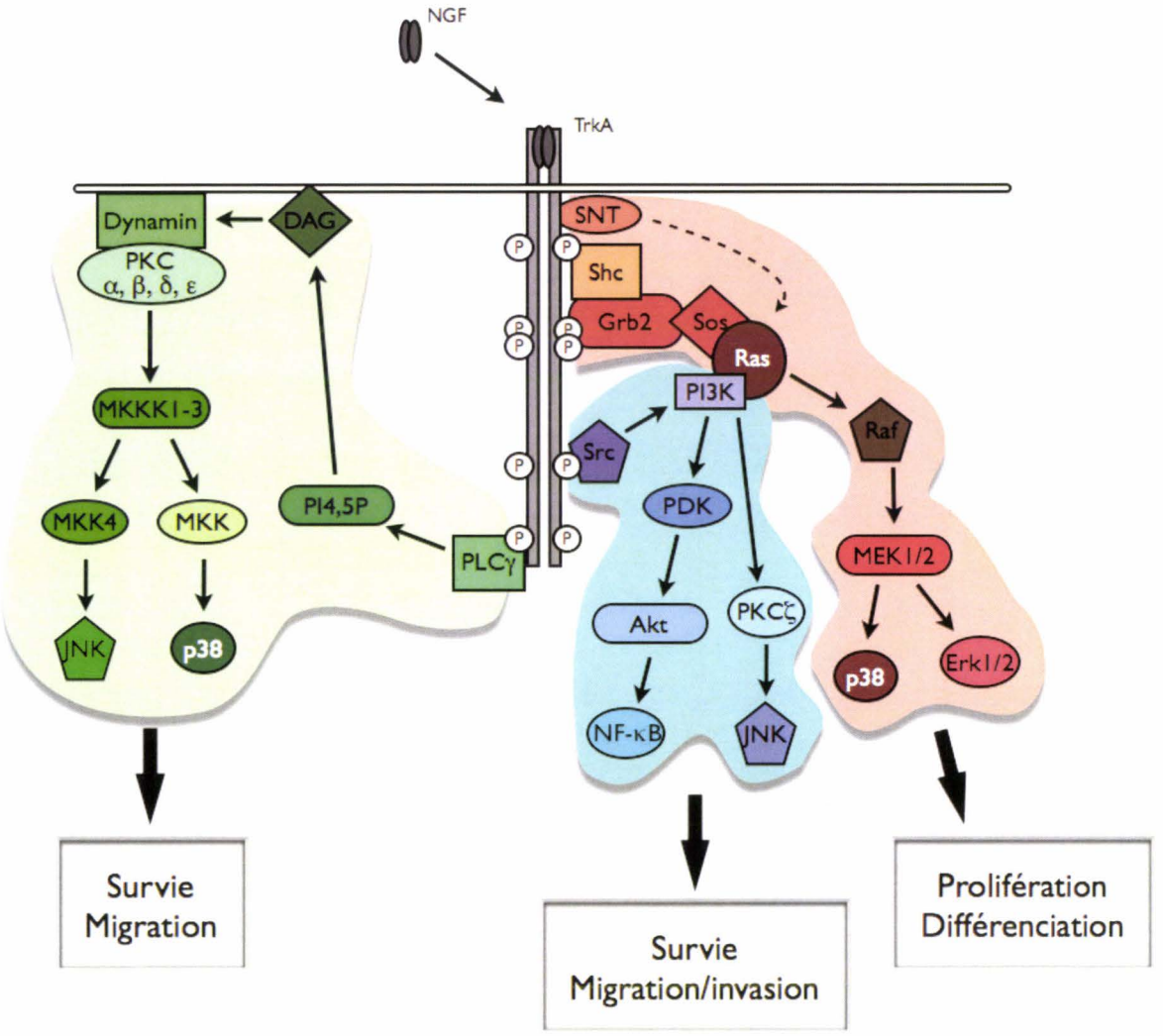

Figure 16 : *Schéma de la signalisation de TrkA.* Après fixation du NGF, TrkA se dimérise, s'ensuit alors une trans-phosphorylation des tyrosines 490, 674/675, 751 et 785. Ces phosphorylations permettent le recrutement d'adaptateurs et l'activation des voies PI3K/Akt et Ras/MAPK/ERK et PLCγ (d'après (Dolle et al. 2003; Schramm et al. 2005; Micera et al. 2007). PKC : Protein Kinase C ; MKKK1-3 : Mitogen-activated protein Kinase Kinase Kinase 1-3 ; MKK (4) : MAP Kinase Kinase (4) ; JNK : c-jun N-terminal Kinase; p38 : p38 MAP kinase ; Erk1/2 : Extracellular signal-regulated kinase 1/2 ; DAG : Diacylglycerol ; PI4,5P : Phosphatidyl 4,5 Phosphate ; PLCγ : Phospholipase C γ ; PDK : 3-phosphoinositide-dependent protein kinase ; SNT : suc-associated neurotriphic phosphotyrosine ; Src : ; Shc : SH2 domain protein C ; Grb2 : Growth factor receptor binding protein 2 ; Sos : Son of sevenless ; NF-κB : Nuclear Factor κB ; Ras : Ras GTPase activating protein ; Raf : Raf proto-oncogene serine/threonine-protein kinase.

II. C. 3. Interaction entre TrkA et p75^{NTR}

Il semble que TrkA et p75^{NTR} puissent jouer un rôle de manière totalement indépendante l'un de l'autre. Cependant, des études dans différents types cellulaires montrent une interaction entre ces deux récepteurs. Ainsi, Rabizadeh et Bredesen ont proposé une théorie intéressante faisant intervenir le rapport entre TrkA et p75^{NTR}, ainsi que les concentrations du NGF et des autres neurotrophines dans les cellules de neuroblastomes (Rabizadeh and Bredesen 2003). En particulier, le NGF provoque une survie accrue des cellules qui expriment à la fois TrkA et p75^{NTR} par rapport aux cellules n'exprimant qu'un seul type de récepteur. Plusieurs modèles de coopération entre TrkA et p75^{NTR} ont été proposés. En effet, Epa et ses collaborateurs (2004) ont montré que l'association entre les deux récepteurs via Shc augmente l'activité de la voie MAPK/ERK, conduisant ainsi à une différenciation des cellules PC12 (Diolaiti et al. 2007). D'autre part, Wehrman et ses collaborateurs (Wehrman et al. 2007) ont proposé la formation d'un complexe p75NTR/NGF/TrkA 1 :2 :1 qu'ils considèrent comme possible du fait de la polarité inverse de la fixation du NGF entre p75^{NTR} et TrkA (Figure 17).

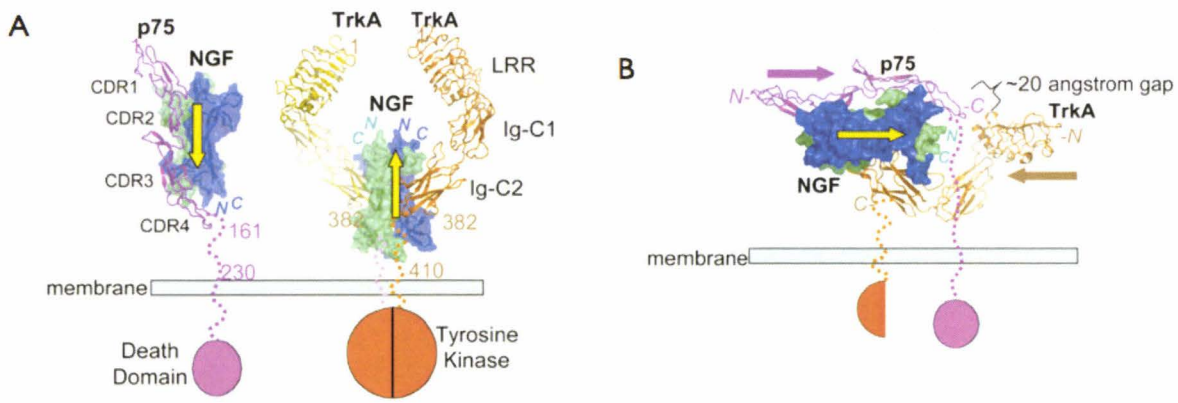

Figure 17 : *Schéma de la structure tridimensionnelle des complexes faisant intervenir TrkA, p75^{NTR} et NGF.* A, complexes p75^{NTR}/NGF et TrkA/NGF. B, complexe p75^{NTR}/NGF/TrkA. La flèche jaune représente la polarité du NGF dans les complexes (Wehrman et al. 2007).

II. C. 4. Protéines de fusion impliquant TrkA et leur pouvoir oncogénique

TrkA a été pour la première fois décrit comme protéine de fusion en association avec la tropomyosine (TRK) dans les cancers colorectaux, cette protéine de fusion a été par la suite retrouvée dans les carcinomes thyroïdiens papillaires. Depuis, d'autres protéines de fusion ont été découvertes (Pierotti and Greco 2006). Ainsi, dans les tumeurs thyroïdiennes papillaires, on peut en trouver 4 protéines faisant intervenir au moins le domaine tyrosine-kinase de TrkA (Figure 18):

- TRK : fusion avec une partie de la tropomyosine TPM3 (1q22-23),
- TRK-T1 : fusion avec une courte séquence de la nucléoporine TPR (1q25),
- TRK-T2 : fusion avec une longue séquence de la nucléoporine TPR (1q25),
- TRK-T3 : fusion avec la protéine TFG (TRK-Fused Gene protein) (3q11-12).

Il est à remarquer que ces protéines, avec lesquelles TrkA peut fusionner, ont également été trouvées fusionnées avec d'autres protéines kinases comme ALK (Anaplasic Lymphoma Kinase), NORI (Neuron-derived Orphan Receptor 1) et HGFR (Hepatocyte Growth Factor Receptor) dans des chondrosarcomes ou des lymphomes (Pierotti and Greco 2006).

Les protéines de fusion se dimérisent spontanément via les domaines SH2 présents dans les protéines TPM3, TPR et TFG, conduisant à l'activation constitutive des voies MAPK et PI3K/Akt. Ces protéines sont de ce fait considérées comme des protéines oncogéniques.

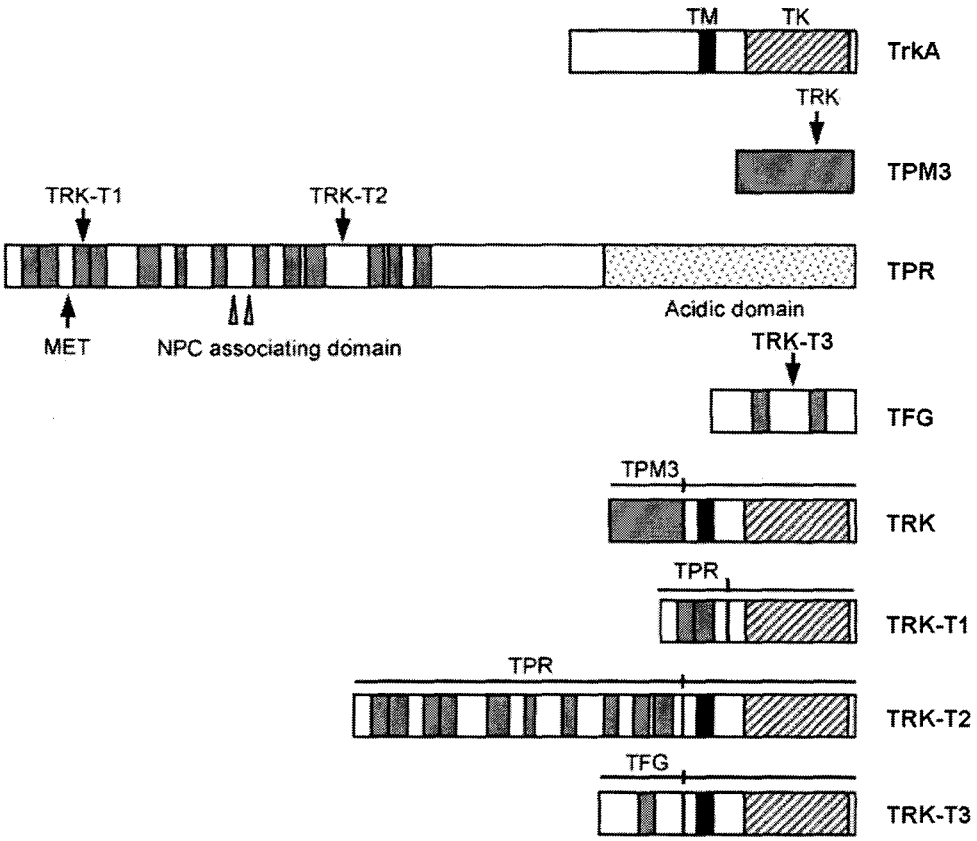

Figure 18 : *Schémas des protéines de fusion faisant intervenir TrkA.* TPM3 : tropomyosine ; TPR : Nucleoporin ; TFG : TRK-Fused Gene protein ; NPC : Nuclear Pore Complexe . TM, transmembrane domain; TK, tyrosine kinase domain (d'après Pierotti and Greco 2006).

II. D. Rôle du NGF et de TrkA dans les tumeurs

Le rôle du NGF dans le développement et la maturation du système nerveux central et périphérique est aujourd'hui bien établi. Il est impliqué dans le contrôle de la prolifération, de la différenciation et de l'apoptose des cellules nerveuses. Cependant, de plus en plus de données montrent que le NGF est également impliqué dans le développement normal et tumoral de tissus non neuronaux. Dans ce chapitre, nous nous efforcerons de résumer les connaissances actuelles sur le rôle de l'axe NGF/TrkA dans les différentes tumeurs. Ce facteur de croissance peut, en effet, exercer une action anti- ou pro-tumorale en fonction de l'origine tissulaire de la tumeur.

II. D. 1. Dans les neuroblastomes

Les neuroblastomes sont des tumeurs solides communes chez l'enfant. Ils prennent leurs origines dans les cellules progénitrices sympathoadrenales dans les crêtes nerveuses. Dans ces tumeurs, la surexpression de TrkA est correlée à un bon pronostic (Kogner et al. 1993; Eggert et al. 2000). En effet, la stimulation par le NGF des cellules de neuroblastomes induit leur différenciation *via* l'activation de TrkA. De plus, la surexpression de TrkA dans les cellules de neuroblastomes réduit l'angiogenèse tumorale dans des modèles de xénogreffes (Eggert et al. 2002). Plus récemment, Tacconelli et ses collaborateurs ont montré l'expression d'une isoforme particulière de TrkA (isoforme TrkA-III) associée à une diminution d'expression des TrkA-I et TrkA-II lors de la progression tumorale (Tacconelli et al. 2004). Cette isoforme est capable de s'autoactiver et d'antagoniser, de manière NGF indépendante, la signalisation de TrkA-I et –II. Ainsi TrkA-III active la voie PI3K/Akt/NF-κB et augmente la survie des cellules. De plus, TrkA-III augmente la tumorogenèse et l'angiogenenèse dans un modèle de xénogreffes.

Dans les neuroblastomes, l'axe NGF/TrkA peut jouer un rôle dual en fonction du stade de la progression tumorale : au stade précoce, cet axe exerce un effet anti-tumoral ; à un stade plus avancé, l'expression préférentielle de l'isoforme TrkA-III augmente l'agressivité tumorale.

II. D. 2. Dans les carcinomes thyroïdiens

TrkA est exprimé dans les tissus thyroïdiens hyperplasiques et dans les carcinomes médullaires thyroïdiens, alors qu'il n'est pas exprimé dans les tissus normaux (McGregor et al. 1999). De plus, le NGF stimule la prolifération des cellules de carcinomes médullaires thyroïdiens et la sécrétion de Calcitonine, une hormone utilisée comme marqueur pour ces carcinomes (Goretzki et al. 1987). D'autre part, comme nous l'avons vu précédemment (Chapitre II.C.4), les carcinomes papillaires (80% des carcinomes thyroïdiens) expriment fréquemment des protéines de fusion impliquant TrkA. Ces protéines de fusion possèdent un pouvoir oncogénique du fait de l'activation constitutive

du domaine tyrosine kinase de TrkA. Ainsi, TrkA joue un rôle pro-tumoral dans les carcinomes thyroïdiens.

II. D. 3. Dans les cancers pulmonaires

Les carcinomes pulmonaires peuvent se différencier en 2 groupes principaux : les cancers à petites cellules (SCLC, Small Cells Lung Cancer) et les cancers non à petites cellules (non-SCLC). Selon le type de cancer, le NGF et TrkA ne vont pas avoir la même influence sur leur développement.

II. D. 3. a) Cancers pulmonaires à petites cellules (SCLC)

Les SCLC représentent 20% des cancers pulmonaires et sont issus de cellules neuroendocrines pulmonaires. Ils sont très agressifs et se disséminent dès les stades précoces du développement tumoral. Les cellules cancéreuses des SCLC expriment le récepteur TrkA (Missale et al. 1998). Un traitement par le NGF inhibe la prolifération, la croissance sans ancrage et la migration cellulaire. De plus, des études de xénogreffes ont montré que l'injection de NGF inhibe la formation et la croissance tumorales (Missale et al. 1998). Cependant, ces données restent encore fragmentaires, des études complémentaires sont nécessaires pour comprendre le rôle physiopathologique de l'axe NGF/TrkA dans ce type de cancer.

II. D. 3. b) Cancers pulmonaires non à petites cellules (non-SCLC)

Les non-SCLC regroupent principalement les carcinomes épidermoïdes (50%), les adénocarcinomes (30%) et les carcinomes bronchiolo-alvéolaires. Ces tumeurs peuvent exprimer soit le NGF soit TrkA (Koizumi et al. 1998; Ricci et al. 2001; Ricci et al. 2005). Dans un tiers des cancers bronchiolo-alvéolaires, on retrouve une co-expression du NGF et de TrkA (Hoyle 2003). Dans des lignées issues de tumeurs non-SCLC, le NGF stimule la croissance des cellules en agar mou (Oelmann et al. 1995). De plus, l'inhibition de TrkA

par K252a induit l'apoptose des cellules A549 issues d'adénocarcinomes pulmonaires (Perez-Pinera et al. 2007). Ainsi, l'axe NGF/TrkA pourrait favoriser le développement des tumeurs non-SCLC, contrairement aux tumeurs SCLC.

II. D. 4. Dans les carcinomes pancréatiques

Les cellules pancréatiques normales expriment les neurotrophines ainsi que leurs récepteurs Trk respectifs (Friess et al. 1999; Zhu et al. 1999). Sur les cellules normales, le NGF a un effet anti-apoptotique *via* TrkA (Navarro-Tableros et al. 2004). Cet effet de survie pourrait impliquer également l'insuline, car un traitement des cellules pancréatiques par le NGF provoque une augmentation de la sécrétion d'insuline qui joue un rôle anti-apoptotique sur les îlets (Miao et al. 2005; Miao et al. 2006). NGF et TrkA sont surexprimés dans les adénocarcinomes ductales pancréatiques, mais aucune corrélation n'est observée entre leurs niveaux d'expression et les stades/grades histopathologiques des carcinomes (Zhu et al. 1999; Schneider et al. 2001; Miknyoczki et al. 2002). L'axe NGF/TrkA stimule la croissance (Sakamoto et al. 2001; Zhu et al. 2001) et la migration des cellules pancréatiques cancéreuses *in vitro*. De plus, les cellules pancréatiques surexprimant le NGF sont plus tumorigènes chez les souris *nude* (Zhu et al. 2002). Enfin, l'axe NGF/TrkA augmente l'innervation tumorale et la douleur du patient (Zhu et al. 1999). Ces données montrent clairement l'implication du NGF et de son récepteur TrkA dans le développement des carcinomes pancréatiques.

II. D. 5. Dans les carcinomes prostatiques

TrkA n'est pas exprimé dans les cellules prostatiques normales, son expression est augmentée au cours de la progression tumorale prostatique. Inversement, $p75^{NTR}$ est exprimé dans les cellules prostatiques normales et son expression diminue lors de la progression tumorale (Papatsoris et al. 2007). L'activation de TrkA par NGF stimule la survie, la prolifération et la migration des cellules prostatiques cancéreuses (Weeraratna et al. 2000; Festuccia et al. 2007). L'inhibition de l'axe NGF/TrkA dans des modèles de

xénogreffes de souris réduit la croissance tumorale (Miknyoczki et al. 2002). L'expression ectopique de $p75^{NTR}$ dans les cellules cancéreuses induit un arrêt du cycle cellulaire (Khwaja et al. 2006). Ainsi, le NGF favorise le développement tumoral via TrkA, alors qu'il peut agir en tant que suppresseur de tumeur via $p75^{NTR}$ (Figure 19) (Krygier and Djakiew 2001; Krygier and Djakiew 2002).

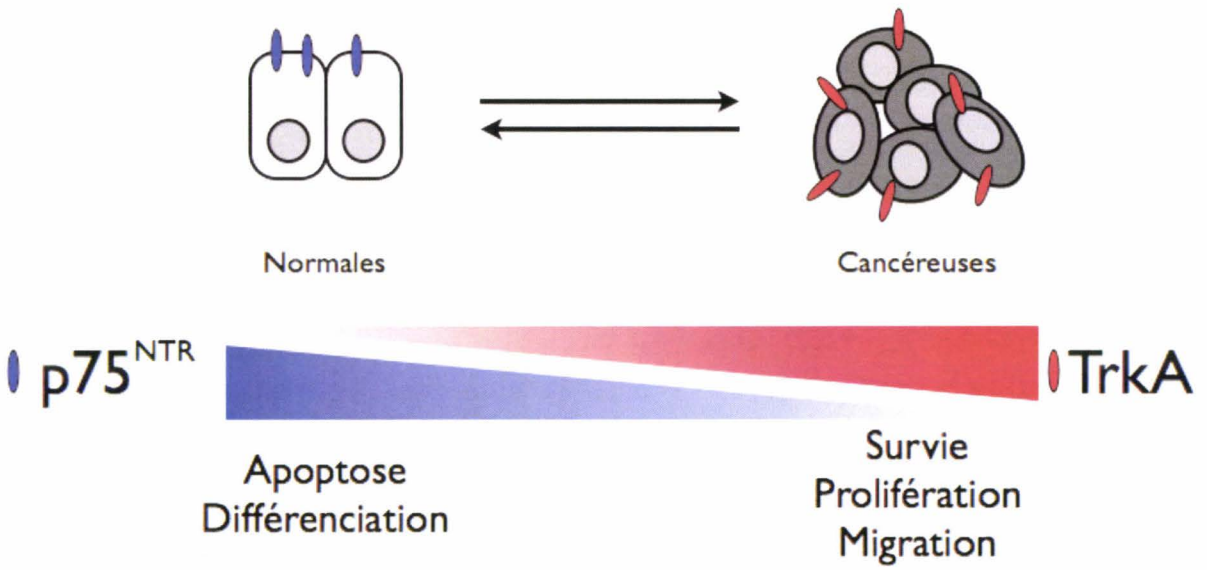

Figure 19 : Expression et rôle de TrkA et de p75NTR dans les cellules prostatiques.

II. D. 6. Dans les carcinomes ovariens

Les cellules ovariennes normales expriment le NGF et ses récepteurs (Campos et al. 2007). Le NGF participe au développement de l'ovaire en stimulant l'expression du récepteur à la FSH (FSHR) et la sécrétion d'œstrogènes ainsi qu'en réduisant l'expression de la progestérone (Dissen et al. 2001; Romero et al. 2002; Salas et al. 2006). De manière intéressante, des études ont montré que l'expression de FSHR au niveau des cellules de l'épithélium de surface des ovaires peut induire la néoplasie. Le NGF peut alors participer à la tumorigenèse ovarienne *via* son effet sur l'expression de FSHR (Bose 2005). Dans les carcinomes ovariens, Davidson et ses collaborateurs ont montré que le niveau d'expression de phospho-TrkA est correlé à un mauvais pronostic. De plus, la co-expression du NGF, de phospho-TrkA et de molécules angiogéniques dans les cellules endothéliales des carcinomes ovariens suggère un rôle de l'axe NGF/TrkA dans

l'angiogenèse tumorale (Davidson et al. 2003; Odegaard et al. 2007). De manière intéressante, le NGF ne semble pas avoir d'effet sur la croissance de cellules ovariennes normales (Salas et al. 2006). Ainsi, non seulement le NGF joue un rôle dans la progression tumorale en stimulant l'angiogenèse, mais il pourrait dans certains cas participer à la carcinogenèse.

II. D. 7. Dans les carcinomes mammaires

Les cellules normales de sein expriment TrkA (Descamps et al. 2001), mais pas NGF (Dolle et al. 2003). Le NGF exogène n'a aucun effet sur la croissance des cellules normales (Descamps et al. 1998). De manière intéressante, dans les cancers du sein, l'expression de NGF semble associée à un mauvais pronostic (Davidson et al. 2004). D'autre part, la forme active de TrkA (phospho-TrkA) est retrouvée très fréquemment dans les effusions (93%) et les récurrences locorégionales (92%), alors qu'elle est retrouvée de manière moins fréquente dans les tumeurs primaires (41%). Il semble donc que l'activation de TrkA soit associée à un caractère tumoral plus agressif. Nous avons montré au laboratoire que les cellules mammaires cancéreuses sécrètent du NGF qui à son tour stimule la survie, la prolifération et la migration *via* une boucle autocrine (Descamps et al. 2001; Dolle et al. 2005). L'inhibition du NGF (Anticorps neutralisant, siRNA) et de TrkA (K252a) induit une forte réduction de la croissance tumorale dans des modèles de xénogreffes (Adrieanssens et al. 2008).

En résumé, l'axe NGF/TrkA favorise le développement de tumeurs d'origine tissulaire différente, à l'exception des tumeurs d'origine neurale (neuroblastomes et cancers pulmonaires à petites cellules). Cependant, l'effet pro-tumoral de l'axe NGF/TrkA peut être influencé par $p75^{NTR}$. Ainsi, $p75^{NTR}$ contre-balance l'effet de NGF/TrkA dans les tumeurs pancréatiques et prostatiques, alors qu'il renforcerait cette axe NGF/TrkA dans les carcinomes thyroïdiens et mammaires.

RESULTATS

I. TrkA prévient l'apoptose via son interaction avec Ku70 dans les cellules de cancer du sein MCF-7 (Article 1).

Publié dans Molecular and Cellulare Proteomics 2007

Le premier chapitre de cette partie « résultats » est présenté d'un article publié dans Molecular and Cellular Proteomics. Dans cette article, nous avons identifié la protéine Ku70 comme partenaire de TrkA spécifique aux cellules cancéreuses de sein. Dans nos conditions, Ku70 semble essentiel à l'induction de la survie des cellules cancéreuses mammaires par l'axe NGF/TrkA.

MCP Papers in Press. Published on July 7, 2007 as Manuscript M700119-MCP200

Nerve Growth Factor Receptor TrkA Signaling in Breast Cancer Cells Involves Ku70 to Prevent Apoptosis

Emmanuelle Com[1], Chann Lagadec[1], Adeline Page[2], Ikram El Yazidi-Belkoura[1], Christian Slomianny[3], Ambre Spencer[4], Djilali Hammache[4], Brian B. Rudkin[4] & Hubert Hondermarck[1*]

[1] INSERM ERI-8 (JE-2488), "Growth factor signaling in breast cancer. Functional proteomics", [2] Mass spectrometry facility, [3] INSERM U800, IFR 147, University of Sciences and Technologies Lille, 59655 Villeneuve d'Ascq, France. [4] Differentiation and Cell Cycle Group, Laboratory for Molecular Biology of the Cell, CNRS/INRA U1237/ENS Lyon, IFR 128, Ecole Normale Supérieure de Lyon, France.

* Correspondence: Hubert Hondermarck, INSERM ERI-8 (JE-2488), "Growth factor signaling in breast cancer. Functional proteomics", University of Sciences and Technologies Lille, 59655 Villeneuve d'Ascq, France. Tel: +33(0)3 20 43 40 97, Fax: +33(0)3 20 43 40 38, hubert.hondermarck@univ-lille1.fr

Running title: TrkA signaling involves Ku70.

Key words: Nerve growth factor / Trk tyrosine kinase receptors / Signaling / Cell survival / Breast cancer.

ABBREVIATIONS

EGF: epidermal growth factor; ERK: extracellular signal-regulated kinase; FGF: fibroblast growth factor; GFP: green fluorescent protein; NGF: nerve growth factor; PDGF: platelet-derived growth factor; PI3K: phosphatidylinositol-3-OH kinase; pY: phosphotyrosine; siRNA: small-interfering RNA; TRAIL: TNF-related apoptosis inducing ligand; VCP: valosin-containing protein.

SUMMARY

The nerve growth factor (NGF) - tyrosine kinase receptor TrkA plays a critical role in various neuronal and non-neuronal cell types by regulating cell survival, differentiation and proliferation. In breast cancer cells, TrkA stimulation results in the activation of cellular growth but downstream signaling largely remains to be described. Here we used a proteomics-based approach to identify partners involved in TrkA signaling in breast cancer cells. Wild type and modified TrkA chimeric constructs with green fluorescent protein were transfected in MCF-7 cells and co-immunoprecipitated proteins were separated by SDS-PAGE before NanoLC-MS/MS analysis. Several TrkA putative signaling partners were identified, among which the DNA repair protein Ku70 which is increasingly reported for its role in cell survival and carcinogenesis. Physiological interaction of Ku70 with endogenous TrkA was induced upon NGF stimulation in non-transfected cells and co-localization was observed with confocal microscopy. Mass spectrometry analysis and western-blotting of phosphotyrosine immunoprecipitates demonstrated the induction of Ku70 tyrosine phosphorylation upon NGF stimulation. Interestingly, no interaction between TrkA and Ku70 was detected in PC12 cells, in the absence or presence of NGF, suggesting that it is not involved in the initiation of neuronal differentiation. In breast cancer cells, RNA interference indicated that whereas Ku70 depletion had no direct effect on cell survival, it induced a strong potentiation of apoptosis in TrkA overexpressing cells. In conclusion, TrkA signaling appears to be pro-apoptotic in the absence of Ku70 and this protein might therefore play a role in the long-time reported ambivalence of tyrosine kinase receptors that can exhibit both anti- and eventually pro-apoptotic activities.

INTRODUCTION

Nerve growth factor (NGF) is the prototypic member of the neurotrophin family of proteins that is mainly described for promoting survival and differentiation of neuronal cells during nervous system development (1). NGF neurotrophic activities are mediated through two membrane receptors, the tyrosine kinase receptor TrkA and the receptor $p75^{NTR}$, a member of the tumor necrosis factor (TNF) receptor superfamily. NGF binding to its receptors leads to a variety of intracellular signaling events in neuronal cells (2), starting with dimerization and activation of the tyrosine kinase activity of TrkA and its subsequent transphosphorylation which creates docking sites for adaptor proteins leading to the activation of intracellular signaling cascades. Among described signaling cascades are the Ras/extracellular signal regulated kinase (ERK)/ mitogen activated protein kinase (MAP-kinase), the phosphatidylinositol-3-OH kinase (PI3K)/Akt kinase and the phospholipase C-γ1 (PLC-γ1) pathways.

Aside from neurotrophism, other NGF activities were described in non neuronal cell types and the involvement of this growth factor in oncogenesis of neuronal and non neuronal origin has been documented. This is particularly the case in brain, ovarian, prostatic, pancreatic, lung and breast cancer in which NGF production has been reported and eventually impacts tumor cell growth (2-7). In breast cancer, NGF is overexpressed and acts as a paracrine/autocrine factor to enhance tumor cell growth and survival (8-10). TrkA and $p75^{NTR}$ are expressed in the majority of breast tumors and are related to prognosis of breast tumors (11-13). Interestingly, TrkA cooperates with the membrane tyrosine kinase p185 (HER2) to activate the proliferation of breast cancer cells (14) and the suppression of TrkA activity by endocannabinoids results in the inhibition of breast cancer cell growth (15). Importantly, the reference drug used in hormonotherapy of breast cancer, Tamoxifen, inhibits the proliferative effect of NGF in breast cancer (16), indicating that targeting NGF signaling in breast cancer is of potential interest for the development of future therapeutic approaches.

To date, TrkA signaling has not been extensively described in breast cancer cells. It is known that TrkA activation leads to a stimulation of cell proliferation that is mediated by the MAP-kinase pathway (9, 16) and a better knowledge of the signaling molecules involved would be important to a better understanding of mammary oncogenesis and the identification of new molecular targets. In the present work, we have used a proteomic strategy to decipher TrkA signaling pathway in MCF-7 breast cancer cells. TrkA-green fluorescent protein (GFP) constructs were used to co-immunoprecipitate proteins that interact with TrkA and these proteins were separated by SDS-PAGE before analysis with nanoLC-MS/MS. 13 TrkA putative interacting partners were identified among which the Ku70 protein initially described as a regulatory subunit of the DNA-dependent protein kinase (DNA-PK) that is crucial to DNA repair. Ku70 is important for the control of cell survival, particularly in proliferating cells in which DNA synthesis must be accompanied by efficient DNA repair, and the implication of Ku70 in oncogenesis is increasingly reported (17). In the present study, the involvement of Ku70 in TrkA signaling pathway was revealed and our results suggest its implication in the control of TrkA activity and survival of breast cancer cells.

EXPERIMENTAL PROCEDURES

Materials. Cell culture reagents were purchased from Bio-Whittaker. Rat tail type I collagen was obtained from Upstate. Recombinant NGF was from R&D systems. Nucleobond plasmid, DNA purification kit was purchased from Machery-Nagel. Nucleofection reagents were from Amaxa Biosystems. Dynabeads protein A and protein G were obtained from Dynal Biotech. Electrophoresis reagents, bicinchoninic acid reagents, protease inhibitor cocktail and rabbit polyclonal anti-actin antibody were from Sigma. Sequencing grade-modified trypsin was provided by Promega. ZipTip$_{C18}$ pipette tips were obtained from Millipore. The rabbit polyclonal anti-GFP antibody (BD Living colors^{TM} Full-Lengh) and the mouse monoclonal anti-Ku70 IgG1 (clone 15) were purchased from BD Biosciences. The mouse

monoclonal anti-GFP (B-2) and anti-phosphotyrosine residues (PY99) antibodies were from Santa Cruz Biotechnology, Inc. The rabbit polyclonal anti-TrkA IgG was from Upstate and the rabbit polyclonal anti-Ku70 antisera (AHP316) was from Serotec. Peroxidase-conjugated donkey anti-rabbit IgG and goat anti-mouse IgG were purchased from Jackson Immunoresearch Laboratories, Inc. SuperSignal West Pico Chemiluminescent Substrate was from Pierce. Lab-Tek chamber slides were obtained from Nalge Nunc International. Alexa Fluor dyes-conjugated secondary antibodies were from Invitrogen. SiRNA were purchased from Eurogentec.

Cell Culture and NGF stimulation. The MCF-7 human breast cancer cell line and the PC12 rat adrenal pheochromocytoma cell line were purchased from the American Type Culture Collection. MCF-7 cells were routinely maintained in MEM Eagle-Earle's BSS supplemented with 2 mM L-glutamine, 1% non-essential amino acids, 10% fetal calf serum, 40 U/ml penicillin-streptomycin, 40 µg/ml gentamycin and 10 µg/ml insulin. PC12 cells were routinely grown in DMEM containing 2 mM L-glutamine, 10% fetal calf serum, 5% horse serum and 20 U/ml penicillin-streptomycin. All cells were cultured at 37°C in a humidified atmosphere of 5% CO_2. NGF stimulation of MCF-7 and PC12 cells was performed after 16 h serum-starvation by addition of 200 ng/ml NGF for 10 min.

Plasmid and siRNA transfection. TrkA-GFP chimeras were constructed as previously described (18). Plasmid DNA purification was carried out using Nucleobond kit according to manufacturer's instructions. MCF-7 cells were transiently transfected using the Nucleofection technology according to Amaxa Biosystems protocol. Briefly, $2x10^6$ cells were resuspended in 100 µl of Cell Line Nucleofector™ Solution V and cell suspension was mixed with 2 µg of TrkA-GFP vector. The sample was transferred into an electroporation cuvette and transfection was performed using the program E-14 according to manufacturer's instructions.

Immediately after nucleofection, cells were transferred into prewarmed complete maintenance medium and were cultured as described before.

SiRNA against Ku70 (sense 5'-GAUGCCCUUUACUGAAAAA-3' and antisense 5'-UUUUUCAGUAAAGGGCAU-3') were those defined and previously tested by Ayene, 2005 (19). MCF-7 cells were transiently nucleofected with 3 µg of siRNA directed against Ku70 as described above.

Determination of apoptotic cells. 24 h after transfection, cells were deprived in a serum-free media for 12 h, stimulated with 200 ng/ml of NGF during 1 h and treated with 200 ng/ml of NGF and 5 ng/ml of TNF-related apoptosis inducing ligand (TRAIL) for 6 h. Apoptosis was determined by morphological analysis after fixation with methanol (10 min, -20°C) and staining with 1 µg/ml Hoechst 33258 (10 min, room temperature, in dark). A minimum of 500-1000 cells was examined for each case under fluorescent microscope and the results represented the number of apoptotic cells over the total number of counted cells.

Protein extraction, immunoprecipitation and SDS-PAGE. Cells were harvested by scraping in lysis buffer (50 mM Tris-HCl pH 7.5, 150 mM NaCl, 1% NP40, 1 mM sodium orthovanadate and protease inhibitor cocktail). After centrifugation (10,000g, 3 min, 4°C), the supernatant proteins were quantified using the bicinchoninic acid method. TrkA-GFP and interacting proteins were co-immunoprecipitated from 5 mg of proteins using 25 µg of anti-GFP antibody (BD Living colors™ Full-Length) and Dynabeads protein A according to manufacturer's instructions. For the immunoprecipitation of phosphorylated proteins, 5 mg (for MS identification) or 1 mg (for immunoblot detection) of proteins were used with 25 µg or 5 µg respectively, of anti-phosphotyrosine antibody (PY99) and Dynabeads protein G. The endogenous TrkA immunoprecipitation was performed from 1 mg of proteins using 5 µg of anti-TrkA and Dynabeads protein A. Immunoprecipitated proteins were eluted in Laemmli

buffer (62.5 mM Tris-HCl pH 6.8, 2% SDS, 10% glycerol, 5% 2-mercaptoethanol and 0.002% bromophenol blue) and boiled 5 min before analysis on 10% polyacrylamide gels. For colloidal Coomassie staining (20), SDS-polyacrylamide gels were fixed overnight in solution containing 50% ethanol and 1.4% orthophosphoric acid. After 3 washes for 30 min in MilliQ water, gels were incubated in impregnation solution (1.3 M ammonium sulfate, 34% methanol, 1.4% orthophosphoric acid) for 1 h and placed in staining solution (1.3 M ammonium sulfate, 34% methanol, 1.4% orthophosphoric acid, 0.07% Coomassie Brillant Blue G250) for 24 h. Finally gels were destained with several washes of MilliQ water until the backgroung was clear.

In gel trypsin digestion. Coomassie blue-stained protein bands were excised from SDS-PAGE gel and processed for trypsin digestion as previously described (21) with minor modifications. In brief, gel bands were destained twice for 10 min in solution containing 100 mM NH_4HCO_3 and 50% acetonitrile, dehydrated in acetonitrile and dried in a vacuum centrifuge. Gel pieces were then rehydrated at 4°C for 45 min in a digestion buffer (50 mM NH_4HCO_3, 12.5 ng/µl trypsin). The supernatant was replaced by 40 µl of 50 mM NH_4HCO_3 and the samples were incubated overnight at 37°C. The tryptic peptides were recovered by 10 min incubations, once in 25 mM NH_4HCO_3, 50% acetonitrile and twice in 25 mM NH_4HCO_3, 50% acetonitrile, 5% formic acid. All supernatants were pooled and dried in a vacuum centrifuge.

Protein identification by mass spectrometry. For MALDI-TOF analyses, tryptic digests were resuspended in 1% formic acid and were desalted and concentrated using $ZipTip_{C18}$ pipette tips according to manufacturer's instructions. Peptides were spotted on MALDI target with 10 mg/ml DHB in 50% acetonitrile using the dried droplet method. MALDI-TOF mass spectra were acquired using Voyager DE STR instrument (Applied Biosystems) in reflector positive ion mode. For mass fingerprint analysis, each raw spectrum was opened in Voyager

Data Explorer software (version 4.6), treated using advanced baseline correction and noise removal 2 functions. It was calibrated with two peptides resulting of trypsin autolysis (m/z 842.5100 and 2211.1046). Filter peak list for monoisotopic masses only was enabled, the peak detection threshold was manually adjusted over the background and then peaks list was copied to Mascot public interface (version 2.1) and searched against Swissprot database 51.3 (250293 sequences, 91444238 residues) using following parameters: trypsin as enzyme, 2 possible missed cleavages, oxydated methionine as variable modification, MH+ monoisotopic masses and peptides tolerance of 70 ppm. Results were scored using Probability Based Mowse Score (protein score is -10*Log(P), where P is the probability that the observed match is a random event. Protein scores greater than 66 are significant ($p<0.05$)). NanoLC-NanoESI-MS/MS analyses were performed on an ion trap mass spectrometer (LCQ Deca XP^+, Thermo-electron) equipped with a nano-electrospray ion source coupled with a nano high-pressure liquid chromatography system (LC Packings Dionex). Tryptic digests were resuspended in 4 µl of 0.1% HCOOH and 1.4 µl were injected into the mass spectrometer using the Famos auto-sampler (LC Packings Dionex). It was first desalted and then concentrated on a reverse phase precolumn of 5 mm x 0.3 mm i.d. (Dionex) by a solvent A (H_2O/Acetonitrile-95/5-0.1% HCOOH) delivered by the Switchos pumping device (LC Packings, Dionex) at a flow rate of 10 µl/min for 3 min. Peptides were separated on a 15 cm x 75 µm i.d., 3 µm, C18 Pepmap column from Dionex. The flow rate was set at 200 nl/min. Peptides were eluted using a 5 to 70% linear gradient of solvent B in 45 min (H_2O/Acetonitrile-20/80-0.08% HCOOH). Coated nanoelectrospray needles (360 µm o.d., 20 µm i.d., 10 µm tip i.d., standard coating) were obtained from New Objective (Woburn). Spray voltage was set at 1.5 kV, and capillary temperature at 170°C. The mass spectrometer was operated in positive ionization mode. Data acquisition was performed in a data-dependent mode consisting of alternatively in a single run, a full scan MS over the range m/z 500-2000 and a full scan MS/MS of the ion selected in an exclusion dynamic mode (the most intense ion is selected and excluded for further selection for a duration of 3

min). MS/MS data were acquired using a 2 m/z units ion isolation window and a 35% relative collision energy. MS/MS .raw data files were transformed in .dta files with Bioworks 3.1 software (Thermo-electron). The .dta files generated were next merged with merge.bat Software to be downloaded in MASCOT software (version 2.1) for database searches in SwissProt 51.3 (250293 sequences, 91444238 residues). Search parameters were the following: *Homo sapiens* for taxonomy, one allowed missed cleavage, methionine oxidation as variable modification, 2 Da for peptide tolerance and 0.8 Da for MS/MS tolerance. Results were scored using Probability Based Mowse Score (Protein score is -10*Log(P), where P is the probability that the observed match is a random event. Protein scores greater than 66 are significant ($p<0.05$). To ascertain unambiguous identification, searches were performed in parallel with Phenyx software using the same parameters. It should be noted that protein can appear in databases under different names and accession number. In addition, as shared sequence may represent a problem, a minimum of 2 peptides with individual score of at least 40 were considered for identification and all sequences obtained by MS/MS analysis were checked using the BLAST public interface (version 2.2.13) to exclude that sequence sharing with other proteins could interfer with the reliability of the identification.

Western blot. After separation on SDS-PAGE, co-immunoprecipitated proteins were electro-transferred onto nitrocellulose membrane using a semi-dry transfer system (Trans-Blot SD cell, Bio Rad). Efficiency of transfer and relative equal loading was checked with Ponceau S staining. Non specific protein binding sites were saturated for 1 h at room temperature in TBS-0.1% Tween-20 reagent (TBST) containing either 5% nonfat dry milk for Ku70 immunodetection, 3% nonfat dry milk for TrkA immunodetection or 5% BSA for GFP and actin immunodetection. Membranes were then incubated overnight at 4°C with 1:5,000 anti-Ku70 (AHP316), 1:1,000 anti-Ku70 (clone 15), 1:500 anti-TrkA, 1:1000 anti-GFP (B-2) or 1:5000 anti-actin. After washes in TBST, peroxidase-conjugated anti-rabbit or anti-mouse IgG diluted in saturated solution was added for 1 h at room temperature and the membranes

were washed several times in TBST before detection of peroxidase activity using chemiluminescent system.

Immunocytochemistry and confocal microscopy. MCF-7 cells were seeded on Lab-tek chamber slide system precoated with 1% type I collagen. Cells were washed in PBS pH 7.5, fixed in 4% paraformaldehyde for 20 min and permeabilized in PBS pH 7.5 containing 0.05% saponine and 50 mM ammonium choride. Non specific protein binding sites were then blocked in PBS pH 7.5 containing 0.05% saponine and 2% BSA and cells were incubated in blocking solution containing 10 µg/ml rabbit anti-TrkA and 10 µg/ml mouse anti-Ku70 (clone 15) antibodies overnight at 4°C. After washes in PBS pH 7.5, 10 µg/ml Alexa Fluor 546 goat anti-rabbit IgG and 10 µg/ml Alexa Fluor 488 donkey anti-mouse IgG were added for 1h at 37°C. Cells were washed in PBS pH 7.5 and mounted in Mowiol®. Scanning fluorescence images were acquired using a Zeiss Axiophot microscope.

RESULTS

Identification of TrkA co-immunoprecipitated proteins. Human MCF-7 cells were transiently transfected with TrkA-GFP construct Δ0, corresponding to the full length TrkA or the Δ8 construct lacking functional intracellular domain of TrkA (Fig. 1A). The full length TrkA-GFP chimera was used in the first step of our experiments to increase the amount of TrkA and to have a bait to co-immunoprecipitate TrkA and its signaling protein complex. TrkA-GFP constructs were well characterized and the full-length chimera have the same biological properties as the endogenous TrkA, such as the tyrosine phosphorylation after NGF stimulation, receptor internalization and trafficking, the activation of MAPK and the differentiation of PC12 cells (18). Moreover we have used a TrkA-GFP construct with a

truncated intracellular domain of the receptor, lacking tyrosine kinase domain and tyrosine-based signaling motifs Y_{499}, $Y_{679;683;684}$ and Y_{794} so that it is unable to bind downstream signaling partners and to transduce NGF signaling (18). After NGF stimulation, cell lysates were subjected to GFP immunoprecipitation and eluates were resolved on SDS-PAGE and visualized with colloidal coomassie blue staining (Fig. 1B). Several differential bands were detected in the Δ0-transfected cells compared to those expressing Δ8, corresponding to proteins that may specifically be bound to the intracellular domain of TrkA. These bands were excised for identification via mass spectrometry.

MALDI-TOF and MS/MS allowed the identification of the two proteins derived from the TrkA-GFP constructs (Table 1). For Δ0 (TrkA-GFP full length), both peptide mass fingerprint and sequence information on the 1403.70 Da peptide are displayed in Fig. 2A. The analysis of the MALDI-TOF spectrum showed 21/35 experimental tryptic peptide masses that matched to theoretical masses from TrkA sequence and GFP sequence, leading to 18% sequence coverage with an average error mass of 33 ppm (Table 1) and a score of 167. This identification was consolidated by MS/MS sequence informations of the 1092.52, 1194.52, 1403.70 and 1517.77 Da peptides for TrkA and the 1049.51, 1346.65, 1476.76 and 1502.65 Da peptides for GFP. Similarly, Δ8 (TrkA-GFP truncated in the TrkA intracellular domain) was identified by peptide mass fingerprint and by sequence information on the 1517.77 Da peptide (Fig. 2B). 15/24 experimental tryptic peptides were matched for the identification by peptide mass fingerprint of TrkA-GFP, leading to 14% sequence coverage with an average error mass of 51 ppm (Table 1) and a score of 116. MS/MS sequence information on 2 peptides for TrkA (1403.7 Da and 1517.77 Da) and 4 peptides for GFP (1346.65 Da, 1476.76 Da, 1502.65 Da and 1541.78 Da) strengthened this identification.

For the identification of TrkA-GFP co-immunoprecipitated proteins, the nanoLC/nanoESI ion trap analyses of SDS-PAGE bands have led to the identification of 13 putative signaling partners from 53 peptide sequences. A large number of peptides have not been assigned to a protein based on our stringent criteria for identification, omitting proteins with low

probabilistic value. Thus, the proteins that we report here have been unambiguously identified (Table 2). The confidence of the identification was expressed by the Mascot score and the expected value of each peptide ($p<0.01$). The list of co-immunoprecipitated proteins includes GTPase activator (Ras GTPase-activating-like protein IQGAP1), heterogeneous nuclear ribonucleoprotein U, valosin-containing protein (ATPase), the elongation factor 2 (EF-2), the 78 kDa glucose-related protein (GRP78), the heat shock cognate 71 kDa protein, the DNA repair protein Ku70, the ATP-dependent RNA helicase DDX5, actin and interleukin enhancer binding factor-2, nucleophosmin, Proliferating cell nuclear antigen (PCNA) and fibrillarin. The known molecular function of each protein, according to the Human Protein Reference Database (http://hprd.org), is indicated (Table 2). Among the identified proteins, the DNA repair protein family Ku70 was intriguing. Ku70 is increasingly appearing as being involved in carcinogenesis and it has not been reported to interact with TrkA nor participate in its downstream signaling. DNA repair is required during cell proliferation, otherwise leading to cell death. Since NGF stimulates both proliferation and survival of breast cancer cells, the identification of Ku70 as a TrkA co-immunoprecipitated protein (i.e. putative signaling partner) was of particular interest and further experiments, described below, were designed to explore the involvement of Ku70 in TrkA signaling and cellular responses.

Ku70 interaction with TrkA is induced by NGF stimulation. In order to validate the interaction between endogenous TrkA and Ku70 in physiological conditions, we have first investigated the possible cellular co-localization of these two proteins in non-transfected breast cancer cells (Fig. 3A). In confocal microscopy, TrkA (red fluorescence) was mainly located in the cytoplasm and cytoplasmic membrane (arrow in lane TrkA) of MCF-7 cells, but also slightly observed in the nucleus (arrowhead in lane TrkA). This localization corresponded to what has previously been reported in other cell types (18) and, in addition, nuclear translocation of tyrosine kinase receptors is increasingly described (22). Concerning Ku70, green fluorescence was observed in the nucleus (arrowhead in lane Ku70) with a

weaker localization in the cytoplasm (arrow in lane Ku70). The overall co-localization of TrkA and Ku70 in both the cytoplasm and the nucleus of MCF-7 cells was reflected by the yellow-orange merge fluorescence (arrowhead and arrow in lane merge). In conclusion, the cellular localization of TrkA and Ku70 that we observed in confocal microscopy is compatible with an interaction of these two proteins. The interaction of TrkA and Ku70 was further studied after immunoprecipitation from nontransfected MCF-7 cells followed by a western blot immunodetection of Ku70 (Fig. 3B). The results validated Ku70 co-immunoprecipitation with TrkA and indicated that this was observed only upon cell stimulation with NGF, whereas it was not observed in control unstimulated cells. Therefore, the interaction between TrkA and Ku70 in breast cancer cells is induced by NGF stimulation. Interestingly, no interaction between TrkA and Ku70 was detected in the neuronal-like cells PC12 indicating a differential regulation between neuronal and non-neuronal cell types and a non involvement of Ku70 in TrkA signaling leading to cell differentiation.

Ku70 is tyrosine phosphorylated upon NGF stimulation. Tyrosine phosphorylation is the prime post-translational modification initiated by TrkA signaling. The immunoprecipitation of proteins phosphorylated on tyrosine in response to NGF stimulation in breast cancer cells was performed using phospho-tyrosine specific antibodies (pY). A TrkA immunoblot following the pY immunoprecipitation showed the activation of TrkA after NGF stimulation (Fig. 4A). After separation on SDS-PAGE, pY-immunoprecipitated proteins were visualized. A 72 kDa band, corresponding to the molecular mass of Ku70, was specifically detected in NGF-stimulated MCF-7 cells (Fig. 4A, upper panel) and was subjected to peptide mass fingerprint identification. The MALDI-TOF analysis (Fig. 4B) of the tryptic digestion peptides indicated that 19/40 peptides matched the theoretical tryptic peptides of the Ku70 protein with a high accuracy (32 ppm), covering 39% of its sequence (Fig. 4C) with a score of 148. In addition, the immunoprecipitation of phosphotyrosine proteins in MCF-7 cells with or without NGF treatment, followed by Ku70 immunodetection by western blot, revealed a band

corresponding to phosphorylated Ku70 only in NGF-stimulated MCF-7 cells (Fig. 4D). Interestingly, no phosphorylation of Ku70 was induced in PC12 cells upon NGF stimulation. These results indicated that NGF stimulation of breast cancer cells resulted in the induction of Ku70 tyrosine phosphorylation.

Ku70 is involved in TrkA signaling and survival of breast cancer cells. It has been reported that Ku70 can prevent cell death (23) and we have previously shown that NGF stimulates the survival and proliferation of breast cancer cells (9). Since an interaction between TrkA and Ku70 has been identified, we have explored the possibility of a regulation of Ku70 anti-apoptotic activity by TrkA. In our experiments, we have induced breast cancer cell death using the pro-apoptotic agent TRAIL (TNF-Related Apoptosis Inducing Ligand). The data presented in Fig. 5A show that whereas RNA interference against Ku70 had no pro-apoptotic effect by itself, it induced a strong potentiation of TRAIL-induced apoptosis in breast cancer cells overexpressing TrkA. Condensation and fragmentation of the nucleus, characteristics of apotosis, can be observed in Fig. 5B, particularly in the situation of Ku70 depletion by specific siRNA. Since there is no potentiation of TRAIL-induced apoptosis when TrkA is not overexpressed, we hereby propose Ku70 as a new player involved in TrkA-mediated survival signaling in breast cancer cells. Together, our data indicate that in the absence of Ku70, TrkA signaling is pro-apoptotic and therefore this protein might be an important key to understanding the well known paradox of anti- versus pro- apoptotic activity of tyrosine kinase receptors. The data presented in Fig. 5C show the efficiency of RNA interference and cell transfection in decreasing the level of Ku70 and overexpressing TrkA respectively.

DISCUSSION

NGF-induced TrkA signaling pathway has mostly been studied in neuronal cells and little is known about intracellular events occurring in breast cancer cells. The aim of the present work was to decipher the signaling initiated by TrkA in breast cells using a proteomics approach combining the co-immunoprecipitation of TrkA plus its putative intracellular partners and the identification of these proteins by mass spectrometry. Similar experimental protocols were previously used to elucidate epidermal growth factor (EGF), platelet-derived growth factor (PDGF) or fibroblast growth factor (FGF) signaling pathways (24-29), allowing the identification of new partners involved in tyrosine kinase receptor signaling. For example, it has been shown that Vav-2 is a substrate of the EGF and PDGF receptors (26), that NSAP1 and TOM1/1 are involved in FGF signaling cascade (27) and that the valosin-containing protein (VCP) and actin are targeted by the serine/threonine kinase Akt (28, 29). In essence, the use of co-immunoprecipitation to study receptor signaling offers the advantage of enabling the detection of previously unsuspected signaling elements.

Some of the putative TrkA signaling partners that we have identified here were already described in growth factor mediated pathways. This is for example the case for the ras GTPase-activating-like protein IQGAP1 known as a scaffold protein that interacts with multiple components of signaling cascades (30). A mass spectrometry-based proteomic study combining the stable isotopic amino acids in cell culture (SILAC) and affinity purification showed that IQGAP1 is recruited by the activated Grb2-EGF receptor complex (31). Moreover a direct binding of IQGAP1 with the MAPK/ERK kinase (MEK) 1/2 and Erk2 has been demonstrated, suggesting that IQGAP1 is a scaffold for mitogen activated protein kinase signaling. Since TrkA signaling involves activation of the MAP kinase cascade in breast cancer cells (9, 16), leading to the stimulation of cellular growth, IQGAP1 could also be a scaffold protein in this mitogenic pathway. Another protein already described in growth factor signaling was the valosin-containing protein (VCP) that belongs to the ATPases Associated with various cellular Activities (AAA) family and is involved in several ATP-

dependent processes including ubiquitin- mediated proteolysis, DNA repair, apoptosis or cell cycle control (32). Recently it was demonstrated that VCP is a target of Akt signaling (33) and is necessary for the anti-apoptotic effect of Akt in breast cancer cells (28). The PI-3K/Akt pathway is one of the cascade activated by TrkA in neuronal cells and our present work suggests that VCP could also be involved in this pathway in breast cancer cells. In line with this, the cytoskeleton protein actin and its associated proteins have been shown to be targeted by Akt signaling (29, 34), leading to cytoskeleton reorganization, and the fact we have identified actin in our experiments corroborates other studies arguing in favour of the presence of actin in complex with TrkA and its involvement in TrkA signalling (18, 35). Another putative TrkA partner that we have identified is the nucleophosmin, also known as B23 or numatrin. Nucleophosmin is a protein implicated in cell growth and proliferation, whose expression rapidly increases in response to mitogenic stimuli and nucleophosmin was found at high levels in proliferative and malignant cells (36). Interestingly, it has recently been shown that nucleophosmin mediates the anti-apoptotic effect of NGF via the PIKE (PI 3-kinase enhancer)/PI3K pathway (37, 38). Together with our present work, these data indicate that the role of nucleophosmin in the cytoprotective activities of NGF might be regulated by TrkA activation in breast cancer cells.

It should be noticed that co-immunoprecipitation and denaturing elution bring down a lot of immunoglobulins which may mask some real interaction partners, while eluting some proteins that are not real TrkA partners. Therefore it is important to emphasize that new putative interaction partners identified in co-immunoprecipitation experiments must subsequently be validated by implementing a combination of approaches such as antibody recognition, confocal microscopy analysis and functional validation by RNA interference. In our present study, this was the case for the protein Ku70, that was not known to be involved in TrkA signaling, and for which we have been able to go through the full validation process. Our results show that Ku70 interacts with TrkA and is tyrosine phosphorylated upon NGF stimulation of breast cancer cells. The interaction of Ku70 with another growth factor receptor, the EGF receptor, has already been reported (39). This work demonstrated, by co-

immunoprecipitation, that Ku70 can bind to the EGF receptor when it is inhibited with a blocking monoclonal antibody. The authors suggested a role of the EGF receptor in the sequestration of Ku70 in the cytoplasm thereby preventing its action in DNA repair as opposed to a direct role of Ku70 in the EGF signaling pathway. Although Ku70 is mainly localized in the nucleus, a cytosolic form of Ku70 has also been described (40-42). This is in agreement with our confocal microscopy study that showed a colocalization between TrkA and Ku70 in the cytoplasm of MCF-7 cells. In addition, we have shown that Ku70 is phosphorylated on tyrosine as a consequence of TrkA activation by NGF. Although we have not been able to map the tyrosine residues that are actually phosphorylated after NGF stimulation, potential sites of phosphorylation were identified on tyrosine 321 and 408 (data not shown) by *in silico* analysis using Scansite software (43). In addition, the possible role of Ku70 in the TrkA signaling pathway was investigated by using the inhibition of its expression by RNA interference. Our results showed that whereas depletion in Ku70 had no effect on its own on breast cancer cell survival and sensitivity to apoptosis, in contrast, in cells overexpressing TrkA a decrease in Ku70 level resulted in a potentiation of apoptosis. Interestingly, a previous study has reported that the cytosolic form of Ku70 binds to the pro-apoptotic signaling protein Bax and can inhibit Bax-mediated apoptosis by suppressing its mitochondrial relocalization from the cytosol (23) and it is tempting to propose that the hypersensitivity to TRAIL-induced apoptosis that we have observed with the inhibition of Ku70 expression could be due to the decrease of Bax sequestration in the cytosol. Alternatively, the DNA repair activities of Ku70 could also be at play here as this protein belongs to the DNA repair family of proteins and is a regulatory subunit of the DNA-dependent protein kinase (DNA-PK). It is well established that DNA repair is necessary during cell proliferation and that its impairment can lead to cell death, but to date, no relationships between TrkA signaling and DNA repair have been described. Further targeted investigations would be necessary to determine if TrkA stimulation impacts DNA repair. While, at this stage, the mechanism of Ku70 involvement cannot be ascertained, our results

show that TrkA signaling in breast cancer cells involves Ku70, and that in absence of Ku70, TrkA signaling can potentiate apoptosis.

An old and still unresolved paradigm in growth factor signaling resides in the fact that common signaling pathways can lead to a different cellular effect depending on cell types and physiological environment. This is well illustrated with the pheochromocytoma PC12 cells in which EGF induces cell proliferation whereas NGF stimulates cell differentiation based on similar signaling events and phosphorylation cascades (44, 45). Although the time course and kinetics of phosphorylation cascades, such as transient or sustained MAP-kinase activation (46, 47) have been proposed to explain the differential biological effect observed with tyrosine kinase receptor stimulation, it still cannot be excluded that specific effectors would be differentially involved (48). Interestingly, in our experiments, we have not detected any interaction between Ku70 and TrkA in PC12 cells, suggesting that Ku70 has no function in the stimulation of neuronal cell differentiation observed upon NGF stimulation. In breast cancer cells, we have also identified the proliferating cell nuclear antigen (PCNA) which is a marker of proliferation specifically overexpressed during the S phase of the cell cycle. It has been previously demonstrated that NGF regulates cell cycle arrest and neuronal differentiation by inducing, among others things, the expression of $p21^{ci1/waf1}$ (49) and a decrease of PCNA expression in PC12 cells. In contrast, NGF is anti-apoptotic and mitogenic for breast cancer cells (8-10), and NGF stimulation results in an *increase* in PCNA expression (unpublished observation). Together, our data suggest that Ku70 is not involved in TrkA signaling that leads to the differentiation of PC12 cells but is more specifically implicated in cell growth and anti-apoptotic NGF signaling in the context of breast cancer cells. Another illustration of the duality of tyrosine kinase receptor signaling is represented by their eventual ability to induce apoptosis. Although tyrosine kinase receptors have widely been described as stimulating cell survival, a pro-apoptotic effect of tyrosine kinase stimulation have long-time been described in a variety of cell types and physiological conditions (50-57). Interestingly, our RNA interference experiments also show that, in the absence of Ku70, TrkA signaling enhances apoptosis of breast cancer cells. TrkA was long-

known to generally have an ambivalent effect on cell survival (58) and a pro-apoptotic effect of TrkA signaling has already been reported (56, 57). In our experiments, TrkA potentiates TRAIL-induced apoptosis only in the absence of Ku70, and therefore Ku70 can prevent TrkA from inducing apoptosis in breast cancer cells. These data suggest that Ku70 might be a switch for the regulation of the apparently ambivalent effect of TrkA, and more generally tyrosine kinase receptors, between prevention and induction of apoptosis.

In conclusion, our work provides for the first time, a list of putative partners (plus some contaminants) of TrkA signaling in breast cancer cells and reveals Ku70 as an important component of this pathway. The functional validation of the implication of these proteins in the control of breast cancer cell growth and survival will have to be further explored, as was done here in case of Ku70, and their precise functions in the deregulation of multiprotein signaling complexes occurring in cancer cells will have to be defined. Previous studies have shown variable levels of TrkA expression in human breast tumors as well as a relationship between TrkA and estrogen receptor levels, resulting in a prognostic value associated to the expression of TrkA (11-13). Ku70 is increasingly regarded as crucially involved in carcinogenesis (59) and based on our present results, it could be postulated that targeting Ku70 in tumors overexpressing TrkA might be a relevant way to induce targeted apoptosis of cancer cells. This hypothesis nevertheless requires further *in vitro* and *in vivo* investigations, but it should be emphasized that Ku70, as well as the other proteins identified in this study, potentially represent new molecular targets whose interest for future therapeutic strategies against breast cancer will have to be investigated.

REFERENCES

1. Bibel, M. and Barde, Y. A. (2000) Neurotrophins: key regulators of cell fate and cell shape in the vertebrate nervous system. *Genes Dev.* **14**, 2919-37.

2. Huang, E. J. and Reichardt, L. F. (2001) Neurotrophins: roles in neuronal development and function. *Annu Rev Neurosci.* **24**, 677-736.

3. Davidson, B., Reich, R., Lazarovici, P., Nesland, J. M., Skrede, M., Risberg, B., Trope, C. G.and Florenes, V. A. (2003) Expression and activation of the nerve growth factor receptor TrkA in serous ovarian carcinoma. *Clin Cancer Res.* **9**, 2248-59.

4. Geldof, A. A., Van Haarst, E. P.and Newling, D. W. (1998) Neurotrophic factors in prostate and prostatic cancer. *Prostate Cancer Prostatic Dis.* **1**, 236-241.

5. Zhu, Z., Kleeff, J., Kayed, H., Wang, L., Korc, M., Buchler, M. W.and Friess, H. (2002) Nerve growth factor and enhancement of proliferation, invasion, and tumorigenicity of pancreatic cancer cells. *Mol Carcinog.* **35**, 138-47.

6. Ricci, A., Graziano, P., Mariotta, S., Cardillo, G., Sposato, B., Terzano, C.and Bronzetti, E. (2005) Neurotrophin system expression in human pulmonary carcinoid tumors. *Growth Factors* **23**, 303-12.

7. Dolle, L., Adriaenssens, E., El Yazidi-Belkoura, I., Le Bourhis, X., Nurcombe, V.and Hondermarck, H. (2004) Nerve growth factor receptors and signaling in breast cancer. *Curr Cancer Drug Targets* **4**, 463-70.

8. Descamps, S., Lebourhis, X., Delehedde, M., Boilly, B.and Hondermarck, H. (1998) Nerve growth factor is mitogenic for cancerous but not normal human breast epithelial cells. *J Biol Chem.* **273**, 16659-62.

9. Descamps, S., Toillon, R. A., Adriaenssens, E., Pawlowski, V., Cool, S. M., Nurcombe, V., Le Bourhis, X., Boilly, B., Peyrat, J. P.and Hondermarck, H. (2001) Nerve growth factor stimulates proliferation and survival of human breast cancer cells through two distinct signaling pathways. *J Biol Chem.* **276**, 17864-70.

10. Dolle, L., El Yazidi-Belkoura, I., Adriaenssens, E., Nurcombe, V.and Hondermarck, H. (2003) Nerve growth factor overexpression and autocrine loop in breast cancer cells. *Oncogene* **22**, 5592-601.

11. Descamps, S., Pawlowski, V., Revillion, F., Hornez, L., Hebbar, M., Boilly, B., Hondermarck, H.and Peyrat, J. P. (2001) Expression of nerve growth factor receptors and their prognostic value in human breast cancer. *Cancer Res.* **61**, 4337-40.

12. Aragona, M., Panetta, S., Silipigni, A. M., Romeo, D. L., Pastura, G., Mesiti, M., Cascinu, S.and La Torre, F. (2001) Nerve growth factor receptor immunoreactivity in breast cancer patients. *Cancer Invest.* **19**, 692-7.

13. Davidson, B., Reich, R., Lazarovici, P., Ann Florenes, V., Nielsen, S.and Nesland, J. M. (2004) Altered expression and activation of the nerve growth factor receptors TrkA and p75 provide the first evidence of tumor progression to effusion in breast carcinoma. *Breast Cancer Res Treat.* **83**, 119-28.

14. Tagliabue, E., Castiglioni, F., Ghirelli, C., Modugno, M., Asnaghi, L., Somenzi, G., Melani, C.and Menard, S. (2000) Nerve growth factor cooperates with p185(HER2) in activating growth of human breast carcinoma cells. *J Biol Chem.* **275**, 5388-94.

15. Melck, D., De Petrocellis, L., Orlando, P., Bisogno, T., Laezza, C., Bifulco, M.and Di Marzo, V. (2000) Suppression of nerve growth factor Trk receptors and prolactin receptors by endocannabinoids leads to inhibition of human breast and prostate cancer cell proliferation. *Endocrinology* **141**, 118-26.

16. Chiarenza, A., Lazarovici, P., Lempereur, L., Cantarella, G., Bianchi, A.and Bernardini, R. (2001) Tamoxifen inhibits nerve growth factor-induced proliferation of the human breast cancerous cell line MCF-7. *Cancer Res.* **61**, 3002-8.

17. Downs, J.A., and Jackson, S.P. (2004) A means to a DNA end: the many roles of Ku. Nature. **5**, 367-378.

18. Jullien, J., Guili, V., Derrington, E. A., Darlix, J. L., Reichardt, L. F.and Rudkin, B. B. (2003) Trafficking of TrkA-green fluorescent protein chimerae during nerve growth factor-induced differentiation. *J Biol Chem.* **278**, 8706-16.

19. Ayene, I.S., Ford, L.P., Koch, C.J. (2005) Ku protein targeting by Ku70 small interfering RNA enhances human cancer cell response to topoisomerase II inhibitor and gamma radiation. *Mol Cancer Ther.* **4**, 529-36.

20. Neuhoff, V., Arold, N., Taube, D., Ehrhardt, W. (1988) Improved staining of proteins in polyacrylamide gels including isoelectric focusing gels with clear background at nanogram sensitivity using Coomassie Brilliant Blue G-250 and R-250. *Electrophoresis* **9**:255-62.

21. Com, E., Evrard, B., Roepstorff, P., Aubry, F. and Pineau, C. (2003) New insights into the rat spermatogonial proteome: identification of 156 additional proteins. *Mol Cell Proteomics.* **2**, 248-61.

22. Schlessinger, J., Lemmon, M.A. (2006) Nuclear signaling by receptor tyrosine kinases: the first robin of spring. *Cell* **127**:45-8.

23. Sawada, M., Sun, W., Hayes, P., Leskov, K., Boothman, D. A. and Matsuyama, S. (2003) Ku70 suppresses the apoptotic translocation of Bax to mitochondria. *Nat Cell Biol.* **5**, 320-9.

24. Pandey, A., Andersen, J. S. and Mann, M. (2000) Use of mass spectrometry to study signaling pathways. *Sci STKE.* 2000 (37),PL1.

25. Vercoutter-Edouart, A., Lemoine, J., Smart, C. E., Nurcombe, V., Boilly, B., Peyrat, J.and Hondermarck, H. (2000) The mitogenic signaling pathway for fibroblast growth factor-2 involves the tyrosine phosphorylation of cyclin D2 in MCF-7 human breast cancer cells. *FEBS Lett.* **478**, 209-15.

26. Pandey, A., Podtelejnikov, A. V., Blagoev, B., Bustelo, X. R., Mann, M.and Lodish, H. F. (2000) Analysis of receptor signaling pathways by mass spectrometry: identification of vav-2 as a substrate of the epidermal and platelet-derived growth factor receptors. *Proc Natl Acad Sci USA.* **97**, 179-84.

27. Hinsby, A. M., Olsen, J. V., Bennett, K. L.and Mann, M. (2003) Signaling initiated by overexpression of the fibroblast growth factor receptor-1 investigated by mass spectrometry. *Mol Cell Proteomics.* **2**, 29-36.

28. Vandermoere, F., El Yazidi-Belkoura, I., Slomianny, C., Demont, Y., Bidaux, G., Adriaenssens, E., Lemoine, J.and Hondermarck, H. (2006) The valosin-containing protein (VCP) is a target of Akt signaling required for cell survival. *J Biol Chem.* **281**, 14307-13.

29. Vandermoere, F., El Yazidi-Belkoura, I., Demont, Y., Slomianny, C., Antol, J., Lemoine, J.and Hondermarck, H. (2007) Proteomic exploration reveals that actin is a signaling target of the kinase Akt. *Mol Cell Proteomics* **6**:114-24.

30. Brown, M. D. andSacks, D. B. (2006) IQGAP1 in cellular signaling: bridging the GAP. *Trends Cell Biol.* **16**, 242-9.

31. Blagoev, B., Kratchmarova, I., Ong, S. E., Nielsen, M., Foster, L. J.and Mann, M. (2003) A proteomics strategy to elucidate functional protein-protein interactions applied to EGF signaling. *Nat Biotechnol.* **21**, 315-8.

32. Wang, Q., Song, C.and Li, C. C. (2004) Molecular perspectives on p97-VCP: progress in understanding its structure and diverse biological functions. *J Struct Biol.* **146**, 44-57.

33. Klein, J. B., Barati, M. T., Wu, R., Gozal, D., Sachleben, L. R., Jr., Kausar, H., Trent, J. O., Gozal, E.and Rane, M. J. (2005) Akt-mediated valosin-containing protein 97 phosphorylation regulates its association with ubiquitinated proteins. *J Biol Chem.* **280**, 31870-81.

34. Stambolic, V., Woodgett, J.R. (2006) Functional distinctions of protein kinase B/Akt isoforms defined by their influence on cell migration. *Trends Cell Biol.* **9**:461-6.

35. Thomas, D., Patterson, S. D., and Bradshaw, R. A. (1995) Src homologous and collagen (Shc) protein binds to F-actin and translocates to the cytoskeleton upon nerve growth factor stimulation in PC12 cells. *J Biol Chem.* **270**, 28924-28931.

36. Grisendi, S., Mecucci, C., Falini, B.and Pandolfi, P. P. (2006) Nucleophosmin and cancer. *Nat Rev Cancer.* **6**, 493-505.

37. Ahn, J. Y., Liu, X., Cheng, D., Peng, J., Chan, P. K., Wade, P. A.and Ye, K. (2005) Nucleophosmin/B23, a nuclear PI(3,4,5)P(3) receptor, mediates the antiapoptotic actions of NGF by inhibiting CAD. *Mol Cell.* **18**, 435-45.

38. Ye, K. (2005) PIKE/nuclear PI 3-kinase signaling in preventing programmed cell death. *J Cell Biochem.* **96**, 463-72.

39. Bandyopadhyay, D., Mandal, M., Adam, L., Mendelsohn, J.and Kumar, R. (1998) Physical interaction between epidermal growth factor receptor and DNA-dependent protein kinase in mammalian cells. *J Biol Chem.* **273**, 1568-73.

40. Fewell, J. W. andKuff, E. L. (1996) Intracellular redistribution of Ku immunoreactivity in response to cell-cell contact and growth modulating components in the medium. *J Cell Sci.* **109**, 1937-46.

41. Bakalkin, G., Yakovleva, T., Hurd, Y. L., Nussenzweig, A., Li, G. C.and Terenius, L. (1998) Autoantigen Ku in the brain. Developmentally regulated expression and subcellular localization. *Neuroreport.* **9**, 2147-51.

42. Koike, M. (2002) Dimerization, translocation and localization of Ku70 and Ku80 proteins. *J Radiat Res (Tokyo).* **43**, 223-36.

43. Obenauer, J. C., Cantley, L. C.and Yaffe, M. B. (2003) Scansite 2.0: Proteome-wide prediction of cell signaling interactions using short sequence motifs. *Nucleic Acids Res.* **31**, 3635-41.

44. Chao, M. V. (1992) Growth factor signaling: where is the specificity? *Cell.* **68**, 995-7.

45. Vaudry, D., Stork, P.J., Lazarovici, P., Eiden, L.E. (2002) Signaling pathways for PC12 cell differentiation: making the right connections. *Science* **296**, 1648-9.

46. Kao, S., Jaiswal, R. K., Kolch, W.and Landreth, G. E. (2001) Identification of the mechanisms regulating the differential activation of the mapk cascade by epidermal growth factor and nerve growth factor in PC12 cells. *J Biol Chem.* **276**, 18169-77.

47. Marshall, C. J. (1995) Specificity of receptor tyrosine kinase signaling: transient versus sustained extracellular signal-regulated kinase activation. *Cell.* **80**, 179-85.

48. Meakin, S. O., Macdonald, J. I., Gryz, E. A., Kubu, C. J.and Verdi, J. M. (1999) The signaling adapter FRS-2 competes with Shc for binding to the nerve growth factor receptor TrkA. A model for discriminating proliferation and differentiation. *J Biol Chem.* **274**, 9861-70.

49. Billon, N., Van Grunsven, L. A.and Rudkin, B. B. (1996) The CDK inhibitor p21WAF1/Cip1 is induced through a p300-dependent mechanism during NGF-mediated neuronal differentiation of PC12 cells. *Oncogene* **13**, 2047-54.

50. Armstrong D.K., Kaufmann, S.H., Ottaviano, Y.L., Furuya, Y., Buckley, J.A., Isaacs, J.T., Davidson, N.E. (1994) Epidermal growth factor-mediated apoptosis of MDA-MB-468 human breast cancer cells. *Cancer Res.* **54**, 5280-3.

51. Gulli, L.F., Palmer, K.C., Chen, Y.Q., Reddy, KB. (1996) Epidermal growth factor-induced apoptosis in A431 cells can be reversed by reducing the tyrosine kinase activity. *Cell Growth Differ.* **7**,173-8.

52. Maloof, P., Wang, Q., Wang, H., Stein, D., Denny, T.N., Yahalom, J., Fenig, E., Wieder, R. (1999) Overexpression of basic fibroblast growth factor (FGF-2) downregulates Bcl-2 and promotes apoptosis in MCF-7 human breast cancer cells. *Breast Cancer Res Treat.* **56**, 153-67.

53. Mansukhani, A., Bellosta, P., Sahni, M., Basilico, C. (2000) Signaling by fibroblast growth factors (FGF) and fibroblast growth factor receptor 2 (FGFR2)-activating mutations blocks mineralization and induces apoptosis in osteoblasts. *J Cell Biol.* **149**, 1297-308.

54. Matteucci, E., Modora, S., Simone, M., Desiderio, M.A. (2003) Hepatocyte growth factor induces apoptosis through the extrinsic pathway in hepatoma cells: favouring role of hypoxia-inducible factor-1 deficiency. *Oncogene*. **22**, 4062-73.

55. Kim, M.S., Kim, C.J., Jung, H.S., Seo, M.R., Juhnn, Y.S., Shin, H.Y., Ahn, H.S., Thiele, C.J., Chi, J.G. (2004) Fibroblast growth factor 2 induces differentiation and apoptosis of Askin tumour cells. *J Pathol.* **202**, 103-12.

56. Muragaki, Y., Chou, T.T., Kaplan, D.R., Trojanowski, J.Q., Lee, V.M. (1997) Nerve growth factor induces apoptosis in human medulloblastoma cell lines that express TrkA receptors. *J Neurosci.* **17**, 530-42.

57. Lavoie, J.F., Lesauteur, L., Kohn, J., Wong, J., Furtoss, O., Thiele, C.J., Miller, F.D., Kaplan, D.R. (2005) TrkA induces apoptosis of neuroblastoma cells and does so via a p53-dependent mechanism. *J. Biol. Chem.* **280**, 29199-207.

58. Bredesen, D. E. andRabizadeh, S. (1997) p75NTR and apoptosis: Trk-dependent and Trk-independent effects. *Trends Neurosci.* **20**, 287-90.

59. Gullo, C., Au, M., Feng, G.and Teoh, G. (2006) The biology of Ku and its potential oncogenic role in cancer. *Biochim Biophys Acta.* **1765**, 223-34.

FOOTNOTES

This work was supported by grants from the Ligue Nationale Contre le Cancer (Equipe labellisée 2006), the Region Nord-pas-de-Calais, a French national Research Agency (ANR) RIB grant (BBR), an ARCUS grant from the French Ministry of Foreign Affairs, and the Rhône-Alpes Region (MIRA) (BBR) and the Association pour la Recherche sur le Cancer. C.L. was a recipient of a fellowship from the French Ministry for Research and Education and the Association pour la Recherche sur le Cancer and E.C. financial support was from the INSERM.

FIGURE LEGENDS

Figure 1. Immunoprecipitation of TrkA-GFP in breast cancer cells. A) Schematic representation of TrkA-GFP constructs. Δ0 is the full-length TrkA-GFP chimera and Δ8 is a truncated mutant that lacks the majority of the intracellular domain of TrkA (tyrosine kinase domain and tyrosine-based signaling motifs Y_{499}, $Y_{679;683;684}$ and Y_{794}). Extra, extracellular domain; TM, transmembrane domain; intra, intracellular domain; EGFP, enhanced green fluorescent protein fusion. **B)** SDS-PAGE pattern of TrkA-GFP co-immunoprecipitated proteins in MCF-7 cells. After transient transfection by TrkA-GFP vectors Δ0 or Δ8, cells were stimulated with NGF at 200 ng/ml for 10 min. Cell lysates were then subjected to GFP immunoprecipitation and the eluates were separated on a 10% SDS-polyacrylamide gel. Bands were visualized using colloidal coomassie blue staining. Numbers indicated the positions of bands from the Δ0 lane (except the band Δ8) that were excised for mass spectrometry identification. The position where IgG were detected are indicated (*).

Figure 2. Mass spectrometry identification of TrkA-GFP constructs. A) MALDI-TOF spectrum of tryptic digest from band Δ0 in Fig. 1B and tandem mass spectrum of the doubly-charged ion at m/z 703.14. Mass spectra allowed the identification of TrkA-GFP Δ0 by peptide mass fingerprint and by sequence information on the 1403.70 Da peptide. Peptides that matched with the theoretical tryptic peptides are indicated. **B)** MALDI-TOF spectrum of tryptic digest from band Δ8 in Fig. 1B and tandem mass spectrum of the doubly charged ion at m/z 760.21. Mass spectra allowed the identification of TrkA-GFP Δ8 by peptide mass fingerprint and by sequence information on the 1517.77 Da peptide. Matched peptides on the MALDI-TOF spectra and y ions on the MS/MS spectra are indicated.

Figure 3. Ku70 interacts with TrkA in NGF-stimulated MCF-7 cells. A) Immuno-fluorescent co-localization of TrkA and Ku70 in MCF-7 cells. Cellular localization of TrkA and

Ku70 were assessed with secondary antibodies directed against rabbit anti-TrkA and mouse anti-Ku70 coupled to Alexa Fluor dyes 546 (red) and 488 (green), respectively. The red fluorescence (TrkA) was mainly observed in the cytoplasm and cytoplasmic membrane (arrow in lane TrkA) but also in the nucleus (arrowhead in lane TrkA). The green fluorescence (Ku70) was mainly located in the nucleus (arrowhead in lane Ku70) but was also detected in the cytoplasm (arrow in lane Ku70). The co-localization of TrkA and Ku70 was reflected by the yellow-orange merge fluorescence in both the cytoplasm and the nucleus (arrow and arrowhead in lane merge). The scales represent 20 µm and a higher magnification is shown in the right column. **B)** Immunoprecipitation of TrkA (IP TrkA) in PC12 and MCF-7 cells after NGF treatment (200 ng/ml for 10 min) was followed by an immunoblot (IB) of Ku70 (clone 15 antibody) and TrkA. NGF stimulation enhanced the interaction between TrkA and Ku70 in MCF-7 cells. No detection was observed in PC12 cells. The presence of Ku70 in both cell types was assessed by immunoblot.

Figure 4. The protein Ku70 is tyrosine-phosphorylated upon NGF stimulation in breast cancer cells. A) Immunoprecipitation of tyrosine-phosphorylated proteins (pY IP) in MCF-7 cells stimulated with 200 ng/ml NGF for 10 min revealed a 72 kDa differential band (indicated by an arrow) by coomassie blue staining that was subjected to trypsin digestion before mass spectrometry identification. Ab, antibodies used as equiloading control. The activation of TrkA after NGF stimulation was checked by pY immunoprecipitation followed by immunobloting (IB) with anti-TrkA. **B)** MALDI-TOF spectrum of the 72 kDa band observed in panel A. Peptides that matched with the theoretical tryptic peptides from human Ku70 are indicated. **C)** Peptide mass fingerprint identification of human Ku70. Masses of the experimental charged tryptic peptides (MH+ submitted) and of their corresponding theoretical peptides (MH+ matched) are listed and the peptide masses are indicated in Daltons (Da). Sequences corresponding to each tryptic peptide are indicated with the position of the first and the last amino acid under brackets. Peptides sequenced by tandem mass spectrometry are underlined. Mox means a methionine oxydation and pyro-glu (N-term Q), a

pyroglutamate modification of the N-terminal glutamine. **D)** Immunoprecipitation of tyrosine phosphorylated proteins (pY IP) in PC12 and MCF-7 cells after NGF treatment (200 ng/ml for 10 min) followed by an immunoblot (IB) of Ku70 (AHP 316 antibody) showed the tyrosine phosphorylation of Ku70 in NGF stimulated MCF-7 cells. Ab, Ponceau detection of antibodies used as equiloading control.

Figure 5. Ku70 is involved in the TrkA-mediated survival of breast cancer cells. A) MCF-7 cells were transiently transfected with TrkA-GFP constructs Δ0 (full length TrkA construct) and/or siRNA directed against Ku70. One day after transfection, cells were serum starved for 16 h, treated with 200 ng/ml of NGF for 1 h before co-treatment with 5 ng/ml Trail and 200 ng/ml NGF during 6 h. Apoptosis was assessed by Hoechst staining and percentage of apoptotic cells are presented as the mean of four measurements. **B)** Hoechst staining of MCF-7 cells overexpressing TrkA shows that characteristic apoptotic nuclear fragmentation is increased after treatment by siRNA against Ku70. **C)** The efficiency of cell transfection and treatment by Ku70 siRNA was verified by immunoblotting against GFP and Ku70 (AHP 316 antibody) respectively. The loading was assessed by anti-actin immunoblotting.

Δ0	MH+ submitted	MH+ matched	Error (Da)	Sequence
TrkA	845,46	845,48	-0,02	(53)AGTLNTLR(60)
	882,46	882,41	0,05	(669)IGDFGMSR(676)
	898,40	898,40	0,00	(669)IGDFGMSR(676) Mox
	1093,52	1093,52	0,00	(517)WELGEGAFGK(526)
	1118,51	1118,57	-0,06	(548)ALKETSENAR(557)
	1195,57	1195,52	0,05	(677)DIYSTDYYR(685)
	1291,69	1291,64	0,05	(696)WMPPESILYR(705)
	1404,76	1404,70	0,06	(105)FVAPDAFHFTPR(116)
	1518,87	1518,77	0,10	(82)LEFEDLQGLGELR(94)
	1818,09	1817,96	0,13	(563)EAELLTMLQHQHIVR(577)
	1833,97	1833,96	0,01	(563)EAELLTMLQHQHIVR(577) Mox
	2031,10	2031,04	0,06	(78)DLQRLEFEDLQGLGELR(94)
GFP	821,36	821,39	-0,03	(80)QHDFFK(85)
	1050,56	1050,51	0,05	(114)FEGDTLVNR(122)
	1266,60	1266,57	0,03	(86)SAMPEGYVQER(96)
	1282,57	1282,57	0,00	(86)SAMPEGYVQER(96) Mox
	1347,62	1347,65	-0,03	(97)TIFFKDDGNYK(107)
	1477,80	1477,76	0,04	(110)AEVKFEGDTLVNR(122)
	1503,70	1503,65	0,05	(27)FSVSGEGEGDATYGK(41)
	1973,88	1973,90	-0,02	(141)LEYNYNSHNVYIMADK(156)
	1989,87	1989,89	-0,02	(141)LEYNYNSHNVYIMADK(156) Mox

Δ8	MH+ submitted	MH+ matched	Error (Da)	Sequence
TrkA	845,48	845,48	0,00	(53)AGTLNTLR(60)
	1404,76	1404,7	0,06	(105)FVAPDAFHFTPR(116)
	1518,84	1518,77	0,07	(82)LEFEDLQGLGELR(94)
	2031,13	2031,04	0,09	(78)DLQRLEFEDLQGLGELR(94)
	2474,44	2474,2	0,24	(295)AVEQHHWCIPFSVDGQPAPSLR(316)
GFP	821,42	821,39	0,03	(80)QHDFFK(85)
	1050,52	1050,51	0,01	(114)FEGDTLVNR(122)
	1266,63	1266,57	0,06	(86)SAMPEGYVQER(96)
	1282,5	1282,57	-0,07	(86)SAMPEGYVQER(96) Mox
	1347,6	1347,65	-0,05	(97)TIFFKDDGNYK(107)
	1477,81	1477,76	0,05	(110)AEVKFEGDTLVNR(122)
	1503,55	1503,65	-0,1	(27)FSVSGEGEGDATYGK(41)
	1542,68	1542,78	-0,1	(128)GIDFKEDGNILGHK(141)
	1973,79	1973,9	-0,11	(141)LEYNYNSHNVYIMADK(156)
	1989,88	1989,89	-0,01	(141)LEYNYNSHNVYIMADK(156) Mox

Table 1 : Mass spectrometry identification of bands Δ0 (TrkA-GFP full length) and Δ8 (TrkA-GFP deleted from intracellular domain) observed in Fig. 1B. Masses of submitted charged tryptic peptides and of their corresponding theoretical matched peptides in TrkA or GFP sequences are listed and peptide masses are indicated in Dalton (Da). Sequences corresponding to each tryptic peptide are indicated with the position of the first and the last amino-acid under brackets. Peptides sequenced by tandem mass spectrometry are underlined. Mox means methionine oxidation.

Band number	Protein name	Swissprot accession no.	Peptide sequences	Observed precursor m/z	Theoretical precursor neutral mass	Delta mass (Da)	Expected value	Mascot score	% of Coverage	Molecular function
1	Ras GTPase-activating-like protein IQGAP1	P46940	TLQALQIPAAK	577.36	1152.69	0.01	5.9e-05	213	2	GTPase activator
			ATFYGEQVDYYK	742.33	1482.67	-0.02	1.8e-05			
			SNQQLENDLNLMDIK	896.00	1789.85	0.14	2.8e-10			
2	Heterogenous nuclear ribonucleoprotein U	Q00839	FIEIAAR	819.35	818.46	-0.12	3.0e-01	283	9	Ribonucleoprotein
			NGQDLGVAFK	525.50	1047.53	1.45	2.5e-02			
			GYFEYIEENK	646.59	1290.58	0.59	7.6e-0.3			
			YNILGTNTIMDK Mox	700.04	1397.69	0.39	5.7e-04			
			NFILDQTNVSAAAQR	824.60	1646.84	0.34	1.9e-04			
			GYFEYIEENKYSR	849.65	1696.77	0.52	2.5e-03			
			SSGPTSLFAVTVAPPGAR	858.01	1713.90	0.09	1.0e00			
3	Valosin-containing protein	P55072	EMVELPLR Mox	501.83	1001.52	0.12	5.0e00	176	6	ATPase activity
			LEILQIHTK	547.91	1093.65	0.16	8.7e-04			
			GILLYGPPGTGK	586.74	1171.66	-0.20	3.2e-03			
			GDIFLVRGGMR Mox	619.83	1235.64	1.99	3.7e01			
			LDQLIYIPLPDEK	778.36	1555.85	-1.15	1.8e-4			
	Elongation factor 2	P13639	VNFTVDQIR	546.79	1090.58	0.99	3.8e-02	77	2	Translation regulator
			VFSGLVSTGLK	554.65	1106.63	0.66	7.6e-03			
4	78 kDa glucose-regulated protein	P11021	DAGTIAGLNVMR Mox	617.64	1232.62	0.65	5.6e-03	523	19	Chaperone
			NELESYAYSLK	658.97	1315.63	0.29	1.8e00			
			TWNDPSVQQDIK	716.02	1429.68	0.35	2.8e-03			
			ITPSYVAFTPEGER	783.98	1565.77	0.18	2.6e-03			
			KSDIDEIVLVGGSTR	795.19	1587.89	0.52	8.1e-09			
			TKPYIQVDIGGGQTK	803.11	1603.86	0.35	1.3e-04			
			NQLTSNPENTVFDAK	839.55	1676.80	0.28	5.4e-06			
			IINEPTAAAIAYGLDKR	908.65	1814.99	0.30	3.1e-05			
			SQIFSTASDNQPTVTIK	919.34	1835.93	0.73	7.3e-06			

Band number	Protein name	Swissprot accession no.	Peptide sequences	Observed precursor m/z	Theoretical precursor neutral mass	Delta mass (Da)	Expected value	Mascot score	% of Coverage	Molecular function
5	Heat shock cognate 71 kDa protein	P11142	DAGTIAGLNVLR	600.50	1197.67	0.32	2.8e-02	554	18	Heat shock protein
			MVNHFIAEFK Mox	626.55	1250.61	0.47	9.3e-03			
			MKEIAEAYLGK Mox	635.10	1267.65	0.54	6.6e-03			
			NSLESYAFNMK Mox	660.49	1318.59	0.38	9.1e-05			
			SQIHDIVLVGGSTR	741.88	1480.80	0.94	1.5e-04			
			TTPSYVAFTDTER	744.35	1486.69	0.03	4.6e-03			
			SFYPEEVSSMVLTK Mox	816.91	1631.77	0.02	1.5e-04			
			IINEPTAAAIAYGLDK	830.67	1658.89	0.43	4.2e-05			
			NQVAMNPTNTVFDAK Mox	833.48	1664.78	0.15	1.4e-05			
			IINEPTAAAIAYGLDKK	894.69	1786.98	0.38	3.7e-07			
	Ku70 (ATP-dependent DNA helicase)	P12956	SDSFENPVLQQHFR	568.86	1702.81	0.76	5.9e-03	133	8	DNA repair
			IMLFTNEDNPHGNDSAK Mox	640.78	1917.85	1.47	1.5e-05			
			TEGDEEAEEEQEENLEASGDYK	1251.20	2499.99	0.39	2.4e-01			
6	Probable ATP-dependent RNA helicase DDX5	P17844	KWNLDELPK	572.52	1141.61	1.41	2.9e00	127	7	RNA binding
			TTYLVLDEADR	648.66	1294.64	0.66	1.0e00			
			NFYQEHPDLAR	695.60	1388.65	0.54	3.6e-02			
			TGTAYTFFTPNNIK	787.94	1573.78	0.09	7.0e-04			
7	Actin beta/gamma	P60709 P63261	GILTLK	644.41	643.43	-0.02	3.3e00	294	21	Structural constituent of cytoskeleton
			GYSFTTTAER	567.20	1131.52	0.87	2.5e-04			
			EITALAPSTMK Mox	589.62	1176.61	0.62	1.8e01			
			AVFPSIVGRPR	600.25	1197.70	0.80	4.2e-04			
			QEYDESGPSIVHR	758.97	1515.70	0.22	2.1e-03			
			IWHHTFYNELR	758.98	1514.79	1.21	1.1e-02			
			VAPEEHPVLLTEAPLNPK	977.89	1953.06	0.71	5.3e-06			
	Interleukin enhancer binding factor 2	Q12905	WFEENASQSTVK	713.86	1424.66	1.05	7.1e-04	131	7	Transcription factor
			VKPAPDETSFSEALLK	866.46	1730.91	0.01	1.5e-06			

Band number	Protein name	Swissprot accession no.	Peptide sequences	Observed precursor m/z	Theoretical precursor neutral mass	Delta mass (Da)	Expected value	Mascot score	% of Coverage	Molecular function
8	Nucleophosmin	P06748	GQESFK	696.17	694.33	0.84	3.1e01	47	8	Chaperone
			FINYVK	783.35	782.43	-0.09	1.6e00			
			VDNDENEHQLSLR	785.06	1567.72	0.38	9.4e-01			
9	Fibrillarin	P22087	DLINLAK	786.35	785.46	-0.13	4.5e01	241	19	Ribonucleoprotein
			IVALNAHTFLR	628.16	1253.72	0.58	2.8e-04			
			VSISEGDDKIEYR	756.26	1509.73	0.77	5.7e-05			
			DHAVVVGVYRPPPK	767.76	1532.85	0.67	5.0e-05			
			MQQENMKPQEQLTLEPYER 2Mox	809.06	2423.11	1.05	7.0e-02			
	Proliferating cell nuclear antigen (PCNA)	P12004	FSASGELGNGNIK	647.94	1292.64	1.23	8.7e-04	59	11	Regulation of cell cycle
			NLAMGVNLTSMSKILK	859.75	1718.94	-1.46	2.3e00			

Table 2: Identification of TrkA co-immunoprecipitated proteins. GFP co-immunoprecipitated proteins were separated by SDS-PAGE (Fig. 1B) and bands differentially found between Δ0 (TrkA-GFP full length) and Δ8 (TrkA-GFP deleted from TrkA intracellular domain) were cut out of the gel and digested with trypsin before nanoLC-nanoESI-MS/MS analysis. Band number, Protein name, Swissprot accession number, peptide sequences, the Mascot score and the percentage of coverage were reported for each protein. The observed precursor m/z, the theoretical precursor neutral mass, the delta mass in Da and the expected value ($p < 0.01$) delivered by Mascot search programm were indicated for each peptide. The molecular function of each protein, according to the Human Protein Reference Database (www.hprd.org) is indicated. Mox means a methionine oxidation. Representative MS/MS spectra of each identified proteins are shown in Supplemental data.

A

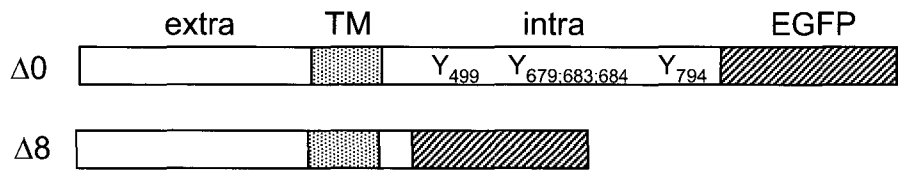

B

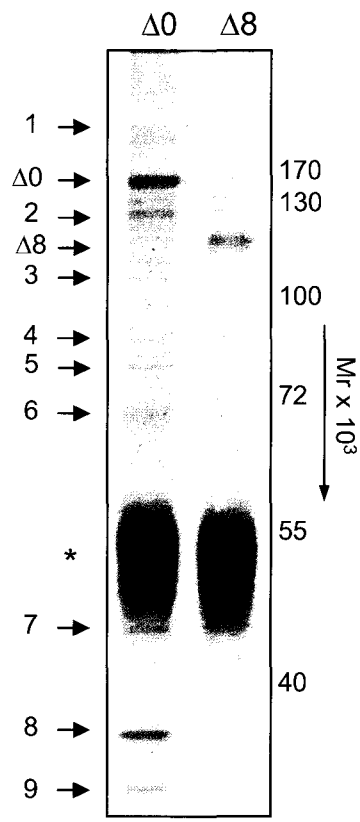

Figure 1

Com *et al.*

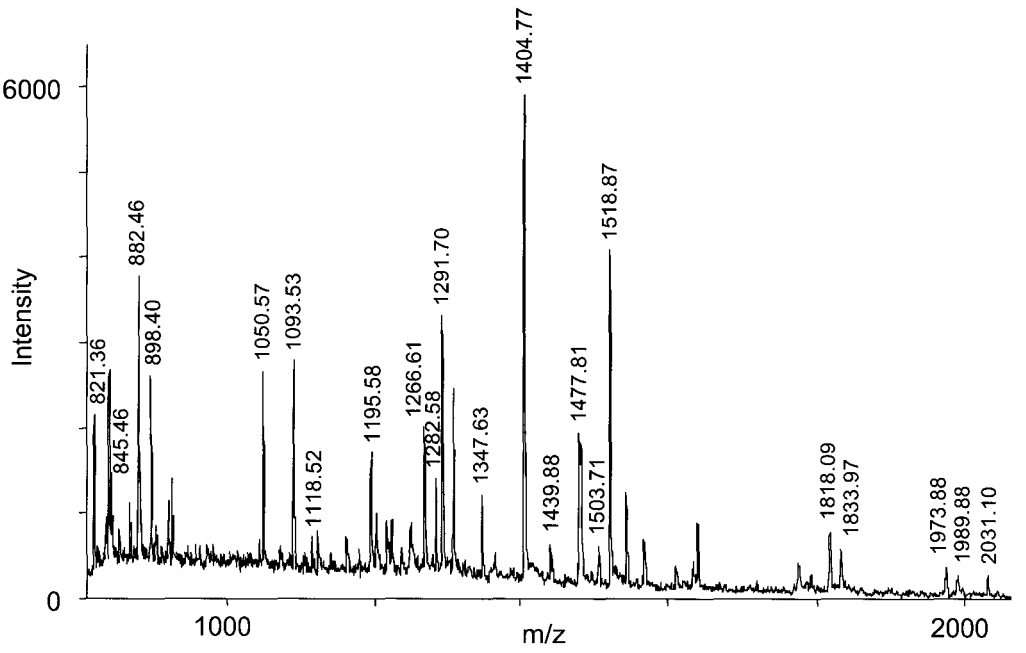

FVAPDAFHFTPR

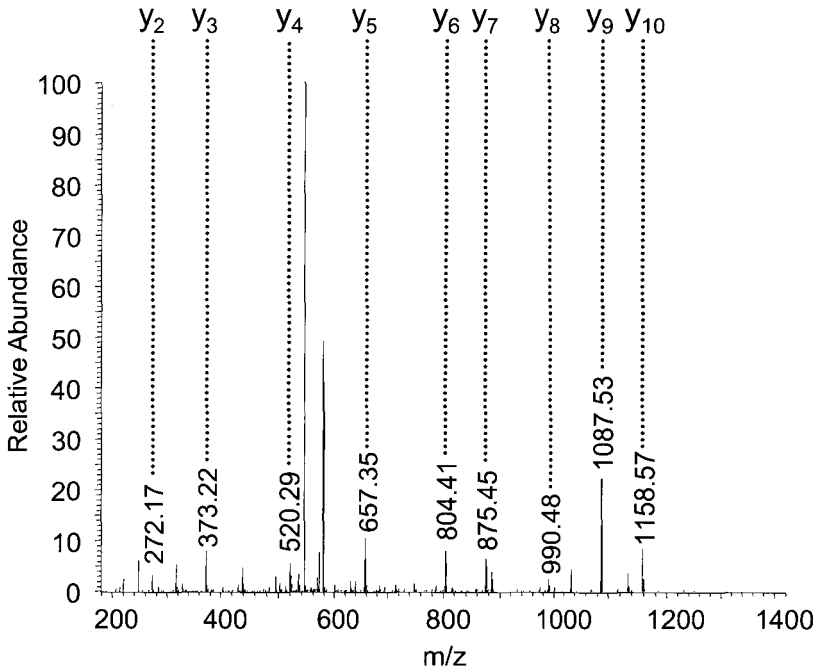

Figure 2A

Com *et al.*

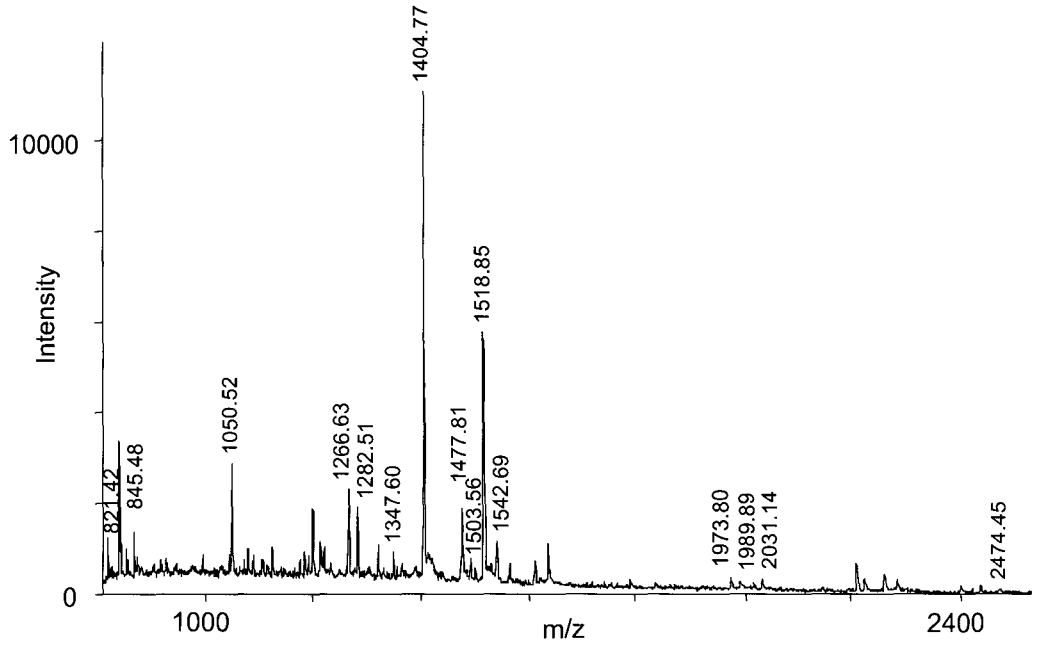

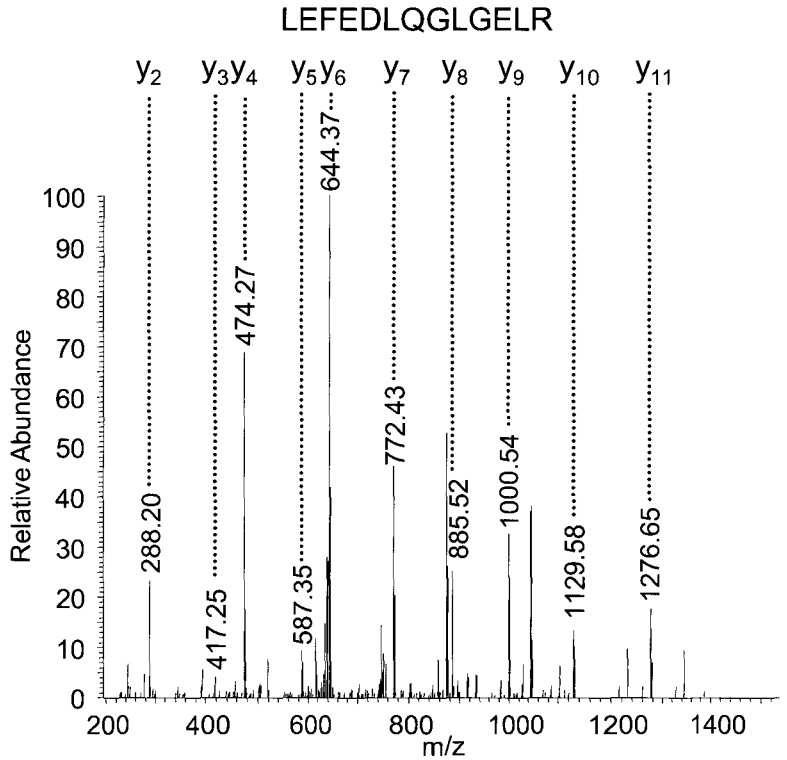

Figure 2B

Com *et al.*

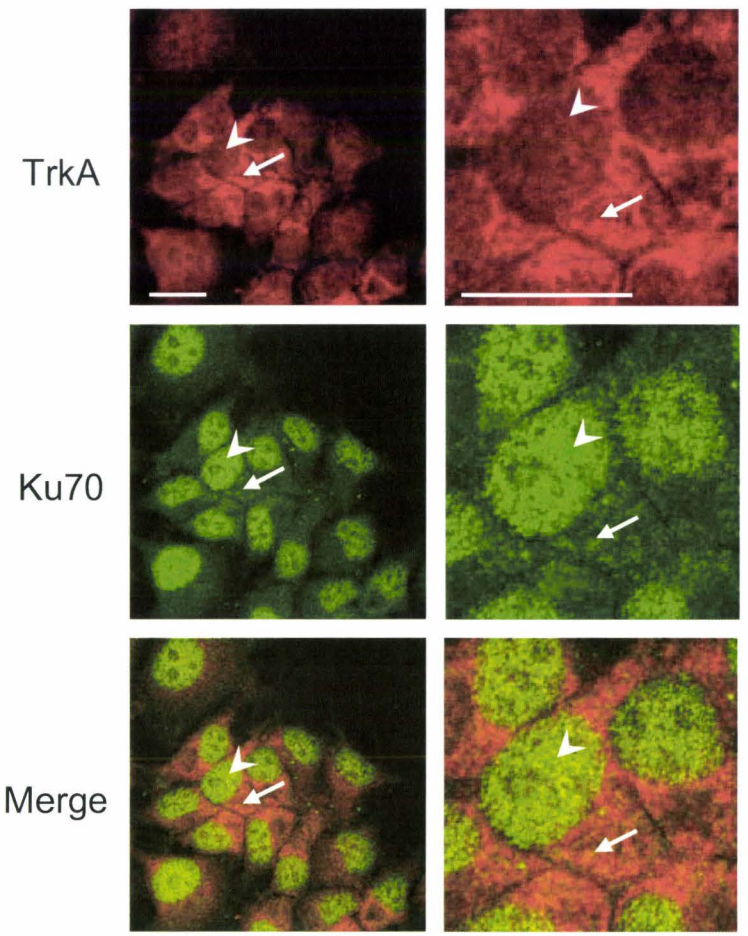

Figure 3 A

Com *et al.*

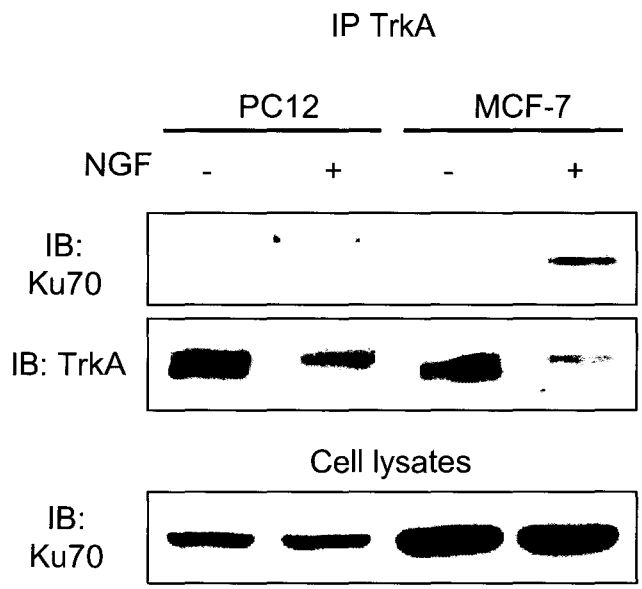

Figure 3B

Com *et al.*

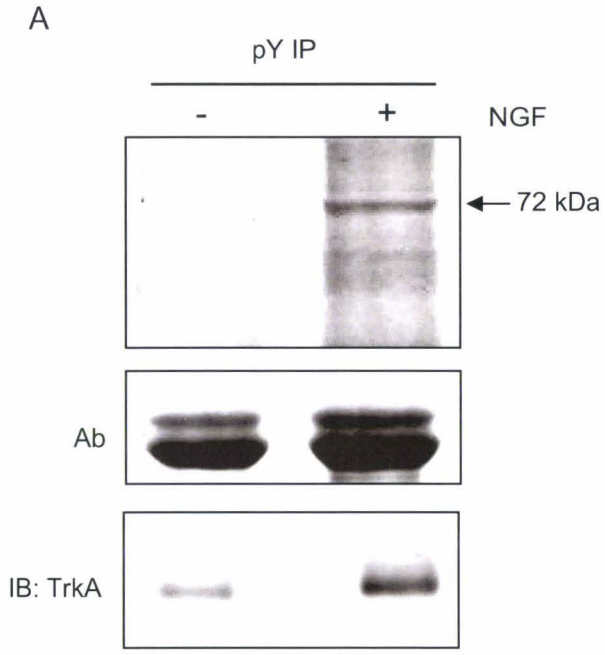
A
pY IP
-
+
NGF
72 kDa
Ab
IB: TrkA

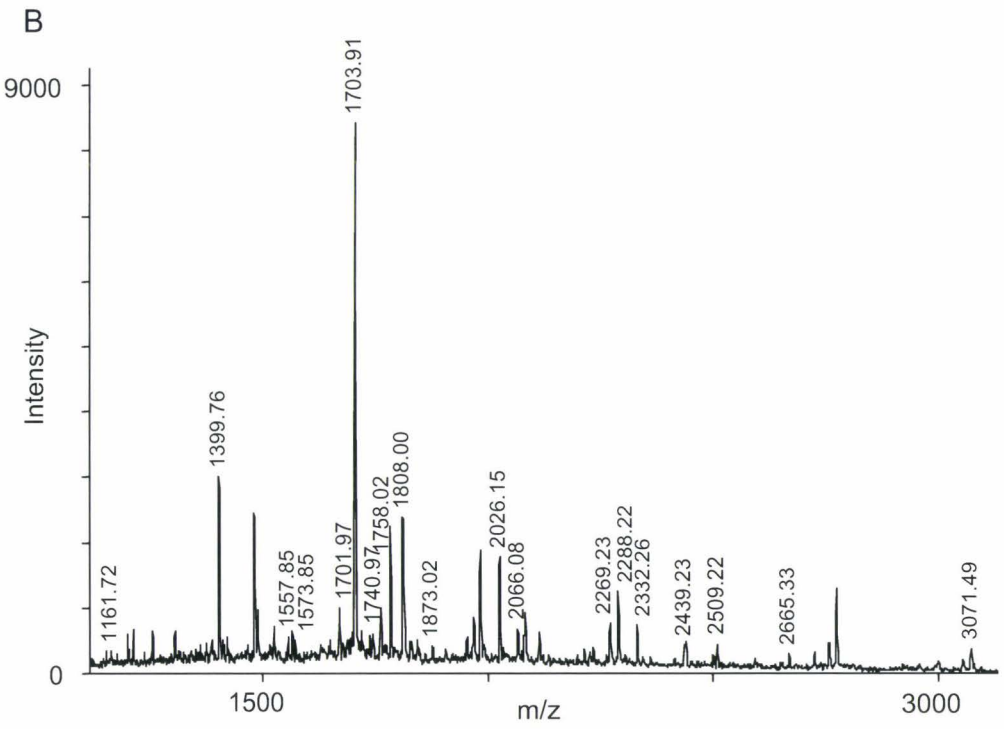
B
9000
0
Intensity
1500
m/z
3000
1161.72
1399.76
1557.85
1573.85
1701.97
1703.91
1740.97
1758.02
1808.00
1873.02
2026.15
2066.08
2269.23
2288.22
2332.26
2439.23
2509.22
2665.33
3071.49

Figure 4 AB

C

MH+ submitted	MH+ matched	Error (Da)	Sequence
1161.72	1161.65	0.07	(114)RILELDQFK(122)
1399.76	1399.73	0.03	(206)KPGGFDISLFYR(217)
1557.86	1557.91	-0.05	(591)SGLKKQELLEALTK(604)
1573.85	1573.81	0.04	(100)NIYVLQELDNPGAK(113)
1701.97	1701.87	0.10	(230)VHFEESSKLEDLLR(243)
1703.91	1703.81	0.10	(474)SDSFENPVLQQHFR(487)
1740.97	1740.93	0.04	(325)QIILEKEETEELKR(338) Pyro-glu (N-term Q)
1758.02	1757.96	0.06	(325)QIILEKEETEELKR(338)
1808.00	1807.95	0.05	(301)TFNTSTGGLLLPSDTKR(317)
1873.02	1873.02	0.00	(451)IMATPEQVGKMKAIVEK(467)
2026.15	2026.08	0.07	(74)IISSDRDLLAVVFYGTEK(91)
2066.08	2066.04	0.04	(445)MPFTEKIMATPEQVGKMK(462)
2269.23	2269.20	0.03	(74)IISSDRDLLAVVFYGTEKDK(93)
2288.22	2288.24	-0.02	(424)IQVTPPGFQLVFLPFADDKR(443)
2332.26	2332.12	0.14	(218)DIISIAEDEDLRVHFEESSK(237)
2439.23	2439.26	-0.03	(488)NLEALALDLMEPEQAVDLTLPK(509) Mox
2509.22	2509.24	-0.02	(517)LGSLVDEFKELVYPPDYNPEGK(538)
2665.33	2665.34	-0.01	(516)RLGSLVDEFKELVYPPDYNPEGK(538)
3071.49	3071.55	-0.06	(218)DIISIAEDEDLRVHFEESSKLEDLLR(243)

D

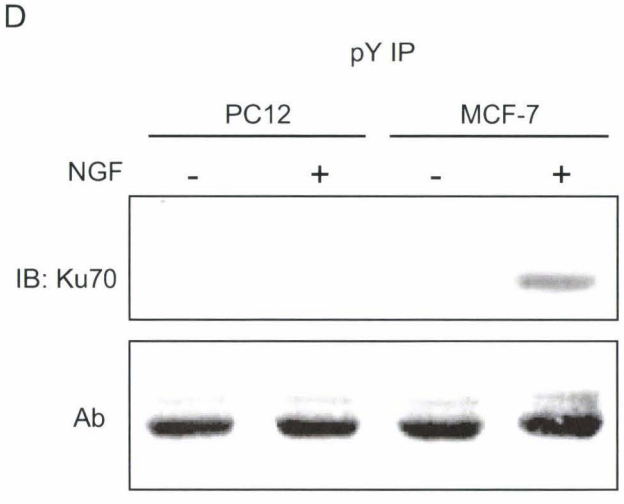

Figure 4 CD

A

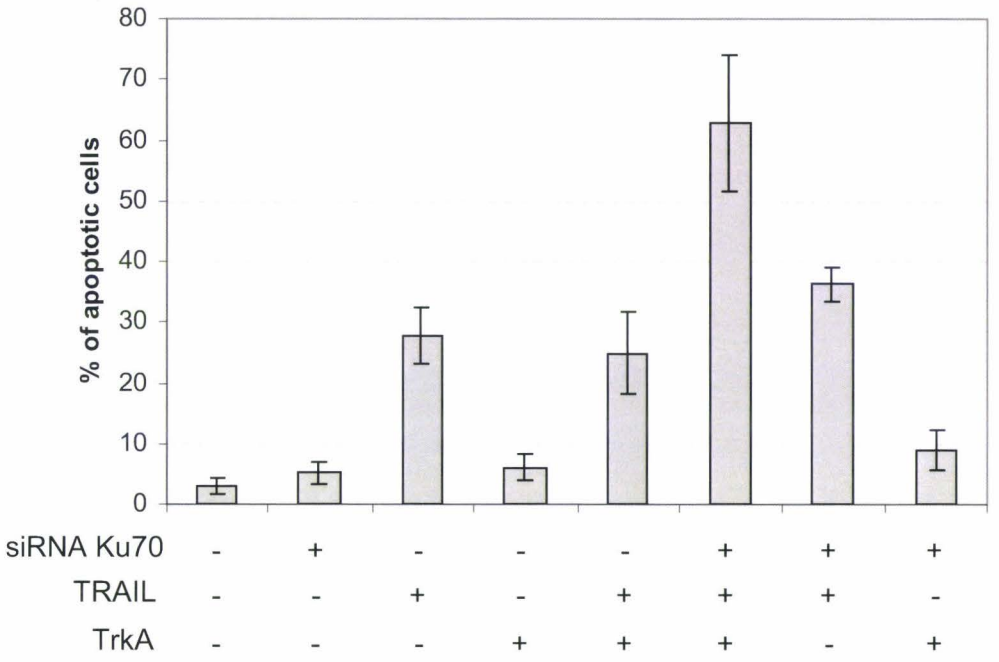

B

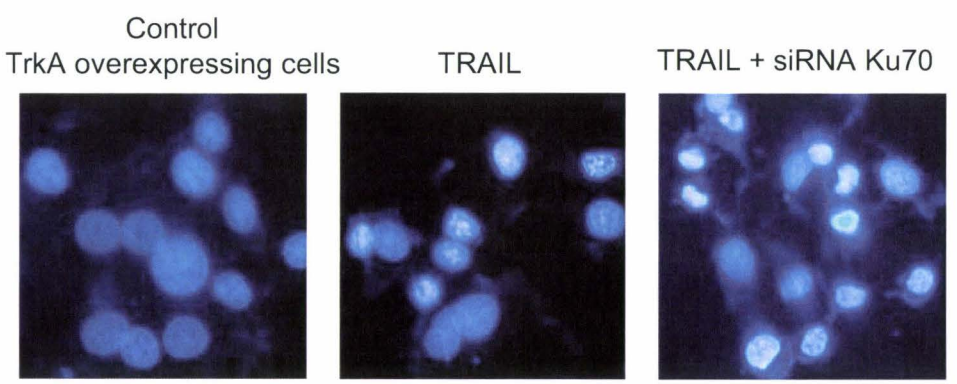

Figure 5AB

Com *et al.*

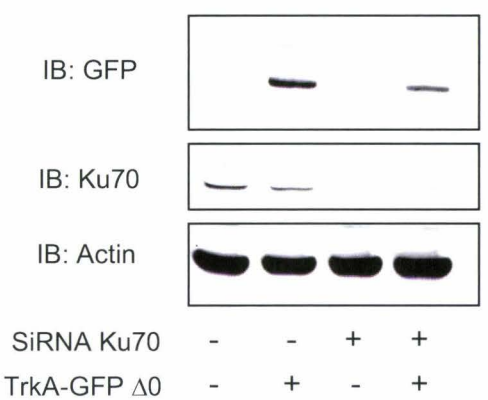

Figure 5C

Com *et al.*

II. La surexpression de TrkA augmente la croissance et la métastase des cellules cancéreuses de sein MDA-MB-231 (Article 2).

Soumis dans Cancer Cell.

Ce deuxième chapitre décrit l'obtention et la caractérisation biologique des cellules MDA-MB-231 surexprimant stablement TrkA. L'ensemble des résultats obtenus fait l'objet d'un manuscrit soumis dans Cancer Cell. Dans cette étude, nous avons montré que les cellules surexprimant TrkA présentent des caractéristiques d'agressivité accrues (augmentation de la prolifération, de la survie et de l'invasion). De plus, nous résultats indiquent que les voies PI3K/Akt et ERK/p38 MAP Kinase sont essentielles aux effets biologiques observés dans les cellules surexprimant TrkA. Nous avons confirmé l'augmentation de l'agressivité des cellules surexprimant TrkA par un modèle de xénogreffes chez des souris SCID. En effet, les souris ayant reçues les cellules surexprimant TrkA développent des tumeurs plus importantes et des métastases plus nombreuses. Nos résultats indiquent donc que TrkA peut être considéré comme une cible importante dans le développement de nouvelles thérapies anti-cancéreuses.

TrkA overexpression promotes growth and metastasis of breast cancer cells

Chann Lagadec, Eric Adriaenssens, Rodrigue Romon, Robert-Alain Toillon, Samuel Meignan, Elsa Vanhecke, Bénédicte Oxombre, Hubert Hondermarck, Xuefen Le Bourhis*

INSERM ERI-8 (JE-2488) "Growth factor signaling in breast cancer. Functional proteomics" IFR 147, University of Sciences and Technologies Lille, Villeneuve d'Ascq, France

*Correspondence: xuefen.lebourhis@univ-lille1.fr

Running title: TrkA overexpression promotes tumor growth and metastasis

Summary

The Trk family of neurotrophin receptors is emerging as an important player in carcinogenic progression. In the present study, we have generated MDA-MB-231 breast cancer cells stably overexpressing TrkA. We show that (a) TrkA overexpression promotes cell growth, migration and invasion *in vitro* as well as tumor development *in vivo*; (b) overexpression of TrkA confers constitutive activation of its tyrosine kinase activity; (c) signal pathways including PI3k-Akt, and ERK/p38 MAP kinases are activated by TrkA signaling and are required for the maintenance of an aggressive phenotype; (d) breast cancer samples presented high levels of TrkA and phospho-TrkA compared to normal breast tissues. Our results point to TrkA as an important target for anticancer therapy, and provide proof-of-concept for further development of clinical testing of inhibition of TrkA signaling.

Significance

Increased receptor tyrosine kinase activity has been found in a number of different human cancers, motivating development of pharmacological inhibitors designed to abrogate their functional contributions. While elevated expression of TrkA and its ligand NGF has been reported for several human cancers, the TrkA signaling system has not been a prominent target for anticancer therapy. This report demonstrates that overexpression of TrkA concomitantly promotes cancer cell proliferation, survival, migration and invasion as well as host angiogenesis. These data point to TrkA as an important target for anticancer therapy, and provide proof-of-concept for further development of clinical testing of inhibition of TrkA signaling.

Introduction

Breast cancer progression depends not only on primary tumor growth but also on the capacity of tumor cells to metastasize to distant sites. Several sets of growth factors and their cognate receptors are known to be importantly involved in the regulation of these processes (Buck and Knabbe, 2006; Burger et al., 2005; Chan et al., 2006; Chang et al., 2007; Chong et al., 2007; Mercurio et al., 2005; Roussidis et al., 2007; Ursini-Siegel et al., 2007). Thus, disruption of growth factor and receptor signalization is a current strategy for the development of anticancer drugs. So far, some drugs have shown therapeutic efficiency such as Herceptin (specific inhibitor of Erb-B2), but their use is limited due to tumor heterogeicity (only 20% of breast cancers overexpress Erb-B2). Identification of other growth factors and their receptors implicated in tumor development is essential to improve cancer therapy.

Neurotrophins consist of nerve growth factor (NGF), brain-derived neurotrophic factor (BDNF), neurotrophin 3 (NT-3), and NT-4/5. Neurotrophins bind two classes of receptors, the receptor tyrosine kinase family of Trk receptors (TrkA, TrkB, TrkC) and the p75 neurotrophin receptor ($p75^{NTR}$). Neurotrophins selectively bind Trk receptors to activate several signaling pathways that regulate cell survival and differentiation (Reichardt, 2006). The p75 receptor ($p75^{NTR}$) binds all neurotrophins with similar affinities (Chao, 1994). $p75^{NTR}$ does not possess kinase activity, but instead regulates cellular processes through interactions between the cytoplasmic domain of $p75^{NTR}$ and effector molecules (Mukai et al., 2003). Although neurotrophin-mediated signaling has been extensively studied in PC12 and neuronal cells, their effects on non-neuronal cells are not clear. Accumulating data have demonstrated that aberrant expression of NGF and NGF receptors are present in different cancers. For example, upregulation of TrkA has been shown in many types of non-neuronal cancers including medullary

thyroid carcinoma (McGregor et al., 1999), lung (Ricci et al., 2001), pancreatic (Friess et al., 1999; Zhu et al., 1999), prostate (Festuccia et al., 2007; Weeraratna et al., 2000), ovarian (Campos et al., 2007; Davidson et al., 2003) and breast carcinomas (Davidson et al., 2004).

Upregulation of TrkA expression is positively correlated with aggressive tumor progression in ovarian and prostate cancers (Katzir et al., 2003; McGregor et al., 1999), increased levels of activated TrkA are observed in breast cancer effusions compared to primary cancers (Davidson et al., 2004). NGF is expressed by several types of malignant, but not normal cells, implicating NGF in autocrine stimulation of non-neuronal carcinogenesis (Campos et al., 2007; Dionne et al., 1998; Dolle et al., 2003). Together, these studies suggest that upregulation of TrkA and NGF may function as a mechanism for abnormal NGF sensitivity in many types of carcinoma. In breast cancer, we showed that NGF is overexpressed and acts as a paracrine/autocrine factor to enhance tumor cell growth both *in vitro* and *in vivo* (Adriaenssens et al., 2007; Dolle et al., 2003). Moreover, specific targeting of NGF and/or TrkA can delay tumor growth in preclinical xenograft models (Adriaenssens et al., 2007). To further determine the functional importance of TrkA in breast cancer development, we stably transfected TrkA in MDA-MB-231 human breast cancer cells. We showed that TrkA overexpression increased cell growth and invasion both *in vitro* and *in vivo*. Moreover, TrkA overexpression strongly enhanced anoikis resistance, leading to increased metastatic spread of breast cancer cells to vital organs such as lung, liver and brain.

Results

Generation of TrkA overexpressing MDA-MB-231 cells

MDA-MB-231 breast cancer cells that express low levels of TrkA were transfected with either pcDNA3.1-hygro/TrkA expression vector or pcDNA3.1-hygro empty vector, followed by selection for hygromycin resistance. Resistant clones were expanded and maintained as pools to avoid artifacts due to the use of single clones. As shown in Figure 1A, a 4-fold increase of mRNA expression was observed compared to empty vector transfectants. Immunochemistry analysis confirmed increased expression of TrkA (Figure 1B). Western blot analysis of TrkA (Figure 1C) revealed an increase of 2 major bands at the expected molecular weight, with the upper and the lower ones being the 140 and 110 kDa glycosylated forms. A third minor band of about 80 kDa was also observed which could correspond to non glycosylated form of TrkA. Moreover, a strong increase of phosphorylated TrkA (pTrkA) was also observed in TrkA overexpressing cells, indicating that TrkA was activated following its overexpression in MDA-MB-231 breast cancer cells.

TrkA overexpression promotes cell growth, migration and invasion

On standard cell culture plastics, TrkA overexpression resulted in accelerated cell growth by 2-fold after 6 days of culture (Figure 2A). Addition of NGF stimulated the growth of empty-vector transfected cells (mock) but not TrkA overexpressing cells. We next performed *in vitro* migration and invasion assays to examine the role of NGF/TrkA axis in the invasiveness of cells. When cell migration was evaluated using the standard Transwell assay, TrkA overexpression induced a 2-fold increase of cells migrated to the bottom chamber than did the empty-vector transfected cells. NGF

treatment further increased cell migration in both mock and TrkA overexpressing cells (Figure 2B). Similar results were obtained using wound healing method (Figure 2C). The invasive capacities of the cells were assessed using Transwells with filters coated with Matrigel (BD Bioscience) and were found to be enhanced in TrkA overexpressing cells. NGF further enhanced cell invasion in both mock and TrkA overexpressing cells (Figure 2D). Such an increase in migration and invasion was not due to differences in cell growth as cells showed comparable growth rates in short time culture (Figure 2A). Increased migration could be the results of modified capacity of cell adhesion, we then evaluated the adhesive abilities of cells in fibronectin-, collagen- and Matrigel-coated plastics. No significant differences were detected between empty-vector transfected and TrkA overexpressing cells (data not shown). To determine whether TrkA can stimulate anchorage-independent cell survival, we cultured cells on poly-HEMA coated-wells that effectively inhibit cell attachment. In suspension, empty-vector transfected cells underwent cell death rapidly, resulting in more than 80% of cell death after 120 h (Figure 2E and F). In contrast, TrkA overexpressing cells could survive and proliferate as large spheroid aggregates in suspension, resulting in a 2-fold increase of cells by 48 h of culture. Of note, during different times of culture the viability of TrkA overexpressing cells remained superior or similar to that at the beginning of the experiment (Figure 2E and F). The enhanced survival of TrkA overexpressing cells was further supported by a soft-agar assay (Figure 2G and H), which reinforced the fact that TrkA overexpression bypasses the need for anchorage. Interestingly, while NGF had no effect on anoikis resistance, it stimulated the colony formation in soft agar in both control and TrkA overexpressing cells. To address whether TrkA can also enhance resistance of cells to known apoptosis-inducing agents, we treated cells with TRAIL

and showed that TrkA overexpression reduced apoptosis induction (Figure 2I). NGF reduced apoptosis induction only in empty-vector transfected cells but not in TrkA overexpressing cells. Similar results were obtained when cells were treated with doxorubicin or 5-fluorouacil (data not shown).

Collectively, these data showed that NGF/TrkA axis increased cell growth, invasion as well as resistance to anoikis and classic apoptosis induction.

PI3K-Akt and MEK MAP kinase are required for TrkA overexpression-promoted migration and anchorage-independent survival

To determine the specific effects of TrkA overexpression and the downstream signaling pathways, we analyzed migration, anoikis and colony formation in soft agar by using different pharmacological inhibitors (TrkA tyrosine inhibitor K252a, PI3K inhibitor LY294002, Akt inhibitor III, MEK inhibitor U0126 and p38 inhibitor II). The levels of phospho-Akt (pAkt), phospho-ERK (pERK) and phospho-p38 (pp38) were elevated in TrkA overexpressing cells when compared to control cells (Figure 3A). Inhibition of TrkA phosphorylation by K252a strongly reduced the levels of pAkt, pERK and pp38 without any effect on the total levels of corresponding proteins. This implies that overexpressed TrkA was functional in signal transduction by activating PI3K-Akt and ERK/p38 MAP kinases. Moreover, inhibition of PI3K and Akt decreased ERK phosphorylation without any effect on p38.

TrkA tyrosine inhibitor K252a had no effect on migration and survival of empty vector transfected cells, but reduced migration, anoikis resistance and colony formation in TrkA overexpressing cells (Figure 3B, C and H). This indicates that phosphorylated TrkA is responsible of the observed biological effects in TrkA overexpressing cells.

Inhibition of PI3K-Akt reduced migration and anoikis resistance in TrkA overexpressing cells, indicating that PI3K-Akt is essential in the control of these processes. Interestingly, PI3K-Akt seemed to be crucial for colony formation in soft agar as cells (overexpressing TrkA or no) did not survive in the presence of LY294002 or Akt inhibitor III (Figure 3H). ERK inhibition by U0126 efficiently counterbalanced TrkA overexpression-induced migration, anoikis resistance and colony formation (Figure 3B, F and H). In contrast, inhibition of p38 did not modify migration (Figure 3B), slightly reduced anoikis resistance (Figure 3G) but diminished colony formation in TrkA overexpressing cells (Figure 3H).

TrkA overexpression accelerates tumor growth by enhancing cell proliferation and angiogenesis

MDA-MB-231 cells were subcutaneously inoculated into SCID mice. All animals implanted with tumor cells formed tumors at the site of injection, but the dynamics of tumor growth rates were quite different: tumors formed by TrkA overexpressing cells were palpable 2 weeks after injection, and attained a size of 2,000 mm^3 5 weeks after injection. In contrast, empty vector transfected cells formed palpable tumors with a latency of 5 weeks and took 10 weeks to form tumors of similar size (2,000 mm^3) (Figure 4A). To determine whether apoptosis, cell proliferation and angiogenesis were modified in tumors formed by TrkA overexpressing cells, we then performed TUNEL assay, immuno-staining of PCNA and vWF which are markers of apoptosis, cell proliferation and angiogenesis, respectively. No difference in TUNEL-positive cells was observed between tumors formed by empty vector transfected and TrkA overexpressing cells. In contrast, 3- and 2.5-fold increases of PCNA- and vWF-positive cells were found in TrkA overexpressing tumor sections (Figure 4B).

These data indicate that accelerated tumor growth is due to the enhanced proliferation of TrkA overexpressing cells and increased angiogenesis.

TrkA overexpression promotes tumor metastasis by enhancing anoikis resistance

The metastatic property of TrkA overexpressing cells was evaluated by subcutaneous injection of GFP-positive MDA-MB-231 cells into SCID mice. These GFP-positive cells exhibited the same levels of TrkA, the similar proliferative and invasive capacities compared to their parental counterparts. Individual tumor burden per organ was measured by quantifying GFP-positive cells using FACS (Figure 5). All animals formed lung and liver metastases, however, TrkA overexpression induced 2- and 3-fold increases of metastatic burden in lungs and livers, respectively. Interstingly, three animals among eight bearing empty vector transfected cells developed low brain metastases with GFP-positive cells being inferior to 0.2%, while 9/9 animals receiving TrkA overexpressing cells developed brain metastasis with an average tumor burden higher than control animals (Figure 5, Table 1). Histological analysis of tumor sections showed the predominance of micrometastatic foci and confirmed increased metastases of TrkA overexpression in lung, liver and brain. Of note, metastatic foci were found to be frequently near vascular vessels (Figure 5). We then attempted to determine the mechanism of TrkA-drived metastasis. For this, TrkA overexpressing cells derived from lungs of 9 animals were isolated and cultured separately to evaluate their behavior in terms of growth, migration and resistance to TRAIL-induced apoptosis, as well as resistance to anoikis (Figure 6). As shown in Figure 6A, the levels of TrkA and phospho-TrkA in recovered metastatic TrkA overexpressing cells were slightly increased compared to cells before injection. No

modification in cell growth, migration and resistance to TRAIL-induced apoptosis was observed when compared to TrkA overexpressing cells before injection (Figure 6B-D). By contrary, the recovered metastatic TrkA overexpressing cells presented enhanced anoikis resistance compared to parental TrkA overexpressing cells. More interestingly, TrkA inhibition with K252a totally abolished anoikis resistance of these metastatic cells (Figure 6E and F). Thus, enhanced lung metastasis of TrkA overexpressing cells is due to the increased anoikis resistance.

Increased levels of TrkA and phospho-TrkA in breast tumor biopsies

To determine the relevance of our in vitro findings, we first compared mRNA expression in both normal and tumor breast biopsies by real time PCR. As shown in Figure 7A, the levels of TrkA mRNA in tumor biopsies were about 10-fold higher than in normal samples. The increased TrkA expression was further confirmed at protein levels, as higher levels of both TrkA and phospho-TrkA were detected in cancer biopsies compared to normal ones (Figure 7B). Interestingly, there was no strict correlation between the levels of TrkA and phospho-TrkA in breast cancers. We then extended our analysis by immunochemical staining of breast tissue microarrays. As shown in Figure 7C and D, the staining intensities for TrkA and phospho-TrkA were significantly elevated in cancer biopsies compared to normal tissues.

Figure 1. Generation of TrkA overexpressing cells

A: MDA-MB-231 cells were stably transfected with pcDNA3.I expression vector containing the full length sequence of TrkA cDNA. Mock and TrkA transfected cells were analyzed for TrkA mRNA expression by RT-PCR.

B: TrkA immunostaining of mock and TrkA transfected cells.

C: Western blots of TrkA and phospho-TrkA (pTrkA).

A

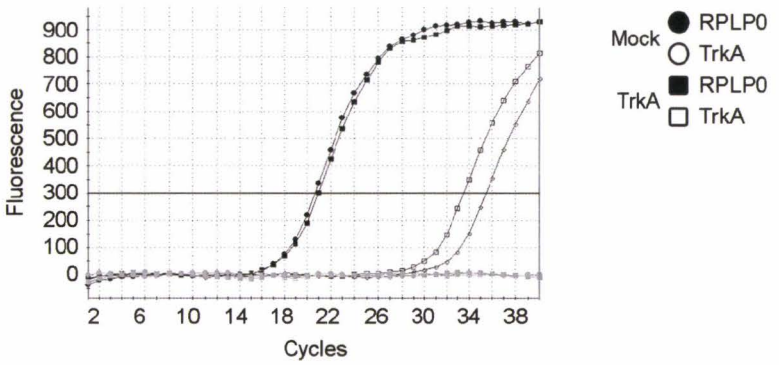

B

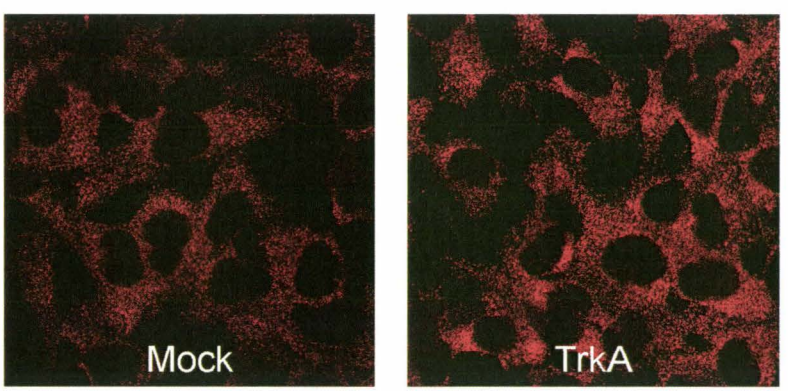

C

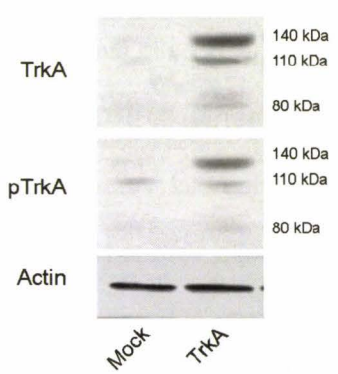

Figure 1 Lagadec *et al.*

Figure 2. Pleiotropic *in vitro* effects of TrkA overexpression

A: Growth Assay on standard culture plastics. Cells were treated with NGF (200 ng/ml) for different periods of time. Results are mean of 3 independent experiments. *, $p<0.01$, TrkA overexpressing cells versus mock cells; ¥, $p<0.01$, NGF treated mock cells versus NGF non treated mock cells.

B: Migration assay using transwell. Cells were treated with NGF for 6 h. Results are mean of 3 independent experiments. * $p<0.01$, TrkA overexpressing cells versus mock cells; ¥, $p<0.01$, NGF-treated mock cells versus NGF-non treated mock cells; #, $p<0.01$, NGF-treated TrkA overexpressing cells versus NGF-non treated TrkA overexpressing cells.

C: Representative photographs of wound-healing assay. Cells were treated with NGF for 24 h.

D: Matrigel invasion assay. Cells were treated with NGF for 16 h. Results are mean of 3 independent experiments. *, $p<0.01$, TrkA overexpressing cells versus mock cells; ¥, $p<0.01$, NGF-treated mock cells versus NGF-non treated mock cells; #, $p<0.01$, NGF-treated TrkA overexpressing cells versus NGF-non treated TrkA overexpressing cells.

E: Anoikis assay. Cells were seeded in poly-HEMA-coated 96-wells plates and cell viability was determined by MTS. Results are the mean of 3 independent experiments. *, $p<0.01$, TrkA overexpressing cells versus mock cells.

F: Representative photographs of cells cultured during 72 h in poly-HEMA-coated 96-wells.

G: Colony formation in soft agar. Cells were treated with NGF at the beginning of the experiments. Colonies of more than 20 cells were counted after 3 weeks of culture. Results are mean of 3 independent experiments. *, $p<0.01$, TrkA overexpressing cells versus mock cells; ¥, $p<0.01$, NGF-treated mock cells versus NGF-non treated mock cells; #, $p<0.01$, NGF-treated TrkA overexpressing cells versus NGF-non treated TrkA overexpressing cells.

H: Representative photographs of cells cultured in soft agar.

I: Resistance to apotosis induction by TRAIL. Results are mean of 3 independent experiments. *, $p<0.01$, TrkA overexpressing cells versus mock cells; ¥, $p<0.01$, NGF-treated mock cells versus NGF-non treated mock cells.

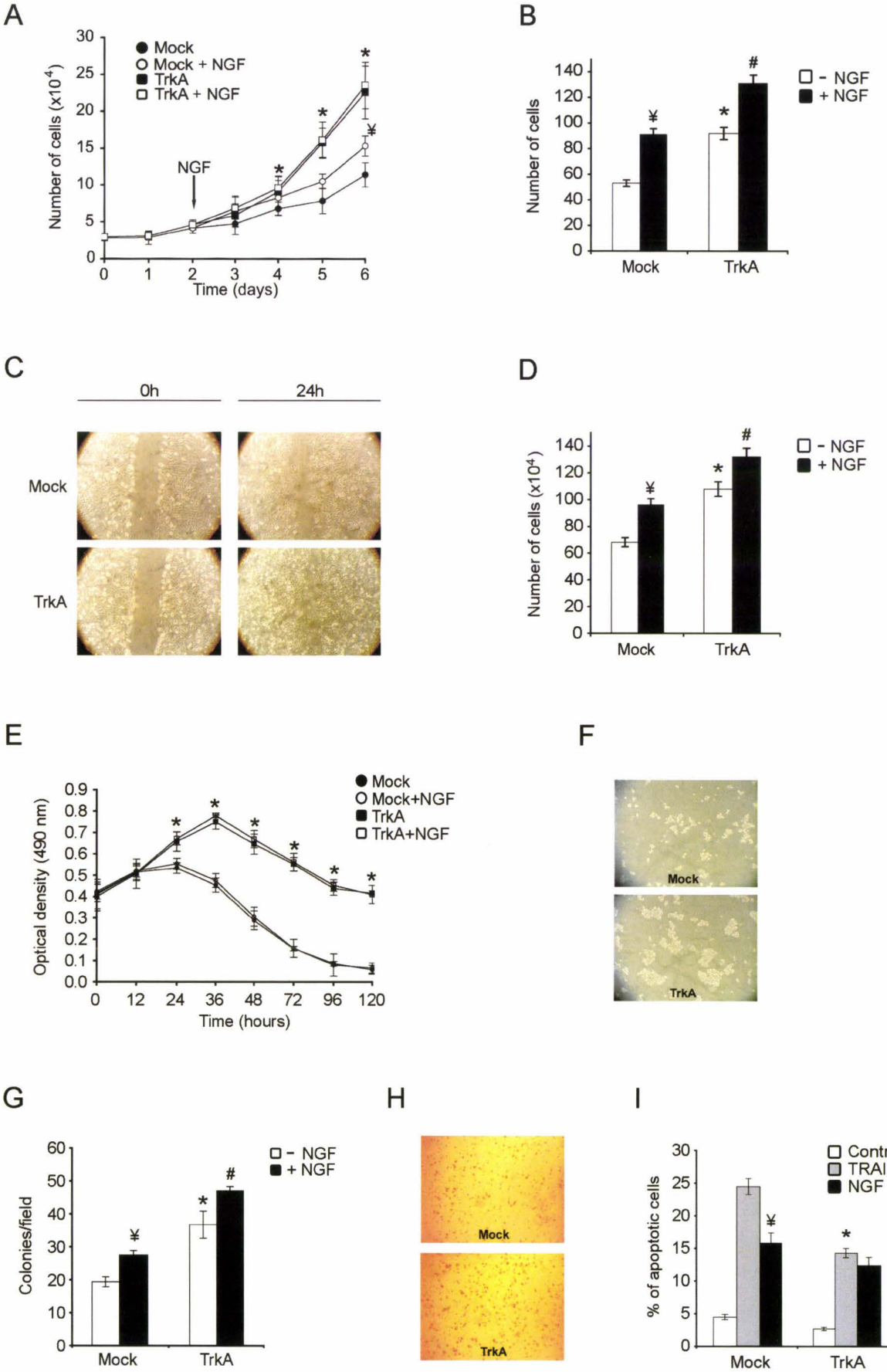

Figure 2

Lagadec *et al.*

Figure 3. Involvement of PI3K-Akt and ERK/p38 MAP Kinases in TrkA-mediated biological effects

A: Cells were treated in EMEM serum free-medium for 30 min with specific pharmacologic inhibitors (10 μM K252a, 15 μM LY294002, 15 μM Akt inhibitor III, 10 μM U0126 and 10 μM p38 inhibitor II). Lysates were made and subjected to immunoblot using the indicated antibodies.

B: Cells were preincubated with different inhibitors for 30 min and then cultured in Transwell for migration assay in the presence of different inhibitors for 6 h. Results are mean of 3 independent experiments. *, $p<0.01$, inhibitors-treated TrkA overexpressing cells versus vehicle-treated TrkA overexpressing cells.

C-G: Cells were preincubated with different inhibitors for 30 min and then cultured in poly-HEMA coated 96-wells plates in the presence of different inhibitors for anoikis assay. Results are mean of 3 independent experiments.

H: Cells were preincubated with different inhibitors for 30 min and then cultured in soft agar in the presence of different inhibitors. Results are mean of 3 independent experiments. *, $p<0.01$, inhibitors-treated TrkA overexpressing cells versus vehicle-treated TrkA overexpressing cells.

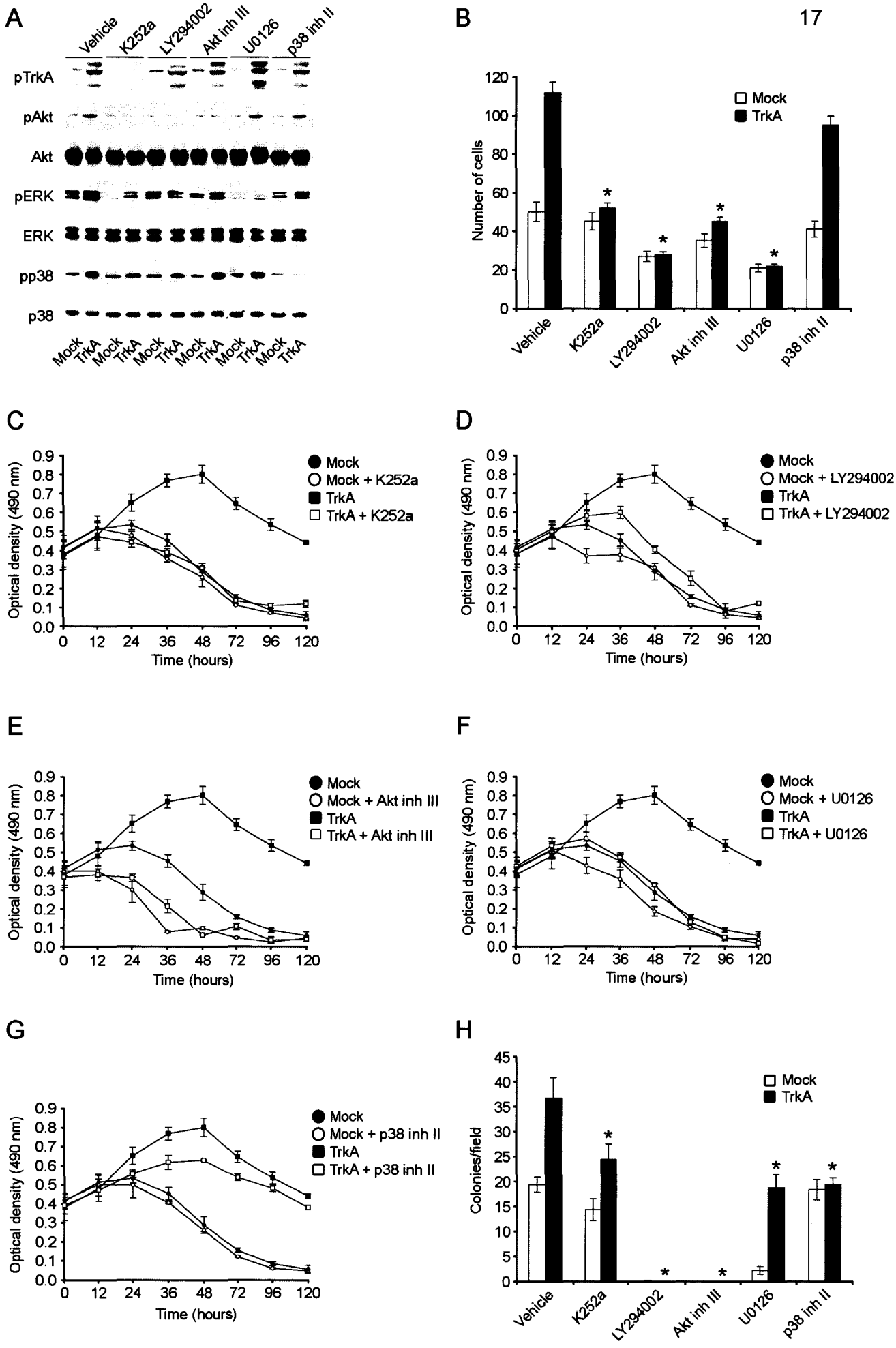

Figure 3

Lagadec *et al.*

Figure 4. Xenograft tumor growth in SCID mice

A: Cells (2×10^6) were subcutaneously injected into mice (9 mice par group). Tumor growth was monitored weekly until mean tumor volume approached 2,000 mm^3. Results are mean of 3 independent experiments. *, $p<0.01$.

B: Paraffin sections from tumors were stained using TUNEL or anti-PCNA, anti-vWF antibodies.

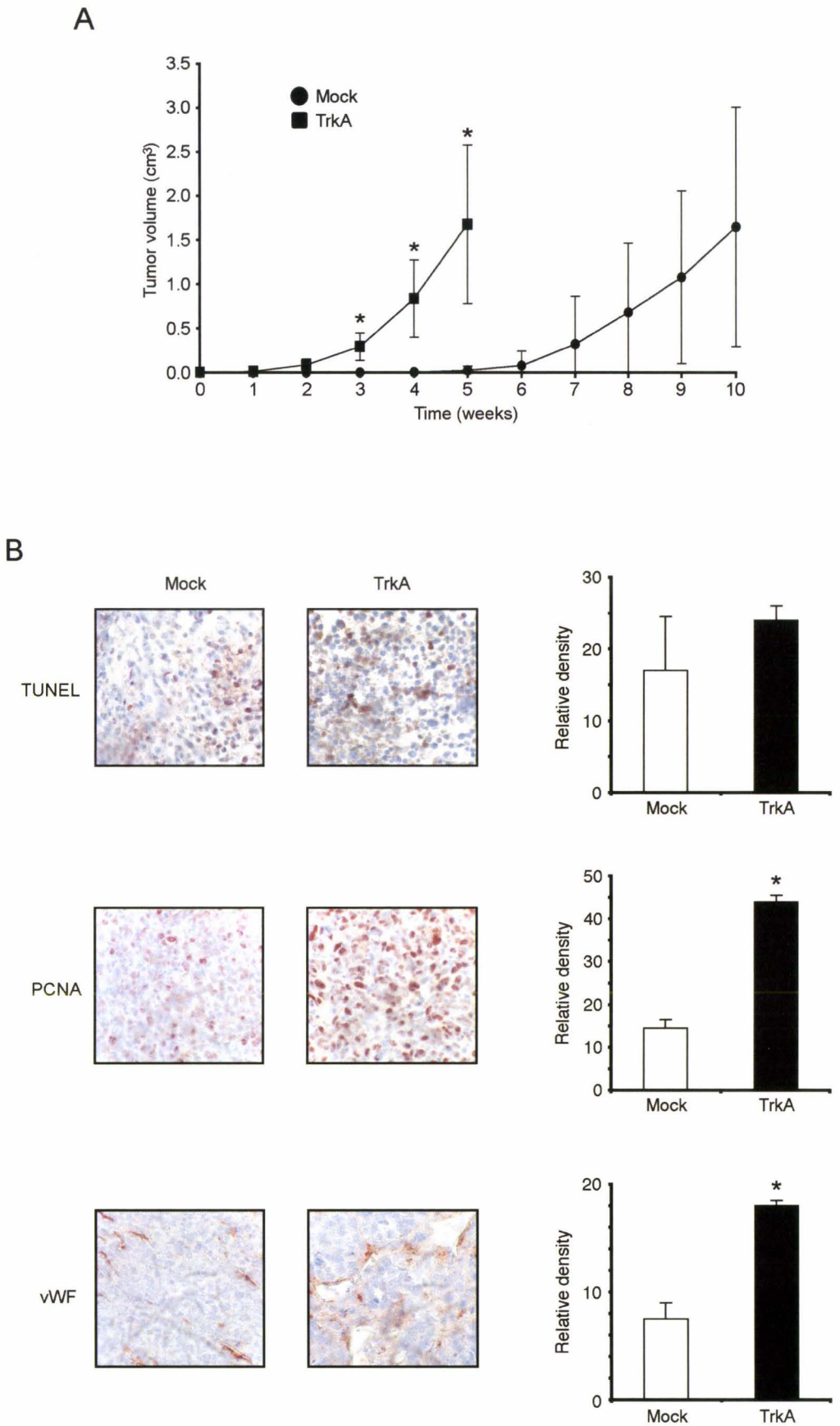

Figure 4 Lagadec *et al.*

Figure 5. Metastasis assessment in lung, liver and brain

A: GFP-mock or GFP-TrkA overexpressing cells were subcutaneously injected to SCID mice. When tumor volume approached 2,000 mm^3. Mice were sacrificed; lung, liver and brain were removed and digested with trypsin, collagenase and hyaluronidase to obtain individual cells. Metastasis was quantified by FACS analysis of GFP-positive cells. GFP-positive MDA-MB-231 cells were used as positive control; lung, liver and brain of a mouse receiving subcutaneous injection of GFP-negative MDA-MB-231 were used as negative controls. Histograms represent the analysis of 8 mice injected with mock cells and 9 mice injected with TrkA overexpressing cells. *, $p<0.01$. Paraffin sections of lung, liver and brain were stained with nuclear red and picroindigo carmine. Arrows indicate metastatic cells.

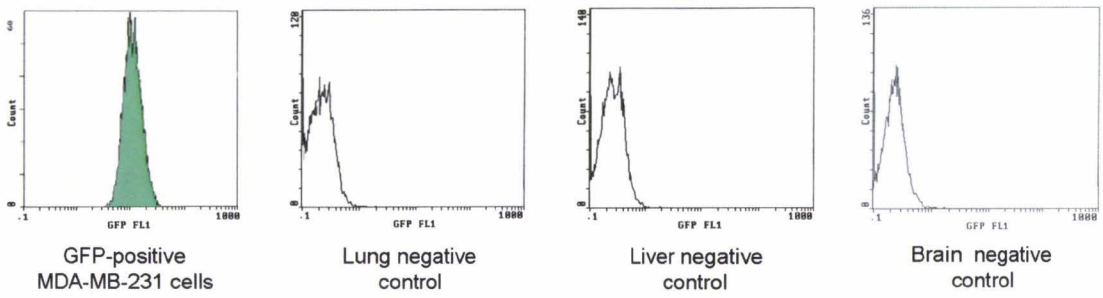

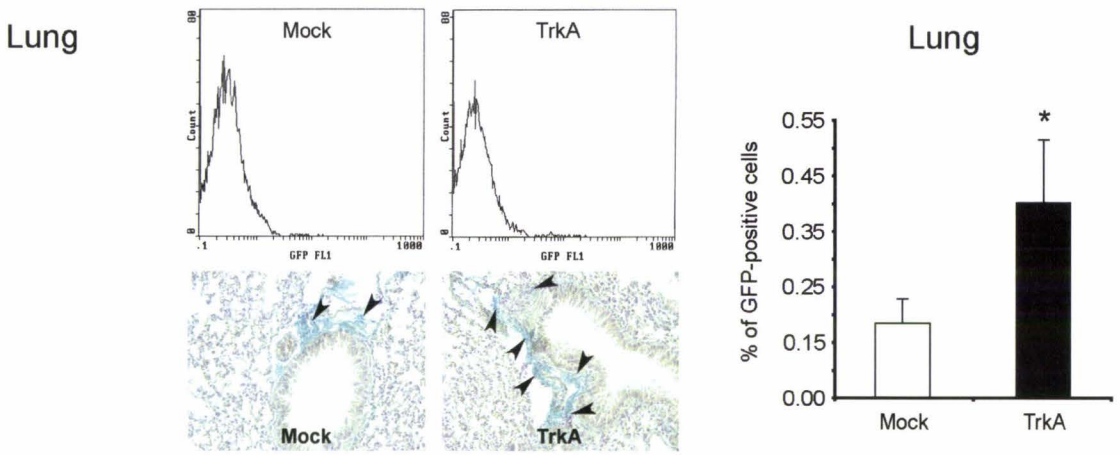

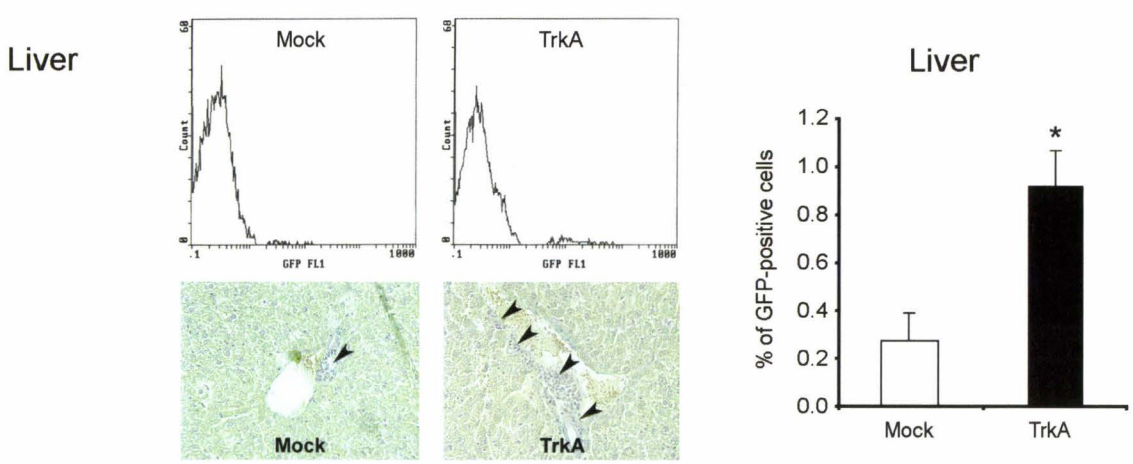

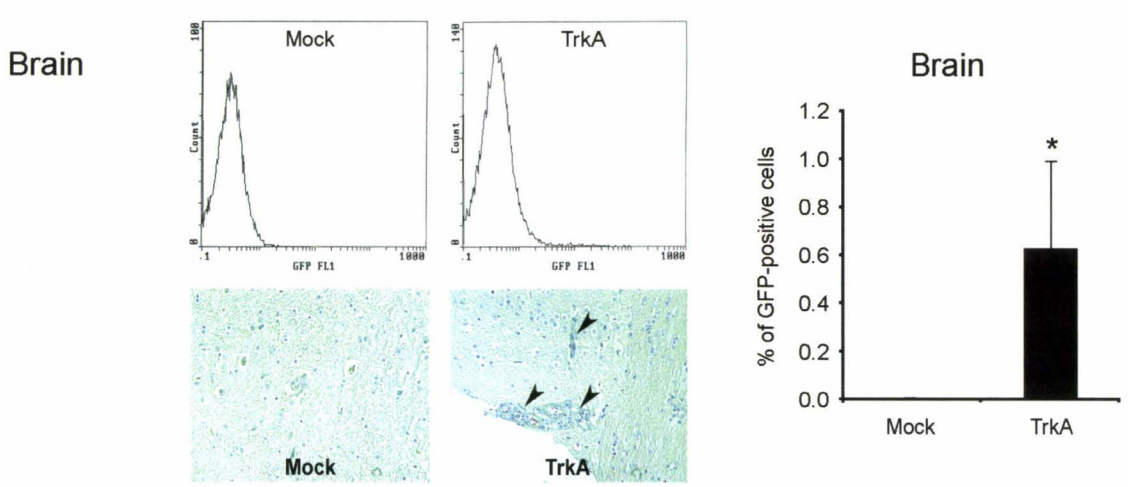

Figure 5 Lagadec *et al.*

Figure 6. Properties of lung metastatic TrkA overexpressing cells

A: Lung metastatic TrkA overexpressing cells were recultivated (13 cultures) from lungs of 9 mice subcutaneously injected with TrkA overexpressing cells. Immunoblots show the levels of pooled metastatic cells.

B: Growth assay on standard culture plastics.

C: Migration assay using Transwells.

D: Resistance to TRAIL-induced apoptosis.

E and F: Anoikis resistance of cells treated or no with K252a.

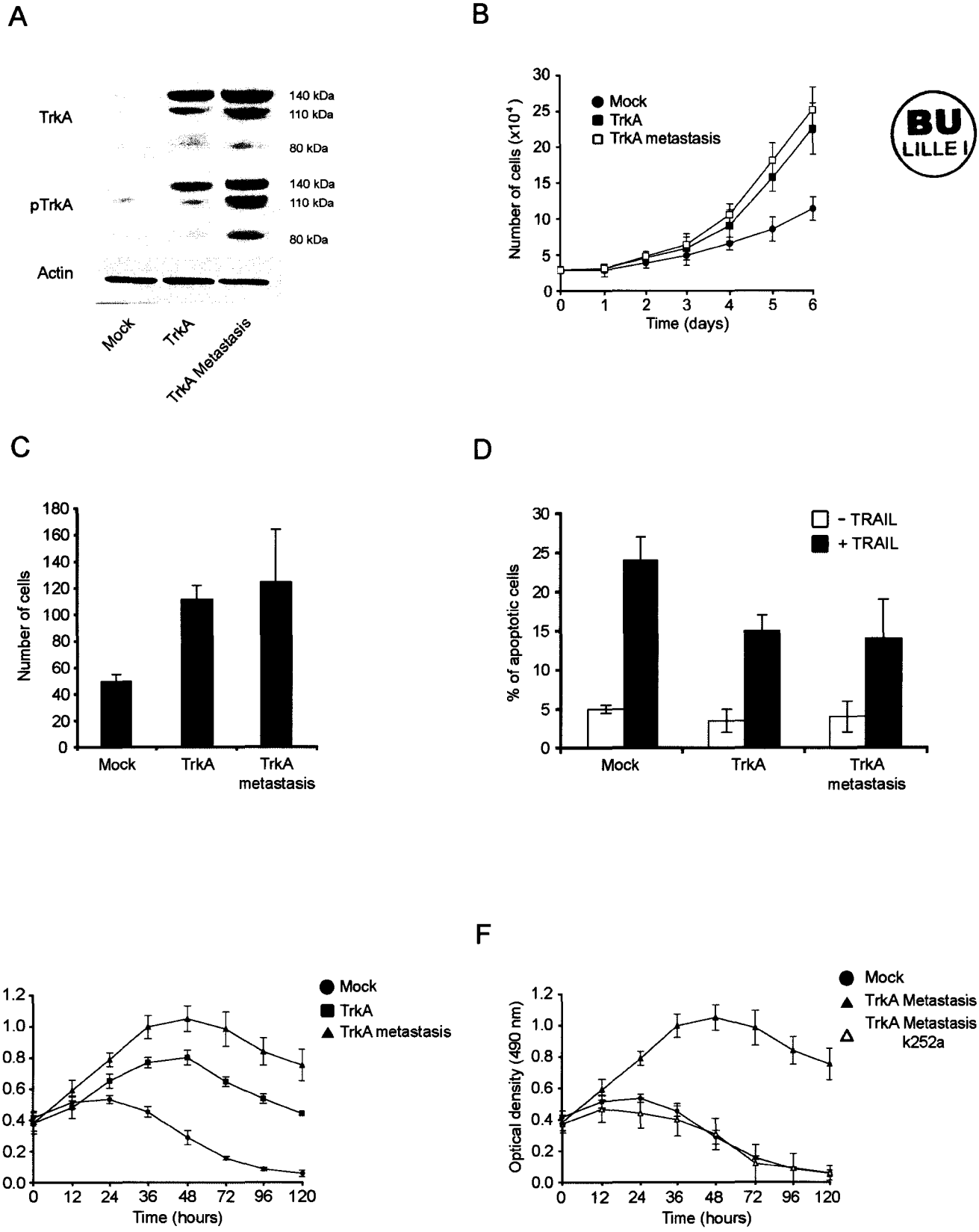

Figure 6 Lagadec *et al.*

Figure 7. Detection of TrkA and phospho-TrkA (pTrkA) in breast biopsies

A: Real time PCR detection of TrkA mRNA in normal and tumor biopsies which were mainly infiltrating ductal carcinoma. Levels of TrkA mRNA were expressed as relative quantity compared to that expressed by mock MDA-MB-231 breast cancer cells.

B: Western blot analysis of TrkA and pTrkA. Cancer biopsies used are: infiltrating lobular carcinoma (IL), infiltrating ductal carcinoma (ID) infiltrating mixed carcinoma (IM).

B and C: TrkA (B) and pTrkA (C) staining from breast cancer tissue microarrays. Breast cancer tissue microarrays (Cliniscience) included 10 normal breast samples and 37 tumor breast samples (2 ductal carcinoma *in situ*, 3 infiltrating lobular carcinoma, 32 infiltrating ductal carcinoma). Representative staining of normal tissue, infiltrating lobular carcinoma and infiltrating ductal carcinoma were shown. *, $p<0,01$.

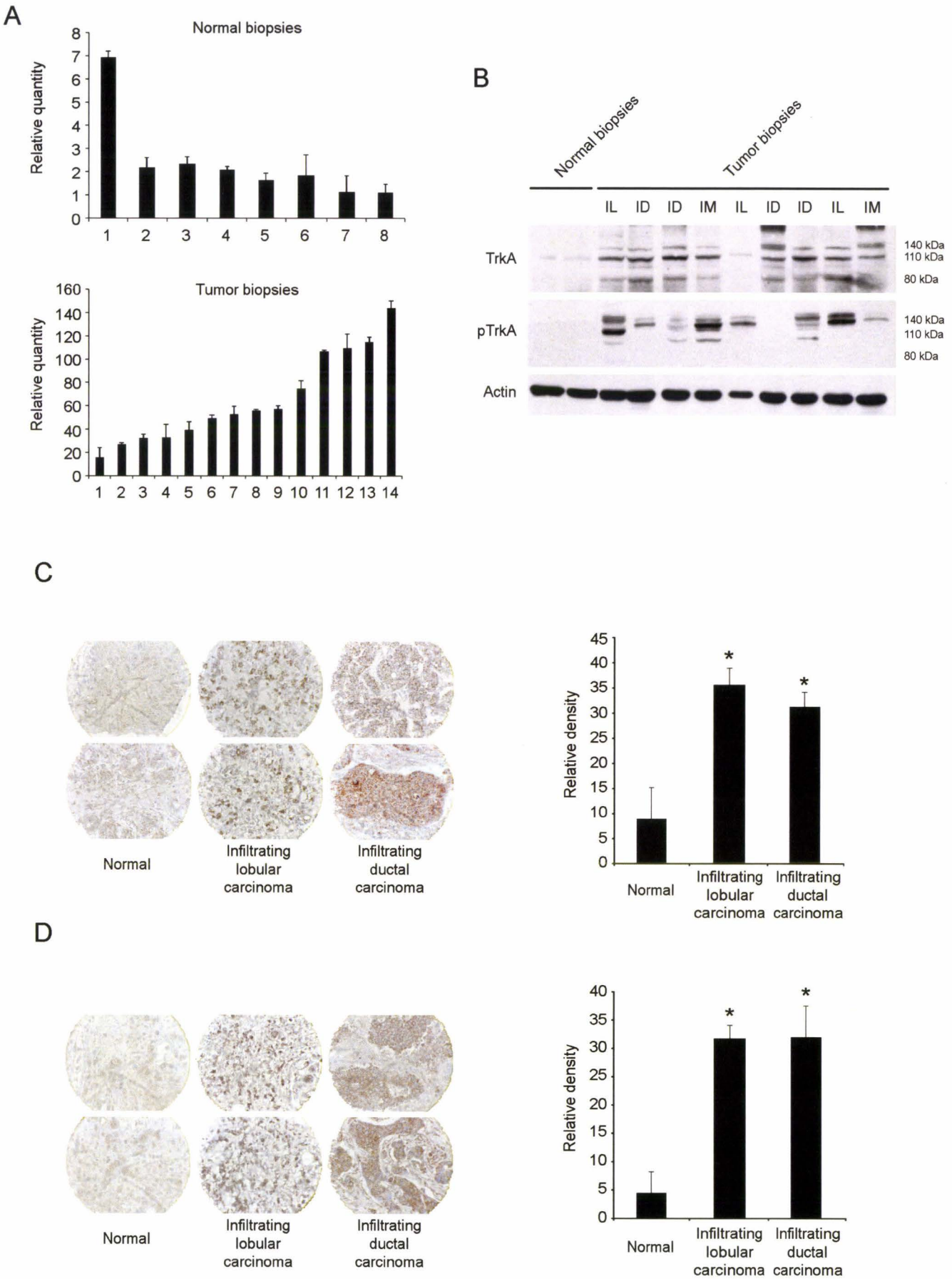

Figure 7 Lagadec *et al.*

Table 1. Effect of TrkA overexpression on incidence and severity of metastasis

	Mock				TrkA			
% of GFP positive cells	<0.2%	0.2-0.5%	0.5-1%	>1%	<0.2%	0.2-0.5%	0.5-1%	>1%
liver	2/8	4/8	1/8	1/8	0/9	3/9	5/9	1/9
lung	6/8	2/8	0/8	0/8	4/9	4/9	1/9	0/9
brain	3/8	0/8	0/8	0/8	1/9	5/9	2/9	1/9

Mice (8) injected with mock cells and mice (9) injected withTrkA overexpressing cells were killed when the average volume of primery tumors approached 2,000 mm^3. Liver, lung and brain of each mouse were recovered and digested with trypsin (2.5 mg/ml), collagenase (0.5 mg/ml) and hyaluronidase (0.5 mg/ml) for 1 h at 37°C to obtain individual cells. GFP-positive cells were then analysed using a Coulter Epics XL/XL-MCI cytometer.

Discussion

The biological effects as well as signaling pathways of NGF/TrkA are largely documented in neurones, but remain unclear in non-neuronal cells. Accumulating evidence suggests a role of NGF/TrkA axis in tumor growth and progression (Adriaenssens et al., 2007; Davidson et al., 2004; Dolle et al., 2003). We have previously shown that NGF can stimulate breast cancer cell growth while has no effect on normal breast epithelial cells (Descamps et al., 1998). Moreover, TrkA activation by NGF in cancer cells leads to cell proliferation *via* ERK MAP kinase activation. Here, we showed different degrees of stimulation by NGF/TrkA axis in MDA-MB-231 breast cancer cells depending on TrkA levels. Hence, cell growth on standard culture plastics and resistance to TRAIL-induced apoptosis were increased by NGF only in empty vector transfected cells (low levels of TrkA) but not in TrKA overexpressing cells. In contrast, cell migration and invasion as well as colony formation were stimulated by NGF whatever the levels of TrkA. These differences of sensitivity to NGF may reflect different intracellular downstream signalization pathways. We showed that TrkA overexpression enhanced phosphorylation of Akt, ERK and p38 MAP kinases. Moreover, PI3K-Akt and ERK were essential in TrkA-promoted cell growth, migration and survival. However, the downstream targets responsible of cell growth, migration and survival are different (Manning and Cantley, 2007). No further stimulation by exogenous NGF in TrkA overexpressing cells may by explained by the fact that one or more downstream targets are already saturated. Apart from PI3K-Akt and ERK pathways, p38 MAP kinase is also implicated in survival of TrkA overexpressing cells when cultured in suspension or soft agar. This is somewhat surprising, as p38 is generally considered as a pro-apoptotic kinase (Wada and Penninger, 2004). However, it has been reported that p38 is a mediator

of H-ras induced cell mobility and invasion in MCF-10A human breast epithelial cells. Moreover, p38 acts in concert with ERK to increase cell migration and invasion (Kim et al., 2003). p38 can also activate the pro-survival PI3-Akt pathway in fibroblasts (Horowitz et al., 2004). Therefore, the consequences of p38 activation may vary according to cell context. Clearly, more work is required to fully comprehend signaling pathways of TrkA-mediated biological effects in breast cancer cells.

Another important finding of our work is increased anoikis resistance in TrkA overexpressing cells. Anoikis resistance seemed to be specific to TrkA overexpression, as exogenous NGF had no effect in either empty vector transfected or TrKA overexpressing cells. Anoikis is defined as apoptosis caused by lack of adhesion (Frisch and Screaton, 2001). However, the corresponding molecular mechanisms are not fully elucidated. We showed that pharmalogical inhibition of PI3K, Akt and ERK abrogated anoikis resistance, while p38 inhibition only slightly reduced it. This indicates that the PI3K-Akt pathway as well as ERK MAP kinase are essential for inhibition of anoikis in TrkA overexpressing breast cancer cells. It has been recently found that in mouse embryo fibroblasts transformed by the ETV6-NTRK3 chimeric tyrosine kinase, an intact insulin-like growth factor I receptor axis is essential for suppression of anoikis (Martin et al., 2006). Similarly, TrkB suppresses anoikis in rat intestinal epithelial cells through activation of the PI3K-Akt pathway, (Douma et al., 2004; Geiger and Peeper, 2007). In contrast, suppression of anoikis in ovarian carcinoma cells through E-cadherin–mediated activation of ErbB1 requires induction of the Ras-ERK1/2 cascade but not PI3K-Akt (Shen and Kramer, 2004). Moreover, other pathways such as Janus-activated kinase-signal transducers and activators of transcription-3 signaling are also implicated in anchorage-independent growth (Zhang et al., 2006). It is therefore likely that cell context is important for

determining the exact molecular mechanisms used for this process (Frisch and Screaton, 2001; Grossmann, 2002). The common theme is that the activation of tyrosine kinases may be critical for suppression of anoikis in tumor cells.

Acquisition of resistance to anoikis may allow survival of cancer cells during systemic circulation and facilitate tumor dormancy or metastasis in distant organs. Accordingly, a functional genomic screen for genes that suppress anoikis leads to the identification of neurotrophic receptor TrkB as an oncoprotein associated with metastatic capacity (Douma et al., 2004). Overexpression of TrkB renders normal intestinal epithelial cells anoikis resistant and highly tumorigenic. Moreover, TrkB overexpressing cells form highly invasive and metastatic tumors in nude mice. Here, we provide the first evidence that TrkA can also promote breast tumor metastasis by enhancing anoikis resitance. However, given the complexity of metastasis process, cancer cells must acquire a series of traits that enable them to overcome multiple barriers erected by normal tissues. The observed enhancement in cell migration and invasion may also potentiate metastasis of TrkA overexpressing cells. Therfore, TrkA overexpression can endow cancer cells with various capacities for metastasis.

Not only is metastasis promoted by TrkA overexpression, our in vivo study showed also that TrkA overexpressing cells exhibit accelerated primary tumor growth which is associated with increased cell proliferation and angiogenesis. This is consistent with our previous work showing that inhibition of TrkA by tyrosine inhibitor K252a efficiently inhibited tumor growth, cell proliferation and angiogenesis (Adriaenssens et al., 2007). NGF has already been suspected as angiogenic as it can stimulate proliferation and tubule formation of human umbilical vein endothelial cells (Cantarella et al., 2002). In addition, some *in vivo* evidence suggests an NGF-mediated pro-angiogenic activity in ovarian cancer (Davidson et al., 2003),

although it is not yet known if this results from a direct or indirect stimulation of endothelial cells, as NGF can also induce the expression of pro-angiogenic factors such as VEGF (Campos et al., 2007). Similarly, it needs to be clarified how TrkA overexpressing tumor cells can stimulate tumor angiogenesis.

In conclusion, we show that TrkA overexpression per se can enhance tumor growth and metastasis in a mouse xenograft model. Moreover, high levels of TrkA and phospho-TrkA were fond in breast cancer samples. These findings imply that development of targeting of TrkA dependent signaling is justified. Furthermore, given the correlation of anoikis resistance and metastatic potential, suppression of anoikis resistance would contribute to limiting metastasis and could be useful in combination with treatments that directly targets primary tumor growth (Sledge and Miller, 2003).

Experimental procedures

Human breast biopsies. Normal breast tissues were obtained from individuals treated by mastectomy at the hospital of Lille (France). Breast carcinoma specimens were obtained from Clinique du Croisé la roche (Lille, France) and were selected on the basis of being the first and unilateral cancer; these samples were collected with institutional safety review board approval. Breast cancer tissue microarrays (Cliniscience) included 10 normal breast samples and 37 tumor breast samples (2 ductal carcinoma *in situ*, 3 infiltrating lobular carcinoma, 32 infiltrating ductal carcinoma).

Cell culture, transfection and generation of TrkA overexpressing cancer cells. The MDA-MB-231 breast cancer cell line was obtained from the American Type Culture Collection. Cells were maintained in EMEM medium supplemented with 10% fetal calf serum (FCS). The TrkA expression vector (pcDNA3.1-hygro/TrkA) was prepared by inserting TrkA cDNA from MDA-MB-231 cells into the EcoRI cloning site of the pcDNA3.1-hygro vector (invitrogen) Cell transfections were done using LipofectAMINE 2000 (Invitrogen) according to the manufacturer's instruction. Cells were selected with 800 µg/ml hygromycin, The resulted hygromycin resistant pools were stored as frozen stocks and used for all the experiments within 20 passages. Expression of TrkA by Western blot showed no change with passages *in vitro* and after growth to form primary tumors *in vivo*. For metastasis assay, MDA-MB-231 cells (empty vector transfected and TrkA overexpressing cells) were stably transfected with a pGFP-C1 expression vector (invitrogen) and selected with 1000 µg/ml G418. GFP-positive cells were selected by fluorescence-activated cell sorting (FACS). The

selected cells expressed similar levels of GFP, and presented the same properties as their parental cells in terms of TrkA expression, cell morphology, migration and growth.

Real Time PCR (RT-PCR). Total RNAs were isolated with the Nucleospin RNAII isolation kit (Macherey-Nagel, Belgium). Reverse transcription was performed with 1 µg of RNAs, 1 µg of random hexamers, 20 units of Moloney murine leukemia virus reverse transcriptase (Invitrogen life technologies, USA) for 10 min at 25 °C, 50 min at 37 °C and 15 min at 70 °C in a final volume of 20 µl for 1 h at 37 °C in a final volume of 100 µl. TrkA RT-PCR was performed using Hs_NTRK1_SG_1 QuantiTect® Primer Assays (Qiagen, France). The subsequent PCR conditions were 40 cycles, carried out in the following manner: 95 °C for 15 sec, 60 °C for 20 sec, and 72 °C for 30 sec. Data were analyzed using the MX4000 PCR system software (Stratagene). Quantification of TrkA mRNA in breast biopsies was performed as previously described (Adriaenssens et al., 2007), and levels of TrkA mRNA were expressed as relative quantity compared to that expressed by mock MDA-MB-231 breast cancer cells.

Western blot analysis. The proteins were separated by SDS-PAGE and then transferred to polyvinylidene difluoride membranes (Millipore, Bedford, MA). Blots were blocked and then probed with antibodies against TrkA (1:500 dilution, cell signalling), phospho-TrkA (1:1,000 dilution; Santa Cruz Biotechnology), Akt (1:1,000 dilution; Santa Cruz Biotechnology), phospho-Akt (Ser473; 1:400 dilution; Santa Cruz Biotechnology), extracellular signal-regulated kinase (ERK; 1:1,000 dilution; Santa Cruz Biotechnology), phospho-ERK (Tyr204; 1:400 dilution; Santa Cruz

Biotechnology), p38 (1:1,000 dilution, Cell Signaling), phospho-p38 (1:1,000 dilution, Cell Signaling) and ß-actin (1:5,000 dilution; Sigma). After washing, the blots were incubated with horseradish peroxidase–conjugated secondary antibodies and visualized by super ECL detection reagent (Pierce).

Growth assay. Cells (3 x10^4) were plated in EMEM 10% FCS. Twenty-four hours later, cells were starved in EMEM serum-free medium for 24 h and then treated with NGF (200 ng/ml) in EMEM 0.1% FCS. Cell numbers were evaluated every day using Malassey's cell.

Apotosis analysis. Cells were starved in serum-free medium (12 h) and then pretreated with 200 ng/ml NGF (1 h) before treatment with 5 ng/ml TRAIL, 2 µM doxorubicin, or 10 µM 5-fluorouacil in the presence of NGF for 6 h. Apoptosis was determined by morphological analysis as previously described (Lagadec et al., 2007).

Anoikis assay. Cells were seeded on poly-HEMA (Sigma)-coated 96 wells plates (15 mg/ml) (1x10^5 cells/well) in EMEM 1% FCS and cultured in the presence or absence of NGF (200 ng/ml) for different periods of time. Cell viability was analyzed by 3-(4,5-dimethylthiazol-2-yl)-5-(3-carboxymethoxyphenyl)-2-(4-sulfophenyl)-2H tetra-zolium (MTS, Promega) assay according to the user manual.

Migration and Matrigel chemoinvasion assays. For cell migration assay, 5 x 10^4 cells were seeded on polycarbonate membrane insert (6.5 mm in diameter with 8 µm pores) in a Transwell apparatus (BD Bioscience) and maintained in EMEM containing 0.1% FCS. NGF (200 ng/ml) was added to the lower chamber. After 6 h of culture,

the insert was washed with PBS, and cells on the top surface of the insert were removed by wiping with a cotton swab. For the Matrigel chemoinvasion assay, the procedure was similar with the cell migration assay, except that the Transwell membrane was coated with Matrigel (BD Biosciences), and the cells were incubated for 16 h. Cells that migrated to the bottom surface of the insert were fixed with methanol and stained by Hoechst 33258 and then subjected to fluorescence microscopic inspection. Cells were counted on 10 random fields at x200.

Wound-healing assay. Cells were plated onto a 35 mm culture dish and allowed to form a confluent monolayer then wounded using a pipette tip. Cells were then treated with 200 ng/ml NGF for further 24 h in EMEM containing 0.1% FCS. Wounded cultures were photographed at the beginning and the end of the experiment.

Adhesion assay. Cells were plated on fibronectin-, collagen I-, Collagen IV- and matrigel-coated 96-well plates (10 $\mu g/cm^2$) ($5x10^4$ cells/well) and cultured for 30, 60, and 90 minutes, respectively. Nonattached cells were removed by three washings with PBS. Attached cells were analyzed by MTS assay according to the user manual (Promega).

Soft agar assay for colony formation. The procedure was based on a modified method as described (Toillon et al., 2002). MDA-MB-231 cells were plated in six-well plates at a density of 500 per well and treated with 200 ng/ml NGF. After 3 weeks of culture, colonies of more than 20 cells were counted. Three independent wells were examined for each experiment.

Tumor growth. Six-week-old female SCID mice were purchased from Charles River Laboratories (France), and acclimatized for at least 2 weeks. Mice were maintained under a 12 h light/dark cycle at a temperature of 20-22°C. Food and water were available *ad libitum*. Mice were maintained in accordance with the Institutional Animal Care and Use Committee procedures and guidelines. MDA-MB-231 mock and TrkA overexpressing cells were harvested and resuspended in PBS before subcutaneous injection into flanks ($2x10^6$ cells/flank) of 8-week-old SCID mice. The tumor volume was determined every week by measuring the length (l) and width (w) and then calculating the volume as $\frac{\pi}{6} lw \frac{(l+w)}{2}$.

Immunohistochemistry and TUNEL staining. TrkA and phospho-TrkA stainging was performed using tissue microarrays according to the manufacturer's instructions. Xenograft tumor samples were fixed in 10% neutral formalin buffer, embedded in paraffin, sectioned at 5 µm, dewaxed by methylcyclohexane (3 x10 min) and rehydrated through a graded series of ethanol and water. For Immunohistochemistry, tissue sections were incubated with tri sodium citrate buffer 10 mM (pH 6) for 40 min at 100°C. Mouse monoclonal antibody against PCNA (1:80) from Calbiochem and rat monoclonal antibody against vWF (1:50) from Novus Biological were used. These primary antibodies were incubated 1 h at 37°C. Biotinylated goat anti-mouse or anti-rat antibodies (Sigma-Aldricht) were used as the secondary antibodies (1:200, 1 h at room temperature). The slides were treated with the Renaissance TSA Biotin System kit (from Perkin Elmer) according to manufacturer's instruction. The signals were visualized with SIGMAFAST™ 3,3′-Diaminobenzidine tablets (Sigma-Aldrich) for 5 min. The sections were then counterstained with hematoxylin (Sigma-Aldricht) and mounted with Dako Glycergel (Dakocytomation). All sections were washed

(3 x 5 min) with TNT buffer (pH 7.6) after each step. Negative controls included substitution of the primary antibody with PBS. For terminal deoxynucleotidyl transferase-mediated dUTP nick end labelling (TUNEL) assay, tissue sections were rehydrated and then incubated with proteinase K for 30 min at 37°C. Apoptotic cells were detected by the TUNEL assay *in situ* cell death detection kit (Roche Molecular Biochemicals) according to the manufacturer's instructions. Positive TUNEL staining was visualized using SIGMAFAST™ 3,3′-Diaminobenzidine tablets (Sigma-Aldricht).

Computer-assisted image analysis. The immunostained cells were quantitatively analyzed using a computer-assisted image analysis system as previously described (Jallal et al., 2007). Briefly, images of stained sections were captured with an Olympus digital camera and processed using Photoshop CS3 extended edition (Adobe System). The total pixel areas (in $pixel^2$) of stained cells and of all cells were quantified by the software. The percentages of stained cells in the microscopic field were then calculated.

Assessment of metastasis. GFP-positive cells were subcutaneously injected into flanks ($2x10^6$ cells/flank) of 8-week-old SCID mice as described above. Once the average tumor size was >2,000 mm^3, the mice were sacrificed and their lung, liver and brain were removed for further analysis. The organs were cupped to 2 parts: One half for histological analysis, total numbers of metastases per organ were determined by collecting serial lung sections, at distances of approximately 0.3 mm. The other half of organ was digested with enzymes (2.5 mg/ml trypsine, 0.5 mg/ml collagenase, 0.5 mg/ml hyalluronidase) for 1 h at 37°C before quantification of metastatic cells (GFP-postive) by FACS analysis. Cultured GFP-positive MDA-MB-231 cells were

used as positive control. Cells derived from lung, liver and brain of a mice inoculated with GFP-negative MDA-MB-231 cells were used as negative control. To recultivate metastatic cells from lungs, enzymatic digests were washed once in 10 ml EMEM 10% FCS and seeded in cell culture dishes in DMEM 10% FCS with 800 µg/ml hygromycin for 2-3 weeks. Selected tumor cells were then confirmed by analysis of GFP and TrkA expression.

Statistical analysis. Statistical differences were determined with two-tailed Student's *t* tests. All *p* values were two-sided. $p<0.05$ was considered as statistically significant.

ACKNOWLEDGMENTS

Grant support: INSERM, la Ligue Nationale Contre le Cancer (Equipe labellisée 2006), le Ministère de l'Education Nationale and the Région Nord/Pas-de-Calais. Chann Lagadec was the recipient of a fellowship from the Association pour la Recherche sur le Cancer (ARC).

References

Adriaenssens, E., Vanhecke, E., Saule, P., Mougel, A., Page, A., Romon, R., Nurcombe, V., LeBourhis, X., Hondermarck, H., and (2007). Nerve Growth Factor is a Potential Molecular Target in Breast Cancer Submitted in Cancer Research.

Buck, M. B., and Knabbe, C. (2006). TGF-beta signaling in breast cancer. Ann N Y Acad Sci *1089*, 119-126.

Burger, A. M., Leyland-Jones, B., Banerjee, K., Spyropoulos, D. D., and Seth, A. K. (2005). Essential roles of IGFBP-3 and IGFBP-rP1 in breast cancer. Eur J Cancer *41*, 1515-1527.

Campos, X., Munoz, Y., Selman, A., Yazigi, R., Moyano, L., Weinstein-Oppenheimer, C., Lara, H. E., and Romero, C. (2007). Nerve growth factor and its high-affinity receptor trkA participate in the control of vascular endothelial growth factor expression in epithelial ovarian cancer. Gynecol Oncol *104*, 168-175.

Cantarella, G., Lempereur, L., Presta, M., Ribatti, D., Lombardo, G., Lazarovici, P., Zappala, G., Pafumi, C., and Bernardini, R. (2002). Nerve growth factor-endothelial cell interaction leads to angiogenesis in vitro and in vivo. Faseb J *16*, 1307-1309.

Chan, S. K., Hill, M. E., and Gullick, W. J. (2006). The role of the epidermal growth factor receptor in breast cancer. J Mammary Gland Biol Neoplasia *11*, 3-11.

Chang, C. F., Westbrook, R., Ma, J., and Cao, D. (2007). Transforming growth factor-beta signaling in breast cancer. Front Biosci *12*, 4393-4401.

Chao, M. V. (1994). The p75 neurotrophin receptor. J Neurobiol *25*, 1373-1385.

Chong, Y. M., Subramanian, A., Sharma, A. K., and Mokbel, K. (2007). The potential clinical applications of insulin-like growth factor-1 ligand in human breast cancer. Anticancer Res *27*, 1617-1624.

Davidson, B., Reich, R., Lazarovici, P., Ann Florenes, V., Nielsen, S., and Nesland, J. M. (2004). Altered expression and activation of the nerve growth factor receptors TrkA and p75 provide the first evidence of tumor progression to effusion in breast carcinoma. Breast Cancer Res Treat *83*, 119-128.

Davidson, B., Reich, R., Lazarovici, P., Nesland, J. M., Skrede, M., Risberg, B., Trope, C. G., and Florenes, V. A. (2003). Expression and activation of the nerve growth factor receptor TrkA in serous ovarian carcinoma. Clin Cancer Res *9*, 2248-2259.

Descamps, S., Lebourhis, X., Delehedde, M., Boilly, B., and Hondermarck, H. (1998). Nerve growth factor is mitogenic for cancerous but not normal human breast epithelial cells. J Biol Chem *273*, 16659-16662.

Dionne, C. A., Camoratto, A. M., Jani, J. P., Emerson, E., Neff, N., Vaught, J. L., Murakata, C., Djakiew, D., Lamb, J., Bova, S., *et al.* (1998). Cell cycle-independent

death of prostate adenocarcinoma is induced by the trk tyrosine kinase inhibitor CEP-751 (KT6587). Clin Cancer Res *4*, 1887-1898.

Dolle, L., El Yazidi-Belkoura, I., Adriaenssens, E., Nurcombe, V., and Hondermarck, H. (2003). Nerve growth factor overexpression and autocrine loop in breast cancer cells. Oncogene *22*, 5592-5601.

Douma, S., Van Laar, T., Zevenhoven, J., Meuwissen, R., Van Garderen, E., and Peeper, D. S. (2004). Suppression of anoikis and induction of metastasis by the neurotrophic receptor TrkB. Nature *430*, 1034-1039.

Festuccia, C., Gravina, G. L., Muzi, P., Pomante, R., Ventura, L., Ricevuto, E., Vicentini, C., and Bologna, M. (2007). In vitro and in vivo effects of bicalutamide on the expression of TrkA and P75 neurotrophin receptors in prostate carcinoma. Prostate *67*, 1255-1264.

Friess, H., Zhu, Z. W., di Mola, F. F., Kulli, C., Graber, H. U., Andren-Sandberg, A., Zimmermann, A., Korc, M., Reinshagen, M., and Buchler, M. W. (1999). Nerve growth factor and its high-affinity receptor in chronic pancreatitis. Ann Surg *230*, 615-624.

Frisch, S. M., and Screaton, R. A. (2001). Anoikis mechanisms. Curr Opin Cell Biol *13*, 555-562.

Geiger, T. R., and Peeper, D. S. (2007). Critical role for TrkB kinase function in anoikis suppression, tumorigenesis, and metastasis. Cancer Res *67*, 6221-6229.

Grossmann, J. (2002). Molecular mechanisms of "detachment-induced apoptosis--Anoikis". Apoptosis *7*, 247-260.

Horowitz, J. C., Lee, D. Y., Waghray, M., Keshamouni, V. G., Thomas, P. E., Zhang, H., Cui, Z., and Thannickal, V. J. (2004). Activation of the pro-survival phosphatidylinositol 3-kinase/AKT pathway by transforming growth factor-beta1 in mesenchymal cells is mediated by p38 MAPK-dependent induction of an autocrine growth factor. J Biol Chem *279*, 1359-1367.

Jallal, H., Valentino, M. L., Chen, G., Boschelli, F., Ali, S., and Rabbani, S. A. (2007). A Src/Abl kinase inhibitor, SKI-606, blocks breast cancer invasion, growth, and metastasis in vitro and in vivo. Cancer Res *67*, 1580-1588.

Katzir, I., Shani, J., Shabashov, D., Dagan, J., and Lazarovici, P. (2003). Establishment and characterization of pheochromocytoma tumor models expressing different levels of trkA receptors. Cancer Lett *200*, 177-185.

Kim, M. S., Lee, E. J., Kim, H. R., and Moon, A. (2003). p38 kinase is a key signaling molecule for H-Ras-induced cell motility and invasive phenotype in human breast epithelial cells. Cancer Res *63*, 5454-5461.

Lagadec, C., Adriaenssens, E., Toillon, R. A., Chopin, V., Romon, R., Van Coppenolle, F., Hondermarck, H., and Le Bourhis, X. (2007). Tamoxifen and TRAIL synergistically induce apoptosis in breast cancer cells. Oncogene.

Manning, B. D., and Cantley, L. C. (2007). AKT/PKB signaling: navigating downstream. Cell *129*, 1261-1274.

Martin, M. J., Melnyk, N., Pollard, M., Bowden, M., Leong, H., Podor, T. J., Gleave, M., and Sorensen, P. H. (2006). The insulin-like growth factor I receptor is required for Akt activation and suppression of anoikis in cells transformed by the ETV6-NTRK3 chimeric tyrosine kinase. Mol Cell Biol *26*, 1754-1769.

McGregor, L. M., McCune, B. K., Graff, J. R., McDowell, P. R., Romans, K. E., Yancopoulos, G. D., Ball, D. W., Baylin, S. B., and Nelkin, B. D. (1999). Roles of trk family neurotrophin receptors in medullary thyroid carcinoma development and progression. Proc Natl Acad Sci U S A *96*, 4540-4545.

Mercurio, A. M., Lipscomb, E. A., and Bachelder, R. E. (2005). Non-angiogenic functions of VEGF in breast cancer. J Mammary Gland Biol Neoplasia *10*, 283-290.

Mukai, J., Suvant, P., and Sato, T. A. (2003). Nerve growth factor-dependent regulation of NADE-induced apoptosis. Vitam Horm *66*, 385-402.

Reichardt, L. F. (2006). Neurotrophin-regulated signalling pathways. Philos Trans R Soc Lond B Biol Sci *361*, 1545-1564.

Ricci, A., Greco, S., Mariotta, S., Felici, L., Bronzetti, E., Cavazzana, A., Cardillo, G., Amenta, F., Bisetti, A., and Barbolini, G. (2001). Neurotrophins and neurotrophin receptors in human lung cancer. Am J Respir Cell Mol Biol *25*, 439-446.

Roussidis, A. E., Theocharis, A. D., Tzanakakis, G. N., and Karamanos, N. K. (2007). The importance of c-Kit and PDGF receptors as potential targets for molecular therapy in breast cancer. Curr Med Chem *14*, 735-743.

Shen, X., and Kramer, R. H. (2004). Adhesion-mediated squamous cell carcinoma survival through ligand-independent activation of epidermal growth factor receptor. Am J Pathol *165*, 1315-1329.

Sledge, G. W., Jr., and Miller, K. D. (2003). Exploiting the hallmarks of cancer: the future conquest of breast cancer. Eur J Cancer *39*, 1668-1675.

Toillon, R. A., Chopin, V., Jouy, N., Fauquette, W., Boilly, B., and Le Bourhis, X. (2002). Normal breast epithelial cells induce p53-dependent apoptosis and p53-independent cell cycle arrest of breast cancer cells. Breast Cancer Res Treat *71*, 269-280.

Ursini-Siegel, J., Schade, B., Cardiff, R. D., and Muller, W. J. (2007). Insights from transgenic mouse models of ERBB2-induced breast cancer. Nat Rev Cancer *7*, 389-397.

Wada, T., and Penninger, J. M. (2004). Mitogen-activated protein kinases in apoptosis regulation. Oncogene *23*, 2838-2849.

Weeraratna, A. T., Arnold, J. T., George, D. J., DeMarzo, A., and Isaacs, J. T. (2000). Rational basis for Trk inhibition therapy for prostate cancer. Prostate *45*, 140-148.

Zhang, W., Zong, C. S., Hermanto, U., Lopez-Bergami, P., Ronai, Z., and Wang, L. H. (2006). RACK1 recruits STAT3 specifically to insulin and insulin-like growth factor 1 receptors for activation, which is important for regulating anchorage-independent growth. Mol Cell Biol *26*, 413-424.

Zhu, Z., Friess, H., diMola, F. F., Zimmermann, A., Graber, H. U., Korc, M., and Buchler, M. W. (1999). Nerve growth factor expression correlates with perineural invasion and pain in human pancreatic cancer. J Clin Oncol *17*, 2419-2428.

III. La stimulation de la migration des cellules cancéreuses de sein par TrkA implique Ku86 (Article 3).

En préparation.

Ce 3ème chapitre constitue une étude plus approfondie du mécanisme moléculaire de l'action de TrkA par protéomique fonctionnelle (modifications du protéomes par aprroche globale et recherche de partenaire de TrkA après immunoprécipitation). On y trouvera les protéines dont le niveau d'expression est modifié dans les cellules surexprimant TrkA. Nous avons notamment montré que l'expression de Ku86 est augmentée dans ces cellules. De plus, Ku86 participe à l'augmentation de la migration cellulaire induite par la surexpression de TrkA. L'ensemble des résultats obtenu est présenté sous forme d'un article.

Upregulation of Ku86 is crucial for TrkA-stimulated migration of breast cancer cells

Chann Lagadec, Christophe Tastet, Samuel Meignan, Emmanuelle Com, Adeline Page, Hubert Hondermarck and Xuefen Le Bourhis

INSERM ERI-8 (JE-2488) "Growth factor signaling in breast cancer. Functional proteomics" IFR 147, University of Sciences and Technologies Lille, Villeneuve d'Ascq, France

*Correspondence: xuefen.lebourhis@univ-lille1.fr

Running title: Ku86 upregulation contributes to TrkA-stimulated migration

Abstract

We have previously shown that TrkA overexpression increases the aggressive phenotype of breast cancer cells. Identification of specific effector proteins is of major interest for the understanding of TrkA function in breast carcinoma. Here we used a functional proteomic approach to identify molecules involved in TrkA-mediated biological effects in MDA-MB-231 TrkA overexpressing breast cancer cells. We first separated proteins using a cup-loading two-dimensional electrophoresis system and then identified a series of putative modified proteins by MALDI and LC-MS/MS mass spectrometry analysis. Interestingly, the major increased protein in TrkA overexpressing cells was found to be Ku86. Moreover, Ku 86 was required for TrkA-stimulated migration while it was not involved in TrkA-induced resistance to anokis or apoptosis induction by TRAIL. Ku86 seemed to function independently of Ku70, though both Ku86 and Ku70 were co-immunoprecipitated with TrkA and their levels at cell surface were found to be increased in TrkA overexpressing cells. Together, these data identify Ku86 as a new mediator of TrkA-stimulated migration.

Introduction

Several sets of growth factors and their cognate receptors are known to be importantly involved in the regulation of cancer development (Burger et al. 2005; Mercurio et al. 2005; Buck and Knabbe 2006; Chan et al. 2006; Chang et al. 2007; Chong et al. 2007; Roussidis et al. 2007; Ursini-Siegel et al. 2007). Nerve growth factor (NGF) is the prototypic member of the neurotrophin family of proteins that is mainly described for promoting survival and differentiation of neuronal cells during nervous system development. However, accumulating data indicate that NGF may also play a role in cancer development (Nakagawara 2001; Papatsoris et al. 2007). NGF exerts its effects through two membrane receptors: the tyrosine kinase receptor TrkA and the receptor $p75^{NTR}$, a common receptor for all neurotrophins and pro-neurotropins. NGF binding to TrkA induces TrkA receptor dimerisation and autophosphorylation of cytoplasmic tyrosines leading to the activation of various signaling pathways, including the Ras/MAPK pathway, the PLCγ pathway, and the PI3K/Akt pathway (Patapoutian and Reichardt 2001). The biological consequences of TrkA activation vary according to cell types. Hence, activation of TrkA by NGF induces differentiation of neuronal precursors and neuroblastoma cells, whereas it induces proliferation in breast adenocarcinoma cells and apoptosis in medulloblastoma cells (Descamps et al. 1998; Schramm et al. 2005; Micera et al. 2007). Upregulation of TrkA has been shown in many cancers including medullary thyroid carcinoma (McGregor et al. 1999), lung (Ricci et al. 2001), pancreatic (Friess et al. 1999; Zhu et al. 1999), prostate (Weeraratna et al. 2000; Festuccia et al. 2007), ovarian (Davidson et al. 2003; Campos et al. 2007) and breast carcinomas (Davidson et al. 2004). Moreover, it has been described that phospho-TrkA, the active form of

NGF tyrosine kinase receptor, is associated with an aggressive phenotype and a bad prognosis in breast cancers (Davidson et al. 2004).

We have previously demonstrated that NGF can stimulate growth and migration of breast cancer cells through an autocrine loop (Descamps et al. 1998; Dolle et al. 2003; Dolle et al. 2005). In additional way, neutralizing antibody or siRNA against NGF, or inhibition of TrkA by K252a induce a strong reduction of tumor growth in breast cancer (Adriaenssens et al. submitted in Cancer Research). More recently, we have shown that TrkA overexpression in MDA-MB-231 breast cancer cells increases cell growth, migration, invasion as well as resistance to anoikis. Primary tumor growth and matstasis were also enhanced in a xenograft model of SCID mice (Lagadec et al. submitted in Cancer Cell). Therefore, TrkA overexpression in breast cancer cells increases further their aggressive phenotype. Despite these findings of TrkA implication in breast cancer development, the underlying molecular mechanisms are largely unknown.

As the identification of specific effector proteins is of major interest for the understanding of TrkA function in solid tumors particularly in breast carcinoma, we have used a functional proteomic approach to identify molecules involved in TrkA-mediated biological effects. For this, we first separated proteins using a cup-loading two-dimensional electrophoresis (2D) system and then identified a series of putative modified proteins by MALDI and LC-MS/MS mass spectrometry analysis. We found that Ku86, initially described to form a heterodimer with ku70 to regulate DNA-dependent protein kinase (DNA-PK) that is crucial to DNA repair, was upregulated in TrkA overexpressing cells. Moreover, Ku 86 was required for TrkA-stimulated

migration while it was not involved in TrkA-induced resistance to anokis or apoptosis induction by TRAIL.

Experimental procedures

Materials

Cell culture reagents were purchased from Bio-Whittaker. Recombinant NGF was from R&D systems. Nucleofection reagents were from Amaxa Biosystems. Dynabeads protein A and protein G were obtained from Dynal Biotech. Electrophoresis reagents, bicinchoninic acid reagents, protease inhibitor cocktail and rabbit polyclonal anti-actin antibody were from Sigma. Sequencing grade-modified trypsin was provided by Promega. ZipTip$_{C18}$ pipette tips were obtained from Millipore. The monoclonal anti-Ku86 for immunofluorescence (S5C11) and neutralizing antibodies Anti-Ku70 (clone N3H10) and anti-Ku86 (clone 111 or S10B1) were purchased from Thermo Scientific. For Western blotting, the polyclonal anti-Ku70 (AHP316), the monoclonal anti-Ku86 (111) and the polyclonal anti-actin were purchased from AbD Serotec, GeneTex and Sigma, respectively. The rabbit polyclonal anti-TrkA IgG was from Upstate. Peroxidase-conjugated donkey anti-rabbit IgG and goat anti-mouse IgG were purchased from Jackson Immunoresearch Laboratories, Inc. SuperSignal West Pico Chemiluminescent Substrate was from Pierce. Lab-Tek chamber slides and Boyden chamber (8 mm) were obtained from Nalge Nunc International. Alexa Fluor dyes-conjugated secondary antibodies were from Invitrogen. siRNA were purchased from Eurogentec.

Cell Culture

The MDA-MB-231 human breast cancer cell line was from the American Type Culture Collection. MDA-MB-231 TrkA overexpressing cells were stably transfected and characterized in our laboratory (Lagadec et al, submitted to Cancer Cell). Cells were routinely maintained in EMEM supplemented with 2 mM L-glutamine, 1% non-

essential amino acids, 10% fetal calf serum (FCS), 40 U/ml penicillin-streptomycin, 40 µg/ml gentamycin and 10 µg/ml insulin. All cells were cultured at 37°C in a humidified atmosphere of 5% CO_2.

Sample preparation and 2D electrophoresis

Cells were harvested by centrifugation, rinsed in PBS and resuspended in homogeneization buffer (0.25M sucrose, 10 mM Tris-HCl, pH 7.5, 1 mM EDTA). Proteins were extracted as previously described (Tastet et al. 2003). Briefly, a buffer volume approximatively equal to the packed cell volume was used. The suspension was transferred to a polyallomer ultracentrifuge tube and the cells were lysed by the addition of 4 volumes (respective to the suspension volume) of 8.75 M urea, 2.5 M thiourea, 25 mM spermine base and 50 mM DTT. After 30 min at room temperature, the extracts were ultracentrifuged using an airfuge (10 min, 20 psi). The supernatant was then collected and the protein concentration was determined by a Bradford assay, using bovine serum albumin as a standard. Carrier ampholytes (0.2% final concentration) were added and the protein extracts were stored at -20°C until use.

Isoelectric focusing was carried out using 18 cm Immobiline DryStrips pH 3-10 (GE Healthcare Bio-Sciences). IPG strips were reswollen overnight in 345 µl DeStreak (hydroxyethyl disulfide, GE Healthcare Bio-Sciences) rehydratation solution and 0.2% (v/v) carrier ampholytes 3-10 (Bio-Lyte® ; Bio-Rad), under 2 ml mineral oil. Prior to IEF, protein samples (150 µg) were first reduced (1 h) by adding tributylphosphine (TBP) to a final concentration of 5 mM and secondly alkylated in the dark with 15 mM iodoacetamide for 90 min at room temperature. The samples were then cup-loaded near the anode of the IPG strips and focused in a Protean IEF cell (Bio-Rad) at a temperature of 20 °C. The IPG strips were initially conditioned for 30 min at 250 V (rapid voltage ramping), linearly ramped to 1,000 V (1 h) and

maintained at 1,000 V for 1 h more. Then the electric voltage was slowly increased to reach 10 000 V in 1 hr and focused at this voltage to give a total of 60 kVh. Focused strips were stored in rehydration/equilibration trays at -20 °C until second-dimension separation could be performed. For second-dimension separations, IPG strips were first equilibrated at room temperature for 15 min in 6 M Urea, 30% w/v glycerol, 2% w/v SDS, 13 mM DTT, 0.125 M Tris, 0.1 M HCl, and 2.5% iodoacetamide for an additional 15 min (Gorg et al. 1988). The IPG strips were aligned on filter paper along one edge to remove excess liquid before they were applied and sealed at the top of the 1 mm vertical second dimensional gel as previously described (Tastet et al. 2003). Second-dimension electrophoresis (SDS-PAGE) was performed on homogenous running gels (10%T) of 18 x 20 cm in a Protean II Xi cell (Bio-Rad) at 11°C constant. The separation was realised using Tris–taurine as trailing ion (Tris 150/0.6) (Tastet et al. 2003) and was conducted at 25 V for 1 h, and then at 9W/gel until the bromophenol blue reached the bottom of the gel. The gel patterns were visualized by silver nitrate staining (Sinha et al. 2001)for analytical purposes or by colloidal CBB G-250 (Neuhoff et al. 1988) in the case of micropreparative separations.

2D gel evaluation

Digitalized images of 2D gels were acquired by scanning with a GS-800 calibrated densitometer under control of PDQuest Advanced software version 8.0 (Bio-Rad), which was also used for image analysis and construction of a local 2D database. Three gels per protein extraction and 3 extractions from independent experiments were made (9 gels in total per condition) for this analysis.

Real Time PCR (RT-PCR)

Total RNAs were isolated from control or TrkA overexpressing cells with the Nucleospin RNAII isolation kit (Macherey-Nagel, Belgium). RNA concentration was quantified using a spectrophotometer at a wavelength of 260 nm. Reverse transcription was performed with 1 µg of RNAs, 1 µg of random hexamers, 20 units of Moloney murine leukemia virus reverse transcriptase (Invitrogen life technologies, USA) for 1 h at 37°C in a final volume of 100 µl. Real time PCR amplifications were performed using a Quantitect SYBR®Green PCR kit (Qiagen, France) with 2 µl of cDNA and 500 nM of primers. The primers used were as following : 5'-CCCCAATTCAGCAGCATATT-3' and 5'-CCTTCAGCCAGACTGGAGAC-3' for Ku86, 5'-AAAAGACTGGGCTCCTTGGT-3' and 5'-TGTGGGTCTTCAGCTCCTCT-3' for Ku70, 5-GTGATGTGCAGCTGATCAAGACT-3 and 5-GATGACCAGCCCAAAGGAGA-3 for RPLP0 (human acidic ribosomal phosphoprotein P0), which was used as a reference gene. The amplification was performed with one denaturing cycle at 95 °C for 5 min, then 40 cycles at 95 °C for 30 s, at 55 °C for 30 s, at 72 °C for 30 s, and one final extension at 95 °C for 1 min. Data were analyzed using the MX4000 PCR system software (Stratagene, Amsterdam, The Netherlands) with the SYBRGreen option (with dissociation curves).

Protein extraction, immunoprecipitation and SDS-PAGE

Cells were harvested by scraping in lysis buffer (50 mM Tris-HCl pH 7.5, 150 mM NaCl, 1% NP40, 1 mM sodium orthovanadate and protease inhibitor cocktail). After centrifugation (10,000 g, 3 min, 4°C), the supernatant proteins were quantified using the bicinchoninic acid method. TrkA and interacting proteins were co-immunoprecipitated from 5 mg of proteins using 25 µg of anti-TrkA antibody (Upstate) and Dynabeads protein A according to manufacturer's instructions.

Immunoprecipitated proteins were eluted in Laemmli buffer (62.5 mM Tris-HCl pH 6.8, 2% SDS, 10% glycerol, 5% 2-mercaptoethanol and 0.002% bromophenol blue) and boiled 5 min before analysis on 10% polyacrylamide gels. For staining, SDS-polyacrylamide gels were fixed overnight in solution containing 50% ethanol and 1.4% orthophosphoric acid. After 3 washes for 30 min in MilliQ water, gels were incubated in impregnation solution (1.3 M ammonium sulfate, 34% methanol, 1.4% orthophosphoric acid) for 1 h and placed in staining solution (1.3 M ammonium sulfate, 34% methanol, 1.4% orthophosphoric acid, 0.07% Coomassie Brillant Blue G250) for 24 h. Finally, gels were destained with several washes of MilliQ water until the backgroung was clear.

In gel trypsin digestion

Coomassie blue-stained protein bands were excised from SDS-PAGE gel and processed for trypsin digestion as previously described (Com et al. 2003) with minor modifications. In brief, gel bands were destained twice for 10 min in solution containing 100 mM NH_4HCO_3 and 50% acetonitrile, dehydrated in acetonitrile and dried in a vacuum centrifuge. Gel pieces were then rehydrated at 4°C for 45 min in a digestion buffer (50 mM NH_4HCO_3, 12.5 ng/µl trypsin). The supernatant was replaced by 40 µl of 50 mM NH_4HCO_3 and the samples were incubated overnight at 37°C. The tryptic peptides were recovered by 10 min incubations, once in 25 mM 50 mM NH_4HCO_3, 50% acetonitrile and twice in 25 mM 50 mM NH_4HCO_3, 50% acetonitrile, 5% formic acid. All supernatants were pooled and dried in a vacuum centrifuge.

Protein identification by mass spectrometry

For MALDI-TOF analyses, tryptic digests were resuspended in 1% formic acid and were desalted and concentrated using $ZipTip_{C18}$ pipette tips according to

manufacturer's instructions. Peptides were spotted on MALDI target with 10 mg/ml DHB in 50% acetonitrile using the dried droplet method. MALDI-TOF mass spectra were acquired using Voyager DE STR instrument (Applied Biosystems) in reflector positive ion mode. Protein identification was performed using monoisotopic masses of tryptic peptides detected on MALDI-TOF spectra internally calibrated with tryptic autolysis peptides as previously described (Com et al. 2003). NanoLC-NanoESI-MS/MS analyses were performed on an ion trap mass spectrometer (LCQ Deca XP+, Thermo-electron, San Jose, CA) equipped with a nano-electrospray ion source coupled with a nano high-pressure liquid chromatography system (LC Packings Dionex, Amsterdam, The Netherlands). Tryptic digests were resuspended in 4 µl of 0.1% HCOOH and 1.4 µl were injected into the mass spectrometer using the Famos auto-sampler (LC Packings Dionex, Amsterdam, The Netherlands). It was first desalted and then concentrated on a reverse phase precolumn of 5 mm x 0.3 mm i.d. (Dionex) by a solvent A (H_2O/Acetonitrile-95/5-0.1% HCOOH) delivered by the Switchos pumping device (LC Packings Dionex, Amsterdam, The Netherlands) at a flow rate of 10 µl/min for 3 min. Peptides were separated on a 15 cm x 75 µm i.d., 3 µm, C18 Pepmap column from Dionex. The flow rate was set at 200 nl/min. Peptides were eluted using a 5 to 70% linear gradient of solvent B in 45 min (H_2O/Acetonitrile-20/80-0.08% HCOOH). Coated nanoelectrospray needles (360 µm o.d., 20 µm i.d., 10 µm tip i.d., standard coating) were obtained from New Objective (Woburn, MA). Spray voltage was set at 1.5 kV, and capillary temperature at 170°C. The mass spectrometer was operated in positive ionization mode. Data acquisition was performed in a data-dependent mode consisting of alternatively in a single run, a full scan MS over the range m/z 500-2000 and a full scan MS/MS of the ion selected in an exclusion dynamic mode (the most intense ion is selected and excluded for

further selection for a duration of 3 min). MS/MS data were acquired using a 2 m/z units ion isolation window and a 35% relative collision energy. MS/MS .raw data files were transformed in .dta files with Bioworks 3.1 software (Thermo-electron, San Jose, CA). The .dta files generated were next merged with merge.bat Software to be downloading in MASCOT Daemon software (Matrix Science Ltd., London, UK) for database searches in SwissProt 52.0. Search parameters were the following: *Homo sapiens* for taxonomy, one allowed missed cleavage, methionine oxidation as variable modification, 2 Da for peptide tolerance and 0.8 Da for MS/MS tolerance. To ascertain unambiguous identification, searches were performed in parallel with Phenyx software using the same parameters.

Western blot

After 2D electropheresis or SDS-PAGE separation, proteins were electro-transferred onto nitrocellulose membrane using a semi-dry transfer system (Trans-Blot SD cell, Bio Rad). Efficiency of transfer and relative equal loading was checked with Ponceau S staining. Non specific protein binding sites were saturated for 1 h 30 at room temperature in TBS-0.1% Tween-20 reagent (TBST) containing either 5% BSA for Ku70, ku86 and actin immunodetection. Membranes were then incubated overnight at 4°C with 1:5,000 anti-Ku70, 1:500 anti-Ku86, 1:500 anti-TrkA or 1:5000 anti-actin. After washes in TBST, peroxidase-conjugated anti-rabbit or anti-mouse IgG diluted in saturated solution was added for 1 h at room temperature and the membranes were washed several times in TBST before detection of peroxidase activity using chemiluminescent system.

Flow cytometry

Cells detached by Trypsin-EDTA solution were incubated 1 h at 4°C with 20 µg/ml of the indicated antibodies or matched control isotypes at similar concentrations. After washing with PBS containing 0.5% BSA, cells were incubated for 30 min at 4°C with secondary fluorescein-labelled IgG. Cells were then analyzed in Coulter Epics XL/XL-MCl cytometer (Beckman).

Immunocytochemistry and confocal microscopy

MDA-MB-231 cells were seeded on Lab-tek chamber slide precoated with type I collagen. Cells were washed in PBS pH 7.5, fixed in 4% paraformaldehyde for 20 min. Non specific protein binding sites were then blocked in PBS pH 7.5 containing 2% BSA and cells were incubated in blocking solution containing 10 µg/ml rabbit anti-TrkA and 10 µg/ml mouse anti-Ku70 or anti-Ku86 antibodies overnight at 4°C. After washes in PBS pH 7.5, 10 µg/ml Alexa Fluor 546 goat anti-rabbit IgG and 10 µg/ml Alexa Fluor 488 donkey anti-mouse IgG were added for 1 h at 37°C. Cells were washed in PBS pH-7.5 and mounted. Scanning fluorescence images were acquired using a Zeiss Axiophot microscope.

siRNA transfection

MDA-MB-231 control and TrkA overexpressing cells were transiently transfected using the Nucleofection technology according to Amaxa Biosystems protocol. siRNA against Ku70 (sense 5'-GAUGCCCUUUACUGAAAAA-3', antisense 5'-UUUUUCAGUAAAGGGCAU-3'), siRNA against Ku86 (sense 5'-CCAGGUUCUCAACAGGCUG-3', antisense 5'-CAGCCUGUUGAGAACCUGG-3') were transfected by Nucleofection. siRNA against GFP (sense 5'-GCUGACCCUGAAGUUCAU-3', antisense 5'-GAUGAACUUCAGGGUCAG-3') were

used as control. MDA-MB-231 cells were transiently nucleofected with 3 µg of siRNA directed against Ku70 and/or Ku86. Briefly, $2x10^6$ cells were resuspended in 100 µl of Cell Line Nucleofector™ Solution V and cell suspension was mixed with siRNA. The sample was transferred into an electroporation cuvette and transfection was performed using the program X-013 according to manufacturer's instructions. Immediately after nucleofection, cells were cultured in prewarmed complete medium. Twenty-four hours after transfection, cells were seeded for the evaluation of apoptosis induction or migration.

Apotosis analysis

Cells transfected by siRNA were pretreated with 200 ng/ml NGF for 1 h before cotreatment with 200 ng/ml NGF and 5 ng/ml TNF-related apoptosis inducing ligand (TRAIL) for 6 h. Apoptosis was determined by morphological analysis after fixation with methanol (10 min, -20°C) and staining with 1 µg/ml Hoechst 33258 (10 min, room temperature, in the dark). A minimum of 500-1000 cells was examined for each case under fluorescent microscope and the results represented the number of apoptotic cells over the total number of counted cells.

Anoikis assay

Cells were pre-treated with 20 µg/ml of neutralizing antibodies against Ku70 and Ku86 for 30 min and seeded on Poly(2-hydroxyethyl methacrylate) (poly HEMA, Sigma)-coated 96 wells-plates (15mg/ml) ($1x10^5$ cells/well) in EMEM1% FCS and cultured with antibodies against ku70 and Ku86 for different periods of time. Cell viability was analyzed by 3-(4,5-dimethylthiazol-2-yl)-5-(3-carboxymethoxyphenyl)-2-(4-sulfophenyl)-2H tetra-zolium (MTS; Promega) assay according to the user manual.

Migration assay

Cells ($5x10^4$) were seeded on polycarbonate membrane insert (6.5 mm in diameter with 8 μm pores) of a Transwell (BD Bioscience) and maintained in EMEM containing 0.1% FCS. NGF was added to the lower chamber. For antibody neutralization, cells were pre-treated with 20 μg/ml of neutralizing antibodies against Ku70 and Ku86 during 30 min and before seeding. After 6 h of culture, the insert was washed with PBS, and cells on the top surface of the insert were removed by wiping with a cotton swab. Cells that migrated to the bottom surface of the insert were fixed with methanol and stained by Hoechst 33258 and then subjected to fluorescence microscopic inspection. Cells were counted on 10 random fields at x200.

Statistical analysis

Statistical differences were determined with two-tailed Student's *t* tests. All *p* values were two-sided. $p<0.05$ was considered as statistically significant.

Results

Identification of protein expression changes in MDA-MB-231 TrkA overexpressing breast cancer cells

Proteins of mock and TrkA overexpressing cells were separated by 2D electrophoresis (pH3-10) before analysis of protein spots with PDquest software. A representative example of proteins separated on a 2D-gel is shown in Figure 1. Nearly 1500 spots were obtained in the ranges of MW 12-120 kDa and pI 3-10. In TrkA overexpressing cells, 26 spots were found to be down- or upregulated after analysis with PDquest software (Figure 1). To identify proteins in the modified spots, we separated 250 mg proteins by 2D electrophoresis (pH3-10) and colored them with Coomassi blue. After trypsin digestion, we successfully identified the proteins by spectrometry analysis (MALDI-ToF and LC-MS/MS). The identified proteins are shown in Table 1, including accession number, Mascot score, theoretical MW (Da) and pI, number of peptides identified and percentage of coverage. Sixteen spots were found to contain 2 or more proteins, 10 spots were found to contain only one protein. Among these 10 spots, 7 proteins were downregulated (Phosphoribosyl pyrophosphate synthetase 1, spot 10; VDAC2, spot 11; Phosphatidylinositol transfer protein b, spot 12; Tau Tubulin kinase 2, spot 13; HSP70 protein 8, spot 15; hnRNP C, spot 19; PAP1, spot 26) and 3 proteins were upregulated (Elongin B, spot 4; Proteasome b 9 subunit, spot 5; Ku86, spot 14).

Ku86 is upregulated in TrkA overexpressing cells

The most important difference between mock and TrkA overexpressing cells concerned Ku86 (Figure 2A and B) which was found to be increased 4-fold in TrkA overxpressing cells.

MALDI-TOF and LC-MS/MS allowed the clear identification of Ku86 as the only protein presented in spot 14. MALDI-TOF spectrum showed 29 experimental tryptic peptides that matched to theoretical masses, leading to 36% sequence coverage with an average error mass of 0.143 Da (Figure 2C and D). This identification was consolidated by independent MS/MS analysis of spot 14, as sequencing of five peptides revealed 8% sequence coverage with an average error mass of 0.295 Da. (Fig. 2E and F).

We then performed Western blotting analysis of Ku86 and showed that Ku86 was increased in TrkA overexpressing cells (Figure 3A), thus confirming the analysis made by the software PDQuest. However, reel time PCR showed no modifications of Ku86 mRNA (Figure 3B), indicating that upregulation of Ku86 was only at protein level.

Ku 86 and Ku 70 proteins are immunoprecipitated with TrkA

Ku 86 and ku70 are associated to form a heterodimeric regulatory subunit of the DNA-dependent protein kinase (DNA-PK) that is crucial to DNA repair (Collis et al. 2005). Ku proteins are also reported to be involved in cell proliferation, migration and invasion (Muller et al. 2005). More recently, we have shown that Ku70 interacts with TrkA in MCF-7 breast cancer cells to stimulate cell survival in TRAIL-induced apoptosis (Com et al. 2007). To determine if TrkA interacts with Ku proteins in MDA-MB-231 cells, we realized TrkA immunoprecipitation and identification of immunoprecipitated proteins by mass spectrometry LC-MS/MS. Both Ku86 and Ku70 were found to be immunoprecipitated with TrkA. Identification of Ku86 was made thanks to the sequencing of 3 peptides (556.88; 689.45; 690.88) (Figure 4A and B), with a Mascot score of 208 and 4 % coverage (blanket). On the other hand, 2 peptides corresponding to Ku70 were sequenced (586.71 and 568.63), with a Mascot

score of 48 and 3 % of coverage (Figure 4C). Western blot confirmed the presence of Ku 86 and ku70 in TrkA co-immunoprecipitated proteins (Figure 4D).

Ku86 is involved in TrkA-induced migration

We have previously shown that TrkA overexpression induces an increase in cell migration and survival (Com et al. 2007). To determine whether Ku86 was implicated in the TrkA-mediated biological effects and whether Ku86 could function in concert with Ku70, we inhibited Ku by siRNA or neutralizing antibodies. As shown in Figure 5A, specific siRNAs strongly decreased the expression of Ku86 and Ku70. Inhibition of Ku86 with both siRNA and the neutralizing antibody efficiently reduced cell migration, while inhibition of Ku70 had no effect (Figure 5B and C). Interestingly, simultaneous inhibition of both Ku86 and Ku 70 did not reduce more than inhibition of Ku86 alone. This indicted that Ku86 could increase TrkA-mediated migration independently of Ku70.

We then evaluated if Ku proteins could control cell resistance to TRAIL-induced apoptosis. As shown in Figure 5D, siRNAs against Ku86 and Ku70 had no pro-apoptotic effect by themselves; Ku70 siRNA induced a strong potentiation of TRAIL-induced apoptosis in TrkA overexpressing MDA-MB-231cells. By contrary, Ku86 siRNA had no effect on TRAIL-induced apoptosis.

Anoikis is defined as a form of apoptosis induced by loss of adhesion, and the resistance to anoikis is considered as a crucial step in metastasis process (Geiger and Peeper 2005; Rennebeck et al. 2005). Although TrkA overexpression strongly increased anoikis resistance, inhibition of Ku86 and Ku70 with neutralizing antibodies did not modify anoikis resistance in TrkA overexpressing cells (Figure 5E).

Membrane Ku86 and Ku70 are increased in TrkA overexpressing cells

Ku proteins localized at cell surface are found to be involved in both cell proliferation and migration (Watanabe et al. 2003; Paupert et al. 2007). Morover, membrane Ku86 and Ku70 can interact with the metalloprotease MMP9 to facilitate migration and invasion of monocyte-derived macrophages (Monferran et al. 2004; Monferran et al. 2004; Paupert et al. 2007). However, we showed that Ku86 and Ku70 functioned independently of each other in TrkA-mediated biological effects. In an attempt to understand the underlying mechanism in TrkA overexpressing cells, we analysed the levels of cell surface Ku proteins by FACS using specific antidibodies against Ku86 and Ku70. As shown in Figure 6, an increase was observed for both Ku86 and Ku70 in TrkA overexpressing cells compared to mock cells.

Figure 1. 2D gel migration patterns of proteins in TrkA overexpressing MDA-MB-231 breast cancer cells

Cells were lysed and soluble proteins were separated by 2D electrophoresis. Separation of proteins was performed in the first dimension (horizontal) by IEF, and subsequently in the second dimension (vertical) by SDS-PAGE. A, a representative example of proteins separated on 2D electrophoresis gel after silver staining. Twenty-six spots (arrows) were found to be modified (at least 2-fold difference) in TrkA overexpressing cells: 8 spots were upregulated (spots N°2, 3, 4, 5, 7, 8, 14 and 17) and 18 were downregulated (spots N°1, 6, 9, 10, 11, 12, 13, 15, 16, 18, 19, 20, 21, 22, 23, 24, 25 and 26). B, zoomed spots of interest.

A

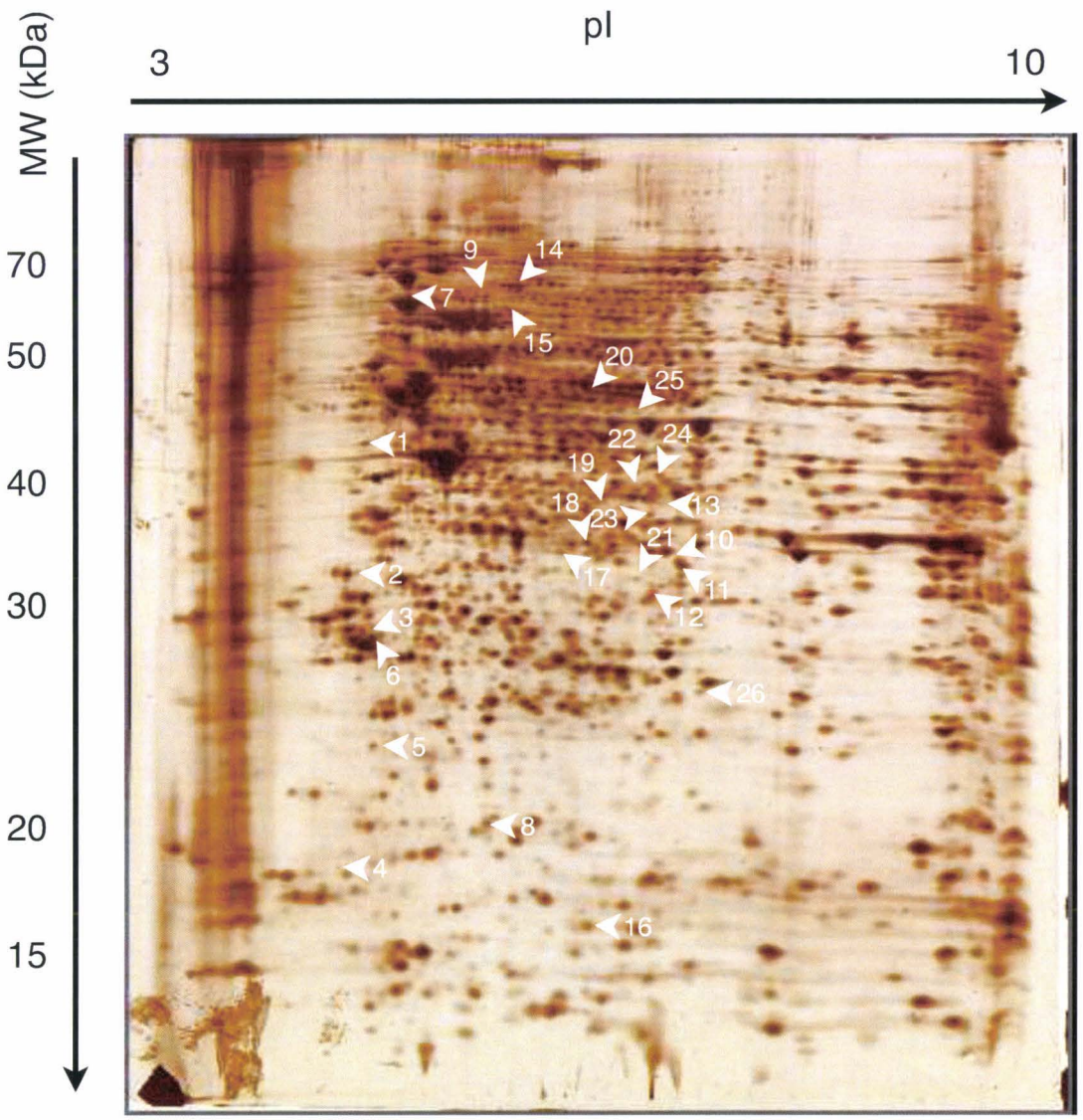

Figure 1A

Lagadec et al.

B

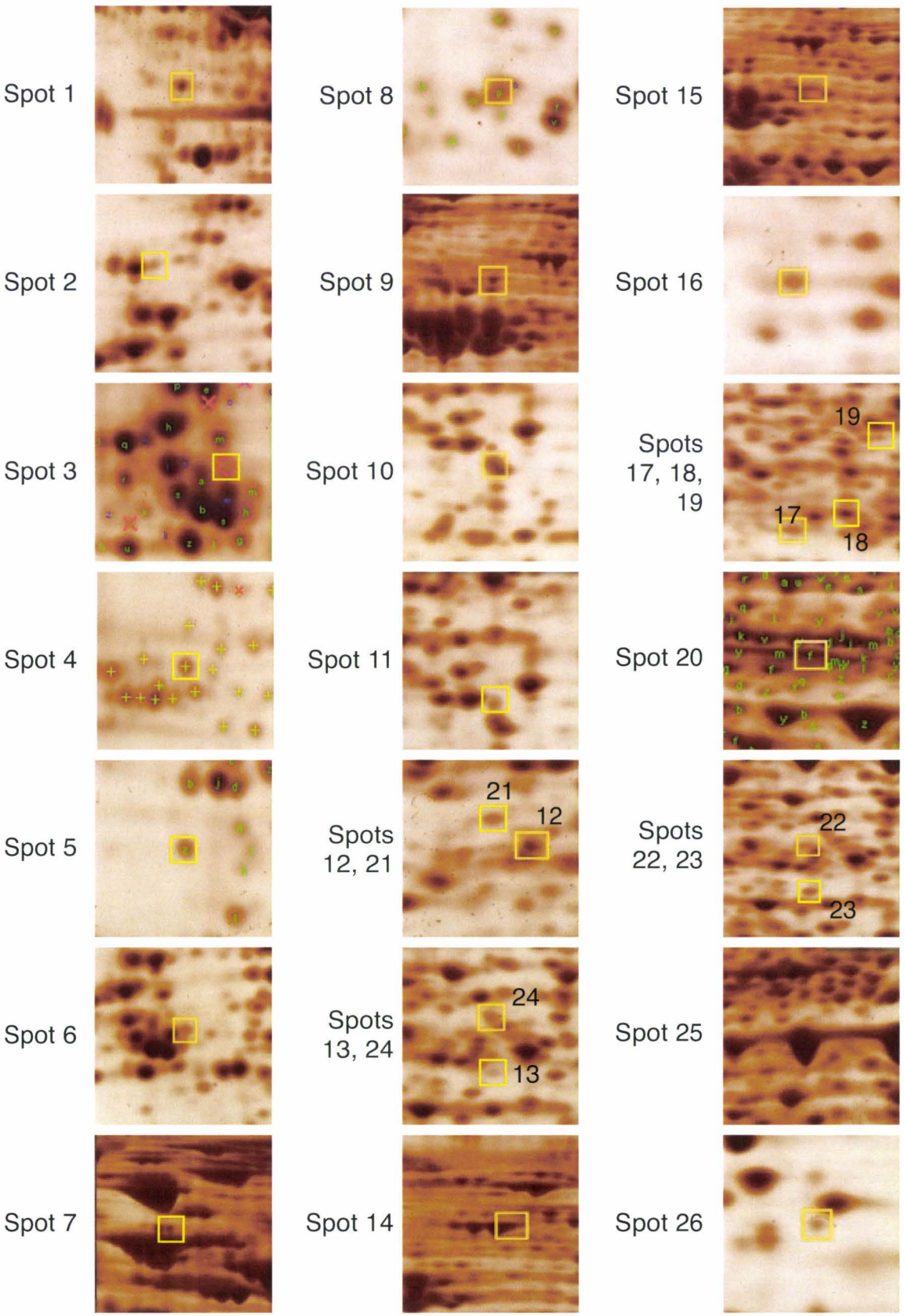

Figure 1B

Lagadec et al.

Table 1. **Identification of proteins modified in TrkA overexpressing cells.** Proteins were separated by 2-DE (Fig. 1); spots with significant difference in abundance between Mock and TrkA overexpressing cells were cut out of the gel and digested with trypsin before nanoLC-nanoESI-MS/MS or MALDI-ToF analysis. Spot number, Protein name, Swissprot accession number, and the Mascot score were reported for each protein. Mascot search program was used to identify proteins.

N°	Name of protein	Accession Nb	Identif.	Score	MW	pI	Nb of peptides	Cov. (%)	Relative difference
1	Vimentin	P08670	LC-MS/MS	135	53,653	5.06	3	6	↓ (x0.3)
	Programmed cell death 2-like	Q9RP1	LC-MS/MS	116	39,391	4.71	2	5	
2	Tyrosine 3/tryptophan 5 - monooxygenase activation protein epsilon	Q53XZ5	LC-MS/MS	253	29,155	4.63	6	21	↑ (x2.2)
	Eukaryotic translation elongation factor 1 beta 2	P32471	LC-MS/MS	60	24,748	4.5	1	5	
	acidic (leucine-rich) nuclear phosphoprotein 32 family, member A	P39687	LC-MS/MS	45	28,568	3.99	1	4	
	14-3-3 gamma	P61981	LC-MS/MS	76	28,357	4.66	2	8	↑ (x2.3)
	Tyrosine 3/tryptophan 5 - monooxygenase activation protein zeta	Q2F831	LC-MS/MS	76	27,728	4.73	2	10	
4	Elongin B isoform a	Q15370	LC-MS/MS	83	13,125	4.73	3	10	↑ (x2.3)
5	Proteasome beta 9 subunit isoform 1	P28065	LC-MS/MS	134	23,25	4.93	3	17	↑ (x3.2)

N°	Name of protein	Accession Nb	Identif.	Score	MW	pI	Nb of peptides	Cov. (%)	Relative difference
6	Tyrosine 3/tryptophan 5 - monooxygenase activation protein beta	Q4VY19	LC-MS/MS	81	28,065	4,76	2	14	↓ (x0.5)
	14-3-3 gamma	P61981	MALDI	78	28,154	4.8	10	36	
7	BIP, GRP78	P11021	LC-MS/MS	486	72,377	5.07	9	14	↑ (x3.9)
	dipeptidyl-peptidase III	Q9NY33	LC-MS/MS	387	82,528	5.04	7	14	
	Erzin, Cytovillin, Villin-2	P15331	LC-MS/MS	92	69,356	5.94	1	2	
8	epididymal secretory protein E1	P61916	LC-MS/MS	106	16,559	7.56	2	17	↑ (x2.8)
	Nm23 protein	P15531	LC-MS/MS	67	20,398	7.07	2	11	
	Signal sequence receptor, delta	P51571	LC-MS/MS	62	18,987	5.76	1	7	
9	Ran GTPase activating protein 1	P46060	LC-MS/MS	253	63,502	4.63	4	8	↓ (x0.2)
	LIM domain and actin-binding protein 1	Q9UHB6	LC-MS/MS	140	85,173	6.41	3	5	
	Calpain 1	P07384	LC-MS/MS	140	81,838	5.49	3	4	
	Eukaryotic translation initiation factor 4B	P23588	LC-MS/MS	45	69,183	5.49	1	2	
10	Phosphoribosyl pyrophosphate synthetase 1 variant	Q53FW2	LC-MS/MS	60	34,841	6.3	5	37	↓ (x0.4)
11	VDAC2, Voltage-dependent anion channel 2	P45880	LC-MS/MS	43	31,575	7.49	1	4	↓ (x0.2)

Table 1

N°	Name of protein	Accession Nb	Identif.	Score	MW	pI	Nb of peptides	Cov. (%)	Relative difference
12	Phosphatidylinositol transfer protein beta isoform	P45739	LC-MS/MS	154	32,389	6.4	5	34	↓ (x0.4)
13	Tau tubulin kinase 2	Q6IQ55	LC-MS/MS	66	182,352	6.58	2	2	↓ (x0.5)
14	***Ku86, ATP-dependent DNA helicase II***	**P13010**	**MALDI (LC-MS/MS)**	**136 (243)**	**82,652**	**5.55**	**29 (6)**	**36 (8)**	**↑ (x4)**
15	HSP70 protein 8 isoform 1	P17066	LC-MS/MS	57,4	70,866	5.3	5	26	↓ (x0.5)
16	Fatty acid binding protein 5	O15540	LC-MS/MS	62	15,155	6.6	3	10	↓ (x0.3)
	40S ribosomal protein S12	P25398	LC-MS/MS	58	14,516	6.3	1	6	
17	Carbonyl reductase 1	P16152	LC-MS/MS	54	30356	8.55	1	5	↑ (x3.1)
	Galectin-1	P09382	MALDI	60	14,575	5.34	12	43	
	Tubulin-specific chaperone B	Q99426	MALDI	114	27,308	5.06	8	47	
	EF-hand domain-containing protein 2	Q96C19	MALDI	70	26,68	5.15	5	46	
18	Lactate dehydrogenase B	P07195	LC-MS/MS	89	36,615	5.71	3	8	↓ (x0.5)
	Heterogenous nuclear ribonucleoprotein H3 isoform a	P31942	LC-MS/MS	58	36,903	6.37	1	3	
	Tubulin-specific chaperone B	Q99426	MALDI	96	27,308	5.06	12	36	
19	Heterogenous nuclear ribonucleoprotein C isoform b	P07910	LC-MS/MS	170	31,947	5.1	3	12	↓ (x0.4)

Table 1

N°	Name of protein	Accession Nb	Identif.	Score	MW	pI	Nb of peptides	Cov. (%)	Relative difference
20	Leucine aminopeptidase	P28838	LC-MS/MS	217	56,014	7.58	5	11	↓ (x0.2)
	Cell proliferation-inducing gene 40 protein	P14868	LC-MS/MS	64	57,156	6.2	1	2	
	Supressor of hairy wing homolog 3	Q8ND82	MALDI	72	83,042	9,29	14	23	
21	Phosphatidylinositol transfer protein, beta	P48739	LC-MS/MS	382	31,52	6.46	10	32	↓ (x0.4)
	Exosome complex exonuclease RRP4	Q13868	LC-MS/MS	56	29,187	6.71	1	4	
22	Heterogeneous nuclear ribonucleoprotein D0	Q14103	LC-MS/MS	133	35,801	8.86	3	9	↓ (x0.3)
	tRNA-guanine transglycosylase	Q9BXR0	LC-MS/MS	79	41,574	6.89	1	3	
23	PDGFA associated protein 1	Q13442	LC-MS/MS	143	20,618	8.84	2	16	↓ (x0.5)
	Transaldolase	P37837	MALDI	72	37,429	6.36	11	20	
24	Heterogeneous nuclear ribonucleoprotein D0	Q14103	LC-MS/MS	126	35,801	8.86	3	9	↓ (x0.5)
	Mitochondrial acetoacetyl-CoA thiolase	P61981	LC-MS/MS	100	45,252	9.07	2	7	

Table 1

N°	Name of protein	Accession Nb	Identif.	Score	MW	pI	Nb of peptides	Cov. (%)	Relative difference
25	Antiquitin	P49419	LC-MS/MS	494	55,331	6.44	13	24	↓ (x0.2)
	Leucine aminopeptidase	P28838	LC-MS/MS	352	56,014	7.58	6	17	
	Inosine-5'-monophosphate dehydrogenase 1	P20839	LC-MS/MS	67	55,414	6.16	1	2	
	Tubulin alpha 6	Q9BQE3	LC-MS/MS	51	49,863	4.96	1	4	
	Sorting and assembly machinery component 50 homolog	Q9Y512	MALDI	65	51,929	6.44	24	40	
26	PDGFA associated protein 1	Q13442	LC-MS/MS	143	20,618	8.84	2	16	↓ (x0.5)

Table 1

Figure 2. Ku86 upregulation in TrkA overexpressing MDA-MB-231 cells

A, enlarged regions of spot 14 from 2D electrophoresis gels. Arrows indicate different forms of Ku86. **B,** relative quantification of Ku86 by PDQuest Biorad software. **C,** MALDI-TOF spectrum of tryptic digest from spot n°14 (Figure 1). **D,** listing of all peptides found by MALDI-TOF. **E,** a tandem mass spectrum of the doubly-charged ion at m/z 1031.24. The bold letters indicate the detected b and y ions matching the predicted ion mass in the database. **F,** LC-MS/MS detected fragments are indicated by red letters in the full sequence of Ku86.

A

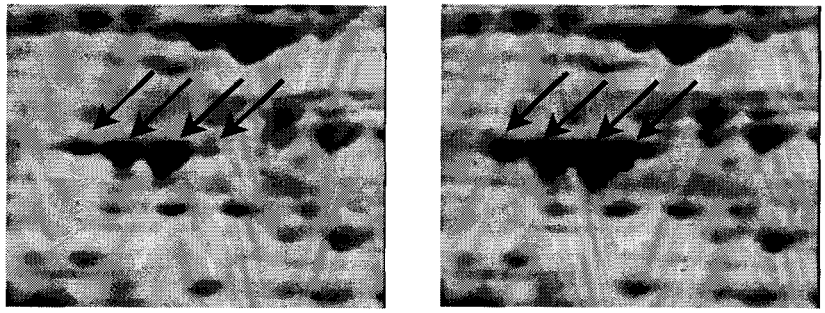

B

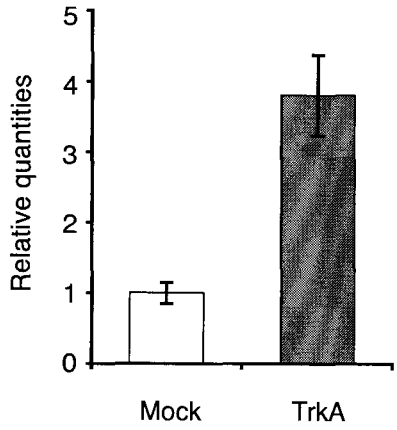

Figure 2A and B

C

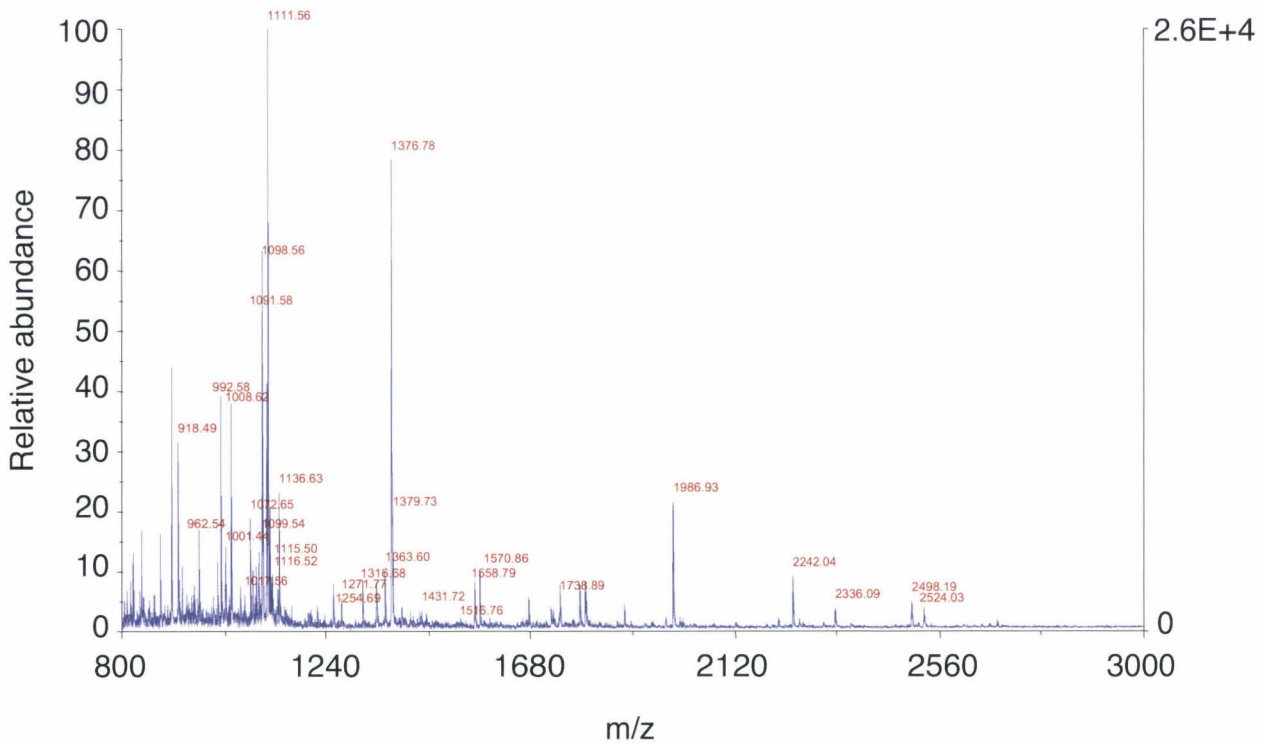

Figure 2C

Lagadec et al.

D

Position	Peptide sequences	Experimental mass	Theoritical precursor neutral mass	Delta mass (Da)
36-44	KVITMFVQR (Ox)	1136.6365	1136.6376	-0.0011
37-44	VITMFVQR	992.5880	992.5477	0.0403
131-141	HIEIFTDLSSR	1316.6862	1316.6725	0.0138
172-184	EDGSGDRGDGPFR	1363.6074	1363.5753	0.0321
179-195	GDGPFRLGGHGPSFPLK	1738.8948	1737.8951	0.9997
185-195	LGGHGPSFPLK	1108.6259	1108.6029	0.0230
196-209	GITEQQKEGLEIVK	1570.8690	1570.8566	0.0124
240-250	IERHSIHWPCR	1431.7218	1432.7146	-0.9928
243-250	HSIHWPCR (Carb)	1091.5891	1091.5083	0.0808
251-260	LTIGSNLSIR	1072.6596	1072.6240	0.0356
275-282	TWTVVDAK	918.4902	918.4811	0.0091
287-307	EDIQKETVYCLNDDDETEVLK	2498.1972	2498.1370	0.0602
316-325	YGSDIVPFSK	1111.5683	1111.5550	0.0133
316-332	YGSDIVPFSKVDEEQMK (Ox)	1986.9381	1986.9245	0.0137
339-347	CFSVLGFCK	1001.4443	1002.4667	-1.0224
354-363	RFFMGNQVLK (Ox)	1254.6996	1254.6543	0.0453
355-363	FFMGNQVLK (Ox)	1098.5673	1098.5532	0.0141
401-413	ANPQVGVAFPHIK	1376.7875	1376.7565	0.0311
432-439	QYMFSSLK (Ox)	1018.5189	1018.4794	0.0396
444-465	YAPTEAQLNAVDALIDSMSLAK (Ox)	2336.0927	2336.1569	-0.0642
470-481	TDTLEDLFPTTK	1379.7318	1379.6820	0.0498
487-497	FQRLFQCLLHR (Carb)	1516.7612	1516.8085	-0.0473
490-497	LFQCLLHR (Carb)	1085.6123	1085.5804	0.0319
533-543	IKTLFPLIEAK	1271.7778	1271.7853	-0.0075
535-543	TLFPLIEAK	1030.6007	1030.6063	-0.0055
546-565	DQVTAQEIFQDNHEDGPTAK	2242.0403	2242.0138	0.0265
641-648	AFREEAIK	962.5435	962.5185	0.0250
649-660	FSEEQRFNNFLK	1558.7948	1557.7576	1.0373
709-732	DKPSGDTAAVFEEGGDVDDLLDMI (Ox)	2524.0383	2524.1163	-0.0780

Figure 2D

E

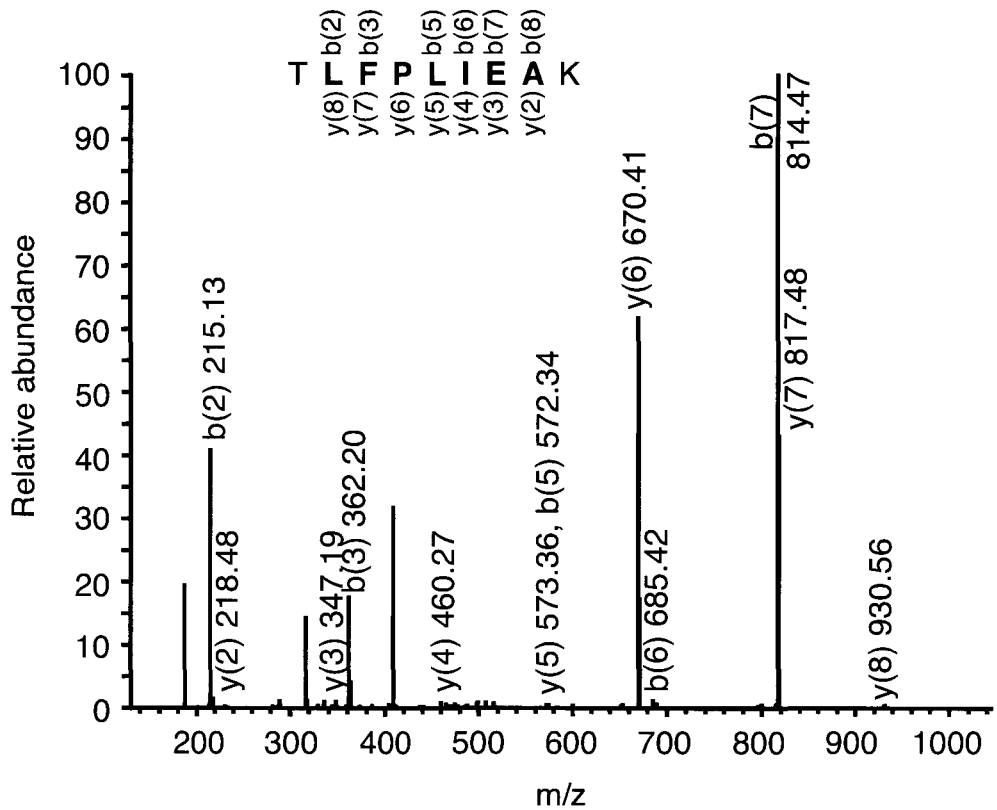

F

MVRSGNKAAV VLCMDVGFTM SNSIPGIESP FEQAKKVITM FVQRQVFAEN
KDEIALVLFG TDGTDNPLSG GDQYQNITVH RHLMLPDFDL LEDIESKIQP
GSQQADFLDA LIVSMDVIQH ETIGKKFEKR HIEIFTDLSS RFSKSQLDII
IHSLKKCDIS LQFFLPFSLG KEDGSGDRGD GPFRLGGHGP SFPLKGITEQ
QKEGLEIVKM VMISLEGEDG LDEIYSFSES LRKLCVFKKI ERHSIHWPCR
LTIGSNLSIR IAAYKSILQE RVKKTWTVVD AKTLKKEDIQ KETVYCLNDD
DETEVLKEDI IQGFR**YGSDI** **VPFSK**VDEEQ MKYKSEGKCF SVLGFCKSSQ
VQRR**FFMGNQ** **VLK**VFAARDD EAAAVALSSL IHALDDLDMV AIVRYAYDKR
ANPQVGVAFP HIKHNYECLV YVQLPFMEDL RQYMFSSLKN SKKYAPTEAQ
LNAVDALIDS MSLAKKDEK**T** **DTLEDLFPTT** **K**IPNPRFQRL FQCLLHRALH
PREPLPPIQQ HIWNMLNPPA EVTTKSQIPL SKIK**TLFPLI** **EAK**KK**DQVTA**
QEIFQDNHED **GPTAK**KLKTE QGGAHFSVSS LAEGSVTSVG SVNPAENFRV
LVKQKKASFE EASNQLINHI EQFLDTNETP YFMKSIDCIR AFREEAIKFS
EEQRFNNFLK ALQEKVEIKQ LNHFWEIVVQ DGITLITKEE ASGSSVTAEE
AKKFLAPKDK PSGDTAAVFE EGGDVDDLLD MI

Figure 2E and F

Figure 3. Analysis of Ku86 expression by Western blot and real time PCR

A, Western blotting. Proteins (200 μg) were electrophoresed in 2D gel and Western blots were performed using an anti-Ku86 antibody. Actin was used to confirm the loading and transfer of equal amounts of protein.

B, real time PCR detection of Ku86 mRNA. RPIP0 was used as an equal loading control.

A

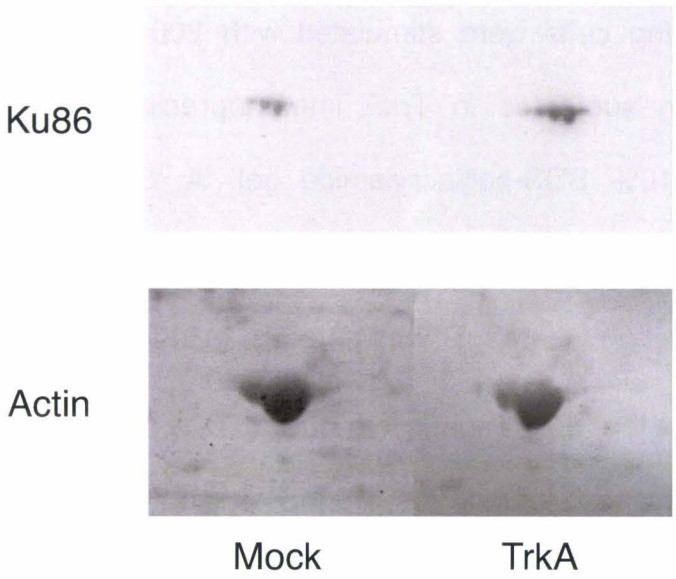

B

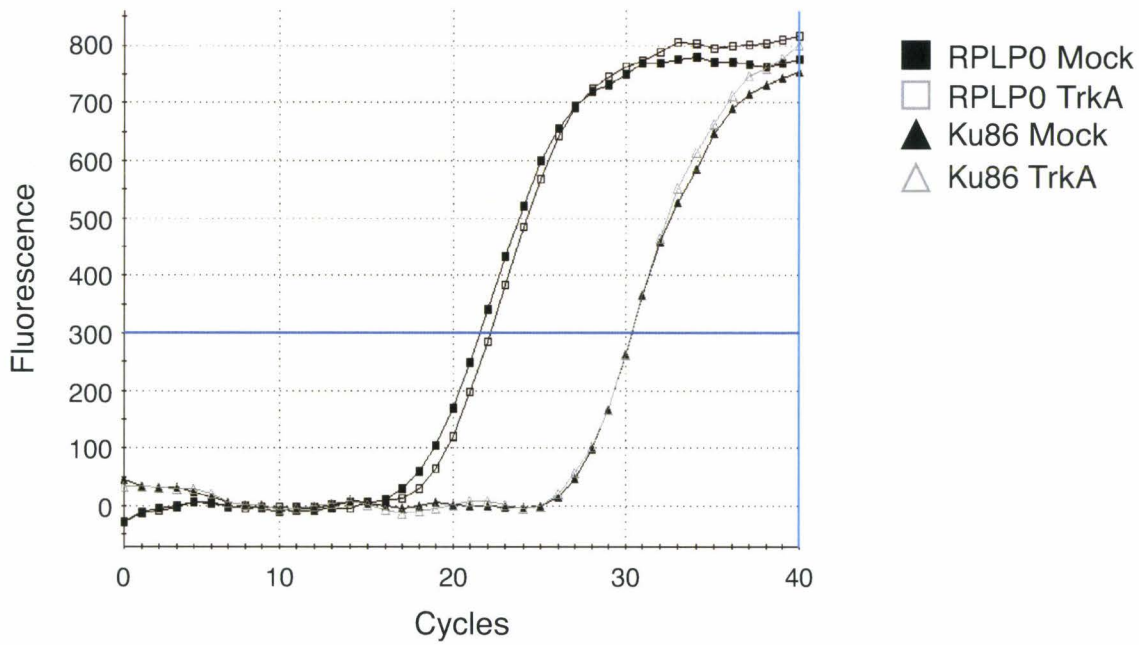

Figure 3A and B

Lagadec et al.

Figure 4. Identification of Ku proteins after TrkA immunoprecipitation

TrkA overexpressing cells were stimulated with 200 ng/m NGF for 10 min. Cell lysates were then subjected to TrkA immunoprecipitation and the elutes were separated on a 10% SDS-polyacrylamide gel. **A**, SDS-polyacrylamide gel after staining with colloidal Coomassie blue. Arrows indicate positions of Ku86 and Ku70 on the gel, the position where IgG was detected is indicated by *. **B** and **C,** Tandem mass spectrum of the doubly charged ions at m/z 1111.74 for Ku86 and at m/z 1171.71 for K70. y and b ions on the MS/MS spectra are indicated. The bold letters indicate the detected b and y ions matching the predicted ion mass in the database. **D,** Western blot of TrkA co-immunoprecipitated Ku proteins. TrkA-overexpressing cells were treated with NGF (200 ng/ml for 10 min), cell lysates were then immunoprecipitated with an anti-TrkA antibody. Co-immunoprecipitated proteins were subjected for immunoblot (IB) of TrkA, Ku86 and Ku70.

A

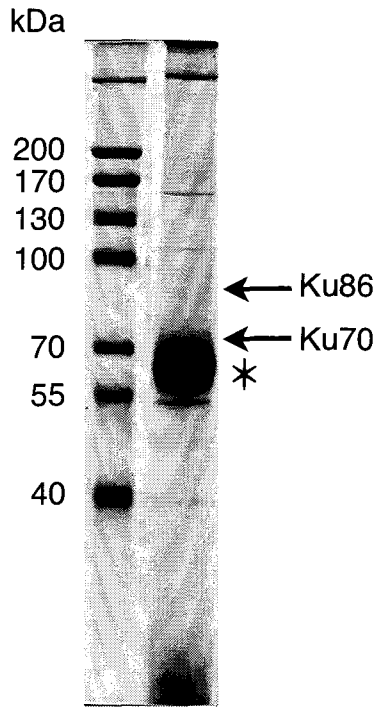

B

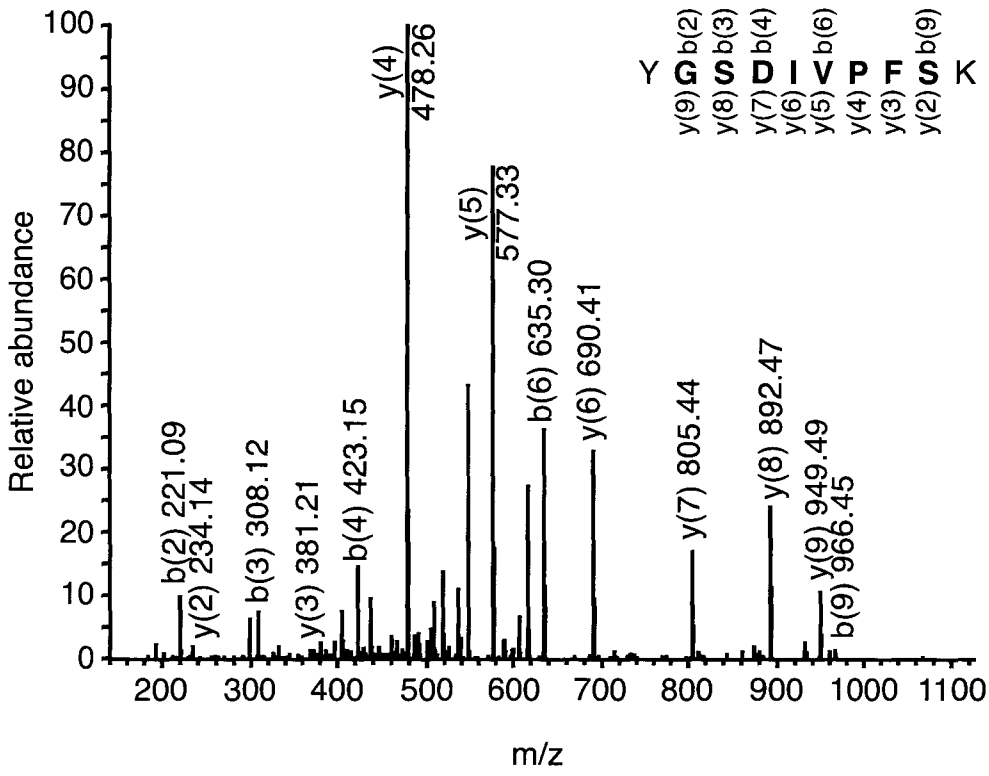

Figure 4A and B

Lagadec et al.

C

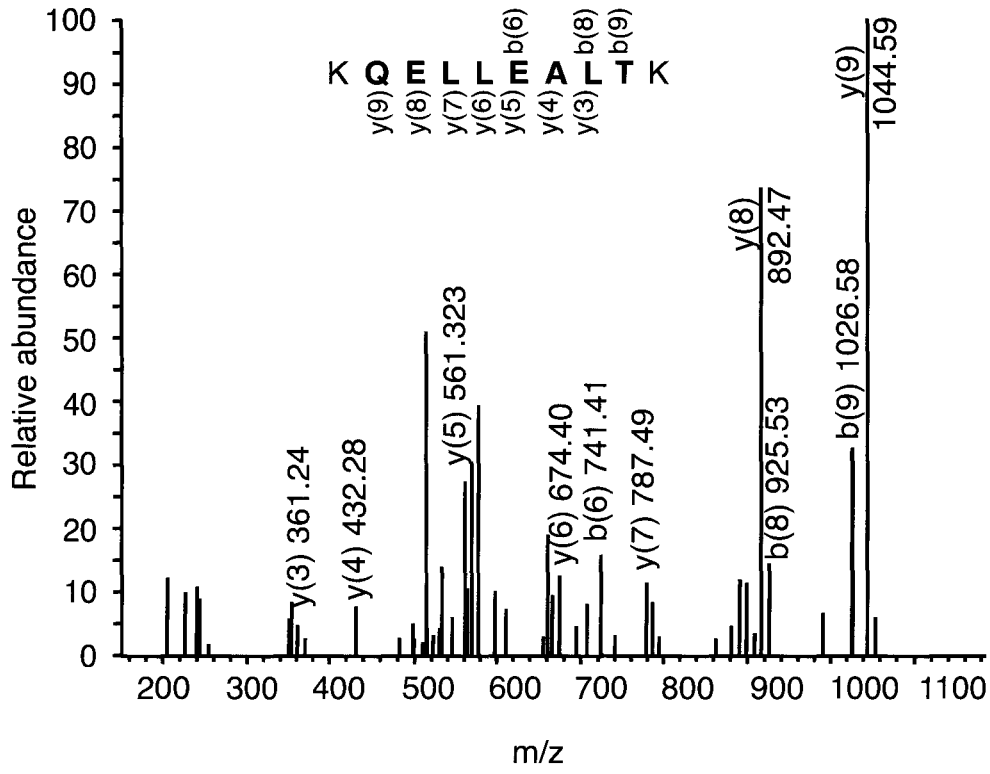

D

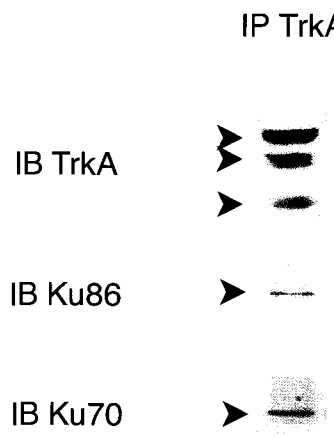

Figure 4C and D

Figure 5. Involvement of Ku proteins in TrkA-mediated biological effects.

A, Western blot analysis of ku proteins after siRNA transfection. MDA-MB-231 mock and TrkA overexpressing cells were transiently with Ku86 siRNA and/or Ku70 siRNA, siRNA directed against GFP (Green Fluorescence Protein) was used as control. The efficiency of siRNA inhibition was verified by immunoblotting against Ku70 and Ku86. **B** and **C,** evaluation of Ku involvement in TrkA-mediated migration. Cells were transfected with Ku siRNAs (**B**) or pretreated with neutralizing antibodies for 30 min at 37°C (**C**) before treatment with 200 ng/ml NGF for 6 h in Transwell. **D,** evaluation of Ku involvement in TrkA-mediated survival upon TRAIL treatment. Cells were transfected with Ku siRNAs, pretreated with NGF (200 ng/ml) for 1 h before co-treatment with TRAIL (5 ng/ml) and NGF (200 ng/ml) during 6 h. Apoptosis was assessed after Hoechst staining. **E,** evaluation of Ku involvement in anoikis resistance. Cells were pretreated with neutralizing antibodies for 30 min at 37°C, then cultured on poly-HEMA coated 96-wells plates with or without neutralizing antibodies. Cell viability was evaluated by MTS assay in different periods of time **(B)**. *, $p<0.01$, siKu70 and siKu86 transfected cells versus siGFP transfected cells, or anti-Ku86 and antiKu70 inhibited cells versus Isotype control inhibited cells.

A

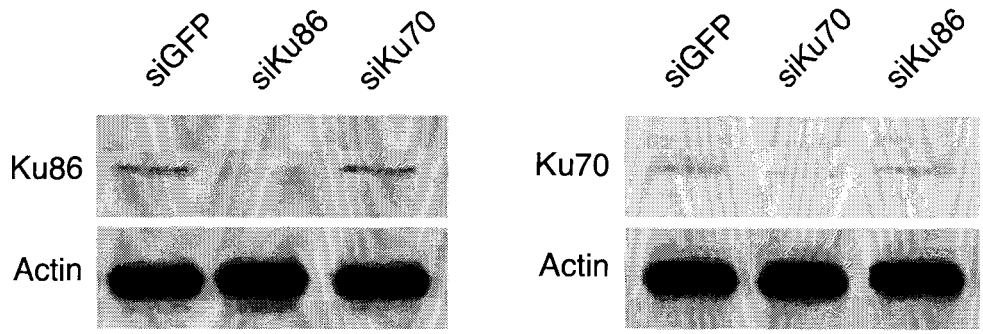

Figure 5A

Lagadec et al.

B

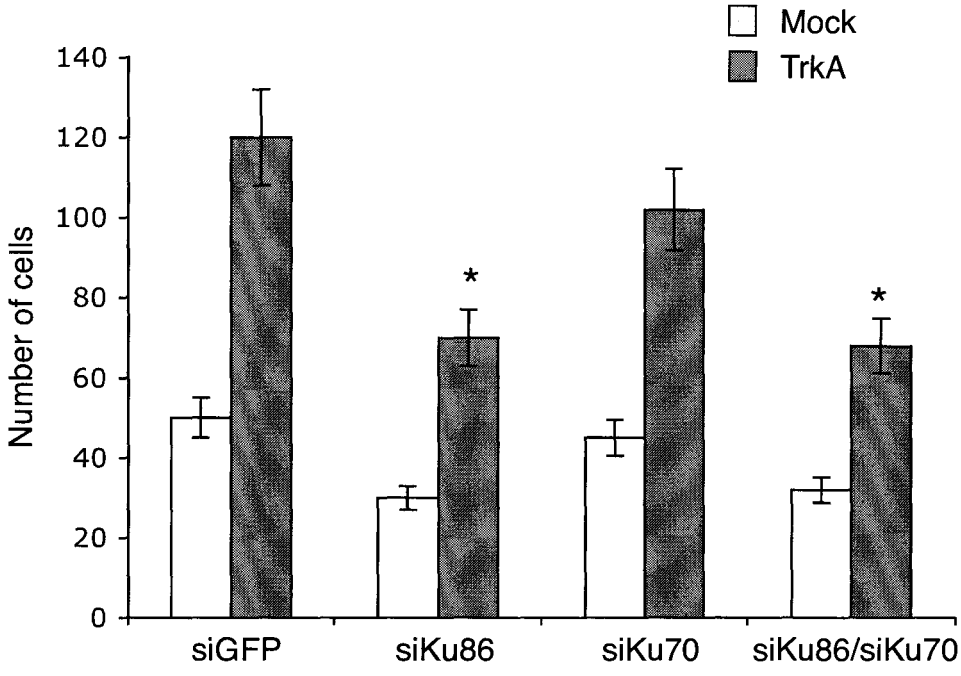

C

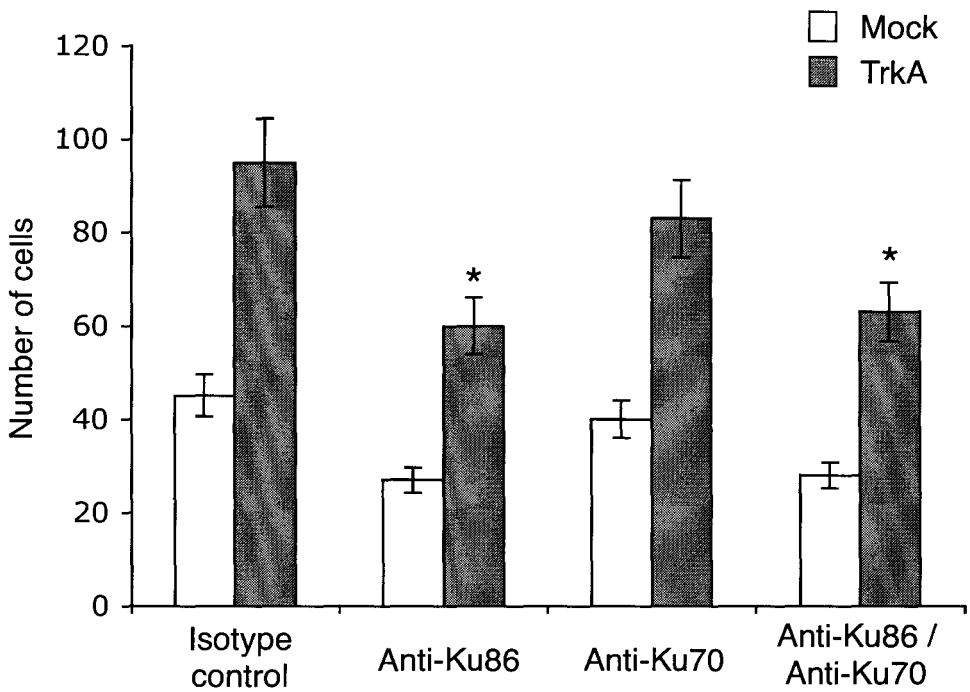

Figure 5B and C

Lagadec et al.

D

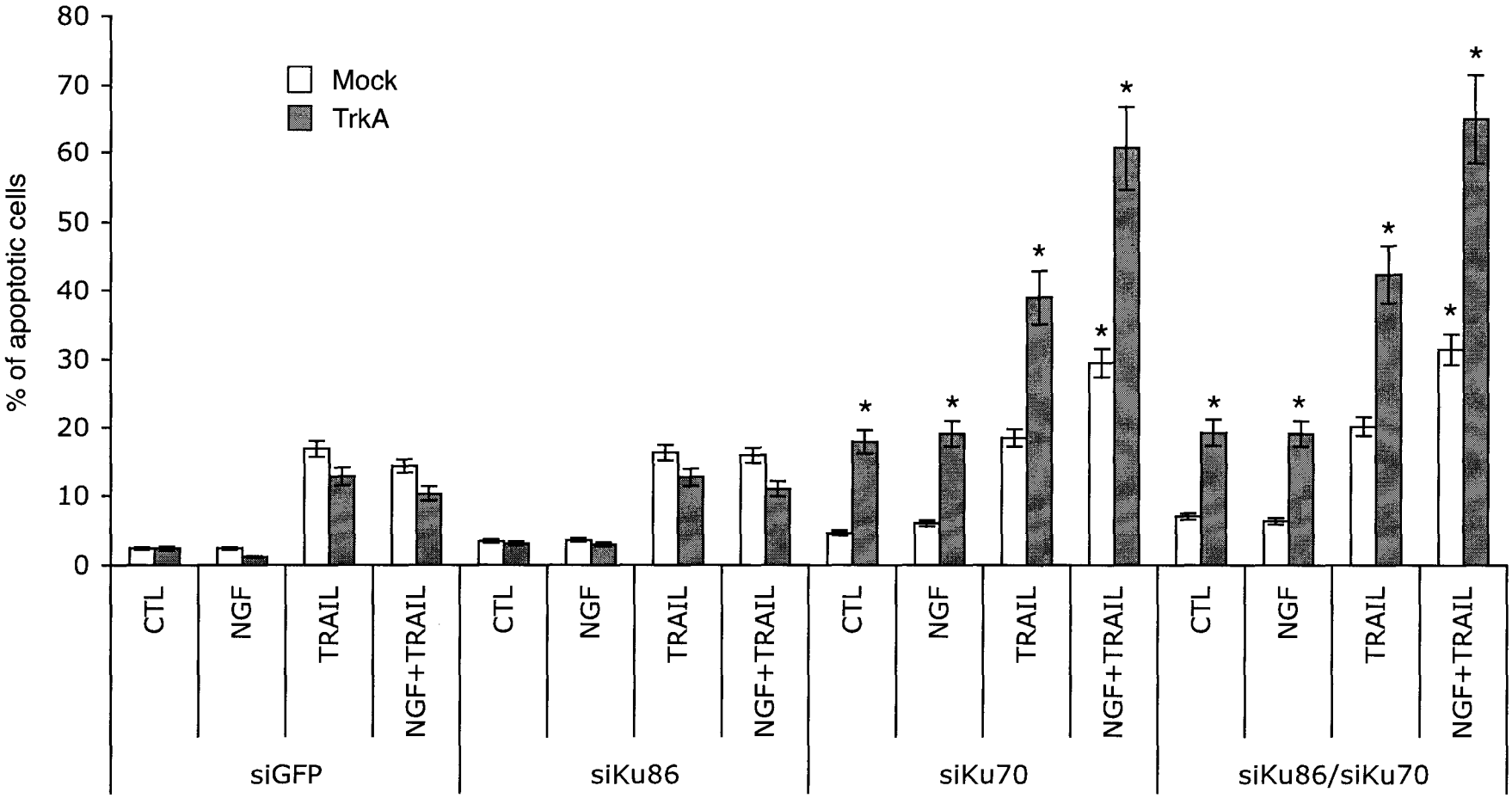

Figure 5D

Lagadec et al.

E

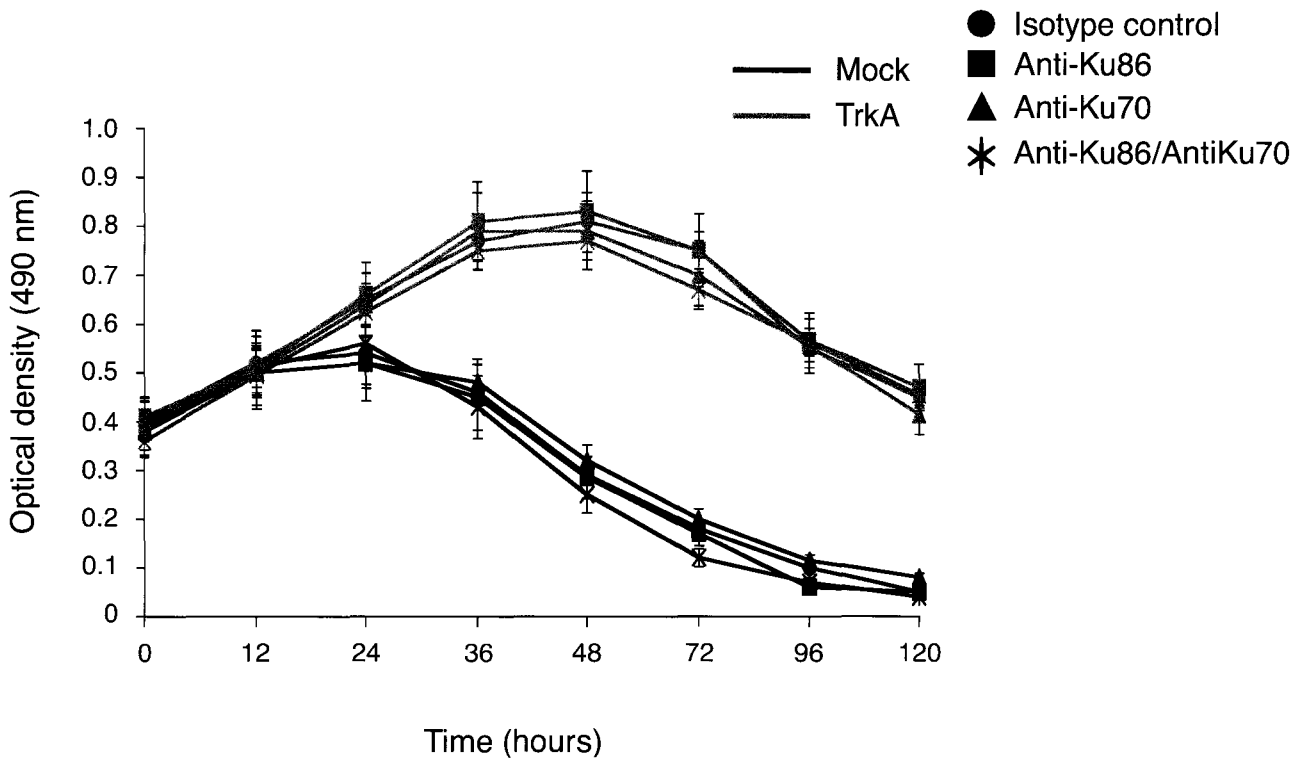

Figure 5E

Lagadec et al.

Figure 6. Detection of cell surface Ku proteins by FACS

Cells were incubated with anti-Ku antibodies, levels of cell surface Ku proteins were analysed by FACS. Dark grey, mock cells; light grey, TrkA overexpressing cells; black, mixed mock and TrkA-overexpressing cells incubated with isotype control antibody. Results are representative of three separate experiments carried out in duplicate.

A

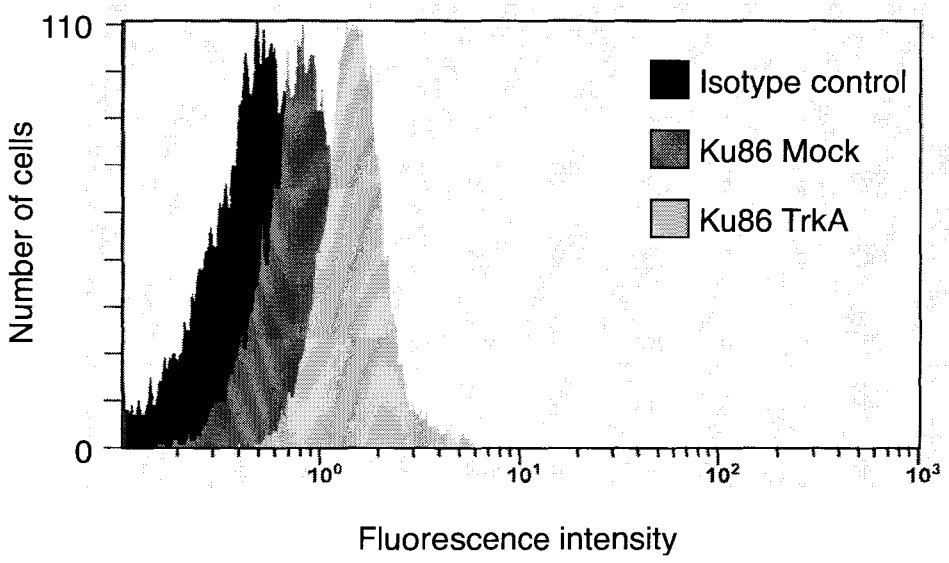

B

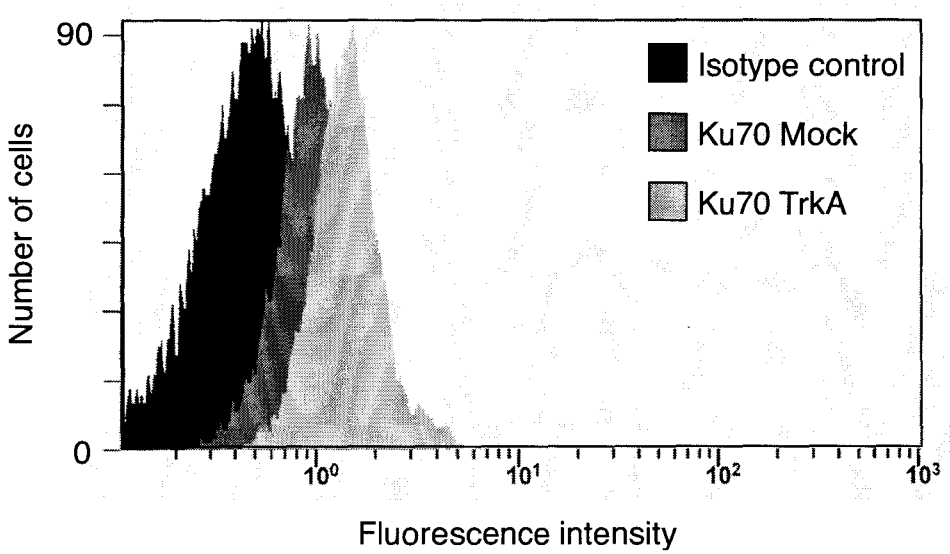

Figure 6

Lagadec et al.

Discussion

We have previously shown that TrkA overexpression in MDA-MB-231 breast cancer cells increases cell growth, migration, as well as survival. In order to understand the underlying mechanism, we have used a functional proteomic approach to identify molecules involved in the TrkA-mediated biological effects. For this, we first separated proteins using a cup-loading two-dimensional electrophoresis system and then identified a series of putative modified proteins in TrkA overexpressing cells by MALDI and LC-MS/MS mass spectrometry analysis. The cup-loading technology allows rapid identification of protein changes between samples on reproducible 2D gels and reduces the inter-experimental variations.

Among modified proteins, we demonstrated that Ku86 was upregulated in TrkA overexpressing cells. Moreover, Ku 86 was required for TrkA-stimulated migration while it was not involved in TrkA-induced resistance to anokis or apoptosis induced by TRAIL. Interestingly, both Ku86 and Ku70 were immunoprecipitated with TrkA. These findings are in agreement with our previous data showing that TrkA is associated with Ku70 in MCF-7 breast cancer cells (Com et al. 2007). The Ku heterodimer (Ku70/Ku86) is an abundant complex located in the nucleus, where it plays a key role in the non-homologous end joining process, which is responsible for repairing a major fraction of DNA double strand breaks in somatic cells of all multicellular eukaryotes (Jackson 2002; Lieber et al. 2003). Ku binds in a sequence-independent specific fashion to virtually all double-stranded DNA. Once bound to DNA ends, Ku recruits the catalytic subunit of DNA dependent protein kinase (DNA-PKcs) to initiate a phosphorylation and protein-protein interaction cascade, that in turn, leads to the recruitment of DSBs repair enzymes (Lees-Miller

and Meek 2003; Collis et al. 2005). The expression of Ku outside the nucleus in both the cytosol and at the cell surface has been described more than 15 years ago but its additional roles have come into focus only recently (Prabhakar et al. 1990; Dalziel et al. 1992). In the cytosol, Ku70 has a cytoprotective function by inhibiting the translocation of Bax to mitochondria (Sawada et al. 2003). More surprisingly, cell surface Ku proteins can regulate cell adhesion, migration and invasion (Paupert et al. 2007).

In this study, we observed that TrkA surexpression increased the expression of Ku86. Nevertheless, we were not able to observe any variation of Ku86 mRNA level by real time PCR, suggesting that Ku86 upregulation is due to more efficient protein synthesis and/or decreased degradation. To determine roles of Ku proteins in TrkA-mediated biological effect in MDA-MB-231 cells, we inhibited Ku proteins with siRNAs and neutralizing antibodies. We showed that Ku86 stimulated cell migration while Ku70 inhibited TRAIL-induced apoptosis in TrkA overexpressing cells. It has been reported that hypoxia induces cell migration and invasion through an upregulation of Ku86 in Kelly neuroblastoma cells and MCF-7 breast carcinoma cells, (Ginis and Faller 2000). In addition, Ku70 and Ku86 can interact with adhesion proteins and extracellular matrix to promote cell migration (Monferran et al. 2004; Muller et al. 2005). Ku 86 and Ku70 can also interact directly with the metalloprotease MMP9 to degrade extracellular matrix, leading to increased invasion (Monferran et al. 2004). We showed that in our model system, Ku86 functioned independently of ku70 to stimulate migration. On the other hand, while inhibition of Ku70 drastically decreased the survival of cells upon TRAIL treatment, Ku86 did not seem be involved in this process.

Anoikis is a form of apoptosis induced by lack of correct extracellular matrix

attachment (Gilmore 2005). Recently, some data indicate that cell-cell interactions can inhibit anoikis (Kang et al. 2007). Interestingly, Teoh and al. (Teoh et al. 1998) have shown that Ku86/Ku70 can be involved in cell-cell adhesion. However, we did not find any involvement of Ku70 and Ku86 in anoikis resistance of TrkA overexpressing cells, suggesting the involvement of other proteins in this process. Of note, FACS analysis showed an increase of cell surface Ku proteins. As TrkA immunoprecipitation also immunoprecipitated Ku proteins, we hypothesize that TrkA could play a role in linking Ku proteins to the plasma membrane. However, more investigations (confocal microscopy, reverse immunoprecipitation) are necessary to confirm this eventuality.

In conclusion, we showed by functional proteomics exploration that Ku86 was upregulated in TrkA overexpressing breast cancer cells. Moreover, Ku86 was involved in TrkA-induced migration. Therefore, upregulation of Ku86 in tumors overexpressing TrkA might be a relevant way to increase metastasis. Further *in vitro* and *in vivo* investigations are required to verify this hypothesis. It should be also emphasized that Ku86 as well as the other proteins identified in this study, may potentially represent new molecular targets whose interest for future therapeutic strategies against TrkA overexpressing breast cancer should be investigated.

Acknowledgments

Grant support: INSERM, la Ligue Nationale Contre le Cancer (Equipe labellisée 2006), le Ministère de l'Education Nationale and the Région Nord/Pas-de-Calais. Chann Lagadec was the recipient of a fellowship from the Association pour la Recherche sur le Cancer (ARC).

References

Adriaenssens, E., E. Vanhecke, P. Saule, A. Mougel, A. Page, R. Romon, V. Nurcombe, X. LeBourhis, H. Hondermarck and (2007). "Nerve Growth Factor is a Potential Molecular Target in Breast Cancer " Submitted in Cancer Research.

Buck, M. B. and C. Knabbe (2006). "TGF-beta signaling in breast cancer." Ann N Y Acad Sci **1089**: 119-26.

Burger, A. M., B. Leyland-Jones, K. Banerjee, D. D. Spyropoulos and A. K. Seth (2005). "Essential roles of IGFBP-3 and IGFBP-rP1 in breast cancer." Eur J Cancer **41**(11): 1515-27.

Campos, X., Y. Munoz, A. Selman, R. Yazigi, L. Moyano, C. Weinstein-Oppenheimer, H. E. Lara and C. Romero (2007). "Nerve growth factor and its high-affinity receptor trkA participate in the control of vascular endothelial growth factor expression in epithelial ovarian cancer." Gynecol Oncol **104**(1): 168-75.

Chan, S. K., M. E. Hill and W. J. Gullick (2006). "The role of the epidermal growth factor receptor in breast cancer." J Mammary Gland Biol Neoplasia **11**(1): 3-11.

Chang, C. F., R. Westbrook, J. Ma and D. Cao (2007). "Transforming growth factor-beta signaling in breast cancer." Front Biosci **12**: 4393-401.

Chong, Y. M., A. Subramanian, A. K. Sharma and K. Mokbel (2007). "The potential clinical applications of insulin-like growth factor-1 ligand in human breast cancer." Anticancer Res **27**(3B): 1617-24.

Collis, S. J., T. L. DeWeese, P. A. Jeggo and A. R. Parker (2005). "The life and death of DNA-PK." Oncogene **24**(6): 949-61.

Com, E., F. Bourgeon, B. Evrard, T. Ganz, D. Colleu, B. Jegou and C. Pineau (2003). "Expression of antimicrobial defensins in the male reproductive tract of rats, mice, and humans." Biol Reprod **68**(1): 95-104.

Com, E., C. Lagadec, A. Page, I. El Yazidi-Belkoura, C. Slomianny, A. Spencer, D. Hammache, B. B. Rudkin and H. Hondermarck (2007). "Nerve growth factor receptor TrkA signaling in breast cancer cells involves KU70 to prevent apoptosis." Mol Cell Proteomics.

Dalziel, R. G., S. C. Mendelson and J. P. Quinn (1992). "The nuclear autoimmune antigen Ku is also present on the cell surface." Autoimmunity **13**(4): 265-7.

Davidson, B., R. Reich, P. Lazarovici, V. Ann Florenes, S. Nielsen and J. M. Nesland (2004). "Altered expression and activation of the nerve growth factor receptors TrkA and p75 provide the first evidence of tumor progression to effusion in breast carcinoma." Breast Cancer Res Treat **83**(2): 119-28.

Davidson, B., R. Reich, P. Lazarovici, J. M. Nesland, M. Skrede, B. Risberg, C. G. Trope and V. A. Florenes (2003). "Expression and activation of the nerve growth factor receptor TrkA in serous ovarian carcinoma." Clin Cancer Res **9**(6): 2248-59.

Descamps, S., X. Lebourhis, M. Delehedde, B. Boilly and H. Hondermarck (1998). "Nerve growth factor is mitogenic for cancerous but not normal human breast epithelial cells." J Biol Chem **273**(27): 16659-62.

Dolle, L., I. El Yazidi-Belkoura, E. Adriaenssens, V. Nurcombe and H. Hondermarck (2003). "Nerve growth factor overexpression and autocrine loop in breast cancer cells." Oncogene **22**(36): 5592-601.

Dolle, L., M. J. Oliveira, E. Bruyneel, H. Hondermarck and M. Bracke (2005). "Nerve growth factor mediates its pro-invasive effect in parallel with the release of a soluble E-cadherin fragment from breast cancer MCF-7/AZ cells." J Dairy Res **72 Spec No**: 20-6.

Festuccia, C., G. L. Gravina, P. Muzi, R. Pomante, L. Ventura, E. Ricevuto, C. Vicentini and M. Bologna (2007). "In vitro and in vivo effects of bicalutamide on the expression of TrkA and P75 neurotrophin receptors in prostate carcinoma." Prostate **67**(12): 1255-64.

Friess, H., Z. W. Zhu, F. F. di Mola, C. Kulli, H. U. Graber, A. Andren-Sandberg, A. Zimmermann, M. Korc, M. Reinshagen and M. W. Buchler (1999). "Nerve growth factor and its high-affinity receptor in chronic pancreatitis." Ann Surg **230**(5): 615-24.

Geiger, T. R. and D. S. Peeper (2005). "The neurotrophic receptor TrkB in anoikis resistance and metastasis: a perspective." Cancer Res **65**(16): 7033-6.

Gilmore, A. P. (2005). "Anoikis." Cell Death Differ **12 Suppl 2**: 1473-7.

Ginis, I. and D. V. Faller (2000). "Hypoxia affects tumor cell invasiveness in vitro: the role of hypoxia-activated ligand HAL1/13 (Ku86 autoantigen)." Cancer Lett **154**(2): 163-74.

Gorg, A., W. Postel, S. Gunther, J. Weser, J. R. Strahler, S. M. Hanash, L. Somerlot and R. Kuick (1988). "Approach to stationary two-dimensional pattern: influence of focusing time and immobiline/carrier ampholytes concentrations." Electrophoresis **9**(1): 37-46.

Jackson, S. P. (2002). "Sensing and repairing DNA double-strand breaks." Carcinogenesis **23**(5): 687-96.

Lagadec, C., E. Adriaenssens, R. Romon, R. Toillon, S. Meignan, E. Vanhecke, B. Oxomdre, H. Hondermarck and X. Lebourhis (2007). "TrkA overexpression promotes growth and metastasis of breast cancer cells." Cancer Cell.

Lees-Miller, S. P. and K. Meek (2003). "Repair of DNA double strand breaks by non-homologous end joining." Biochimie **85**(11): 1161-73.

Lieber, M. R., Y. Ma, U. Pannicke and K. Schwarz (2003). "Mechanism and regulation of human non-homologous DNA end-joining." Nat Rev Mol Cell Biol **4**(9): 712-20.

McGregor, L. M., B. K. McCune, J. R. Graff, P. R. McDowell, K. E. Romans, G. D. Yancopoulos, D. W. Ball, S. B. Baylin and B. D. Nelkin (1999). "Roles of trk family neurotrophin receptors in medullary thyroid carcinoma development and progression." Proc Natl Acad Sci U S A **96**(8): 4540-5.

Mercurio, A. M., E. A. Lipscomb and R. E. Bachelder (2005). "Non-angiogenic functions of VEGF in breast cancer." J Mammary Gland Biol Neoplasia **10**(4): 283-90.

Micera, A., A. Lambiase, B. Stampachiacchiere, S. Bonini, S. Bonini and F. Levi-Schaffer (2007). "Nerve growth factor and tissue repair remodeling: trkA(NGFR) and p75(NTR), two receptors one fate." Cytokine Growth Factor Rev **18**(3-4): 245-56.

Monferran, S., C. Muller, L. Mourey, P. Frit and B. Salles (2004). "The Membrane-associated form of the DNA repair protein Ku is involved in cell adhesion to fibronectin." J Mol Biol **337**(3): 503-11.

Monferran, S., J. Paupert, S. Dauvillier, B. Salles and C. Muller (2004). "The membrane form of the DNA repair protein Ku interacts at the cell surface with metalloproteinase 9." Embo J **23**(19): 3758-68.

Muller, C., J. Paupert, S. Monferran and B. Salles (2005). "The double life of the Ku protein: facing the DNA breaks and the extracellular environment." Cell Cycle **4**(3): 438-41.

Nakagawara, A. (2001). "Trk receptor tyrosine kinases: a bridge between cancer and neural development." Cancer Lett **169**(2): 107-14.

Neuhoff, V., N. Arold, D. Taube and W. Ehrhardt (1988). "Improved staining of proteins in polyacrylamide gels including isoelectric focusing gels with clear background at nanogram sensitivity using Coomassie Brilliant Blue G-250 and R-250." Electrophoresis **9**(6): 255-62.

Papatsoris, A. G., D. Liolitsa and C. Deliveliotis (2007). "Manipulation of the nerve growth factor network in prostate cancer." Expert Opin Investig Drugs **16**(3): 303-9.

Patapoutian, A. and L. F. Reichardt (2001). "Trk receptors: mediators of neurotrophin action." Curr Opin Neurobiol **11**(3): 272-80.

Paupert, J., S. Dauvillier, B. Salles and C. Muller (2007). "Transport of the leaderless protein Ku on the cell surface of activated monocytes regulates their migratory abilities." EMBO Rep **8**(6): 583-8.

Prabhakar, B. S., G. P. Allaway, J. Srinivasappa and A. L. Notkins (1990). "Cell surface expression of the 70-kD component of Ku, a DNA-binding nuclear autoantigen." J Clin Invest **86**(4): 1301-5.

Rennebeck, G., M. Martelli and N. Kyprianou (2005). "Anoikis and survival connections in the tumor microenvironment: is there a role in prostate cancer metastasis?" Cancer Res **65**(24): 11230-5.

Ricci, A., S. Greco, S. Mariotta, L. Felici, E. Bronzetti, A. Cavazzana, G. Cardillo, F. Amenta, A. Bisetti and G. Barbolini (2001). "Neurotrophins and neurotrophin receptors in human lung cancer." Am J Respir Cell Mol Biol **25**(4): 439-46.

Roussidis, A. E., A. D. Theocharis, G. N. Tzanakakis and N. K. Karamanos (2007). "The importance of c-Kit and PDGF receptors as potential targets for molecular therapy in breast cancer." Curr Med Chem **14**(7): 735-43.

Sawada, M., P. Hayes and S. Matsuyama (2003). "Cytoprotective membrane-permeable peptides designed from the Bax-binding domain of Ku70." Nat Cell Biol **5**(4): 352-7.

Schramm, A., J. H. Schulte, K. Astrahantseff, O. Apostolov, V. Limpt, H. Sieverts, S. Kuhfittig-Kulle, P. Pfeiffer, R. Versteeg and A. Eggert (2005). "Biological effects of TrkA and TrkB receptor signaling in neuroblastoma." Cancer Lett **228**(1-2): 143-53.

Sinha, P., J. Poland, M. Schnolzer and T. Rabilloud (2001). "A new silver staining apparatus and procedure for matrix-assisted laser desorption/ionization-time of flight analysis of proteins after two-dimensional electrophoresis." Proteomics **1**(7): 835-40.

Tastet, C., S. Charmont, M. Chevallet, S. Luche and T. Rabilloud (2003). "Structure-efficiency relationships of zwitterionic detergents as protein solubilizers in two-dimensional electrophoresis." Proteomics **3**(2): 111-21.

Tastet, C., P. Lescuyer, H. Diemer, S. Luche, A. van Dorsselaer and T. Rabilloud (2003). "A versatile electrophoresis system for the analysis of high- and low-molecular-weight proteins." Electrophoresis **24**(11): 1787-94.

Teoh, G., M. Urashima, E. A. Greenfield, K. A. Nguyen, J. F. Lee, D. Chauhan, A. Ogata, S. P. Treon and K. C. Anderson (1998). "The 86-kD subunit of Ku autoantigen mediates homotypic and heterotypic adhesion of multiple myeloma cells." J Clin Invest **101**(6): 1379-88.

Ursini-Siegel, J., B. Schade, R. D. Cardiff and W. J. Muller (2007). "Insights from transgenic mouse models of ERBB2-induced breast cancer." Nat Rev Cancer **7**(5): 389-97.

Watanabe, F., K. Shinohara, H. Teraoka, K. Komatsu, K. Tatsumi, F. Suzuki, T. Imai, M. Sagara, H. Tsuji and T. Ogiu (2003). "Involvement of DNA-dependent protein kinase in down-regulation of cell cycle progression." Int J Biochem Cell Biol **35**(4): 432-40.

Weeraratna, A. T., J. T. Arnold, D. J. George, A. DeMarzo and J. T. Isaacs (2000). "Rational basis for Trk inhibition therapy for prostate cancer." Prostate **45**(2): 140-8.

Zhu, Z., H. Friess, F. F. diMola, A. Zimmermann, H. U. Graber, M. Korc and M. W. Buchler (1999). "Nerve growth factor expression correlates with perineural invasion and pain in human pancreatic cancer." J Clin Oncol **17**(8): 2419-28.

DISCUSSION ET PERSPECTIVES

Les travaux réalisés au cours de ma thèse ont permis de caractériser le phénotype des cellules cancéreuses de sein suite à la surexpression du récepteur TrkA. Ainsi, les principales caractéristiques de ces cellules sont une augmentation de la croissance, de la résistance à certains apoptogènes, de la résistance à l'anoïkis et de la invasion (Article 2). Nous avons pu également mettre en évidence des partenaires importants pour l'effet biologique de TrkA : Ku70 agit sur la survie des cellules (Article 1) et Ku86 participe à la migration cellulaire (Article 3).

I. Augmentation de l'agressivité des cellules surexprimant TrkA.

Les cellules MDA-MB-231 ont été initialement prélevées d'une effusion plurale. Elles sont caractérisées par une grande capacité à proliférer, à résister à certains apoptogènes et à migrer (Cailleau et al. 1974; Cailleau et al. 1974; Garcia et al. 1992). Lorsque ces cellules sont injectées à des souris immunodéficientes *nude*, elles forment des adénocarcinomes peu différenciés de grade III (Price et al. 1990). Elles sont donc globalement considérées comme des cellules prototypiques hormono-insensibles d'un stade avancé de la maladie. Malgré l'agressivité préexistante des MDA-MB-231, nous avons montré dans l'article 2 que la surexpression de TrkA par transfection stable induit l'activation constitutive de TrkA et augmente encore le phénotype agressif de ces cellules. Ainsi, leur croissance est accrue tout comme leur migration et leur invasion, elles sont également plus résistantes à l'induction de l'apoptose par des agents chimiothérapeutiques (C2, doxorubicine, 5-Fluorouracile) ou des cytokines telles que TRAIL, et enfin, elles résistent de manière prolongée à l'anoïkis. D'autre part, nos études *in vivo* chez les souris SCID montrent que les cellules surexprimant TrkA forment des tumeurs plus rapidement. La croissance accrue des tumeurs primaires est associée à une augmentation de la prolifération des cellules cancéreuses et à une augmentation de l'angiogenèse tumorale. De manière intéressante, les cellules surexprimant TrkA développent des métastases plus nombreuses au niveau des poumons, du foie et du cerveau. Les cellules métastatiques pulmonaires sont plus résistantes à l'anoïkis comparativement aux cellules avant injection, suggérant l'importance de la résistance à l'anoïkis dans le processus métastatique. Nos

résultats montrent clairement que TrkA est impliqué dans l'augmentation de l'agressivité des cellules tumorales de sein et confortent les observations décrites par Davidson et ses collaborateurs (Davidson et al. 2004). En effet, les auteurs ont montré que la forme active de TrkA (Phospho-TrkA) est fréquemment retrouvée dans les effusions et les récurrences locorégionales alors qu'elle est moins fréquente dans les sites primaires. Ils suggèrent que l'activation de TrkA est associée à un caractère tumoral plus agressif

Dans ce contexte, les recherches sur les inhibiteurs visant TrkA (inhibiteurs pharmacologiques ou anticorps neutralisants) sont des options à prendre en compte dans le traitement du cancer du sein à l'image de ce qui se fait pour les récepteurs d'autres facteurs de croissance tels que l'EGF-R (Ito et al. 2007), le FGF-R (Ornitz and Itoh 2001; Manetti and Botta 2003), l'IGF-R (Pandini et al. 2007; Zavodovskaya et al. 2007), le VEGF-R (Wilmes et al. 2007) et l'HGF-R (Koga et al. 2007; Zou et al. 2007). Cependant, les facteurs de croissance n'agissent pas de façon indépendante. Ainsi, des études sur des cellules bronchiales ont montré que l'EGF-R et le TGFβ1 sont tous les deux nécessaires à l'induction de l'expression de l'oncogène COX-2 (Liu et al. 2007). Dans ce cas précis, EGF-R et TGFβ1 agissent de manière complémentaire pour participer au développement tumoral. Au vue de ces différentes données et afin d'optimiser les futurs traitements, il est nécessaire de viser à la fois les récepteurs spécifiques et les cibles moléculaires communes.

II. Auto-activation de TrkA et de ses voies de signalisation

Nous avons vu dans l'introduction que le récepteur TrkA est capable d'activer de nombreuses voies de signalisation suite à une stimulation par le NGF, aboutissant à des effets très différents en fonction du type et du contexte cellulaire. Dans notre étude, nous avons montré que la surexpression de TrkA induit une augmentation de phospho-TrkA et une activation constitutive des voies de signalisation PI3K/Akt, ERK/p38 MAPK. L'activation de TrkA peut être induite par le NGF sécrété par les cellules ou par sa simple surexpression. En effet, il a été montré qu'il existe une boucle autocrine de NGF dans les lignées de cancer du sein (MDA-MB-231, MCF-7, T47-D...) (Dollé et al. 2003). De plus, il a été décrit la surexpression de TrkA dans des cellules PC12 entraîne une auto-activation du récepteur (Leoni and Valtorta 2002). La surexpression de TrkA peut rendre

sa glycosylation incomplète, or il a été reporté que la glycosylation du récepteur empêche son autoactivation (Watson et al. 1999). Dans notre modèle, il est donc possible que TrkA surexprimé s'autoactive du fait d'une glycosylation incomplète.

Les résultats obtenus montrent que les voies PI3K/Akt et ERK MAPK sont essentielles aux effets biologiques observés dans les cellules surexprimant TrkA. De façon surprenante, la sensibilité des cellules au NGF exogène varie selon les phénotypes étudiés. Ainsi, le NGF stimule la migration et l'invasion des cellules surexprimant TrkA alors qu'il n'a aucun effet sur la prolifération et la résistance à l'apoptose. Ce phénomène pourrait être expliqué par la saturation de certaines cibles en aval des voies de signalisation responsables des effets biologiques.

III. Rôle pléiotropique des protéines Ku70 et Ku86

Initialement, l'hétérodimère de Ku a été découvert pour jouer un rôle central dans la reconnaissance et la réparation des cassures double brin de l'ADN en recrutant la sous unité catalytique DNA-PKcs (DNA Protein Kinase Catalytic sub-unit). Mais plus récemment, diverses autres fonctions ont été imputées à Ku70, à Ku86 ou à l'hétérodimère. Ainsi, alors que Ku70 est principalement nucléaire, il peut également être retrouvé au niveau du cytoplasme des cellules où il joue un rôle cytoprotecteur *via* son interaction avec la protéine pro-apoptotique Bax (Sawada et al. 2003). Nous avons montré que l'interaction entre TrkA et Ku70 est essentielle à la survie des cellules qui surexpriment TrkA (Article 1). Cet effet cytoprotecteur semble indépendant de Ku86 puisque l'inhibition de Ku86 n'a pas d'effet sur la survie des cellules surexprimant TrkA. De plus, une colocalisation de TrkA et de Ku70 est observée au niveau du cytoplasme et du noyau.

Il a été décrit que les protéines Ku peuvent également être exprimées à la surface externe de la membrane plasmique de certaines cellules comme les macrophages dérivés de monocytes (Monferran et al. 2004), les cellules endothéliales humaines de la veine ombilicale (HUVEC) (Ginis et al. 1995), des cellules hématopoiétiques et des cellules cancéreuses d'origines différentes (Prabhakar et al. 1990; Dalziel et al. 1992; Ginis et al. 1995; Ginis and Faller 2000; Lynch et al. 2001). Dans les monocytes, Ku70 et Ku86

membranaires stimulent la migration et l'invasion cellulaires en activant la métalloprotéase MMP9 (Muller et al. 2005). Dans des cellules de neuroblastome et les cellules cancéreuses mammaires MCF-7, Ku86 est impliqué dans la motilité et l'invasion cellulaire (Ginis and Faller 2000). Nous avons observé que la surexpression de TrkA provoque l'augmentation de l'expression de Ku86. De plus, nous avons retrouvé Ku86 lors de l'immunoprécipitation de TrkA. Ku86 est impliqué dans la migration des cellules, cette implication ne nécessite pas la présence de Ku70 (Article 3). Ainsi, dans notre modèle cellulaire, les protéines Ku peuvent jouer des rôles différents indépendamment l'une de l'autre. Au même titre que les protéines Ku, d'autres protéines ont un rôle pléitropique en fonction de leur localisation cellulaire. Ainsi, la protéine chromosomale HMGB1 (High Motility Group Box) est connue pour faciliter l'assemblage de complexes protéiques comme les facteurs de transcription (Récepteur aux stéroïdes, p53, TBP) au niveau de sites spécifiques sur la chromatine (Calogero et al. 1999). Mais, HMGB1 joue aussi un rôle dans l'inflammation et dans la métastase tumorale en stimulant la migration cellulaire lorsqu'elle est sécrétée à la surface des cellules (Wang et al. 1999; Taguchi et al. 2000). De manière relativement troublante, la protéine HMGB1 est capable d'activer la métalloprotéase MMP9 tout comme Ku86 (Monferran et al. 2004) ! À la lumière de ces deux exemples, on peut entr'apercevoir la complexité des mécanismes cellulaires. En effet, 30000 gènes codent plus d'un million de protéines dont les fonctions peuvent non seulement varier selon des modifications post-traductionnelles mais également en fonction de leur localisation cellulaire.

De nombreuses interrogations ont été soulevées depuis la découverte du rôle des Ku86 à la surface des cellules. Par exemple, nous ne savons pas comment est sécrété Ku86 en absence de peptide signal, ni comment il se lie à la membrane et comment il interagit avec TrkA ?

IV. Intérêt des protéines identifiées après 2D

Par une approche de protéomique globale, nous avons repéré 26 spots dont l'intensité varie dans les cellules surexprimant TrkA. Certains spots ne contiennent qu'une seule protéine alors que d'autres spots en contiennent 2 ou plusieurs. Parmi les spots dont l'intensité augmente, nous avons identifié la protéine Ku86. Nous avons montré que cette protéine est impliquée dans la stimulation de la migration induite par TrkA. Il serait donc important d'étudier l'implication d'autres protéines identifiées dans les effets biologiques induits par l'activation de TrkA. Pour cela, il faudra confirmer les variations observées par d'autres méthodes (Western blots, ELISA...) puis valider leur implication dans les effets biologiques induits par TrkA.

V. Avantages et limites de nos approches expérimentales

❖ *Transfection stable*

Nous avons initialement débuté notre recherche sur les cellules MCF-7 à l'aide de transfection transitoire (Article 1). Mais certaines expériences que nous voulions réaliser nécessitaient une expression prolongée de TrkA. Nous avons alors envisagé l'établissement de lignées surexprimant TrkA de façon stable issues des MDA-MB-231. Une des raisons pour lesquelles nous avons opté pour la lignée MDA-MB-231 est que cette lignée cellulaire dérivent moins en culture par rapport au MCF-7. Néanmoins, l'obtention de clones à partir des MDA-MB-231 n'a pas non plus été simple. À titre d'exemple, après sélection à l'antibiotique (Hygromycine B), nous avons isolé 60 clones résistants, malheureusement seuls 5 clones surexprimaient l'ARNm de TrkA et 3 la protéine. Afin d'éviter d'observer des effets clonaux provoqués par la transfection, nous avons utilisé 2 clones que nous avons étudiés en parallèle avec une population totale de cellules surexprimant TrkA.

La surexpression d'une protéine pose le problème de la relevance du niveau d'expression par rapport au niveau physiologique dans les tumeurs. Les travaux

précédents du laboratoire ont montré une hétérogénéité du niveau d'expression de l'ARNm de TrkA dans les échantillons de cancers du sein. Dans l'article 2, une nouvelle étude de l'expression de TrkA a permis de montrer qu'une très grande majorité des tumeurs de sein surexprime TrkA par rapport aux biopsies mammaires normales. Néanmoins, le niveau moyen d'ARNm dans la lignée MDA-MB-231 est 3 fois moins élevé qu' au niveau des tumeurs (Descamps et al. 2001). Nous avons également montré qu'au niveau protéique, les MDA-MB-231 contrôle expriment un faible niveau de TrkA alors que les MDA-MB-231 surexprimant TrkA expriment un niveau globalement équivalent à ce que l'on trouve dans les tumeurs. Le niveau de TrkA dans notre modèle de surexpression reste donc relevant. Cependant, un système inductible aurait pu permettre d'analyser les effets et la signalisation de TrkA en fonction du niveau d'expression du récepteur.

Le modèle de surexpression ne doit être qu'une première étape, car en surexprimant l'un des deux récepteurs du NGF, on provoque un déséquilibre de la balance TrkA/p75^{NTR} qui, nous l'avons vu dans l'introduction, peut s'avérer important pour certains effets biologiques. Ainsi, les effets biologiques que nous avons observés sont bien imputables à TrkA, mais seraient-ils les mêmes si p75^{NTR} était également surexprimé ou réprimé ? En effet, certaines études montre que p75^{NTR} amplifie l'activation des voies de signalisation induites par TrkA et accélère ainsi la différenciation neurales des PC12 (Epa et al. 2004; Diolaiti et al. 2007). Une autre étude a montré que p75^{NTR} ralentit l'ubiquitinilation, l'internalisation et la dégration de TrkA, prolongeant ainsi son activation au niveau de la membrane (Makkerh et al. 2005).

Le « must » aurait été de réaliser des primo-cultures de cellules tumorales surexprimant TrkA ! Notre démarche est donc la première des étapes nécessaires à la compréhension du rôle de TrkA dans le développement tumoral mammaire.

❖ *L'immuno-précipitation (IP)*

Afin de pouvoir diminuer, voire inhiber, les effets de TrkA, il faut connaître ses modes de signalisation. L'étude des partenaires de TrkA s'est faite par IP après 10 min de stimulation au NGF et les identifications ont été réalisées grâce aux outils de spectrométrie de masse. Cela nous a permis d'identifier Ku70 comme médiateur de la

survie des cellules surexprimant TrkA et Ku86 comme étant impliqué dans la migration cellulaire.

L'IP nécessite des quantités très importantes de matériel compatibles avec la coloration des gels au bleu de Coomassie colloïdal et l'identification par spectrométrie de masse. Une telle quantité peut nous faire redouter la présence de faux positifs que l'on enrichirait en même temps que le complexe TrkA. De plus, la surexpression de TrkA dans les cellules pourrait provoquer une association du récepteur avec des protéines non-spécifiques. Des mises au point à chacune des étapes de l'IP (tampon d'extraction, support de l'IP billes magnétique, tampon d'IP, tampon d'élution) ont donc été nécessaires pour obtenir les immuno-précipitats les plus « propres » possible.

Avec plus de recul sur les protocoles mis au point au cours de cette thèse, une spécificité plus importante aurait pu être obtenue en procédant en parallèle à une IP avec des anticorps isotypes contrôles. Ainsi, toutes les protéines identifiées dans les deux IP sont des faux positifs dont il ne faut pas tenir compte car elles ont précipité en se fixant de manière aspécifique sur les billes ou sur les anticorps. Il existe d'autres méthodes permettant l'identification de partenaires d'un complexe qui pourraient être utilisées de manière complémentaire à l'IP. La méthode de double purification dite TAP (Tandem Affinity Purification) a été développée pour les complexes de protéines (Rigaut et al. 1999). La combinaison de deux étiquettes d'affinité différentes a considérablement réduit le nombre de faux-positifs et les résultats dans l'étude de la signalisation du TNFa sont très prometteurs (Puig et al. 2001). Il existe aussi les méthodes de criblage double-hybride (Serebriiskii et al. 2001; Toby and Golemis 2001), de « blue native-PAGE » qui permet la séparation de complexes protéiques sur gels en deux dimensions (Tulp et al. 1999), de Glutathion S transférase-pull down (GST-Pulle Down) (Malloy et al. 2001; Naud et al. 2003) et enfin la méthode de « phage-display » (Mourez and Collier 2004).

Nous avons identifié que peu de protéines de signalisation (12 %) en utilisant les MDA-MB-231 surexprimant TrkA. Par ailleurs, nous n'avons retrouvé qu'un seul partenaire connu de TrkA à savoir PDK1. Plusieurs hypothèses sont possibles pour expliquer ces résultats : les protéines de signalisation sont des protéines exprimées en très faible quantité, les rendant difficilement détectables par les outils de spectrométrie de masse ; d'autre part, les caractéristiques physico-chimiques de certains peptides sont

incompatibles avec la spectrométrie de masse, car ils peuvent précipiter lors des élutions ou très mal voler dans les analyseurs.

❖ *L'électrophorèse bidimensionnelle (2D)*

L'électrophorèse 2D est une technique très performante pour étudier de manière naïve les modifications du protéome suite à un traitement ou, dans notre cas, suite à la surexpression d'une protéine. En effet, elle permet de visualiser sans à priori les modifications de très nombreuses protéines. Néanmoins, il a fallu mettre au point les protocoles d'extraction, d'isofocalisation et de seconde dimension, qui ont été pour moi un véritable parcours du combattant avec des problèmes qui en appellent d'autres en permanence. Toutefois, à force de persévérance et avec l'aide de nombreuses personnes, et notamment le Dr. Christiphe Tastet, nous avons pu mettre au point un protocole d'électrophorèse 2D par « cup-loading » très reproductible pour les gammes de pH 3-10 et 6-11. L'analyse informatique qui suit la production des gels 2D est une étape essentielle pour la détermination des variations (là encore, je du mettre au point des protocoles adaptés aux nouveaux matériels récemment acquis au laboratoire). Malgré une automatisation de plus en plus poussée, les analyses informatiques nécessitent de longues heures de nettoyage manuel et de vérification de détection et d'appariement des spots. Ainsi, la technique d'électrophorèse 2D est composée de très nombreuses étapes clés qui nécessitent une organisation draconienne.

Cette technique comporte certaines limites pour la recherche des modifications sur l'ensemble du protéome. En effet, les protéines de haut poids moléculaires, les protéines hydrophobes, les protéines membranaires ainsi que les protéines acides sont très difficilement analysables. Durant cette analyse, nous n'avons jamais repéré de spots pouvant correspondre à la surexpression de TrkA qui cumule les caractéristiques de contre-indication à la 2D : protéines de haut poids moléculaire et domaine transmembranaire hydrophobe. Néanmoins, nous avons dénombré plus de 1500 spots différents par gel dans une zone de pH comprise entre 3 et 10. Parmi ces spots, 26 ont été observés comme subissant une variation suite à la surexpression de TrkA. L'analyse par spectrométrie a permis d'identifier un certain nombre de protéines pouvant correspondre

à ces spots. Ainsi, dans les cas les plus simples, nous avons identifié une seule protéine, mais parfois les spots s'avéraient être un mélange de plusieurs protéines.

La technique que nous avons utilisée nécessite la comparaison de gels 2D comportant chacun un seul échantillon. Malgré la reproductibilité des gels, les déformations et autres anomalies des gels ont compliqué l'analyse. De plus, la coloration à l'argent que nous avons utilisée n'est que semi-quantitative. De nouvelles méthodes sont disponibles afin de contourner ces contraintes. Par exemple, la 2D-DIGE (Differential Gel Electrophoresis), une méthode basée sur le greffage différentiel de fluorochromes (cyanines) sur les échantillons, permet de comparer jusqu'à 3 échantillons différents sur un seul gel (Marouga et al. 2005). De plus, les difficultés liées aux déformations sont en partie éliminées et la coloration aux cyanines est quantitative car linéaire sur une gamme beaucoup plus importante (5 ordres de magnitude contre 1,5 pour une coloration à l'argent). Plus récemment, des techniques indépendantes de l'électrophorèse 2D ont été développées. Le SILAC (Stable Isotope Labeling with Amino acids in Cell culture) permet une quantification stricte qui se fait à l'aide d'une incorporation d'acides aminés marqués par des isotopiques stables (Mann 2006) suivie d'une analyse systématique des pistes d'un gel 1D. La quantification se fait par spectrométrie de masse. Enfin, des méthodes comme le « Shot-Gun », ne nécessitant pas de gel d'acrylamide, peuvent parfois être utilisées. Le « Shot-Gun » repose sur une séparation des produits de digestion d'échantillons protéiques complexes par chromatographies liquides multidirectionnelles suivie d'une anlayse par spectrométrie de masse en tandem (McDonald and Yates 2003). Par comparaison, les plus récentes analyses ont montré la détection dans un même « run » de « Shot-Gun » de 5130 protéines chez l'homme soit 15% des ORF (Open Reading Frame) prédits, alors que l'électrophorèse n'en détecte que 5% au mieux (Resing 2004). De plus, cette technique permet d'analyser le remaniement de domaines très hydrophobes tels que ceux des centromères (Andersen et al. 2003), des rafts (Foster et al. 2003) et des microsomes (Han et al. 2001).

VI. Conclusion et perspectives

Au cours de ma thèse, nous avons créé un modèle cellulaire surexprimant TrkA. Cette surexpression de TrkA augmente l'agressivité des cellules de cancer du sein *in vitro* et *in vivo*. Nous avons montré que les voies PI3K/Akt et ERK MAPK sont essentielles aux effets biologiques observés. De plus, nous avons démontré l'implication des protéines Ku70 et Ku86 dans la survie et la migration des cellules surexprimant TrkA. Il serait donc important de poursuivre les études sur les mécanismes moléculaires des voies de signalisation de l'axe NGF/TrkA.

De manière plus générale, nos résultats soulèvent de nombreuses questions : Quels sont les voies de signalisation activées par TrkA dans les tumeurs ? Par quels mécanismes TrkA est-il surexprimé ? Y a-t-il amplification génique, modifications épigénétiques ou mutations au niveau du promoteur de TrkA ? Y a-t-il perte progressive de la sensibilité au NGF parallèlement à l'augmentation de l'expression de TrkA, faisant ainsi passer les cellules d'un état autocrine à un état acrine vis-à-vis du NGF ? Une première étude menée au laboratoire montre qu'il n'y a pas de mutations significatives dans la zone promotrice proximale du gène TrkA.

D'autre part, il a été décrit que la surexpression de TrkB transforme les cellules épithéliales intestinales normales de rat et les rend hautement métastatiques (Douma et al. 2004). De plus, la transformation des cellules épithéliales mammaires normales (HMEC) par la télomérase active la signalisation du récepteur à l'EGF en inhibant l'expression de $p57^{KIP2}$ (protéine inhibitrice de la signalisation du récepteur EGF) (Yaswen and Stampfer 2002). Des études précédentes du laboratoire ont permis d'observer que TrkA est exprimé dans les cellules normales de sein mais non activable par le NGF. Il serait donc intéressant de connaître l'impact de la surexpression de TrkA dans des cellules normales de sein. TrkA est-il capable d'induire la carcinogenèse de cellules mammaires normales à l'image de TrkB, ou est-ce une propriété acquise plus tardivement au cours du développement tumoral nécessitant l'accumulation d'autres altérations au niveau de la cellule ?

Mon travail a permis d'ajouter quelques éléments essentiels à la compréhension de l'influence de TrkA sur le développement tumoral et ouvre de nombreuses perspectives de recherche pour les années à venir.

TRAVAUX SUPPLEMENTAIRES

Quand je suis arrivé au laboratoire, nous n'avions ni soutient de l'INSERM. Les thématiques étaient un peu plus variées, ce qui m'a amené à étudier au cours de mon DEA l'influence d'un traitement combiné de Tamoxifen, un agent anticancéreux utilisé en clinique, et TRAIL (Tumor necrosis factor Related Apoptosis Inducing Lingand), une cytokine au fort potentiel anti-tumorale. La labellisation ESPRI/ERI obtenue auprès de l'INSERM a nécessité une homogénéisation des thématiques autour du NGF, c'est ainsi que je me suis intéressé au rôle de TrkA dans le cancer du sein. Néanmoins, les travaux réalisés au cours de mon DEA étaient très prometteurs, nous avons donc décidé de poursuivre cette étude en parallèle de mes travaux de thèse proprement dit.

De plus, d'autres travaux restaient inachevés. Ainsi, Robert-Alain Toillon avait montré au cours de sa thèse que les cellules mammaires normales contrôlent la croissance des cellules cancéreuses *via* la sécrétion de facteurs dans le milieu extracellulaire (Toillon et al. 2000; Toillon et al. 2002a; Toillon et al. 2002b). Nous avons alors entrepris de poursuivre ses recherches afin de déterminer la nature des facteurs solubles responsables de l'induction de l'apoptose des cellules cancéreuses.

Il m'a semblé important de rendre compte de ces travaux, malgré l'absence de liens directs avec TrkA, car ils se sont tous les deux concrétisés par des publications.

I. Tamoxifen et TRAIL induisent de manière synergique l'apoptose des cellules cancéreuses de sein (Article 4).

Publié dans Oncogene 2007.

Les traitements actuels contre le cancer du sein sont la chirurgie, la radiothérapie et la chimiothérapie. Cependant, de nombreuses tumeurs échappent à ces traitements et de effets secondaires sont constatés, c'est pourquoi la recherche de traitements toujours plus efficaces est indispensable. Des traitements combinant l'action de plusieurs agents anti-cancéreux constituent une alternative intéressante en permettant d'être plus efficace tout en diminuant les doses et donc les effets secondaires. Le Tamoxifen est couramment utilisé contre les cancers du sein hormono-sensibles. TRAIL est une cytokine potentiellement anti-tumorale car capable d'induire préférentiellement l'apoptose de nombreux types de cellules cancéreuses sans influencer la survie des cellules normales. Nous avons montré ici que ces deux molécules induisent de manière synergiques l'apoptose des cellules cancéreuses de sein indifféremment de leur statut hormonal. Le co-traitement augmente l'expression de protéines pro-apoptotiques telles que FADD, Bax, Bid, Bid tronqué (tBid) et Caspase 9, et diminue l'expression de protéines anti-apoptotiques comme FLIPs et Bcl-2. Nous avons également confirmé l'efficacité de ce traitement *in vivo* chez les souris SCID. Ainsi, le co-traitement Tamoxifen plus TRAIL arrête la croissance des tumeurs issues des cellules cancéreuses mammaires hormono-insensibles MDA-MB-231. Nos résultats montrent la possibilité d'utiliser un traitement combinant Tamoxifen et TRAIL contre les cancers du sein quelque soit leur statut hormonal.

Oncogene (2007), 1–6

www.nature.com/onc

SHORT COMMUNICATION

Tamoxifen and TRAIL synergistically induce apoptosis in breast cancer cells

C Lagadec[1], E Adriaenssens[1], RA Toillon[1], V Chopin[1], R Romon[1], F Van Coppenolle[2], H Hondermarck[1] and X Le Bourhis[1]

[1]*INSERM ERI-8 (JE2488), Growth Factor Signaling in Breast Cancer. Functional Proteomics. IFR147, Université des Sciences et Technologies de Lille, Villeneuve d'Ascq, France and* [2]*INSERM U800, IFR147, Université des Sciences et Technologies de Lille, Villeneuve d'Ascq, France*

Tamoxifen (TAM), is widely used as a single agent in adjuvant treatment of breast cancer. Here, we investigated the effects of TAM in combination with tumor necrosis factor-related apoptosis-inducing ligand (TRAIL) in estrogen receptor-α (ER-α)-positive and -negative breast cancer cells. We showed that cotreatment with TAM and TRAIL synergistically induced apoptosis regardless of ER-α status. By contrast, cotreatment did not affect the viability of normal breast epithelial cells. Cotreatment with TAM and TRAIL in breast cancer cells decreased the levels of antiapoptotic proteins including FLIPs and Bcl-2, and enhanced the levels of proapoptotic proteins such as FADD, caspase 8, tBid, Bax and caspase 9. Furthermore, cotreatment-induced apoptosis was efficiently reduced by FADD- or Bid-siRNA, indicating the implication of both extrinsic and intrinsic pathways in synergistic apoptosis induction. Importantly, cotreatment totally arrested tumor growth in an ER-α-negative MDA-MB-231 tumor xenograft model. The abrogation of tumor growth correlated with enhanced apoptosis in tumor tissues. Our findings raise the possibility to use TAM in combination with TRAIL for breast cancers, regardless of ER-α status.
Oncogene advance online publication, 3 September 2007; doi:10.1038/sj.onc.1210749

Keywords: breast cancer; tamoxifen; TRAIL; apoptosis; tumor xenograft

Introduction

The antiestrogenic drug, tamoxifen (TAM), a nonsteroidal selective estrogen receptor modulator, has been used as a single agent in the treatment of estrogen receptor-α (ER-α)-positive breast cancer (Lover, 1989; Jordan, 1992). Clinical response to TAM is shown to be associated with both decreased proliferation and increased apoptosis (Gelman, 1997; McClay *et al.*, 2000). Thus, TAM is thought to exert antitumor effect via ER-α-dependent inhibition of cell proliferation and induction of apoptosis. However, an important additional feature of TAM is its effectiveness in the treatment of ER-α-negative neoplasia including breast cancer, malignant gliomas, pancreatic carcinoma and melanoma (Gelman, 1997; McClay *et al.*, 2000). Moreover, at clinical achievable concentrations (1–10 μM), TAM strongly induces apoptosis in both ER-α-positive and ER-α-negative breast cancer cells. The apoptosis-inducing effect is not reversible by addition of estrogens, suggesting that ER-α-independent induction of apoptosis could be a major mechanism of the observed antitumor effect of TAM (Hawkins *et al.*, 2000; Mandlekar and Kong, 2001). TAM can induce apoptosis through several distinct pathways including production of oxidative stress and ceramide, as well as transcriptional regulation of expression of Bcl-2 protein family members (Mandlekar and Kong, 2001; Nazarewicz *et al.*, 2007). Therefore, a critical question remaining is whether TAM, if given in combination with other agents, will be more efficient to eliminate both ER-α-positive and ER-α-negative breast cancer cells.

Tumor necrosis factor-related apoptosis-inducing ligand (TRAIL), has recently emerged as a novel biological agent for cancer therapy (LeBlanc and Ashkenazi, 2003). TRAIL exerts its tumoricidal effect by directly inducing apoptosis of cancer cells via a receptor-mediated process. TRAIL interacts with five different receptors: two functional receptors (DR4 and DR5), two decoy receptors (DcR1 and DcR2) that can bind TRAIL but lack the functional intracellular death domain, thus incapable of transducing a death signal, and one soluble protein (osteoprotegerin) that binds TRAIL at low affinity. Binding of TRAIL to DR4 or DR5 results in the recruitment of the adapter protein FADD, which in turn recruits and activates caspases 8 or 10. These active caspases initiate apoptosis either by direct cleavage of downstream effector caspases (extrinsic pathway) or by cleaving Bid. Truncated Bid (tBid) becomes inserted into mitochondrial membrane to favor the release of proapoptotic factors such as cytochrome *c*, leading to caspase 9 activation and subsequent apoptosis. This mitochondria-mediated signaling cascade is also called intrinsic pathway (LeBlanc and Ashkenazi, 2003).

Correspondence: Professor X Le Bourhis, INSERM ERI-8, Université des Sciences et Technologies de Lille, Villeneuve d'Ascq, 59655, France.
E-mail: xuefen.lebourhis@univ-lille1.fr
Received 23 April 2007; revised 9 July 2007; accepted 27 July 2007

Although the majority of cultured cancer cells show a certain degree of sensitivity to the cytotoxic effect of TRAIL, it has been well documented that cotreatment with TRAIL and chemotherapeutic agents such as topoisomerase inhibitors, antimetabolites and antimicrotubule agents results in a synergistic induction of tumor cell apoptosis and a marked inhibition of tumor growth in murine xenograft models (Duiker *et al.*, 2006).

Despite the existence of plenty of convincing data describing the ability of TRAIL to synergize chemotherapeutic agent-induced apoptosis of cancer cells, nothing is known about the effect of combined treatment with TAM and TRAIL on breast cancer cells, especially in ER-α-negative breast cancer cells. Here, we show that these two agents synergize to induce apoptosis in both ER-α-positive and ER-α-negative breast cancer cells. Moreover, TAM and TRAIL together totally abolish tumor growth in an ER-α-negative MDA-MB-231 tumor xenograft model. Our findings provide a proof of principle that the clinical efficacy of TAM could be enhanced by combined treatment with TRAIL not only for ER-α-positive but also for ER-α-negative breast cancers.

Results and discussion

Cotreatment with TAM and TRAIL enhanced apoptosis induction in breast cancer cells

We investigated whether the combination of TAM and TRAIL could enhance apoptosis more than either agent alone. As shown in Figure 1, TAM (2 μM) and TRAIL (1 ng ml^{-1}) alone only moderately induced apoptosis (10–20%) in breast cancer cells. In contrast, cotreatment with TAM and TRAIL synergistically induced apoptosis in all breast cancer cell lines tested regardless of ER-α status, since the combination index was calculated as being less than 1 (0.4–0.6). Synergistic induction of cell death was also confirmed by MTT assay (Supplementary Figure 1). Interestingly, neither agent alone nor in combination affected apoptosis in normal breast epithelial cells (Figure 1b and Supplementary Figure 1). Since TAM is known to induce cell cycle blockage in ER-α-positive breast cancer cells (Osborne, 1998), we then performed flow cytometric analysis to see if there were any modifications of cell cycle distribution upon cotreatment (Supplementary Table 1). TAM alone or in combination with TRAIL induced an accumulation of ER-α-positive MCF-7 cells in G_1 phase; no significant modifications of cell cycle profile were observed in ER-α-negative MDA-MB-231 cells. However, the percentages of cells in subG_1 were strongly increased by cotreatment in both MCF-7 and MDA-MB-231 cells. Collectively, these results indicated that the combination of TAM and TRAIL synergistically induced apoptosis in breast cancer cells regardless of ER-α status. Results shown were obtained in serum-free culture medium to avoid eventual protective effects of serum-derived survival factors. However, similar results were observed in the presence of 5% serum (data not shown). Of note, the apoptosis-inducing effects of TAM alone or in

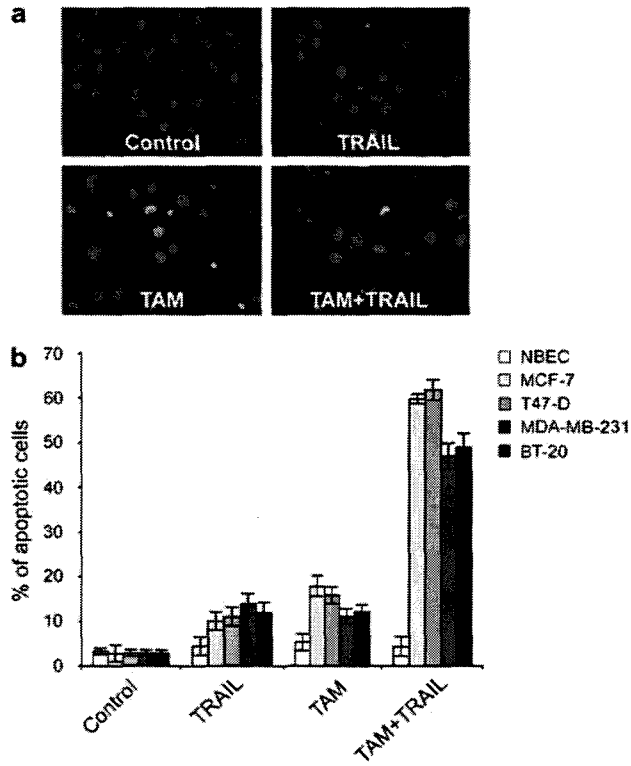

Figure 1 Effects of tamoxifen (TAM) and tumor necrosis factor-related apoptosis-inducing ligand (TRAIL) on apoptosis in breast cancer and normal epithelial cells. ER-α-positive (MCF-7, T47-D) and ER-α-negative (MDA-MB-231, BT-20) human breast cancer cells as well as normal breast epithelial cells (NBEC) were treated in serum-free medium with 2 μM TAM and/or 1 ng ml^{-1} TRAIL for 24 h. (**a**) Hoechst staining of MCF-7 cells. Apoptotic nuclei are condensed or fragmented. (**b**) Percentage of apoptotic cells was determined after Hoechst staining as described (Chopin *et al.*, 2004). Values represent mean±s.d. of three experiments. Synergism was calculated as described (Supplementary Data).

combination with TRAIL were somewhat stronger in ER-α-positive cells. Since TAM can acts through ER-α inhibition to induce apoptosis (Mandlekar and Kong, 2001), it is possible that the superiority of observed effects in ER-α-positive breast cancer cells may be partly mediated by signaling through ER-α. Nevertheless, at clinical achievable concentrations (1–10 μM), TAM has already been shown to induce apoptosis through mechanisms independent of ER-α including production of oxidative stress and ceramide, activation of JNK, as well as transcriptional regulation of expression of Bcl-2 protein family members (Mandlekar and Kong, 2001; Kallio *et al.*, 2005; Nazarewicz *et al.*, 2007). Accordingly, we observed that inhibition of JNK activity, using the specific JNK inhibitor SP600125 or a dominant-negative form of JNK, reduced cotreatment-induced apoptosis (data not shown).

Both extrinsic and intrinsic pathways were involved in cotreatment-induced apoptosis

TRAIL-induced apoptosis in breast cancer cells is known to involve both extrinsic (death receptor) and

intrinsic (mitochondrial) pathways (Suliman *et al.*, 2001). We first determined the effects of cotreatment on the levels of molecular determinants of TRAIL signaling pathways (Figure 2a and Supplementary Table 2). Cotreatment increased the expression of the death receptor adapter FADD and reduced the expression of the short FLICE inhibitory protein (FLIP) isoform (FLIPs) in both MCF-7 and MDA-MB-231 cells. As FLIP competes with procaspase 8 to inhibit procaspase 8 recruitment by FADD, the observed modifications presumably lead to more recruitment of procaspase 8, and therefore increase caspase 8 activation and subsequent cell death. Accordingly, FADD-siRNA efficiently reduced the expression of FADD and the synergistic induction of apoptosis by cotreatment (Figure 3a), confirming the implication of extrinsic pathways in synergistic induction of apoptosis.

Cross talk between the death receptor and mitochondrial pathways can be mediated by caspase 8 cleavage of Bid. tBid translocates to mitochondria and interacts with pro- and antiapoptotic members to activate or antagonize their functions, leading to cytochrome *c* release (LeBlanc and Ashkenazi, 2003). We showed that combined treatment with TAM and TRAIL strongly increased the cleavage of Bid in breast cancer cells (Figure 2a and Supplementary Table 2). Bid-siRNA efficiently reduced the expression of Bid and the synergistic induction of apoptosis by cotreatment (Figure 3b). However, Bid inhibition could not totally abolish apoptosis induced by cotreatment, suggesting that other Bcl-2 family proteins may be also implicated. Indeed, cotreatment increased the levels of pro-apoptotic protein Bax and decreased the levels of antiapoptotic protein Bcl-2. Thus, downregulation of antiapoptotic protein Bcl-2 together with upregulation of proapoptotic proteins tBid and Bax may constitute a complementary positive amplification loop to promote mitochondrial dysfunctions, as confirmed by the release of mitochondrial cytochrome *c* (Figures 2b and c) and enhanced levels of active caspase 9 (Figure 2a and Supplementary Table 2). The mechanism by which cotreatment regulates the levels of Bcl-2 family members

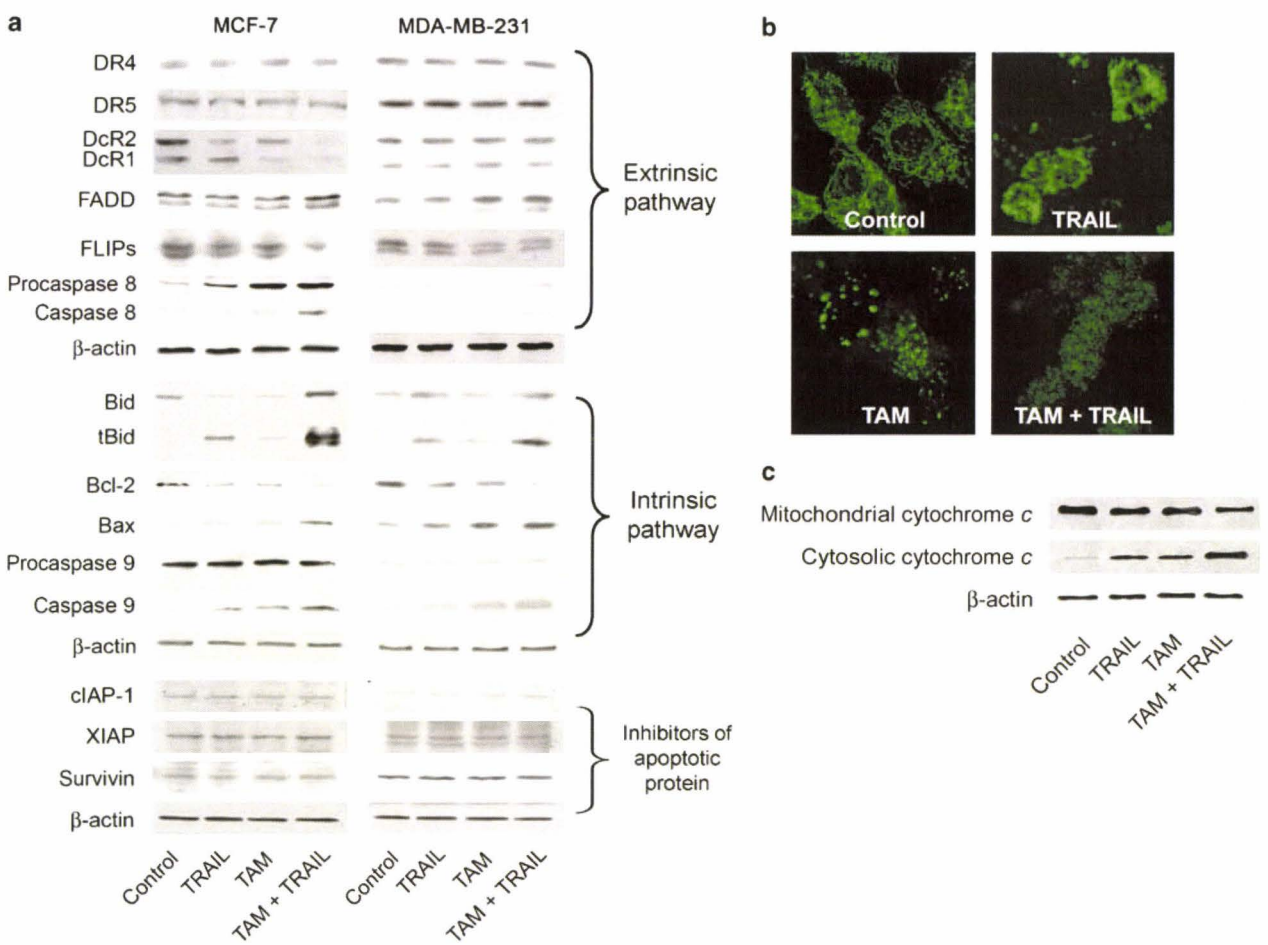

Figure 2 Modulations of apoptosis regulating proteins by cotreatment with tamoxifen (TAM) and tumor necrosis factor-related apoptosis-inducing ligand (TRAIL). MCF-7 and MDA-MB-231 breast cancer cells were treated in serum-free medium with 2 μM TAM and/or 1 ng ml^{-1} TRAIL for 24 h. Western blot and confocal microscopy were then performed as described (Chopin *et al.*, 2004). (**a**) Western blot analysis of whole cell lysates. (**b**) Confocal microscopy analysis of cytochrome *c* in MCF-7 cells. Typical punctuated mitochondrial staining was observed in control cells. A diffuse cytosolic signal was observed in cells treated with TRAIL and TAM alone, or in combination, suggesting the translocation of cytochrome *c* from mitochondria to cytosol. (**c**) Western blot analysis of mitochondrial and cytosolic cytochrome *c* in MCF-7 cells.

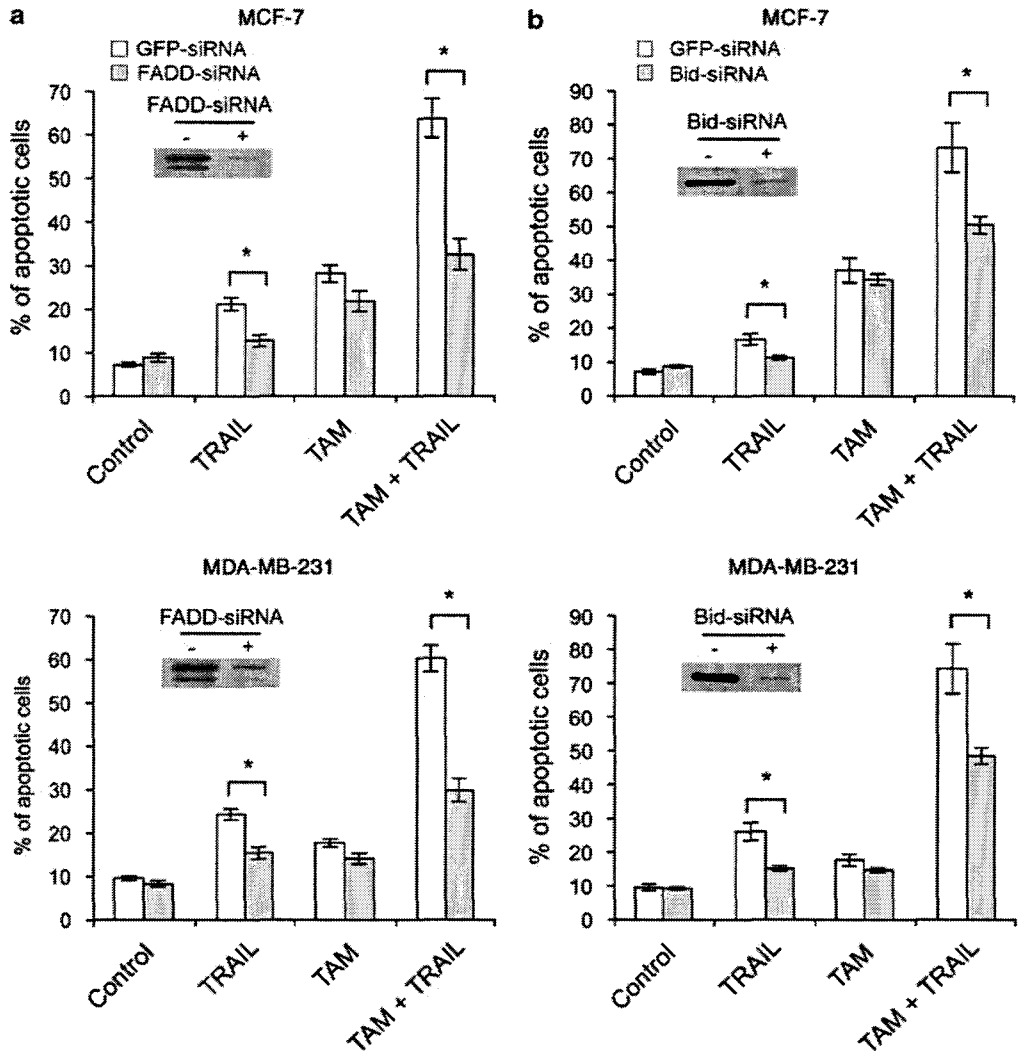

Figure 3 Effects of FADD-siRNA and Bid-siRNA on synergistic apoptosis induction. MCF-7 and MDA-MB-231 cells were subjected to one round of transfection with FADD-specific siRNA (**a**) or two sequential rounds of transfection with Bid-specific siRNA (**b**) as described (Grambihler *et al.*, 2003; Broaddus *et al.*, 2005). Twenty-four hours after transfection, cells were treated in serum-free medium with 2 μM tamoxifen (TAM) and 1 ng ml^{-1} tumor necrosis factor-related apoptosis-inducing ligand (TRAIL) alone or both for 24 h. Results were from one experiment representative of three independent experiments. $^*P<0.05$ (Student's *t*-test).

remains unknown. One explanation might be the involvement of JNK pathway. In this regard, activated JNK has been reported to enhance cleavage of Bid by enhanced activation of caspase 8 and to stimulate the expression of proapoptotic members such as Bid and Bax (Nakano *et al.*, 2006). Moreover, Yanamadala *et al.* (2007) have recently reported that phosphorylation of Bcl-2 by JNK leads to degradation of Bcl-2 protein via the proteasome pathway.

Abrogation of tumor growth by cotreatment with TAM and TRAIL in SCID mice

Because TAM and TRAIL synergized to induce apoptosis of breast cancer cells *in vitro*, we examined the effectiveness of combined treatment in an ER-α-negative breast cancer xenograft model. As shown in Figure 4a, TRAIL slightly reduced tumor growth while TAM had no significant effect when compared to control mice. Interestingly, combined treatment completely arrested tumor growth, as tumor volume remained the same during the periods of treatment. Quantification of terminal deoxynucleotidyl transferase biotin-dUTP nick end labeling (TUNEL)-positive cells in tumor sections showed that TAM had no significant effect on apoptosis induction, whereas TRAIL alone or in combination with TAM induced more than two- or sevenfold increase of apoptosis, respectively (Figures 4b and c). Interestingly, intensity of proliferating cell nuclear antigen (PCNA) expression index, an indicator of cell proliferation, was similar in tumors of different animal groups (Figure 4d). Thus, in the ER-α-negative breast cancer xenograft model, cotreatment induced apoptosis without modification of cell proliferation. Importantly, cotreatment did not affect survival in normal breast epithelial cells *in vitro* and was well tolerated by mice during the periods of treatment, as

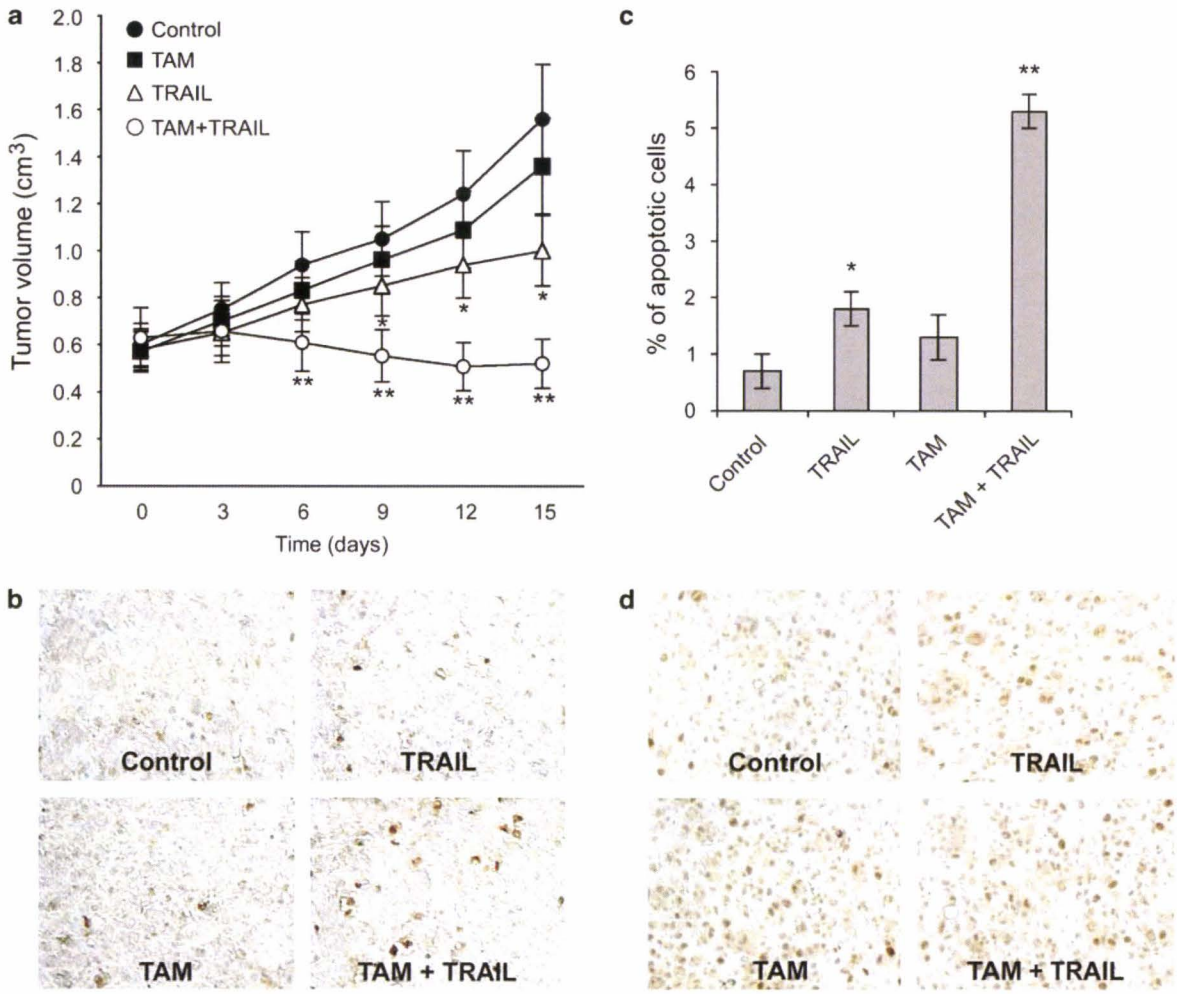

Figure 4 Effects of cotreatment with tamoxifen (TAM) and tumor necrosis factor-related apoptosis-inducing ligand (TRAIL) on tumor growth in SCID mice. The ER-α-negative breast cancer cells MDA-MB-231 (2×10^6) were injected subcutaneously into the right flank of 6-week-old SCID mice (Charles River Laboratories. L'Arbresle, France). Tumor volumes were monitored every 3 days with calipers and calculated using the formula: $4/3\pi \times r1^2 \times r2$, where $r1$ and $r2$ are the minor and the major dimensions, respectively. When tumor volume attained 0.6 cm^3, the animals were grouped ($n=8$ for each group) and treated with an intraperitoneal injection of TRAIL (30 μg in 100 μl PBS) and/or TAM (250 μg in 100 μl corn oil) every other day for 15 days. (**a**) Tumor volumes at different times of treatment. Data represent mean ± s.d. ($n=8$). (**b** and **c**) Analysis of apoptosis after TUNEL staining (ApopTag Peroxidase *in situ* Apoptosis Detection Kit, R&D systems, Lille, France). (**d**) Analysis of cell proliferation after PCNA staining (Santa Cruz, Le Perray en Yvelines, France). Significant differences (Student's *t*-test) between treated and untreated mice are indicated with asterisks. $^*P<0.05$; $^{**}P<0.01$.

there were no abnormal appearance and behavior (ruffled fur/lethargy) in mice. Moreover, no modification in body weight was observed after 15 days of treatment (data not shown).

Up to the present, TAM has been used to treat ER-α-positive breast cancers. However, approximately 40–50% of primary breast cancers are either ER-α-negative or ER-α-positive but resistant to TAM (Osborne, 1998). Thus a substantial proportion of breast cancers are not suited to treatment with TAM. It is now admitted that resistance to apoptosis is a major cause of nonresponsiveness of cancers leading to treatment failure. An exciting outcome from our study is the observation that suboptimal doses of both TAM and TRAIL can synergize to induce cell death even in ER-α-negative breast cancer cells. This raises the possibility to use TAM in combination with TRAIL for breast cancers, regardless of ER-α status. Moreover, cotreatment with low doses may be advantageous since high concentrations found to be active *in vitro* may often not be achieved *in vivo*. This is also of importance in reducing potential toxic side effects of each agent. Altogether, our findings may open up a new therapeutic window in the fight against breast cancers by combined use of TAM and TRAIL.

Acknowledgements

The study is supported by grants from INSERM, la Ligue Nationale Contre le Cancer (Equipe labellisée 2006), le Ministère de l'Education Nationale and the Région Nord/Pas-de-Calais. Chann Lagadec was the recipient of a fellowship from the Association pour la Recherche sur le Cancer (ARC).

References

Broaddus VC, Dansen TB, Abayasiriwardana KS, Wilson SM, Finch AJ, Swigart LB *et al.* (2005). Bid mediates apoptotic synergy between tumor necrosis factor-related apoptosis-inducing ligand (TRAIL) and DNA damage. *J Biol Chem* **280**: 12486–12493.

Chopin V, Slomianny C, Hondermarck H, Le Bourhis X. (2004). Synergistic induction of apoptosis in breast cancer cells by cotreatment with butyrate and TNF-alpha, TRAIL, or anti-Fas agonist antibody involves enhancement of death receptors' signaling and requires P21(waf1). *Exp Cell Res* **298**: 560–573.

Duiker EW, Mom CH, de Jong S, Willemse PH, Gietema JA, van der Zee AG *et al.* (2006). The clinical trail of TRAIL. *Eur J Cancer* **42**: 2233–2240.

Gelman EP. (1997). Tamoxifen for the treatment of malignancies other than breast and endometrial carcinoma. *Semin Oncol* **24**(Suppl): S65–S70.

Grambihler A, Higuchi H, Bronk SF, Gores GJ. (2003). cFLIP-L inhibits p38 MAPK activation: an additional anti-apoptotic mechanism in bile acid-mediated apoptosis. *J Biol Chem* **278**: 26831–26837.

Hawkins RA, Arends MJ, Ritchie AA, Langdon S, Miller WR. (2000). Tamoxifen increases apoptosis but does not influence markers of proliferation in an MCF-7 xenograft model of breast cancer. *Breast J* **9**: 96–106.

Jordan VC. (1992). The strategic use of antiestrogens to control the development and growth of breast cancer. *Cancer* **70**(Suppl): S977–S982.

Kallio A, Zheng A, Dahllund J, Heiskanen KM, Härkönen P. (2005). Role of mitochondria in tamoxifen-induced rapid death of MCF-7 breast cancer cells. *Apoptosis* **10**: 1395–1410.

LeBlanc HN, Ashkenazi A. (2003). Apo2L/TRAIL and its death and decoy receptors. *Cell Death Differ* **10**: 66–75.

Lover RR. (1989). Tamoxifen therapy in primary breast cancer: biology, efficacy, and side effects. *J Clin Oncol* **7**: 803–815.

Mandlekar S, Kong A-NT. (2001). Mechanisms of tamoxifen-induced apoptosis. *Apoptosis* **6**: 469–477.

McClay EF, McClay ME, Monroe L, Baron PL, Cole DJ, O'Brien PH *et al.* (2000). The effect of tamoxifen and cisplatin on the disease-free and overall survival of patients with high risk malignant melanoma. *Br J Cancer* **83**: 16–21.

Nakano H, Nakajima A, Sakon-Komazawa S, Piao JH, Xue X, Okumura K. (2006). Reactive oxygen species mediate crosstalk between NF-kappaB and JNK. *Cell Death Differ* **13**: 730–737.

Nazarewicz RR, Zenebe WJ, Parihar A, Larson SK, Alidema E, Choi J *et al.* (2007). Tamoxifen induces oxidative stress and mitochondrial apoptosis via stimulating mitochondrial nitric oxide synthase. *Cancer Res* **67**: 1282–1290.

Osborne CK. (1998). Tamoxifen in the treatment of breast cancer. *N Engl J Med* **339**: 1609–1618.

Suliman A, Lam A, Datta R, Srivastava RK. (2001). Intracellular mechanisms of TRAIL: apoptosis through mitochondrial-dependent and -independent pathways. *Oncogene* **20**: 2122–2133.

Yanamadala V, Negoro H, Gunaratnam L, Kong T, Denker BM. (2007). Galpha 12 stimulates apoptosis in epithelial cells through JNK1 mediated Bcl-2 degradation and upregulation of Ikappa B-alpha. *J Biol Chem* **282**: 24352–24363.

Supplementary Information accompanies the paper on the Oncogene website (http://www.nature.com/onc).

II. Les cellules épithéliales mammaires mormales induisent l'apoptose des cellules cancéreuses de sein via l'IGFBP-3 (Insulin-Like Growth Factor Binding Protein-3) and la maspine (Article 5).

Publié dans Molecular and cellular Proteomics 2007.

Les cellules mammaires normales sont connues pour exercer un effet apoptotique sur les cellules cancéreuses de sein, suggérant l'existence d'une inhibition paracrine du développement tumoral mammaire. Nous avons, ici, purifié et caractérisé les facteurs sécrétés par les cellules normales de sein, responsables de l'induction de l'apoptose des cellules mammaires cancéreuses. Le milieu conditionné de cellules normales a été concentré puis séparé par chromotographie. L'activité apoptotique des différentes fractions a été testée sur les cellules mammaires cancéreuses MCF-7. L'analyse par LC-MS/MS des fractions actives a permi d'identifier l'IGFBP-3 (Insulin Growth Factor Binding Protein-3) et la maspine. Nous avons montré, par Western blot, que ces 2 protéines sont exprimées spécifiquement par les cellules épithéliales normales et pas par les cellules cancéreuses. Des expériences d'immuno-déplétion ont confirmé l'implication de l'IGFBP-3 et de la maspine dans l'induction de l'apoptose des cellules cancéreuses de sein par les cellules épithéliales mammaires normales. Ces découvertes fournissent un argument moléculaire à l'effet inhibiteur des cellules normales environnantes sur le développement des tumeurs du sein observé depuis longtemps.

Proteomics Demonstration That Normal Breast Epithelial Cells Can Induce Apoptosis of Breast Cancer Cells through Insulin-like Growth Factor-binding Protein-3 and Maspin*

Robert-Alain Toillon‡§, Chann Lagadec‡§¶, Adeline Page‖, Valérie Chopin‡, Pierre-Eric Sautière**, Jean-Marc Ricort‡‡, Jérôme Lemoine§§, Ming Zhang¶¶, Hubert Hondermarck‡, and Xuefen Le Bourhis‡‖‖

Normal breast epithelial cells are known to exert an apoptotic effect on breast cancer cells, resulting in a potential paracrine inhibition of breast tumor development. In this study we purified and characterized the apoptosis-inducing factors secreted by normal breast epithelial cells. Conditioned medium was concentrated by ultrafiltration and separated on reverse phase Sep-Pak C_{18} and HPLC. The proapoptotic activity of eluted fractions was tested on MCF-7 breast cancer cells, and nano-LC-nano-ESI-MS/MS allowed the identification of insulin-like growth factor-binding protein-3 (IGFBP-3) and maspin as the proapoptotic factors produced by normal breast epithelial cells. Western blot analysis of conditioned media confirmed the specific secretion of IGFBP-3 and maspin by normal cells but not by breast cancer cells. Immunodepletion of IGFBP-3 and maspin completely abolished the normal cell-induced apoptosis of cancer cells, and recombinant proteins reproduced the effect of normal cell-conditioned medium on apoptosis of breast cancer cells. Together our results indicated that normal breast epithelial cells can induce apoptosis of breast cancer cells through IGFBP-3 and maspin. These findings provide a molecular hypothesis for the long observed inhibitory effect of normal surrounding cells on breast cancer development. ***Molecular & Cellular Proteomics 6: 1239–1247, 2007.***

Breast cancer is the leading cause of cancer-related deaths in women of the western world, and despite significant improvements in cancer diagnosis and treatment, more than two-thirds of the patients still succumb to the disease (1). However, this pathology progresses slowly, and it has been estimated that the development of a clinically detectable tumor from one tumor cell may require 6–8 years. The normal human breast gland comprises a branching ductal-lobular system lined by an inner layer of luminal epithelial cells and an outer layer of myoepithelial cells separated from the interstitial stroma by an intact basement membrane. The luminal epithelial cells are polarized glandular cells with specialized apical and basolateral membrane domains expressing sialomucin and cell-cell adhesion molecules, respectively (2). The myoepithelial cells contribute significantly to the formation of basement membrane, and their myogenic differentiation is responsible for the contractile function. Breast cancer development involves defined clinical and pathological stages starting with atypical epithelial hyperplasia, progressing to *in situ* then invasive carcinomas, and culminating in metastatic disease (3). In *in situ* breast carcinomas, luminal epithelial cells lose their ability to maintain a single epithelial layer. At the same time, the number of myoepithelial cells decreases, and the number of stromal fibroblasts, lymphocytes, and endothelial cells increases. In invasive carcinoma, myoepithelial cells and the basement membrane are absent, and tumor cells are dispersed into the stroma.

It is now widely documented that tumor evolution is highly dependent on interactions between tumor cells and neighboring normal cells (4, 5). The paracrine interactions between neoplastic cells and adjacent normal cells may determine whether transformed cells undergo apoptosis, remain in a quiescent state, or advance to tumorigenesis. In various experimental tumor models, the microenvironment affects the efficiency of tumor formation, the rate of tumor growth, and the extent of invasiveness (6). Although fibroblasts and endothelial cells have been shown to favor tumor development, normal breast myoepithelial and epithelial cells are reported to have antitumor effects both *in vitro* and *in vivo* (7–13). We have demonstrated that normal breast epithelial

From the ‡INSERM ERI-8 (JE 2488) "Signalisation des facteurs de croissance dans le cancer du sein. Protéomique fonctionnelle," ‖Centre Commun de Mesure de Spectrométrie de Masse, and **CNRS FRE 2933, IFR 147, Université des Sciences et Technologies de Lille, 59655 Villeneuve d'Ascq, France, ‡‡CNRS UMR 8113, Ecole Normale Supérieure, 94230 Cachan, France, §§CNRS UMR 5180, Université Claude Bernard, 69622 Villeurbanne, France, and ¶¶Department of Molecular and Cellular Biology, Baylor College of Medicine, Houston, Texas 77030

Received, December 20, 2006, and in revised form, March 1, 2007
Published, MCP Papers in Press, April 19, 2007, DOI 10.1074/mcp.M600477-MCP200

cells (NBECs)[1] inhibit growth of cancer cells by inducing apoptosis (14, 15). The induction of apoptosis is mediated through a Fas-mediated pathway because conditioned medium from NBECs increases membrane-associated Fas and Fas ligand. More importantly both Fas-neutralizing antibody and dominant negative Fas completely abolish NBEC-induced apoptosis. The mechanisms of the apoptosis-inducing effect of NBECs on breast cancer cells, from the standpoint of both effector molecules and signal transduction, hold promise for the understanding of the natural paracrine tumor suppression as well as for cancer prevention. In the present study, we purified and characterized the apoptosis-inducing factors secreted by NBECs. Mass spectrometry analysis together with immunodepletion assay showed insulin-like growth factor-binding protein-3 (IGFBP-3) and maspin to be the major apoptosis-inducing factors produced by NBECs.

EXPERIMENTAL PROCEDURES

Chemicals—All cell culture reagents were obtained from BioWhittaker except insulin, which was obtained from Organon. Chemicals and anti-β-actin antibody were purchased from Sigma unless otherwise stated. Recombinant IGFBP-3 and anti-IGFBP-3 antibodies for Western blot and for immunodepletion assay were obtained from R&D Systems. Anti-maspin antibodies were produced by Biomerieux. Trypsin and soybean trypsin inhibitor were purchased from Roche Applied Science. GST-maspin was produced in *Escherichia coli* as described previously (16).

Cell Culture and Preparation of Conditioned Medium—NBEC cultures were established as described previously (11) from mammoplasty material (18–30-year-old women) obtained from the Department of Plastic Surgery (Prof. Pellerin) at the Medical University of Lille (Lille, France) in accordance with rules and regulations concerning ethical issues in France. In this study, NBECs from three primary cultures were used. Cells were cultured in DMEM/F-12 medium (1:1) containing 5% FCS, 10 μg/ml insulin, 5 μg/ml cortisol, 2 ng/ml EGF, 100 ng/ml cholera toxin, 100 IU/ml streptomycin, 100 μg/ml penicillin, and 45 μg/ml gentamicin. MCF-7, MDA-MB-231 and T-47D breast cancer cell lines were grown in Eagle's minimal essential medium supplemented with 10% FCS, 5 μg/ml insulin, 100 IU/ml streptomycin, 100 μg/ml penicillin, and 45 μg/ml gentamicin. For all experiments, cells were cultured in basal DMEM/F-12 medium without serum.

For preparation of conditioned medium, cells were plated in 75-cm^2 flasks (Nunc). When they reached preconfluence, they were washed two times with PBS and incubated in basal DMEM/F-12 medium (without serum, insulin, cortisol, EGF, or cholera toxin). Two hours later, the basal DMEM/F-12 medium was changed, and cells were further cultured for 24 h. The medium was then centrifuged at 200 × *g* for 10 min at 4 °C to remove cell debris and stored at −80 °C prior to use.

For immunodepletion of IGFBP-3 and maspin, conditioned medium was incubated with mouse anti-IGFBP-3 and/or anti-maspin antibodies overnight at 4 °C before incubation with protein A-agarose for 2 h on a roller system at 4 °C. Control was performed by incubating conditioned medium with an equal amount of irrelevant mouse immunoglobulin G. After centrifugation (10,000 × *g* for 10 min at 4 °C), the supernatants were used to determine apoptosis induction.

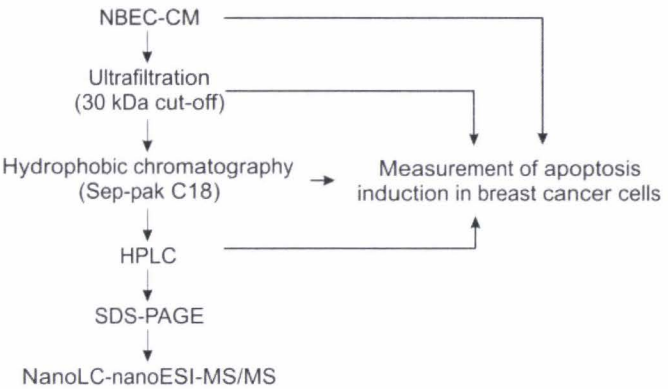

FIG. 1. **Protocol for purification and identification of apoptosis-inducing factors.**

Determination of Apoptotic Cells—Cells were seeded in 35-mm dishes (Nunc). After treatment with NBEC-conditioned medium (NBEC-CM), cells were fixed in cold methanol (−20 °C) for 10 min and washed twice in PBS before staining with 1 μg/ml Hoechst 33258 for 30 min at room temperature in the dark. Cells were then washed with PBS and mounted with coverslips using Glycergel (Dako). Apoptotic cells exhibiting condensed and fragmented nuclei were counted under an Olympus-BH2 fluorescence microscope as described previously (15). At least 500–1,000 cells in randomly selected fields were examined.

Purification Scheme of Apoptosis-inducing Factors—Apoptosis-inducing factors were purified following the protocol described in Fig. 1. To determine the approximate molecular size of apoptosis-inducing factors, size fractionation of NBEC-CM was performed by centrifugation in Centriplus tubes (Millipore) fitted with molecular sieve filters according to the manufacturer's instructions. For further purification, NBEC-CM (10 liters) was concentrated about 1,000 times using an Ultrasette type of ultrafiltration device (Filtron, Pall Gelman Science) (30-kDa cutoff). The concentrate was then loaded onto a reverse phase Sep-Pak C_{18} column and eluted with 50, 80, and 100% acetonitrile. The eluted fractions were freeze-dried and resuspended in DMSO before being loaded onto an HPLC column (Sephasil C_4, 250 × 10 mm, 5 μm; Vydac). Each eluted fraction was tested for its apoptosis-inducing activity in MCF-7 breast cancer cells as described above.

Protein Identification by Mass Spectrometry—The apoptosis-inducing fractions from HPLC were subjected to 12% SDS-PAGE followed by colloidal Coomassie Blue staining and trypsin digestion. The protein bands of interest were trypsin-digested and analyzed as described previously (17). Nano-LC-nano-ESI-MS/MS analysis of the trypsin digests was performed on an ion trap mass spectrometer (LCQ Deca XP^+, Thermo Electron) equipped with a nanoelectrospray ion source coupled with a nano-high pressure liquid chromatography system (LC Packings Dionex). Tryptic digests were resuspended in 10 μl of 0.1% HCOOH, and 1 μl was injected into the mass spectrometer using a Famos autosampler (LC Packings Dionex). The samples were first desalted and then concentrated on a reserve phase precolumn of 5 mm × 0.3-mm inner diameter (Dionex) by solvent A (H_2O/acetonitrile, 0.1% HCOOH (95:5)) delivered by the Switchos pumping device (LC Packings Dionex) at a flow rate of 10 μl/min for 3 min. Peptides were separated on a 15 cm × 75-μm-inner diameter C_{18} PepMap column (Dionex). The flow rate was set at 200 nl/min. Peptides were

[1] The abbreviations used are: NBEC, normal breast epithelial cell; Bax, Bcl-2-associated x protein; Bcl-2, B-cell/lymphoma 2; DMEM, Dulbecco's modified minimum essential medium; EGF, epidermal growth factor; IGF, insulin-like growth factor; IGFBP, insulin-like growth factor-binding protein; NBEC-CM, NBEC-conditioned medium; GST-maspin, recombinant GST-maspin fusion protein; uPA, urokinase plasminogen activator.

eluted using a 5–100% linear gradient of solvent B (H_2O/acetonitrile, 0.08% HCOOH (20:80)) in 45 min. Coated nanoelectrospray needles were obtained from New Objective (Woburn, MA). Spray voltage was set at 1.5 kV, and capillary temperature was set at 170 °C. The mass spectrometer was operated in positive ion mode. Data acquisition was performed in a data-dependent mode consisting of, alternatively in a single run, full-scan MS over the range *m/z* 500–2,000 and full MS/MS of the ion selected in an exclusion dynamic mode (the most intense ion is selected and excluded for further selection for a duration of 3 min). MS/MS data were acquired using a 2 *m/z* unit ion isolation window and a 35% relative collision energy. MS/MS raw data files were transformed to dta files with Bioworks 3.1 software (Thermo Electron). MS/MS spectra indicate primarily fragment ions originating from either the C terminus (y ion series) or N terminus (b ion series) of a peptide. Neutral mass of the precursor and sequence information were used to identify proteins in the Swiss-Prot database through MASCOT public interface using a mass tolerance of 0.8 Da for precursor, trypsin as the digestion enzyme, two possible missed cleavages, and oxidized methionine as a variable modification. Results were scored using probability-based Mowse score (protein score is $-10 \times \log(p)$ where p is the probability that the observed match is a random event. Scores greater than 42 are significant ($p < 0.05$). To ascertain unambiguous identification, searches were performed in parallel with Phenyx software using the same parameters.

Western Ligand Blotting and Western Blotting—Conditioned media (2 ml) of NBECs or MCF-7 cells were loaded onto a G-25 Sephadex gel filtration column. Fractions containing IGFBPs were eluted by 0.03 M ammonium acetate and lyophilized as described previously (18). Proteins from lyophilized samples were size-fractionated by 12.5% polyacrylamide gel electrophoresis under non-reducing conditions and electroblotted onto nitrocellulose membranes. The membranes were then incubated overnight in the presence of ^{125}I-labeled IGF-1 and ^{125}I-labeled IGF-2 (2×10^5 cpm for each ligand) (Amersham Biosciences) followed by washing with Tris-buffered saline (pH 7.2) and exposed to Eastman Kodak Co. X-Omat film for at least 48 h. For Western blotting, concentrated media and cell lysates were loaded onto a 10% SDS-polyacrylamide gel and then electrotransferred to nitrocellulose membrane (Hybond-C extra, Amersham Biosciences). After transfer, the blots were blocked with 3% BSA in TBS-T (20 mM Tris, pH 7.6, 150 mM NaCl, 0.1% Tween 20) at room temperature and then incubated with anti-IGFBP-3 or anti-maspin antibodies (overnight at 4 °C). The detection was performed using a horseradish peroxidase-conjugated secondary antibody (1.5 h at room temperature) and the ECL detection system (Amersham Biosciences).

Statistical Analysis—Statistical significance was measured by Student's paired *t* test. The value of *p* for each data set is shown in the figures.

RESULTS

NBEC-conditioned Medium Induced Apoptosis of Breast Cancer Cells—MCF-7 breast cancer cells were cultured in serum-free medium in the presence of different dilutions of NBEC-conditioned medium. Apoptosis was determined following Hoechst staining (Fig. 2*A*). As shown in Fig. 2*B*, NBEC-conditioned medium induced apoptosis in a dose-dependent manner with a significant increase in apoptosis at a 1:40 dilution of NBEC-conditioned medium and a 4.5-fold increase in apoptosis at a 1:2 dilution. Similar results in apoptosis induction were obtained using a terminal deoxynucleotidyltransferase biotin-dUTP nick end labeling reaction (data not shown). Conditioned medium was then treated with heat and trypsin to determine whether the apoptosis-inducing factors were proteins. As shown in Fig. 2*C*, heating or trypsin treatment totally suppressed the apoptosis-inducing effect of NBEC-conditioned medium. This indicated that the apoptosis-inducing factors were temperature-sensitive proteins. We then evaluated the approximate molecular masses using a Centricon ultrafiltration system. Conditioned medium was concentrated with membrane filters of different cutoffs (10, 30, 50, and 100 kDa), and the apoptotic activity was determined in non-retained fractions. As shown in Fig. 2*C*, the non-retained fractions from 10- and 30-kDa-cutoff filters could not induce apoptosis, indicating that the molecular masses of apoptosis-inducing factors were greater than 30 kDa. In contrast, the total apoptosis-inducing activity was found in the non-retained fractions when filters of 50- and 100-kDa cutoff were used, indicating that the molecular masses of apoptosis-inducing factors were less than 50 kDa. Therefore the approximate molecular masses of apoptosis-inducing factors were estimated at between 30 and 50 kDa.

Purification of Apoptosis-inducing Factors—NBEC-conditioned medium was sequentially processed as described in Fig. 1. For each step, apoptosis induction of MCF-7 cells was determined. Conditioned medium (10 liters) was concentrated (1000-fold) and then subjected to a reverse phase Sep-Pak C_{18} column and eluted at 50, 80, and 100% acetonitrile. Apoptosis-inducing fractions were subsequently subjected to HPLC. The active fractions a and b were identified from HPLC (Fig. 3*A*). Fraction a was eluted at about 43% acetonitrile. After freeze-drying and dilution to a final concentration equivalent to 50% non-concentrated conditioned medium, this fraction induced about 28% of cancer cells into apoptosis. Fraction b was eluted at about 68% acetonitrile and induced about 17% of cells into apoptosis when cells were treated with a final concentration equivalent to 50% non-concentrated conditioned medium.

Identification of Apoptosis-inducing Factors by Mass Spectrometry—The two apoptosis-inducing fractions eluted by analytical HPLC were subjected to 12% SDS-PAGE followed by colloidal Coomassie Blue staining (Fig. 3*B*). Fraction a was revealed as an apparent double band at about 35–40 kDa. Fraction b was revealed as a single band at 42 kDa. These two individual protein bands were excised from a colloidal Coomassie Blue-stained gel and digested by trypsin, and the resulting peptides were processed for analysis by nano-LC-nano-ESI-MS/MS. The MS/MS spectra and the database search results are presented in Fig. 4. Two peptides were sequenced for each band. The 35-kDa band was identified as IGFBP-3 (score, 156; sequence coverage, 10.6%), and the 42-kDa band corresponded to maspin (score, 300; sequence coverage, 7.8%).

Western Blot Analysis of IGFBP-3 and Maspin—The presence of IGFBP-3 in conditioned media from normal and cancer cells was first verified by Western ligand blot (Fig. 5*A*). In NBEC-conditioned medium, three species of IGFBPs were visualized (IGFBP-2, IGFBP-3, and IGFBP-4) with IGFBP-3

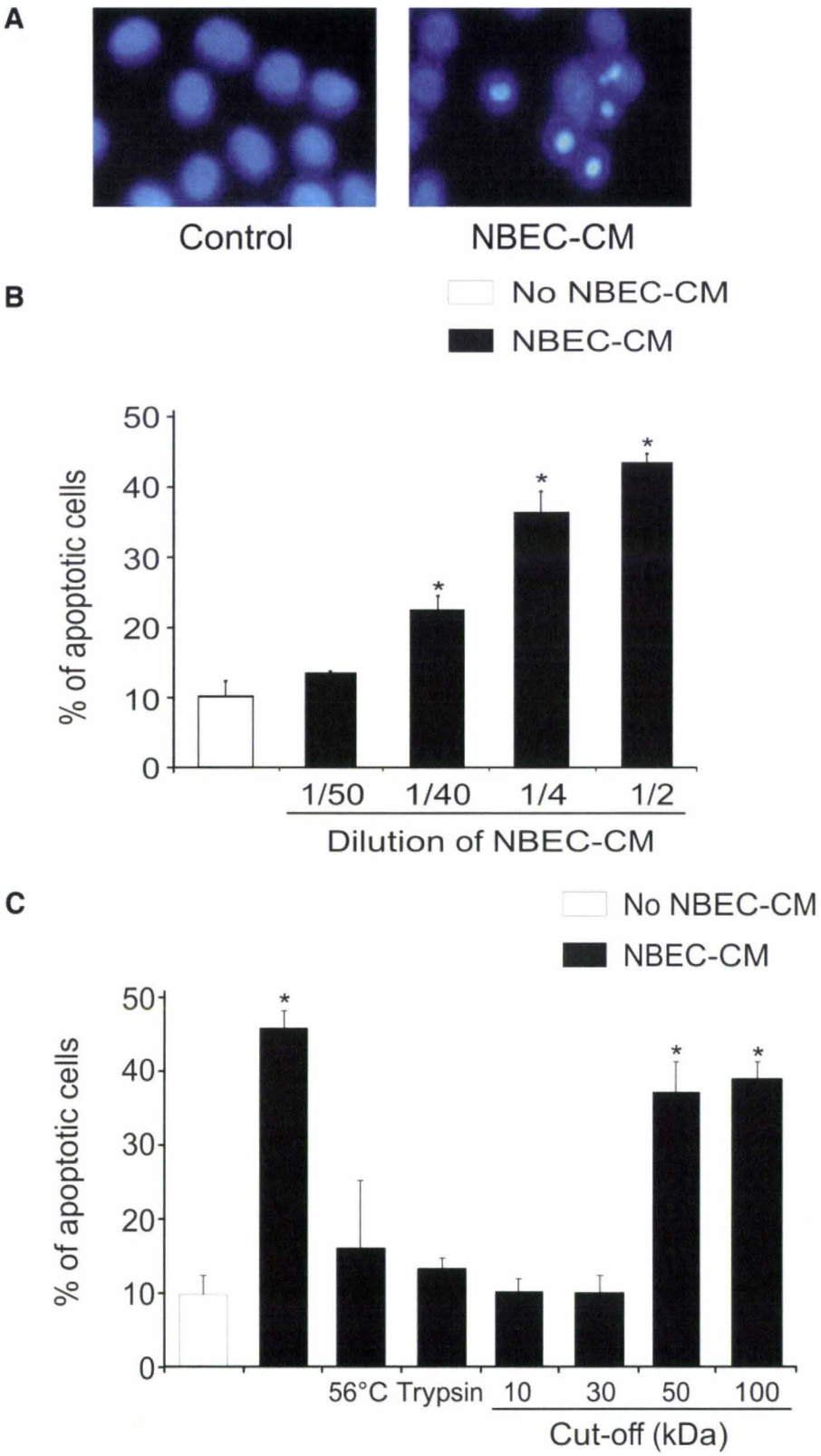

FIG. 2. **NBEC-CM induced apoptosis in MCF-7 breast cancer cells.** Cells were cultured in basal DMEM/F-12 medium for 24 h in the presence or absence of various dilutions of NBEC-CM. *A*, apoptosis detection after Hoechst staining. Apoptotic nuclei are condensed or fragmented. *B*, percentage of apoptotic cells. Data are the mean of three independent experiments. *C*, characterization of apoptosis-inducing activity in NBEC-CM. NBEC-CM was heated at 56 °C for 30 min or incubated with 2.5 μg/ml trypsin at 37 °C for 30 min. Molecular size fractionation of NBEC-CM was performed using 10-, 30-, 50-, and 100-kDa-cutoff sieve filters, and the non-retained fractions were used to determine apoptosis induction in MCF-7 cells as described. Apoptosis experiments were performed with a 1:2 dilution of conditioned medium. *Bars* show S.D. *, $p < 0.01$.

being the most abundant. In medium conditioned by MCF-7 cells, only IGFBP-2 and IGFBP-4 were detected.

The presence of IGFBP-3 and maspin in cell lysates and conditioned media from NBECs and MCF-7 cells was also verified by immunoblot analysis. As shown in Fig. 5, *B* and *C*, both IGFBP-3 and maspin were produced and secreted by

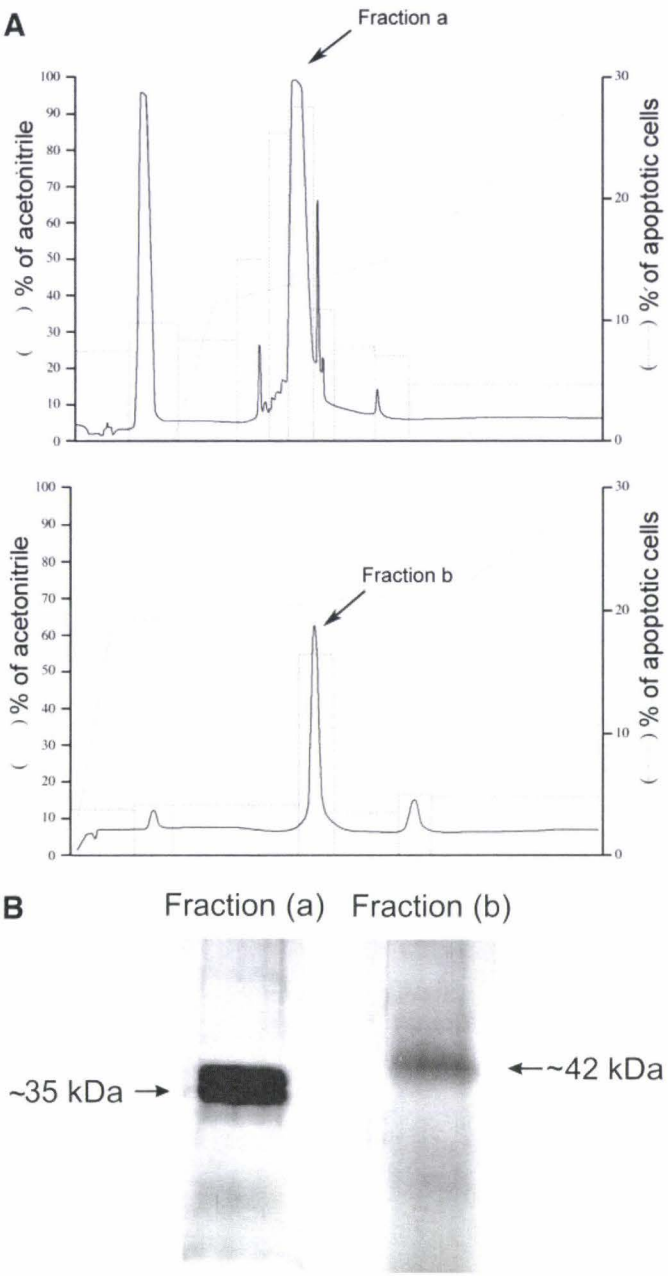

FIG. 3. **Elution profiles of HPLC and SDS-PAGE separation of active fractions.** *A*, HPLC elution profile reveals two active fractions, a and b. HPLC columns were eluted with a linear gradient of 0.1% TFA in acetonitrile. The flow rate was maintained at 1 ml/min, and the absorbance was monitored at 280 nm. Apoptotic activity of collected fractions was determined on MCF-7 cells after Hoechst staining. *B*, SDS-PAGE analysis of HPLC fractions. The active fractions a and b from HPLC were subjected to SDS-PAGE followed by colloidal Coomassie Blue staining.

NBECs. In contrast, neither IGFBP-3 nor maspin was detected in MCF-7 cell lysate and conditioned medium. Altogether these results suggested that IGFBP-3 and maspin were specifically secreted by NBECs but not by MCF-7 breast cancer cells.

Immunodepletion of IGFBP-3 and Maspin Abolished NBEC-CM-induced Apoptosis—To determine the extent to which secreted IGFBP-3 and maspin contributed to apoptosis induction, we immunodepleted IGFBP-3 and/or maspin by incubating NBEC-CM with anti-IGFBP-3 and/or anti-maspin antibodies. As shown in Fig. 6*A*, immunodepletion of NBEC-CM with the anti-IGFBP-3 antibody or the anti-maspin antibody diminished apoptosis induction in MCF-7 cells. Interestingly immunodepletion of both IGFBP-3 and maspin totally abolished apoptosis induction. This confirmed that IGFBP-3 and maspin secreted by NBECs did induce apoptosis of MCF-7 breast cancer cells.

IGFBP-3 and Maspin Synergistically Induced Apoptosis of Breast Cancer Cells—It has been described that both endogenous overexpressed maspin and IGFBP-3 can induce apoptosis or potentiate apoptosis induction by other agents (16, 19–22). To provide further evidence that extracellular IGFBP-3 and maspin could also induce apoptosis in breast cancer cells, recombinant proteins were used. As shown in Fig. 6*B*, IGFBP-3 and maspin alone significantly induced apoptosis. Interestingly the induction of apoptosis was further increased by cotreatment with IGFBP-3 and maspin.

DISCUSSION

Accumulating evidence suggests that dynamic cell-cell interaction may be as great a determinant of the behavior of a tumor cell as the specific oncogenetic or tumor suppressor alterations occurring within the malignant cells themselves (1–5). Normal breast myoepithelial and epithelial cells have been demonstrated to exert an inhibitory effect on breast cancer cells. We have reported previously that conditioned medium of normal breast epithelial cells strongly induces apoptosis of breast cancer cells (14, 15), but so far the apoptosis-inducing factors have yet to be identified. Here we used a proteomics-based approach to purify and identify apoptosis-inducing factors from normal breast epithelial cells. Proteomics offers the possibility of identifying proteins at very low concentrations, and this is of considerable interest in characterizing paracrine regulators as well as therapeutic targets in various pathologies such as breast cancers (23, 24). The use of sequential chromatography and mass spectrometry as well as immunodepletion assay has allowed us to identify IGFBP-3 and maspin as the two apoptogens secreted by normal breast epithelial cells.

IGFBP-3 is the most abundant of the circulating IGFBPs that bind IGFs with high affinity. IGFBP-3 inhibits cell proliferation and induces apoptosis by its ability to bind IGFs as well as through its IGF-independent effects. Hence IGFBP-3 can induce apoptosis by modulating the expression of Bcl-2 proteins in human breast cancer cells (25). More recently, Lee *et al.* (22) have demonstrated that in response to IGFBP-3 the retinoid X receptor-α-binding partner nuclear receptor Nur77 rapidly undergoes translocation from the nucleus to the mitochondria, resulting in rapid caspase activation. This nuclear

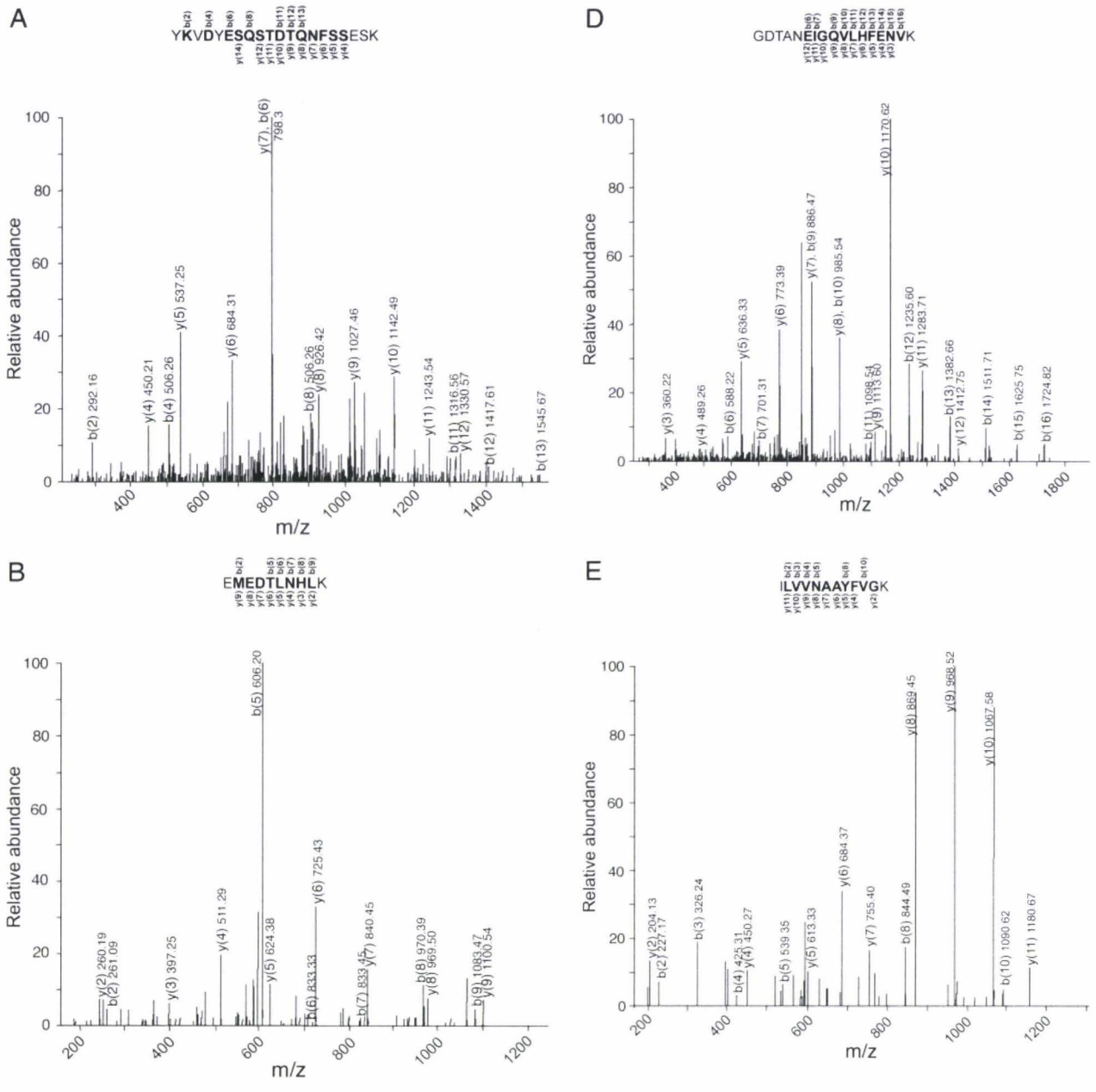

C Insulin-like growth factor binding protein-3
(P 17936)

MQRARPTLWA AALTLLVLLR GPPVARAGAS SGGLGPVVRC
EPCDARALAQ CAPPPAVCAE LVREPGCGCC LTCALSEGQP
CGIYTERCGS GLRCQPSPDE ARPLQALLDG RGLCVNASAV
SRLRAYLLPA PPAPGNASES EEDRSAGSVE SPSVSSTHRV
SDPKFHPLHS KIIIIKKGHA KDSQR**YKVDY** **ESQSTDTQNF**
SSESKRETEY GPCRR**EMEDT** **LNHLK**FLNVL SPRGVHIPNC
DKKGFYKKKQ CRPSKGRKRG FCWCVDKYGQ PLPGYTTKGK
EDVHCYSMQS K

F Maspin
(P 36952)

MDALQLANSA FAVDLFKQLC EKEPLGNVLF SPICLSTSLS
LAQVGAK**GDT** **ANEIGQVLHF** **ENVK**DIPFGF QTVTSDVNKL
SSFYSLKLIK RLYVDKSLNL STEFISSTKR PYAKELETVD
FKDKLEETKG QINNSIKDLT DGHFENILAD NSVNDQTK**IL**
VVNAAYFVGK WMKKFPESET KECPFRLNKT DTKPVQMMNM
EATFCMGNID SINCKIIELP FQNKHLSMFI LLPKDVEDES
TGLEKIEKQL NSESLSQWTN PSTMANAKVK LSIPKFKVEK
MIDPKACLEN LGLKHIFSED TSDFSGMSET KGVALSNVIH
KVCLEITEDG GDSIEVPGAR ILQHKDELNA DHPFIYIIRH
NKTRNIIFFG KFCSP

FIG. 4. **Mass spectrometry identification of IGFBP-3 and maspin.** The SDS-PAGE bands from fractions a and b were subjected to tryptic digestion. The tryptic digests were analyzed by nano-LC-nano-ESI-MS/MS. Spectra of the IGFBP-3 peptides are shown in *A* and *B*, and spectra of maspin are shown in *D* and *E*. The *bold letters* indicate the detected b and y ions matching the predicted ion mass in the database. The detected fragments (*bold letters*) are indicated in the sequence of full-length IGFBP-3 (*C*) and maspin (*F*).

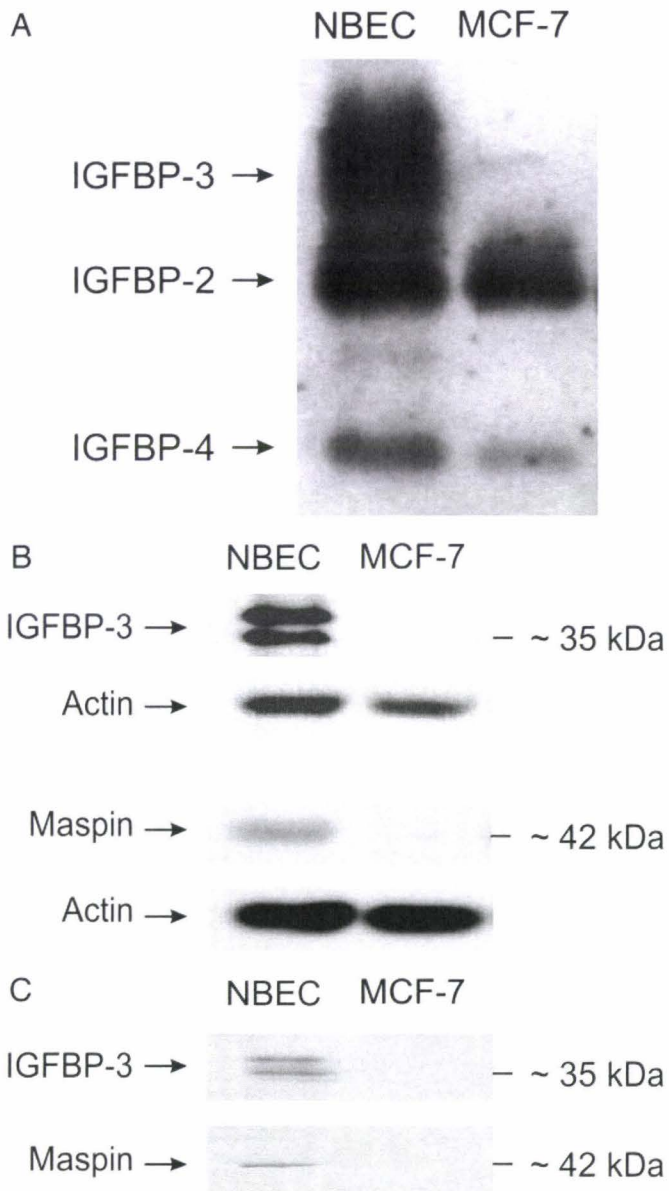

FIG. 5. **Western blot analysis of IGFBP-3 and maspin.** *A*, Western ligand blot analysis of IGFBPs. Conditioned media from NBECs and MCF-7 cells were collected, size-fractionated using 12% SDS-PAGE under non-reducing conditions, electroblotted onto nitrocellulose membranes, and treated with ^{125}I-labeled IGF-1 and -2 as indicated under "Experimental Procedures." *B* and *C*, detection of IGFBP-3 and maspin by Western blotting. Lysates (*B*) and concentrated conditioned media (*C*) from NBECs and MCF-7 cells were subjected to SDS-PAGE and immunoblotted as described under "Experimental Procedures." The loading and transfer of equal amounts of protein were confirmed by immunodetection of actin. The data are representative of three independent experiments.

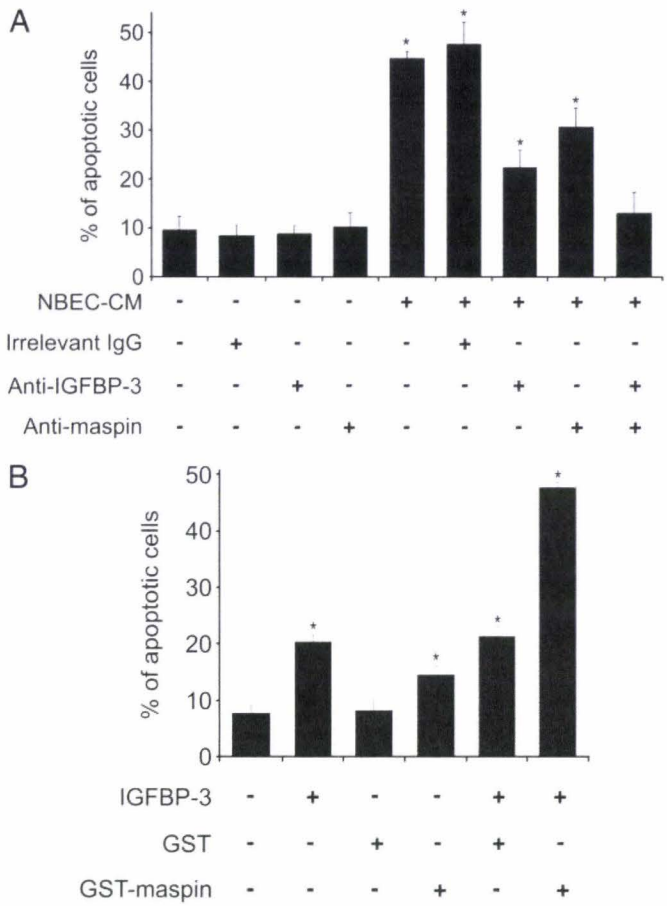

FIG. 6. **Effect of IGFBP-3 and maspin on apoptosis of MCF-7 breast cancer cells.** *A*, effect of IGFBP-3 and maspin immunodepletion from NBEC-conditioned medium. Conditioned medium was incubated with anti-IGFBP-3 and/or anti-maspin antibodies to immunodeplete IGFBP-3 and/or maspin. Irrelevant mouse immunoglobulin G (*IgG*) was used as control. Immunodepleted supernatants were added to MCF-7 cells with a final concentration equivalent to a 1:2 dilution of conditioned medium for 24 h. *B*, effect of recombinant IGFBP-3 and GST-maspin. MCF-7 cells were treated with IGFBP-3 (2.5 ng/ml) or GST-maspin (200 ng/ml) alone or in combination for 24 h. Apoptosis was determined after Hoechst staining. Results are the mean of three independent experiments. Bars show S.D. *, $p < 0.01$.

non-genotypic pathway requires the presence of retinoid X receptor-α. On the other hand, it has also been reported that inducible expression of IGFBP-3 leads to apoptosis induction of MCF-7 breast cancer cells by activating death receptor pathways (21). The level and activity of IGFBP-3 can be controlled by IGFBP-degrading proteases such as metalloproteinases (26, 27). Post-translational modifications including phosphorylation and glycosylation can also modify IGFBP-3 activity. Once phosphorylated, the binding of IGFBP-3 to IGF-I is enhanced (28). Phosphorylation of IGFBP-3 also increases the extracellular translocation of IGFBP-3 into the nucleus to exert IGF-independent effects (29, 30). Glycosylation, which influences bioavailability and cell surface association, may also enhance antiproliferative and proapoptotic effects (31). In our study, IGFBP-3 isolated from NBEC-conditioned medium seemed to be the full-length protein. However, two bands were obtained in the purified HPLC fraction as well as in Western blot analysis. Further studies are required to determine the nature of post-translational modifications of IGFBP-3.

Maspin (mammary serpin) is a serine protease inhibitor with tumor suppression activities. Since its discovery in 1994, maspin has been consistently shown to suppress the aggressive tumor phenotypes, inhibiting cell invasion and mobility *in vitro* and inhibiting tumor growth and metastasis in experimental animal models (32–34). Maspin is localized both in cytoplasmic and nuclear compartments but may also be secreted. Maspin is the only proapoptotic serpin among all the serpins implicated in apoptosis regulation. However, the proapoptotic function of maspin has been so far observed by transfecting cancer cells with maspin cDNA (35). Transfected breast carcinoma cells are more sensitive to multiple apoptotic inducers. This apoptosis-sensitizing effect is mediated through the regulation of Bcl-2 family proteins (20, 35). The intracellular maspin can also translocate to the mitochondria to induce cytochrome *c* release and caspase activation (16). In this work, we showed that both normal breast epithelial cell-secreted maspin and recombinant maspin had the ability to induce apoptosis of breast cancer cells. The underlying mechanism is currently not known; however, maspin has been reported to dramatically decrease both cell-associated uPA/uPA receptor expression and uPA activity (36–38), and it is possible that maspin may induce apoptosis by reducing cell surface-associated prosurvival uPA·uPA receptor complex (34, 39). Alternatively because extracellular maspin is efficiently internalized (36, 40), it is also possible that internalized maspin induces apoptosis in a manner similar to overexpressed intracellular maspin by modulating expression of Bcl-2 family members or by targeting directly mitochondria (16, 20, 35). Consistent with this hypothesis, we have shown previously that conditioned medium from normal breast epithelial cells increases the level of Bax and decreases that of Bcl-2 (41).

Interestingly we showed that the release of IGFBP-3 and maspin is specifically observed for normal breast epithelial cells but not for breast cancer cells. This is consistent with findings that both IGFBP-3 and maspin are transcriptionally down-regulated or silenced by epigenetic changes such as methylation in cancer cells (42, 43). It is important to bear in mind that normal mammary epithelial cells that express high levels of maspin do not undergo detectable apoptosis either *in vitro* or *in vivo* (19). Furthermore maspin expression increases resistance to tumor necrosis factor-related apoptosis-inducing ligand (TRAIL)- and staurosporine-induced apoptosis in normal breast epithelial cells (44). Recombinant IGFBP-3 does not modify growth kinetics of normal cells *per se* but can enhance proliferative effects of EGF in normal immortalized breast epithelial cells (MCF-10A) (45). In agreement with these data, we observed that recombinant IGFBP-3 and maspin alone or in combination did not affect growth of normal breast epithelial cells (data not shown). By contrast, MCF-7 breast cancer cells were dramatically induced into apoptosis when cotreated with IGFBP-3 and maspin. In the present study, apoptosis induction in MCF-7 breast cancer cells was used as a functional test to identify apoptosis-inducing factors produced by normal breast epithelial cells. However, we had shown previously that other breast cancer cell lines such as T-47D and MDA-MB-231 cells can also be induced into apoptosis by conditioned medium from normal breast epithelial cells (14, 15). Moreover recombinant IGFBP-3 and maspin synergistically induced apoptosis of these cells (data not shown). These findings indicate that IGFBP-3 and maspin exert a similar effect on distinct breast cell types.

In conclusion, using a proteomics-based approach we identified IGFBP-3 and maspin as the proapoptotic factors produced by normal breast epithelial cells. Although more physiological conditions, such as reconstituted three-dimensional culture systems and animal models, would be required to confirm *in vivo* the role of IGFBP-3 and maspin in breast epithelial cell homeostasis, our data provide a molecular basis for the long observed inhibitory effect of normal surrounding cells on breast cancer development.

* This work was supported in part by the French Ministry for Research and Education, the INSERM, the "Region Nord-Pas-de-Calais," and the "Ligue Nationale Contre le Cancer" (Equipe labellisée 2006). The costs of publication of this article were defrayed in part by the payment of page charges. This article must therefore be hereby marked "*advertisement*" in accordance with 18 U.S.C. Section 1734 solely to indicate this fact.

§ Both authors contributed equally to this work.

¶ Supported by the French Ministry for Research and Education and the "Association pour la Recherche contre le Cancer."

‖ To whom correspondence should be addressed: INSERM ERI-8 (JE 2488), Bâtiment SN3, Université des Sciences et Technologies de Lille, 59655 Villeneuve d'Ascq, France. Tel.: 33-3-20-43-45-81; Fax: 33-3-20-43-40-38; E-mail: xuefen.lebourhis@univ-lille1.fr.

REFERENCES

1. Lacroix, M., Toillon, R. A., and Leclercq, G. (2004) Stable 'portrait' of breast tumors during progression: data from biology, pathology and genetics. *Endocr. Relat. Cancer* **11,** 497–522
2. Ronnov-Jessen, L., Petersen, O. W., and Bissell, M. J. (1996) Cellular changes involved in conversion of normal to malignant breast: importance of the stromal reaction. *Physiol. Rev.* **76,** 69–125
3. Polyak, K. (2001) On the birth of breast cancer. *Biochim. Biophys. Acta* **1552,** 1–13
4. Bissell, M. G., Radisky, D. C., Rizki, A., Weaver, V. M., and Petersen, O. W. (2002) The organizing principle: micro-environmental influences in the normal and malignant breast. *Differentiation* **70,** 537–546
5. Allinen, M., Beroukhim, R., Cai, L., Brennan, C., Lahti-Domenici, J., Huang, H., Porter, D., Hu, M., Chin, L., Richardson, A., Schnitt, S., Sellers, W. R., and Polyak, K. (2004) Molecular characterization of the tumor microenvironment in breast cancer. *Cancer Cell* **6,** 17–32
6. Elenbaas, B., and Weinberg, R. A. (2001) Heterotypic signaling between epithelial tumor cells and fibroblasts in carcinoma formation. *Exp. Cell Res.* **264,** 169–184
7. Sternlicht, M. D., Kedeshian, P., Shao, Z. M., Safarians, S., and Barsky, S. H. (1997) The human myoepithelial cell is a natural tumor suppressor. *Clin. Cancer Res.* **3,** 1949–1958
8. Alpaugh, M. L., Lee, M. C., Nguyen, M., Deato, M., Dishakjian, L., and Barsky, S. H. (2000) Myoepithelial-specific CD44 shedding contributes to the anti-invasive and antiangiogenic phenotype of myoepithelial cells. *Exp. Cell Res.* **261,** 150–158
9. Nguyen, M., Lee, M. C., Wang, J. L., Tomlinson, J. S., Shao, Z. M., Alpaugh, M. L., and Barsky, S. H. (2000) The human myoepithelial cell displays a multi-faceted anti-angiogenic phenotype. *Oncogene* **19,** 3449–3459
10. Zajchowski, D. A., Band, V., Trask, D. K., Kling, D., Connolly, J. L., and

Sager, R. (1990) Suppression of tumor-forming ability and related traits in MCF-7 human breast cancer cells by fusion with immortal mammary epithelial cells. *Proc. Natl. Acad. Sci. U. S. A.* **87,** 2314–2318
11. Dong-Le Bourhis, X., Berthois, Y., Millot, G., Degeorges, A., Sylvi, M., Martin, P. M., and Calvo, F. (1997) Effect of stromal and epithelial cells derived from normal and tumorous breast tissue on the proliferation of human breast cancer cell lines in co-culture. *Int. J. Cancer* **71,** 42–48
12. Quarrie, L. H., Pitts, J. D., and Finbow, M. E. (1999) Interactions between normal mammary epithelial cells and mammary tumour cells in a model system. *Cell Prolif.* **32,** 351–361
13. Spink, B. C., Cole, R. W., Katz, B. H., Gierthy, J. F., Bradley, L. M., and Spink, D. C. (2006) Inhibition of MCF-7 breast cancer cell proliferation by MCF-10A breast epithelial cells in coculture. *Cell Biol. Int.* **30,** 227–238
14. Toillon, R. A., Chopin, V., Jouy, N., Fauquette, W., Boilly, B., and Le Bourhis, X. (2002) Normal breast epithelial cells induce p53-dependent apoptosis and p53-independent cell cycle arrest of breast cancer cells. *Breast Cancer Res. Treat.* **71,** 269–280
15. Toillon, R. A., Descamps, S., Adriaenssens, E., Ricort, J. M., Bernard, D., Boilly, B., and Le Bourhis, X. (2002) Normal breast epithelial cells induce apoptosis of breast cancer cells via Fas signaling. *Exp. Cell Res.* **275,** 31–43
16. Latha, K., Zhang, W., Cella, N., Shi, H. Y., and Zhang, M. (2005) Maspin mediates increased tumor cell apoptosis upon induction of the mitochondrial permeability transition. *Mol. Cell. Biol.* **25,** 1737–1748
17. Vandermoere, F., El Yazidi-Belkoura, I., Slomianny, C., Demont, Y., Bidaux, G., Adriaenssens, E., Lemoine, J., and Hondermarck, H. (2006) The valosin-containing protein (VCP) is a target of Akt signaling required for cell survival. *J. Biol. Chem.* **281,** 14307–14313
18. Lalou, C., Lassarre, C., and Binoux, M. (1996) A proteolytic fragment of insulin-like growth factor (IGF) binding protein-3 that fails to bind IGFs inhibits the mitogenic effects of IGF-I and insulin. *Endocrinology* **137,** 3206–3212
19. Jiang, N., Meng, Y., Zhang, S., Mensah-Osman, E., and Sheng, S. (2002) Maspin sensitizes breast carcinoma cells to induced apoptosis. *Oncogene* **21,** 4089–4098
20. Liu, J., Yin, S., Reddy, N., Spencer, C., and Sheng, S. (2004) Bax mediates the apoptosis-sensitizing effect of maspin. *Cancer Res.* **64,** 1703–1711
21. Kim, H. S., Ingermann, A. R., Tsubaki, J., Twigg, S. M., Walker, G. E., and Oh, Y. (2004) Insulin-like growth factor-binding protein 3 induces caspase-dependent apoptosis through a death receptor-mediated pathway in MCF-7 human breast cancer cells. *Cancer Res.* **64,** 2229–2237
22. Lee, K. W., Ma, L., Yan, X., Liu, B., Zhang, X. K., and Cohen, P. (2005) Rapid apoptosis induction by IGFBP-3 involves an insulin-like growth factor-independent nucleomitochondrial translocation of RXRα/Nur77. *J. Biol. Chem.* **280,** 16942–16948
23. Hondermarck, H. (2003) Breast cancer: when proteomics challenges biological complexity. *Mol. Cell. Proteomics* **2,** 281–291
24. Hondermarck, H. (ed) (2004) *Biomedical and Pharmaceutical Applications of Proteomics*, Kluwer-Springer, Dordrecht, The Netherlands
25. Butt, A. J., Firth, S. M., King, M. A., and Baxter, R. C. (2000) Insulin-like growth factor-binding protein-3 modulates expression of Bax and Bcl-2 and potentiates p53-independent radiation-induced apoptosis in human breast cancer cells. *J. Biol. Chem.* **275,** 39174–39181
26. Bernard, L., Babajko, S., Binoux, N., and Ricort, J. M. (2002) The amino-terminal region of insulin-like growth factor binding protein-3, (1–95) IGFBP-3, induces apoptosis of MCF-7 breast carcinoma cells. *Biochem. Biophys. Res. Commun.* **293,** 55–60
27. Miyamoto, S., Yano, K., Sugimoto, S., Ishii, G., Hasebe, T., Endoh, Y., Kodama, K., Goya, M., Chiba, T., and Ochiai, A. (2004) Matrix metalloproteinase-7 facilitates insulin-like growth factor bioavailability through its proteinase activity on insulin-like growth factor binding protein 3. *Cancer Res.* **64,** 665–671
28. Mishra, S., and Murphy, L. J. (2003) Phosphorylation of insulin-like growth factor (IGF) binding protein-3 by breast cancer cell membranes enhances IGF-I binding. *Endocrinology* **144,** 4042–4050
29. Schedlich, L. J., Young, T. F., Firth, S. M., and Baxter, R. C. (1998) Insulin-like growth factor-binding protein (IGFBP)-3 and IGFBP-5 share a common nuclear transport pathway in T47D human breast carcinoma cells. *J. Biol. Chem.* **273,** 18347–18352
30. Schedlich, L. J., Nilsen, T., John, A. P., Jans, D. A., and Baxter, R. C. (2003) Phosphorylation of insulin-like growth factor binding protein-3 by deoxyribonucleic acid-dependent protein kinase reduces ligand binding and enhances nuclear accumulation. *Endocrinology* **144,** 1984–1994
31. Firth, S. M., and Baxter, R. C. (1999) Characterisation of glycosylation variants of insulin-like growth factor binding protein-3. *J. Endocrinol.* **160,** 379–387
32. Shi, H. Y., Zhang, W., Liang, R., Kittrell, F., Templeton, N. S., Medina, D., and Zhang, M. (2003) Modeling human breast cancer metastasis in mice: maspin as a paradigm. *Histol. Histopathol.* **18,** 201–206
33. Bailey, C. M., Khalkhali-Ellis, Z., Seftor, E., and Hendrix, M. J. C. (2006) Biological functions of maspin. *J. Cell. Physiol.* **209,** 617–624
34. Sheng, S. (2006) A role of novel serpin maspin in tumor progression: the divergence revealed through efforts to converge. *J. Cell. Physiol.* **209,** 631–635
35. Zhang, W., Shi, H. Y., and Zhang, M. (2005) Maspin overexpression modulates tumor cell apoptosis through the regulation of Bcl-2 family proteins. *BMC Cancer* **5,** 50
36. Biliran, H. Jr., and Sheng, S. (2001) Pleiotropic inhibition of pericellular urokinase-type plasminogen activator system by endogenous tumor suppressive maspin. *Cancer Res.* **61,** 8676–8682
37. Amir, S., Margaryan, N. V., Odero-Marah, V., Khalkhali-Ellis, Z., and Hendrix, M. J. C. (2005) Maspin regulates hypoxia-mediated stimulation of uPA/uPAR complex in invasive breast cancer cells. *Cancer Biol. Ther.* **4,** 400–406
38. Yin, S., Lockett, J., Meng, Y., Biliran, H. J., Blouse, G. E., Li, X., Reddy, N., Zhao, Z., Lin, X., Anagli, J., Cher, M. L., and Sheng, S. (2006) Maspin retards cell detachment via a novel interaction with the urokinase-type plasminogen activator/urokinase-type plasminogen activator receptor system. *Cancer Res.* **66,** 4173–4181
39. Ossowski, L., and Aguirre-Ghiso, J. A. (2000) Urokinase receptor and integrin partnership: coordination of signaling for cell adhesion, migration and growth. *Curr. Opin. Cell Biol.* **12,** 613–620
40. Odero-Marah, V. A., Khalkhali-Ellis, Z., Chunthapong, J., Amir, S., Seftor, R. E., Seftor, E. A., and Hendrix, M. J. C. (2003) Maspin regulates different signaling pathways for motility and adhesion in aggressive breast cancer cells. *Cancer Biol. Ther.* **2,** 398–403
41. Toillon, R. A., Adriaenssens, E., Wouters, D., Lottin, S., Boilly, B., Hondermarck, H., and Le Bourhis, X. (2000) Normal breast epithelial cells induce apoptosis of MCF-7 breast cancer cells through a p53-mediated pathway. *Mol. Cell. Biol. Res. Commun.* **3,** 338–344
42. Hanafusa, T., Shinji, T., Shiraha, H., Nouso, K., Iwasaki, Y., Yumoto, E., Ono, T., and Koide, N. (2005) Functional promoter upstream p53 regulatory sequence of IGFBP3 that is silenced by tumor specific methylation. *BMC Cancer* **5,** 9
43. Futscher, B. W., Oshiro, M. M., Wozniak, R. J., Holtan, N., Hanigan, C. L., Duan, H., and Domann, F. E. (2002) Role for DNA methylation in the control of cell type specific maspin expression. *Nat. Genet.* **31,** 175–179
44. Lockett, J., Yin, S., Li, X., Meng, Y., and Sheng, S. (2006) Tumor suppressive maspin and epithelial homeostasis. *J. Cell. Biochem.* **97,** 651–660
45. Martin, J. L., Weenink, S. M., and Baxter, R. C. (2003) Insulin-like growth factor-binding protein-3 potentiates epidermal growth factor action in MCF-10A mammary epithelial cells. Involvement of p44/42 and p38 mitogen-activated protein kinases. *J. Biol. Chem.* **278,** 2969–2976

Incidence de la surexpression de TrkA sur la croissance des cellules cancéreuses de sein

Nous avons préalablement montré au laboratoire que le NGF stimule la croissance des cellules cancéreuses de sein et ce de manière autocrine *via* deux récepteurs : le récepteur à activité tyrosine kinase TrkA impliqué dans la prolifération cellulaire et $p75^{NTR}$ intervenant dans la survie cellulaire. Afin de comprendre le rôle de TrkA dans le cancer du sein, nous avons établi un modèle cellulaire MDA-MB-231 surexprimant de manière stable TrkA.

Nous avons observé que la surexpression de TrkA augmente la croissance, la clonogénicité en agar mou, la migration et l'invasion des cellules. La surexpression de TrkA diminue également l'anoïkis ainsi que l'apoptose induite par TRAIL ou la doxorubicine. Les voies PI3K/Akt et ERK MAPK sont essentielles aux effets biologiques observés dans les cellules surexprimant TrkA. De plus, des études *in vivo* chez les souris SCID montrent que la surexpression de TrkA augmente la croissance des tumeurs primaires et la métastase dans les poumons, le foie et le cerveau. L'augmentation de la croissance tumorale est corrélée à une prolifération des cellules cancéreuses et à une angiogenèse accrue, tandis que la métastase est corrélée avec une augmentation de la résistance à l'anoïkis.

Enfin, par une approche en protéomique fonctionnelle, nous avons montré que la protéine Ku70 est associée à TrkA et qu'elle est impliquée dans la survie induite par l'activation de TrkA. De plus, la surexpression de TrkA dans les cellules de cancer du sein MDA-MB-231 induit une augmentation de l'expression de Ku86 et plus particulièrement au niveau de la surface cellulaire ; cette augmentation est impliquée dans la stimulation de la migration cellulaire.

L'ensemble de ces résultats montre que la surexpression de TrkA augmente l'agressivité des cellules cancéreuses de sein et ouvre des perspectives encourageantes dans le développement de stratégies thérapeutiques contre le cancer du sein.

BIBLIOGRAPHIE

Andersen, J. S., C. J. Wilkinson, T. Mayor, P. Mortensen, E. A. Nigg and M. Mann (2003). "Proteomic characterization of the human centrosome by protein correlation profiling." Nature **426**(6966): 570-4.

Arnold, A. and A. Papanikolaou (2005). "Cyclin D1 in breast cancer pathogenesis." J Clin Oncol **23**(18): 4215-24.

Austin and Short (1984). Reproduction in Mammalians. Hormonal control of reproduction. C. U. Press. Cambridge. **Book III**.

Beattie, M. S., A. W. Harrington, R. Lee, J. Y. Kim, S. L. Boyce, F. M. Longo, J. C. Bresnahan, B. L. Hempstead and S. O. Yoon (2002). "ProNGF induces p75-mediated death of oligodendrocytes following spinal cord injury." Neuron **36**(3): 375-86.

Benito-Gutierrez, E., J. Garcia-Fernandez and J. X. Comella (2006). "Origin and evolution of the Trk family of neurotrophic receptors." Mol Cell Neurosci **31**(2): 179-92.

Bieche, I. and R. Lidereau (1997). "[Somatic genetics of breast cancer]." Bull Cancer **84**(1):

Birnbaum, D., F. Bertucci, C. Ginestier, R. Tagett, J. Jacquemier and E. Charafe-Jauffret (2004). "Basal and luminal breast cancers: basic or luminous? (review)." Int J Oncol **25**(2): 249-58.

Blancato, J., B. Singh, A. Liu, D. J. Liao and R. B. Dickson (2004). "Correlation of amplification and overexpression of the c-myc oncogene in high-grade breast cancer: FISH, in situ hybridisation and immunohistochemical analyses." Br J Cancer **90**(8): 1612-9.

Bosco, E. E. and E. S. Knudsen (2007). "RB in breast cancer: at the crossroads of tumorigenesis and treatment." Cell Cycle **6**(6): 667-71.

Bose, C. K. (2005). "Role of nerve growth factor and FSH receptor in epithelial ovarian cancer." Reprod Biomed Online **11**(2): 194-7.

Brann, A. B., M. Tcherpakov, I. M. Williams, A. H. Futerman and M. Fainzilber (2002). "Nerve growth factor-induced p75-mediated death of cultured hippocampal neurons is age-dependent and transduced through ceramide generated by neutral sphingomyelinase." J Biol Chem **277**(12): 9812-8.

Buck, M. B. and C. Knabbe (2006). "TGF-beta signaling in breast cancer." Ann N Y Acad Sci **1089**: 119-26.

Burger, A. M., B. Leyland-Jones, K. Banerjee, D. D. Spyropoulos and A. K. Seth (2005). "Essential roles of IGFBP-3 and IGFBP-rP1 in breast cancer." Eur J Cancer **41**(11): 1515-27.

Cailleau, R., B. Mackay, R. K. Young and W. J. Reeves, Jr. (1974). "Tissue culture studies on pleural effusions from breast carcinoma patients." Cancer Res **34**(4): 801-9.

Cailleau, R., R. Young, M. Olive and W. J. Reeves, Jr. (1974). "Breast tumor cell lines from pleural effusions." J Natl Cancer Inst **53**(3): 661-74.

Calogero, S., F. Grassi, A. Aguzzi, T. Voigtlander, P. Ferrier, S. Ferrari and M. E. Bianchi (1999). "The lack of chromosomal protein Hmg1 does not disrupt cell growth but causes lethal hypoglycaemia in newborn mice." Nat Genet **22**(3): 276-80.

Campos, X., Y. Munoz, A. Selman, R. Yazigi, L. Moyano, C. Weinstein-Oppenheimer, H. E. Lara and C. Romero (2007). "Nerve growth factor and its high-affinity receptor trkA participate in the control of vascular endothelial growth factor expression in epithelial ovarian cancer." Gynecol Oncol **104**(1): 168-75.

Chan, S. K., M. E. Hill and W. J. Gullick (2006). "The role of the epidermal growth factor receptor in breast cancer." J Mammary Gland Biol Neoplasia **11**(1): 3-11.

Chang, C. F., R. Westbrook, J. Ma and D. Cao (2007). "Transforming growth factor-beta signaling in breast cancer." Front Biosci **12**: 4393-401.

Chao, M. V. (1994). "The p75 neurotrophin receptor." J Neurobiol **25**(11): 1373-85.

Charafe-Jauffret, E., C. Ginestier, F. Monville, S. Fekairi, J. Jacquemier, D. Birnbaum and F. Bertucci (2005). "How to best classify breast cancer: conventional and novel classifications (review)." Int J Oncol **27**(5): 1307-13.

Chittka, A., J. C. Arevalo, M. Rodriguez-Guzman, P. Perez, M. V. Chao and M. Sendtner (2004). "The p75NTR-interacting protein SC1 inhibits cell cycle progression by transcriptional repression of cyclin E." J Cell Biol **164**(7): 985-96.

Chong, Y. M., A. Subramanian, A. K. Sharma and K. Mokbel (2007). "The potential clinical applications of insulin-like growth factor-1 ligand in human breast cancer." Anticancer Res **27**(3B): 1617-24.

Com, E., C. Lagadec, A. Page, I. El Yazidi-Belkoura, C. Slomianny, A. Spencer, D. Hammache, B. B. Rudkin and H. Hondermarck (2007). "Nerve growth factor receptor TrkA signaling in breast cancer cells involves KU70 to prevent apoptosis." Mol Cell Proteomics.

Cowin, P., T. M. Rowlands and S. J. Hatsell (2005). "Cadherins and catenins in breast cancer." Curr Opin Cell Biol **17**(5): 499-508.

Dalziel, R. G., S. C. Mendelson and J. P. Quinn (1992). "The nuclear autoimmune antigen Ku is also present on the cell surface." Autoimmunity **13**(4): 265-7.

Davidson, B., R. Reich, P. Lazarovici, V. Ann Florenes, S. Nielsen and J. M. Nesland (2004). "Altered expression and activation of the nerve growth factor receptors TrkA and p75 provide the first evidence of tumor progression to effusion in breast carcinoma." Breast Cancer Res Treat **83**(2): 119-28.

Davidson, B., R. Reich, P. Lazarovici, J. M. Nesland, M. Skrede, B. Risberg, C. G. Trope and V. A. Florenes (2003). "Expression and activation of the nerve growth factor receptor TrkA in serous ovarian carcinoma." Clin Cancer Res **9**(6): 2248-59.

Descamps, S., X. Lebourhis, M. Delehedde, B. Boilly and H. Hondermarck (1998). "Nerve growth factor is mitogenic for cancerous but not normal human breast epithelial cells." J Biol Chem **273**(27): 16659-62.

Descamps, S., V. Pawlowski, F. Revillion, L. Hornez, M. Hebbar, B. Boilly, H. Hondermarck and J. P. Peyrat (2001). "Expression of nerve growth factor receptors and their prognostic value in human breast cancer." Cancer Res **61**(11): 4337-40.

Descamps, S., R. A. Toillon, E. Adriaenssens, V. Pawlowski, S. M. Cool, V. Nurcombe, X. Le Bourhis, B. Boilly, J. P. Peyrat and H. Hondermarck (2001). "Nerve growth factor stimulates proliferation and survival of human breast cancer cells through two distinct signaling pathways." J Biol Chem **276**(21): 17864-70.

Dewan, M. Z., S. Ahmed, Y. Iwasaki, K. Ohba, M. Toi and N. Yamamoto (2006). "Stromal cell-derived factor-1 and CXCR4 receptor interaction in tumor growth and metastasis of breast cancer." Biomed Pharmacother **60**(6): 273-6.

Dickson, J., S. E. Davidson, R. D. Hunter and C. M. West (2000). "Pretreatment plasma TGF beta 1 levels are prognostic for survival but not morbidity following radiation therapy of carcinoma of the cervix." Int J Radiat Oncol Biol Phys **48**(4): 991-5.

Diolaiti, D., R. Bernardoni, S. Trazzi, A. Papa, A. Porro, F. Bono, J. M. Herbert, G. Perini and G. Della Valle (2007). "Functional cooperation between TrkA and p75(NTR) accelerates neuronal differentiation by increased transcription of GAP-43 and p21(CIP/WAF) genes via ERK1/2 and AP-1 activities." Exp Cell Res **313**(14): 2980-92.

Dissen, G. A., C. Romero, A. N. Hirshfield and S. R. Ojeda (2001). "Nerve growth factor is required for early follicular development in the mammalian ovary." Endocrinology **142**(5): 2078-86.

Dolle, L., I. El Yazidi-Belkoura, E. Adriaenssens and H. Hondermarck (2003). "Nerve growth factor: from neurons to breast cancer." Research Advances in Cancer.

Dolle, L., I. El Yazidi-Belkoura, E. Adriaenssens, V. Nurcombe and H. Hondermarck (2003). "Nerve growth factor overexpression and autocrine loop in breast cancer cells." Oncogene **22**(36): 5592-601.

Dolle, L., M. J. Oliveira, E. Bruyneel, H. Hondermarck and M. Bracke (2005). "Nerve growth factor mediates its pro-invasive effect in parallel with the release of a soluble E-cadherin fragment from breast cancer MCF-7/AZ cells." J Dairy Res **72 Spec No**: 20-6.

Douma, S., T. Van Laar, J. Zevenhoven, R. Meuwissen, E. Van Garderen and D. S. Peeper (2004). "Suppression of anoikis and induction of metastasis by the neurotrophic receptor TrkB." Nature **430**(7003): 1034-9.

Eggert, A., M. A. Grotzer, N. Ikegaki, X. G. Liu, A. E. Evans and G. M. Brodeur (2002). "Expression of the neurotrophin receptor TrkA down-regulates expression and function of angiogenic stimulators in SH-SY5Y neuroblastoma cells." Cancer Res **62**(6): 1802-8.

Eggert, A., N. Ikegaki, X. G. Liu and G. M. Brodeur (2000). "Prognostic and biological role of neurotrophin-receptor TrkA and TrkB in neuroblastoma." Klin Padiatr **212**(4): 200-5.

Elliott, B. E., W. L. Hung, A. H. Boag and A. B. Tuck (2002). "The role of hepatocyte growth factor (scatter factor) in epithelial-mesenchymal transition and breast cancer." Can J Physiol Pharmacol **80**(2): 91-102.

Epa, W. R., K. Markovska and G. L. Barrett (2004). "The p75 neurotrophin receptor enhances TrkA signalling by binding to Shc and augmenting its phosphorylation." J Neurochem **89**(2): 344-53.

Espie, M., A. Gorin and A. Gorin (1995). "Le sein". Paris.

Festuccia, C., G. L. Gravina, P. Muzi, R. Pomante, L. Ventura, E. Ricevuto, C. Vicentini and M. Bologna (2007). "In vitro and in vivo effects of bicalutamide on the expression of TrkA and P75 neurotrophin receptors in prostate carcinoma." Prostate **67**(12): 1255-64.

Foster, L. J., C. L. De Hoog and M. Mann (2003). "Unbiased quantitative proteomics of lipid rafts reveals high specificity for signaling factors." Proc Natl Acad Sci U S A **100**(10): 5813-8.

Friess, H., Z. W. Zhu, F. F. di Mola, C. Kulli, H. U. Graber, A. Andren-Sandberg, A. Zimmermann, M. Korc, M. Reinshagen and M. W. Buchler (1999). "Nerve growth factor and its high-affinity receptor in chronic pancreatitis." Ann Surg **230**(5): 615-24.

Garcia, M., D. Derocq, G. Freiss and H. Rochefort (1992). "Activation of estrogen receptor transfected into a receptor-negative breast cancer cell line decreases the metastatic and invasive potential of the cells." Proc Natl Acad Sci U S A **89**(23): 11538-42.

Gasco, M., S. Shami and T. Crook (2002). "The p53 pathway in breast cancer." Breast Cancer Res **4**(2): 70-6.

Ginis, I. and D. V. Faller (2000). "Hypoxia affects tumor cell invasiveness in vitro: the role of hypoxia-activated ligand HAL1/13 (Ku86 autoantigen)." Cancer Lett **154**(2): 163-74.

Ginis, I., S. J. Mentzer, X. Li and D. V. Faller (1995). "Characterization of a hypoxia-responsive adhesion molecule for leukocytes on human endothelial cells." J Immunol **155**(2): 802-10.

Goretzki, P. E., R. A. Wahl, R. Becker, C. Koller, D. Branscheid, M. Grussendorf and H. D. Roeher (1987). "Nerve growth factor (NGF) sensitizes human medullary thyroid carcinoma (hMTC) cells for cytostatic therapy in vitro." Surgery **102**(6): 1035-42.

Han, D. K., J. Eng, H. Zhou and R. Aebersold (2001). "Quantitative profiling of differentiation-induced microsomal proteins using isotope-coded affinity tags and mass spectrometry." Nat Biotechnol **19**(10): 946-51.

Hanahan, D. and R. A. Weinberg (2000). "The hallmarks of cancer." Cell **100**(1): 57-70.

Hayes, D. F., K. Miller and G. Sledge (2007). "Angiogenesis as targeted breast cancer therapy." Breast.

Heimann, R., F. Lan, R. McBride and S. Hellman (2000). "Separating favorable from unfavorable prognostic markers in breast cancer: the role of E-cadherin." Cancer Res **60**(2): 298-304.

Hoyle, G. W. (2003). "Neurotrophins and lung disease." Cytokine Growth Factor Rev **14**(6): 551-8.

Hutcheson, I. R., J. M. Knowlden, T. A. Madden, D. Barrow, J. M. Gee, A. E. Wakeling and R. I. Nicholson (2003). "Oestrogen receptor-mediated modulation of the EGFR/MAPK pathway in tamoxifen-resistant MCF-7 cells." Breast Cancer Res Treat **81**(1): 81-93.

Ito, H., H. Nomoto and S. Furukawa (2002). "Role of low-affinity p75 receptor in nerve growth factor-inducible growth arrest of PC12 cells." J Neurosci Res **69**(5): 653-61.

Ito, Y., N. Tokudome, T. Sugihara, S. Takahashi and K. Hatake (2007). "Does lapatinib, a small-molecule tyrosine kinase inhibitor, constitute a breakthrough in the treatment of breast cancer?" Breast Cancer **14**(2): 156-62.

Jacobs, T. W., A. M. Gown, H. Yaziji, M. J. Barnes and S. J. Schnitt (2000). "HER-2/neu protein expression in breast cancer evaluated by immunohistochemistry. A study of interlaboratory agreement." Am J Clin Pathol **113**(2): 251-8.

Khwaja, F., A. Tabassum, J. Allen and D. Djakiew (2006). "The p75(NTR) tumor suppressor induces cell cycle arrest facilitating caspase mediated apoptosis in prostate tumor cells." Biochem Biophys Res Commun **341**(4): 1184-92.

Koga, F., S. Tsutsumi and L. M. Neckers (2007). "Low dose geldanamycin inhibits hepatocyte growth factor and hypoxia-stimulated invasion of cancer cells." Cell Cycle **6**(11): 1393-402.

Kogner, P., G. Barbany, C. Dominici, M. A. Castello, G. Raschella and H. Persson (1993). "Coexpression of messenger RNA for TRK protooncogene and low affinity nerve growth factor receptor in neuroblastoma with favorable prognosis." Cancer Res **53**(9): 2044-50.

Koizumi, H., M. Morita, S. Mikami, E. Shibayama and T. Uchikoshi (1998). "Immunohistochemical analysis of TrkA neurotrophin receptor expression in human non-neuronal carcinomas." Pathol Int **48**(2): 93-101.

Krygier, S. and D. Djakiew (2001). "The neurotrophin receptor p75NTR is a tumor suppressor in human prostate cancer." Anticancer Res **21**(6A): 3749-55.

Krygier, S. and D. Djakiew (2002). "Neurotrophin receptor p75(NTR) suppresses growth and nerve growth factor-mediated metastasis of human prostate cancer cells." Int J Cancer **98**(1): 1-7.

Lakhani, S. R., R. Chaggar, S. Davies, C. Jones, N. Collins, C. Odel, M. R. Stratton and M. J. O'Hare (1999). "Genetic alterations in 'normal' luminal and myoepithelial cells of the breast." J Pathol **189**(4): 496-503.

Lee, T. H., S. Seng, M. Sekine, C. Hinton, Y. Fu, H. K. Avraham and S. Avraham (2007). "Vascular endothelial growth factor mediates intracrine survival in human breast carcinoma cells through internally expressed VEGFR1/FLT1." PLoS Med **4**(6): e186.

Leoni, C. and F. Valtorta (2002). "Constitutive TrkA activity in receptor-overexpressing PC12 clones." Biochem Biophys Res Commun **291**(4): 972-8.

Liu, M., S. C. Yang, S. Sharma, J. Luo, X. Cui, K. A. Peebles, M. Huang, M. Sato, R. D. Ramirez, J. W. Shay, J. D. Minna and S. M. Dubinett (2007). "EGFR Signaling is Required for TGF-{beta}1-mediated COX-2 Induction in Human Bronchial Epithelial Cells." Am J Respir Cell Mol Biol.

Lynch, E. M., R. B. Moreland, I. Ginis, S. P. Perrine and D. V. Faller (2001). "Hypoxia-activated ligand HAL-1/13 is lupus autoantigen Ku80 and mediates lymphoid cell adhesion in vitro." Am J Physiol Cell Physiol **280**(4): C897-911.

Makkerh, J. P., C. Ceni, D. S. Auld, F. Vaillancourt, G. Dorval and P. A. Barker (2005). "p75 neurotrophin receptor reduces ligand-induced Trk receptor ubiquitination and delays Trk receptor internalization and degradation." EMBO Rep **6**(10): 936-41.

Malloy, P. J., W. Zhu, X. Y. Zhao, G. B. Pehling and D. Feldman (2001). "A novel inborn error in the ligand-binding domain of the vitamin D receptor causes hereditary vitamin D-resistant rickets." Mol Genet Metab **73**(2): 138-48.

Mamidipudi, V., C. Lin, M. L. Seibenhener and M. W. Wooten (2004). "Regulation of interleukin receptor-associated kinase (IRAK) phosphorylation and signaling by iota protein kinase C." J Biol Chem **279**(6): 4161-5.

Manetti, F. and M. Botta (2003). "Small-molecule inhibitors of fibroblast growth factor receptor (FGFR) tyrosine kinases (TK)." Curr Pharm Des **9**(7): 567-81.

Mann, M. (2006). "Functional and quantitative proteomics using SILAC." Nat Rev Mol Cell Biol **7**(12): 952-8.

Marouga, R., S. David and E. Hawkins (2005). "The development of the DIGE system: 2D fluorescence difference gel analysis technology." Anal Bioanal Chem **382**(3): 669-78.

Martin-Zanca, D., S. H. Hughes and M. Barbacid (1986). "A human oncogene formed by the fusion of truncated tropomyosin and protein tyrosine kinase sequences." Nature **319**(6056): 743-8.

McDonald, W. H. and J. R. Yates, 3rd (2003). "Shotgun proteomics: integrating technologies to answer biological questions." Curr Opin Mol Ther **5**(3): 302-9.

McGregor, L. M., B. K. McCune, J. R. Graff, P. R. McDowell, K. E. Romans, G. D. Yancopoulos, D. W. Ball, S. B. Baylin and B. D. Nelkin (1999). "Roles of trk family neurotrophin receptors in medullary thyroid carcinoma development and progression." Proc Natl Acad Sci U S A **96**(8): 4540-5.

Mercurio, A. M., E. A. Lipscomb and R. E. Bachelder (2005). "Non-angiogenic functions of VEGF in breast cancer." J Mammary Gland Biol Neoplasia **10**(4): 283-90.

Miao, G., J. Mace, M. Kirby, A. Hopper, R. Peverini, R. Chinnock, J. Shapiro and E. Hathout (2005). "Beneficial effects of nerve growth factor on islet transplantation." Transplant Proc **37**(8): 3490-2.

Miao, G., J. Mace, M. Kirby, A. Hopper, R. Peverini, R. Chinnock, J. Shapiro and E. Hathout (2006). "In vitro and in vivo improvement of islet survival following treatment with nerve growth factor." Transplantation **81**(4): 519-24.

Micera, A., A. Lambiase, B. Stampachiacchiere, S. Bonini, S. Bonini and F. Levi-Schaffer (2007). "Nerve growth factor and tissue repair remodeling: trkA(NGFR) and p75(NTR), two receptors one fate." Cytokine Growth Factor Rev **18**(3-4): 245-56.

Miknyoczki, S. J., W. Wan, H. Chang, P. Dobrzanski, B. A. Ruggeri, C. A. Dionne and K. Buchkovich (2002). "The neurotrophin-trk receptor axes are critical for the growth and progression of human prostatic carcinoma and pancreatic ductal adenocarcinoma xenografts in nude mice." Clin Cancer Res **8**(6): 1924-31.

Missale, C., A. Codignola, S. Sigala, A. Finardi, M. Paez-Pereda, E. Sher and P. F. Spano (1998). "Nerve growth factor abrogates the tumorigenicity of human small cell lung cancer cell lines." Proc Natl Acad Sci U S A **95**(9): 5366-71.

Mohammed, R. A., A. Green, S. El-Shikh, E. C. Paish, I. O. Ellis and S. G. Martin (2007). "Prognostic significance of vascular endothelial cell growth factors -A, -C and -D in breast cancer and their relationship with angio- and lymphangiogenesis." Br J Cancer **96**(7): 1092-100.

Monferran, S., J. Paupert, S. Dauvillier, B. Salles and C. Muller (2004). "The membrane form of the DNA repair protein Ku interacts at the cell surface with metalloproteinase 9." Embo J **23**(19): 3758-68.

Mourez, M. and R. J. Collier (2004). "Use of phage display and polyvalency to design inhibitors of protein-protein interactions." Methods Mol Biol **261**: 213-28.

Muller, C., J. Paupert, S. Monferran and B. Salles (2005). "The double life of the Ku protein: facing the DNA breaks and the extracellular environment." Cell Cycle **4**(3): 438-41.

Nass, S. J. and N. E. Davidson (1999). "The biology of breast cancer." Hematol Oncol Clin North Am **13**(2): 311-32.

Naud, N., A. Toure, J. Liu, C. Pineau, L. Morin, O. Dorseuil, D. Escalier, P. Chardin and G. Gacon (2003). "Rho family GTPase Rnd2 interacts and co-localizes with MgcRacGAP in male germ cells." Biochem J **372**(Pt 1): 105-12.

Navarro-Tableros, V., M. C. Sanchez-Soto, S. Garcia and M. Hiriart (2004). "Autocrine regulation of single pancreatic beta-cell survival." Diabetes **53**(8): 2018-23.

Odegaard, E., A. C. Staff, V. M. Abeler, J. Kopolovic, M. Onsrud, P. Lazarovici and B. Davidson (2007). "The activated nerve growth factor receptor p-TrkA is selectively expressed in advanced-stage ovarian carcinoma." Hum Pathol **38**(1): 140-6.

Oelmann, E., L. Sreter, I. Schuller, H. Serve, M. Koenigsmann, B. Wiedenmann, D. Oberberg, B. Reufi, E. Thiel and W. E. Berdel (1995). "Nerve growth factor stimulates clonal growth of human lung cancer cell lines and a human glioblastoma cell line expressing high-affinity nerve growth factor binding sites involving tyrosine kinase signaling." Cancer Res **55**(10): 2212-9.

Ornitz, D. M. and N. Itoh (2001). "Fibroblast growth factors." Genome Biol **2**(3): REVIEWS3005.

Pandini, G., M. Genua, F. Frasca, S. Squatrito, R. Vigneri and A. Belfiore (2007). "17{beta}-Estradiol Up-regulates the Insulin-like Growth Factor Receptor through a Nongenotropic Pathway in Prostate Cancer Cells." Cancer Res **67**(18): 8932-41.

Papatsoris, A. G., D. Liolitsa and C. Deliveliotis (2007). "Manipulation of the nerve growth factor network in prostate cancer." Expert Opin Investig Drugs **16**(3): 303-9.

Pedraza, C. E., P. Podlesniy, N. Vidal, J. C. Arevalo, R. Lee, B. Hempstead, I. Ferrer, M. Iglesias and C. Espinet (2005). "Pro-NGF isolated from the human brain affected by Alzheimer's disease induces neuronal apoptosis mediated by p75NTR." Am J Pathol **166**(2): 533-43.

Perez-Pinera, P., T. Hernandez, O. Garcia-Suarez, F. de Carlos, A. Germana, M. Del Valle, A. Astudillo and J. A. Vega (2007). "The Trk tyrosine kinase inhibitor K252a regulates growth of lung adenocarcinomas." Mol Cell Biochem **295**(1-2): 19-26.

Pierotti, M. A. and A. Greco (2006). "Oncogenic rearrangements of the NTRK1/NGF receptor." Cancer Lett **232**(1): 90-8.

Polyak, K. (2001). "On the birth of breast cancer." Biochim Biophys Acta **1552**(1): 1-13.

Prabhakar, B. S., G. P. Allaway, J. Srinivasappa and A. L. Notkins (1990). "Cell surface expression of the 70-kD component of Ku, a DNA-binding nuclear autoantigen." J Clin Invest **86**(4): 1301-5.

Price, J. E., A. Polyzos, R. D. Zhang and L. M. Daniels (1990). "Tumorigenicity and metastasis of human breast carcinoma cell lines in nude mice." Cancer Res **50**(3): 717-21.

Puig, O., F. Caspary, G. Rigaut, B. Rutz, E. Bouveret, E. Bragado-Nilsson, M. Wilm and B. Seraphin (2001). "The tandem affinity purification (TAP) method: a general procedure of protein complex purification." Methods **24**(3): 218-29.

Rabizadeh, S. and D. E. Bredesen (2003). "Ten years on: mediation of cell death by the common neurotrophin receptor p75(NTR)." Cytokine Growth Factor Rev **14**(3-4): 225-39.

Resing, K. A. (2004). "Current progress in protein profiling of complex samples." Expert Rev Proteomics **1**(2): 137-40.

Ricci, A., P. Graziano, S. Mariotta, G. Cardillo, B. Sposato, C. Terzano and E. Bronzetti (2005). "Neurotrophin system expression in human pulmonary carcinoid tumors." Growth Factors **23**(4): 303-12.

Ricci, A., S. Greco, S. Mariotta, L. Felici, E. Bronzetti, A. Cavazzana, G. Cardillo, F. Amenta, A. Bisetti and G. Barbolini (2001). "Neurotrophins and neurotrophin receptors in human lung cancer." Am J Respir Cell Mol Biol **25**(4): 439-46.

Rigaut, G., A. Shevchenko, B. Rutz, M. Wilm, M. Mann and B. Seraphin (1999). "A generic protein purification method for protein complex characterization and proteome exploration." Nat Biotechnol **17**(10): 1030-2.

Romero, C., A. Paredes, G. A. Dissen and S. R. Ojeda (2002). "Nerve growth factor induces the expression of functional FSH receptors in newly formed follicles of the rat ovary." Endocrinology **143**(4): 1485-94.

Roussidis, A. E., A. D. Theocharis, G. N. Tzanakakis and N. K. Karamanos (2007). "The importance of c-Kit and PDGF receptors as potential targets for molecular therapy in breast cancer." Curr Med Chem **14**(7): 735-43.

Sakamoto, Y., Y. Kitajima, G. Edakuni, E. Sasatomi, M. Mori, K. Kitahara and K. Miyazaki (2001). "Expression of Trk tyrosine kinase receptor is a biologic marker for cell proliferation and perineural invasion of human pancreatic ductal adenocarcinoma." Oncol Rep **8**(3): 477-84.

Salas, C., M. Julio-Pieper, M. Valladares, R. Pommer, M. Vega, C. Mastronardi, B. Kerr, S. R. Ojeda, H. E. Lara and C. Romero (2006). "Nerve growth factor-dependent activation of trkA receptors in the human ovary results in synthesis of follicle-stimulating hormone receptors and estrogen secretion." J Clin Endocrinol Metab **91**(6): 2396-403.

Sawada, M., W. Sun, P. Hayes, K. Leskov, D. A. Boothman and S. Matsuyama (2003). "Ku70 suppresses the apoptotic translocation of Bax to mitochondria." Nat Cell Biol **5**(4): 320-9.

Schneider, M. B., J. Standop, A. Ulrich, U. Wittel, H. Friess, A. Andren-Sandberg and P. M. Pour (2001). "Expression of nerve growth factors in pancreatic neural tissue and pancreatic cancer." J Histochem Cytochem **49**(10): 1205-10.

Schramm, A., J. H. Schulte, K. Astrahantseff, O. Apostolov, V. Limpt, H. Sieverts, S. Kuhfittig-Kulle, P. Pfeiffer, R. Versteeg and A. Eggert (2005). "Biological effects of TrkA and TrkB receptor signaling in neuroblastoma." Cancer Lett **228**(1-2): 143-53.

Serebriiskii, I. G., G. G. Toby, R. L. Finley, Jr. and E. A. Golemis (2001). "Genomic analysis utilizing the yeast two-hybrid system." Methods Mol Biol **175**: 415-54.

Sorlie, T., R. Tibshirani, J. Parker, T. Hastie, J. S. Marron, A. Nobel, S. Deng, H. Johnsen, R. Pesich, S. Geisler, J. Demeter, C. M. Perou, P. E. Lonning, P. O. Brown, A. L. Borresen-Dale and D. Botstein (2003). "Repeated observation of breast tumor subtypes in independent gene expression data sets." Proc Natl Acad Sci U S A **100**(14): 8418-23.

Sternlicht, M. D., H. Kouros-Mehr, P. Lu and Z. Werb (2006). "Hormonal and local control of mammary branching morphogenesis." Differentiation **74**(7): 365-81.

Stevens, A. and J. Lowe (1992). Histologie.

Tacconelli, A., A. R. Farina, L. Cappabianca, G. Desantis, A. Tessitore, A. Vetuschi, R. Sferra, N. Rucci, B. Argenti, I. Screpanti, A. Gulino and A. R. Mackay (2004). "TrkA alternative splicing: a regulated tumor-promoting switch in human neuroblastoma." Cancer Cell **6**(4): 347-60.

Tacconelli, A., A. R. Farina, L. Cappabianca, A. Gulino and A. R. Mackay (2005). "TrkAIII. A novel hypoxia-regulated alternative TrkA splice variant of potential physiological and pathological importance." Cell Cycle **4**(1): 8-9.

Taguchi, A., D. C. Blood, G. del Toro, A. Canet, D. C. Lee, W. Qu, N. Tanji, Y. Lu, E. Lalla, C. Fu, M. A. Hofmann, T. Kislinger, M. Ingram, A. Lu, H. Tanaka, O. Hori, S. Ogawa, D. M. Stern and A. M. Schmidt (2000). "Blockade of RAGE-amphoterin signalling suppresses tumour growth and metastases." Nature **405**(6784): 354-60.

Thompson, D. and D. Easton (2004). "The genetic epidemiology of breast cancer genes." J Mammary Gland Biol Neoplasia **9**(3): 221-36.

Toby, G. G. and E. A. Golemis (2001). "Using the yeast interaction trap and other two-hybrid-based approaches to study protein-protein interactions." Methods **24**(3): 201-17.

Toillon, R. A., E. Adriaenssens, D. Wouters, S. Lottin, B. Boilly, H. Hondermarck and X. L. Bourhis (2000). "Normal breast epithelial cells induce apoptosis of MCF-7 breast cancer cells through a p53-mediated pathway." Mol Cell Biol Res Commun **3**(6): 338-44.

Toillon, R. A., V. Chopin, N. Jouy, W. Fauquette, B. Boilly and X. Le Bourhis (2002). "Normal breast epithelial cells induce p53-dependent apoptosis and p53-independent cell cycle arrest of breast cancer cells." Breast Cancer Res Treat **71**(3): 269-80.

Toillon, R. A., S. Descamps, E. Adriaenssens, J. M. Ricort, D. Bernard, B. Boilly and X. Le Bourhis (2002). "Normal breast epithelial cells induce apoptosis of breast cancer cells via Fas signaling." Exp Cell Res **275**(1): 31-43.

Tulp, A., D. Verwoerd and J. Neefjes (1999). "Electromigration for separations of protein complexes." J Chromatogr B Biomed Sci Appl **722**(1-2): 141-51.

Ursini-Siegel, J., B. Schade, R. D. Cardiff and W. J. Muller (2007). "Insights from transgenic mouse models of ERBB2-induced breast cancer." Nat Rev Cancer **7**(5): 389-97.

Vogel, C. L. and E. Tan-Chiu (2005). "Trastuzumab plus chemotherapy: convincing survival benefit or not?" J Clin Oncol **23**(19): 4247-50.

Wang, H., J. M. Vishnubhakat, O. Bloom, M. Zhang, M. Ombrellino, A. Sama and K. J. Tracey (1999). "Proinflammatory cytokines (tumor necrosis factor and interleukin 1) stimulate release of high mobility group protein-1 by pituicytes." Surgery **126**(2): 389-92.

Wang, J. J., A. Tasinato, D. W. Ethell, M. P. Testa and D. E. Bredesen (2000). "Phosphorylation of the common neurotrophin receptor p75 by p38beta2 kinase affects NF-kappaB and AP-1 activities." J Mol Neurosci **15**(1): 19-29.

Watson, F. L., M. A. Porcionatto, A. Bhattacharyya, C. D. Stiles and R. A. Segal (1999). "TrkA glycosylation regulates receptor localization and activity." J Neurobiol **39**(2): 323-36.

Weeraratna, A. T., J. T. Arnold, D. J. George, A. DeMarzo and J. T. Isaacs (2000). "Rational basis for Trk inhibition therapy for prostate cancer." Prostate **45**(2): 140-8.

Wehrman, T., X. He, B. Raab, A. Dukipatti, H. Blau and K. C. Garcia (2007). "Structural and mechanistic insights into nerve growth factor interactions with the TrkA and p75 receptors." Neuron **53**(1): 25-38.

Wilmes, L. J., M. G. Pallavicini, L. M. Fleming, J. Gibbs, D. Wang, K. L. Li, S. C. Partridge, R. G. Henry, D. R. Shalinsky, D. Hu-Lowe, J. W. Park, T. M. McShane, Y. Lu, R. C. Brasch and N. M. Hylton (2007). "AG-013736, a novel inhibitor of VEGF receptor tyrosine kinases, inhibits breast cancer growth and decreases vascular permeability as detected by dynamic contrast-enhanced magnetic resonance imaging." Magn Reson Imaging **25**(3): 319-27.

Yaswen, P. and M. R. Stampfer (2002). "Molecular changes accompanying senescence and immortalization of cultured human mammary epithelial cells." Int J Biochem Cell Biol **34**(11): 1382-94.

Zavodovskaya, M., M. J. Campbell, B. A. Maddux, L. Shiry, G. Allan, L. Hodges, P. Kushner, J. A. Kerner, J. F. Youngren and I. D. Goldfine (2007). "Nordihydroguaiaretic acid (NDGA), an inhibitor of the HER2 and IGF-1 receptor tyrosine kinases, blocks the growth of HER2-overexpressing human breast cancer cells." J Cell Biochem.

Zhu, Z., H. Friess, F. F. diMola, A. Zimmermann, H. U. Graber, M. Korc and M. W. Buchler (1999). "Nerve growth factor expression correlates with perineural invasion and pain in human pancreatic cancer." J Clin Oncol **17**(8): 2419-28.

Zhu, Z., J. Kleeff, H. Kayed, L. Wang, M. Korc, M. W. Buchler and H. Friess (2002). "Nerve growth factor and enhancement of proliferation, invasion, and tumorigenicity of pancreatic cancer cells." Mol Carcinog **35**(3): 138-47.

Zhu, Z. W., H. Friess, L. Wang, T. Bogardus, M. Korc, J. Kleeff and M. W. Buchler (2001). "Nerve growth factor exerts differential effects on the growth of human pancreatic cancer cells." Clin Cancer Res **7**(1): 105-12.

Zou, H. Y., Q. Li, J. H. Lee, M. E. Arango, S. R. McDonnell, S. Yamazaki, T. B. Koudriakova, G. Alton, J. J. Cui, P. P. Kung, M. D. Nambu, G. Los, S. L. Bender, B. Mroczkowski and J. G. Christensen (2007). "An orally available small-molecule inhibitor of c-Met, PF-2341066, exhibits cytoreductive antitumor efficacy through antiproliferative and antiangiogenic mechanisms." Cancer Res **67**(9): 4408-17.